Isolation and Structure Elucidation of Anticancer and Antimalarial Natural Products

Yixi Liu

Dissertation submitted to the faculty of the Virginia Polytechnic Institute and State University in partial fulfillment of the requirements for the degree of

Doctor of Philosophy
In
Chemistry

David G. I. Kingston, chair

James M. Tanko

Harry C. Dorn

Webster L. Santos

March 26th 2015
Blacksburg, Virginia

Keywords: Natural Products, Antiproliferative, Antimalarial, α-pyrone, Lignan, Sesquiterpene lactone, Naphthoquinone, Stilbenenoid, Alkaloid, Butanolid, Diterpene.

Isolation, Synthesis and Structure–Activity Relationship Study of Anticancer and Antimalarial Agents from Natural Products

Yixi Liu

ABSTRACT

As part of an International Cooperative Biodiversity Group (ICBG) program and a continuing search for antiproliferative natural products from the Madagascar rainforest, and a collaborative research project established between Virginia Tech and the Institute for Hepatitis and Virus Research (IHVR) focusing on searching for bioactive natural products from tropical forests in South Africa, 20 extracts were selected for investigation based on their antiproliferative activities against A2780 human ovarian cancer cell line or antimalarial activities against the Dd2 strain of *Plasmodium falciparum*. Bioassay-guided fractionation of seven of the extracts yielded twenty new compounds and twenty-four known compounds, and their structures were elucidated by using a combination of 1D (^{1}H and ^{13}C) and 2D NMR spectroscopy including COSY, HASQC, HMQC, HMBC, and NOESY sequences, mass spectrometry, UV, IR, ECD, optical rotation, and chemical conversions. In addition, ten known compounds were isolated from another five of the extracts, while studies on the remaining extracts were suspended due to loss of activity, unworkable small amounts of material, or low structural interest.

The plants and their metabolites are discussed in the following order: five new antimalarial 5,6-dihydro-α-pyrones and six bicyclic tetrahydro-α-pyrone derivatives from *Cryptocarya rigidifolia* (Lauraceae); two new and five known antiproliferative lignans from *Cleistanthus boivinianus* (Phyllanthaceae); two new and two known antiproliferative sesquiterpenes lactones from *Piptocoma antillana* (Asteraceae); one new

antiproliferative 1,4-naphthoquinone, one known antiproliferative isoflovonoid, and five known antiproliferative stilbenoids from *Stuhlmannia moavi* (Leguminosae); four known antiproliferative bisbenzylisoquinoline alkaloids from *Anisocycla grandidieri* (Menispermaceae); one new and two known antiproliferative butanolides, and two new antiproliferative secobutanolides from *Ocotea macrocarpa* (Lauraceae); one new antiproliferative and five known antiproliferative diterpenoids from *Malleastrum rakotozafyi* (Meliceae); and 10 known compounds from *Monoporus sp.* (Myrsinaceae), *Premna corymbosa* (Verbenaceae), *Premna perplexanes* (Verbenaceae), *Epallage longipes* (Asteraceae), and *Cinnamosma fragrans* (Canellaceae).

Table of Contents

List of Tables

List of Schemes

List of Figures

1 Introduction

1.1 Natural Products

In the broadest sense, natural products include any substance produced by life, but the term is commonly used in reference to chemical compounds or substances produced by a living organism found in nature. Natural products often have pharmacological or biological activities. Therefore, humans have relied on nature for their basic needs throughout the ages, especially for the treatment of a wide spectrum of diseases. Plants, in particular, have formed the basis of traditional medicine systems, and records dating from around 2600 BCE document the uses of approximately 1000 plant-derived substances in Mesopotamia.[1]

It is worth discussing the reasons for the important roles played by natural products, especially natural products from plants. Natural products can be characterized as secondary metabolites from natural resources, like plants, marine organisms and microbes. So the first reason can be from a biological point of view. Plants are fixed in a place, thus it is almost impossible for them to kill predators such as insects and animals or to defend themselves by movement. As time passes, they change, recombine and evolve their genes to develop a very effective chemical defensive system, which they do in part by producing numerous compounds with diverse chemical structures.[2] It has been reported that these secondary metabolites are related to predator deterrence.[3] And some of those secondary metabolites produced by the evolved genes can be used utilized by humans as bioactive natural products.

Furthermore, natural products are irreplaceable as the source of lead compounds for future drug design. Natural compounds are friendlier ligands to biological receptors

than pure synthetic compounds, since they come from natural organisms. However, they may not be very effective drugs directly after they are isolated, and chemists may need to use medicinal chemistry to modify their structures to improve their potency or their pharmacokinetic properties.

1.2 Cancer and Anticancer Agents from Natural Products

Cancer is one of the leading causes of death in the world. According to the statistical data from the World Cancer Report, about 8.2 million people died because of cancer in 2012, which means 22,500 deaths per day, among them about 62% are from developing countries and 38% are from developed countries. If this rate continues, 17.5 million cancer deaths per year from cancer can be predicted by 2050.[4, 5] Therefore the cure of cancer has been a worldwide concern for a long time. Plants have proven to be the most reliable source and successful strategy in modern cancer treatment. An impressive number of modern drugs derived from plants have been used to treat many types of cancer, like lymphomas, leukemias and solid tumors.[6] From Newman and Cragg's research, 63% of a total of 155 anticancer drugs marketed from 1981 to 2006 are natural products or analogues of natural products, and most of them come from North America, Europe, and Japan.[7] Butler also lists 79 new anticancer agents that entered clinical trial as natural products or their derivatives in recent years.[8]

The earliest attempt at searching for anticancer agents from plants was in the 1950s. It started with the discovery of the vinca alkaloids. The vinca alkaloids are a series of compounds composed of indole and indoline subunits. They are the first natural products entering into clinical use as anticancer agents and represent one of the most

important classes of anticancer agents. The first two active vinca alkaloids, vinblastine **1.1** and vincristine **1.2**, were isolated from *Catharanthus roseus* (L.) (Apocynaceae family).[9, 10] After the success of the first clinical trials in the 1960s, clinicians started to use these two so-called vinca alkaloids widely in the treatment of different types of cancers, and they were given the trade names of Velban®/ Velbe® and Oncovin®, respectively. Some analogues of the earliest vinca alkaloids have been synthesized and have entered into clinical applications, including vindesine **1.3** (Eldesine®),[11] vinorelbine **1.4** (Navelbine®),[12] and vinflunine **1.5**.[13]

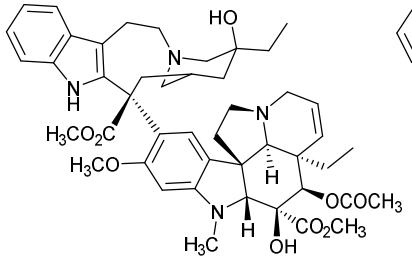

1.1

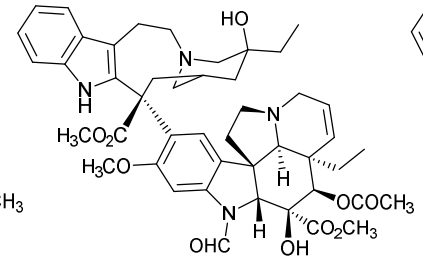

1.2

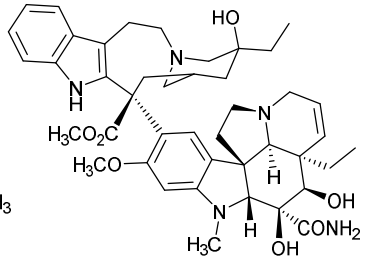

1.3

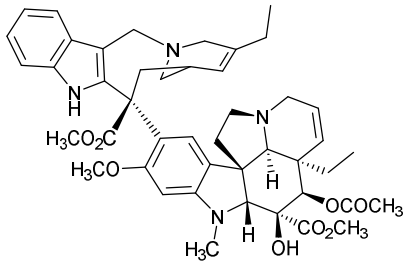

1.4

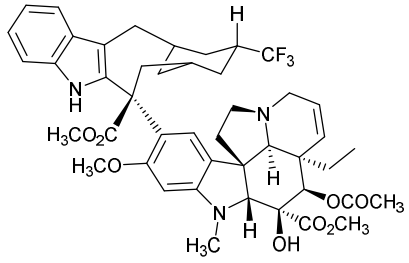

1.5

The important natural product drug Taxol (paclitaxel) **1.6** was first isolated from the bark of *Taxus brevifolia* (Pacific yew) as the major active component in the 1960s. The structure was elucidated by Monroe Wall, Mansukh Wani and Andrew McPhail in 1971.[14] It entered phase I clinical trials in 1984.[15] Phase II trials overcame allergic reactions by using a lengthened infusion period and premedication, and taxol **1.6** was approved by the FDA for the treatment of ovarian and breast cancer in 1992 and 1994,

respectively.[16] Some analogs, including Taxotere **1.7** cabazitaxel **1.8**, showed even better activities in some assays than taxol, were approved by FDA in 1999 and 2009, respectively.[17] [18]

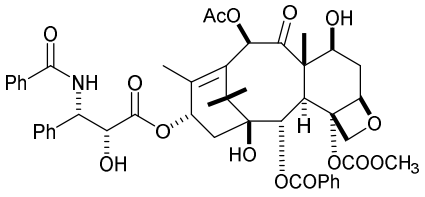

1.6

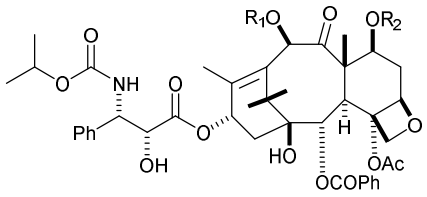

1.7 R_1 = Ac, R_2 = H
1.8 R_1 = R_2 = Me

Another important anticancer natural product is podophyllotoxin (**1.9**), which was first isolated in 1880 from an alcoholic extract of *Podophyllum* rhizome (Podophyllaceae family).[19] Podophyllotoxin (**1.9**), is the major component of podophyllin, and it was found to inhibit mitotic spindle assembly. However, its unacceptable side effects stopped its antitumor study.[19] Fortunately, after many attempts, etoposide (**1.10**) and teniposide (**1.11**) were synthesized as podophyllotoxin glycosides and entered into clinical application as effective anticancer drugs. Etoposide (**1.10**) was approved by the FDA as a drug for testicular cancer in 1983, and teniposide (**1.11**) also entered into the U.S. market in 1992.[20] Nowadays, they are widely used in the treatment of various cancers, such as small cell lung, lymphoma, leukemia, and Kaposi's sarcoma.

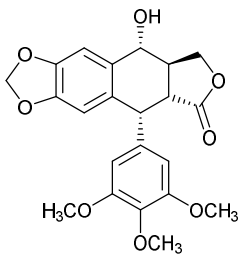

1.9

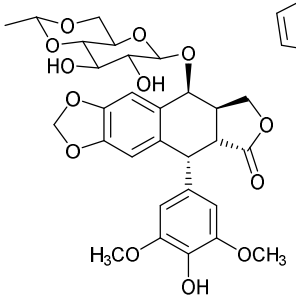

1.10

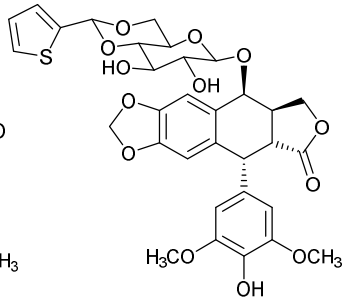

1.11

1.3 Malaria and Antimalarial Agents from Natural Products

Malaria is a mosquito-borne infectious disease caused by eukaryotic parasitic protozoans of the genus *Plasmodium*. Malaria typically causes symptoms including fever, fatigue, vomiting and headaches, and severely yellow skin, which can lead to seizures, coma or death. The disease is widespread throughout tropical and subtropical regions including much of sub-Saharan Africa, Asia, the Pacific Islands, and South America. Malaria remains one of the major infectious diseases that threaten human lives. According to the world malaria report by the World Health Organization (WHO) global malaria programme in 2014, about 219 million cases of malaria and an estimated 660,000 deaths occur from malaria every year, and it is responsible for over 430000 child deaths in Africa every year. Emerging drug- and insecticide-resistance continues to pose a major threat, and if left unaddressed, could trigger an upsurge in deaths.

In the 17th century, quinine (**1.12**) and quinidine (**1.13**) were isolated from the bark of the cinchona tree.[21] They were the first effective antimalarial medicines and were used for centuries until chloroquine (**1.14**) was discovered in the 1940s. Chloroquine is more effective for all types of malaria with fewer side effects.[22] However, resistant strains started to emerge in the 1960s. Other antimalarial agents with similar heterocyclic ring structures were discovered afterwards, including mefloquinone (**1.15**) and mepacrine (**1.16**).

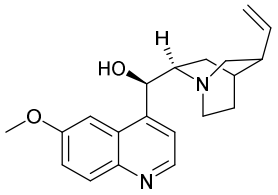

1.12

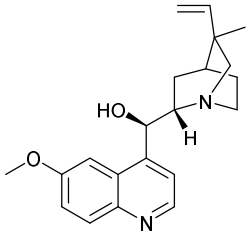

1.13

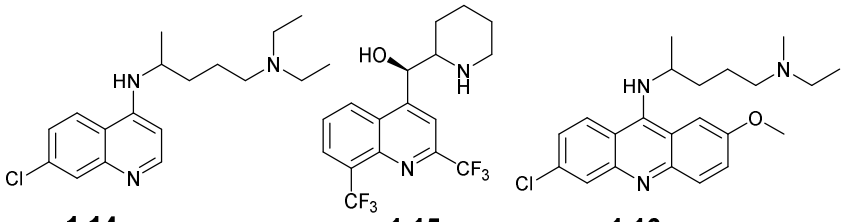

1.14 **1.15** **1.16**

The new type of antimalarial agent artemisinin (**1.17**) was isolated in 1972 from the traditional Chinese medicinal plants, *Artemesia annua* (Asteraceae), which has been used for the treatment of fever and malaria since ancient times. Unlike most of the conventional antimalarial agents, artemisinin is a sesquiterpene lactone peroxide without a heterocyclic aromatic ring. It was found to be an effective drug for antimalarial treatment without obvious side effects.[23] However, because of its low solubility in both oil and water and its rapid biotransformation, it is difficult to administer. Therefore, many semi-synthetic derivatives of artemisinin have been synthesized, including dihydroartemisinin (**1.18**), artesunate (**1.19**), artemether (**1.20**), and artemisone (**1.21**).[24] Among those derivatives, artesunate (**1.19**) is commonly used in antimalarial combination therapy (ACT) at the present time.[25] In addition, a synthetic trioxolane arterolane (OZ-277) **(1.22)**, which was modeled on the artemisinin pharmacophore, is in phase II clinical trial.[8]

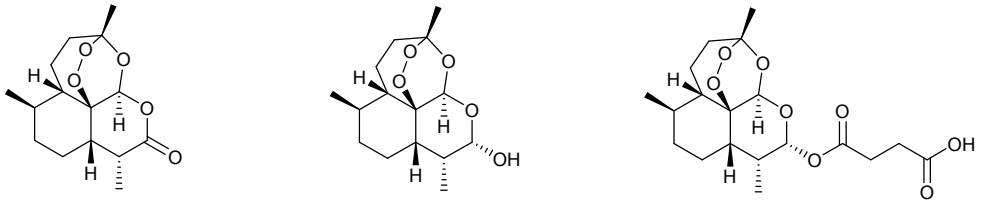

1.17 **1.18** **1.19**

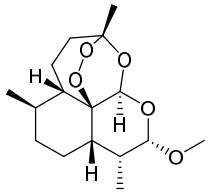

1.20

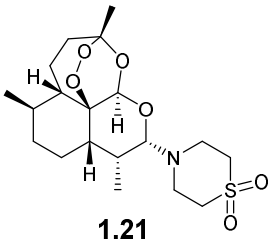

1.21

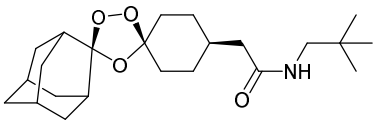

1.22

1.4 Discovery of New Natural Product Drugs

1.4.1 Bioactivity directed fractionation

Since natural products will continue to play a crucial role in the discovery and development of new lead drug candidates, considerable efforts are being and will continue to be made by many groups worldwide for the isolation of natural products. The efforts are usually based on bioassays of crude extracts first to identify those that may contain active compounds. Extracts identified as active in a particular assay are then fractionated and the fractionation procedure is followed by the guidance of bioassays. Conventionally, the fractionation procedure is mainly carried out by chromatography, including open column chromatography, HPLC, and preparative TLC, *etc.*[26] Once a pure active compound has been isolated, its molecular structure is identified by spectroscopic methods, including UV, IR, NMR, and mass spectrometry. This process requires significant amounts of source extracts, a long period of time, and also significant cost.[26] However, the most disappointing thing is that the isolated compounds may turn out to be known compounds. If the known compounds are found to have a novel bioactivity, then the results may still be valuable, but if they are known compounds with a previously known activity, then this result is of little interest. Such known compounds with replicate activities must be recognized at an early stage before carrying out efforts at purification

and structural identification to avoid duplicated compounds. The increased costs of the classical bioactivity-directed fractionation approach and the needs for high throughput bioactive novel compound discovery stimulated a dereplication approach which can differentiate natural product extracts that contain useless or known compounds from those that contain novel compounds which are of interest to us, as early as possible.

1.4.2 Dereplication approach

1.4.2.1 Dereplication

Dereplication is the process of screening samples of mixtures with desired bioactivities, so as to recognize and determine if the activity is due to a previously known substance. Dereplication ensures that the research focus is always on novel chemistry. If a compound has been isolated previously, it should be possible to use the published information to identify the compound when it appears again, avoiding the need to repeat the entire isolation and structure-determination process.

Numerous dereplication approaches have been developed based on the coupling of HPLC with different detection techniques, including LC-UV, LC-UV-DAD (diode-array detector), LC-MS, LC-MS/MS, and LC-NMR, *etc.*[26] The different LC detectors each have their own advantages and disadvantages in resolution, sensitivity, and scale requirement. In recent years, the use of capillary and cryo NMR probes and SPE-NMR is increasing, in order to increase sensitivity and accuracy. Since the dereplication process mainly starts from crude plant extracts which are complex mixtures that may contain hundreds of constituents, the combined application of LC coupled techniques such as LC-UV-MS-NMR is the most effective approach for dereplication. The combination of the

high separation efficiency of HPLC with different detectors can acquire on-line spectroscopic data for the HPLC peaks of interest, even when treating with a very complicated mixture.[27]

1.4.2.2 UV spectroscopy

UV spectroscopy was the first widely used detection method for HPLC. Sensitivity is not a problem to give good data and a diode-array detector allows a complete UV spectrum of each compound eluted to be recorded "on the fly". However, UV spectra are not compound specific, and this approach only works for the compounds that contain distinctive enough chromophore to be recognized, and a database is needed for searching. For example, it is always easy to recognize mycophenolic acid because of its distinctive chromophores. However, problems arise for compounds with less distinctive chromophores, such as peptides.[28] Diode-array UV detectors have advantages over single-wavelength detectors, because the spectra of eluted compounds can be stored in digital form and can be handled by different algorithms, especially for peptides containing aromatic amino acids such as tryptophan, tyrosine, and phenylalanine. However, there are still many compounds that cannot be detected by a UV detector.

1.4.2.3 LC-MS and LC-MS/MS

One of the major advances in recent years has been the coupling of HPLC with MS. LC-MS and LC-MS/MS are very sensitive and facile approaches and can analyze complex mixtures and provide structural information independent of source, sample preparation, or conditions of measurement. The information includes molecular mass and molecular formula, which are highly desired information for dereplication and are easy to

search in most of the commercial databases, such as AntiBase, Dictionary of Natural Products (DNP), MarinLit, and also in SciFinder Scholar or STN International (CAPlus).[26]

MS/MS is a collision induced technique and is used to fragment a precursor ion into several product ions, which are selected and subjected to MS/MS/MS analysis, and so on.[29] This process can identify the fragmentation pathway of a precursor from its first generation fragments (MS/MS) to the n^{th} generation products (MS^n). During the whole process, some neutral products released can also be identified. The molecular formula analysis includes C, H, N, O, and S, which are the basic elements for most natural products. High resolution mass separation and precise mass measurements can be used to identify the molecular formulas of small molecules or ions. Adding up the molecular formulas of small products can lead to the unique determination of the molecular formula of the precursor compounds or ions, and the resulting molecular formula of the precursors can conversely be used to confirm the molecular formula of the small products.[29]

As a successful example of the application of the LC-MS approach, Cordell and Shin[30] studied the fruit extract of *S. anacardium* L. (Anacardiaceae) and found the ion chromatograms at *m/z* 315 and 317 corresponded to the active compounds. Through comparison with the NAPRALERT database and in the DNP, the compounds 1,2-dihydroxy-3-pentadeca-7',10'-dienylbenzene and 2-dihydroxy-3-pentadec-8'-enyl-benzene were identified and were later confirmed. They also studied the root extract of *B. parviflora L.* (Begoniaceae) for its strong cytotoxicity against various human cancer cell lines. Cucurbitacin D (M = 516), hexanorcucurbitacin D (M = 402), cucurbitacin B (M =

558) and dihydrocucurbitacin B (M = 560) were also matched in the NAPRALERT database, and they were confirmed later.

The LC-MS technique enables a rapid and efficient characterization of a natural product, but its main disadvantage is that it is easy to make false identifications. This is caused by the uncertainty regarding the presence of pseudomolecular ions (MH^+, MNa^+, MK^+, MNH_4^+, MCH_4CN^+, etc.), and also by the presence of ions from minor components that ionize more readily than the major ones.[31]

1.4.2.4 LC-NMR spectroscopy

LC-NMR spectroscopy is the most powerful tool for compound identifications, and it can also be used for dereplication, based on the technique of pattern recognition. Unlike UV and MS, NMR data allows ready recognition of a wide variety of functional groups and the environment in which they exist in a compound of interest. By comparing NMR spectra, the identification of known compounds can be rapid, especially with the addition of clues given by UV and MS data. The major limitation of this approach is the high cost of the instrumentation required. In one LC-NMR approach, structural types and even unique compounds can be identified by the presence and chemical shift values of distinctive peaks, such as methyl groups, α-protons in peptides, acetal protons, and aromatic substitution patterns. This approach is a powerful one when it is coupled to a comprehensive database, such as the DNP database.

A modern LC-NMR system consists of a high resolution NMR instrument (400-800 MHz) with an LC-NMR flow probe which is connected to an HPLC system. The control unit of the HPLC is connected to the data acquisition system of the NMR spectrometer, in order to get synchronous data from the two different operating systems.

An obvious concern of the LC-NMR technique is how to recognize signals of compounds in low concentration, in the presence of large signals of HPLC solvent.[32] Most of the HPLC separations are performed by large amounts of binary or ternary solvent mixtures, as it is too expensive to use deuterated solvent for the analysis. The development of solvent suppression, as a fast and reliable technique, eliminates this major concern. By using solvent suppression techniques, even non-deuterated solvents like methanol and acetonitrile can be widely used for reverse phase HPLC analysis to obtain high quality spectra. However, water is usually replaced by D_2O, due to its relatively low price and for the purpose of giving higher quality spectra.[27]

With the development of efficient flow probe design and the use of high magnetic fields, the sensitivity and accuracy of LC-NMR techniques have been highly improved. We can also increase the sample volume, magnetic field strength, quality of the NMR coil, and lower the temperature to obtain more and more mature LC-NMR techniques for dereplication. It is a potentially complementary technique to LC-UV-MS in natural product dereplication, by providing detailed on-line structural analysis of natural products. The access to NMR data at the initial steps of the dereplication of crude extracts significantly accelerates the whole dereplication.[27]

Wolfender and Ndjoko[33] performed LC-UV-MS and LC-NMR for the isolation of compounds from the roots of *Cordia linnaei* (Boraginaceae), which was interesting for its antifungal and larvicidal properties. During the dereplication process, they identified two naphthoquinones as previously known compounds. They also investigated *Lisianthius seemannii*. The LC-MS-NMR analysis indicated the presences of a high molecular weight secoiridoid, and the main constituent was found to be lisianthioside.[33]

1.5 The Madagascar ICBG project

In 1992, three federal institutions of the United States, the National Institutes of Health (NIH), the National Science Foundation (NSF), and the U.S. Agency for International Development (AID) initiated out a program in order to help with the development of natural products drug discovery. This program was a way to promote the conservation of biological diversity and economic development through the formation of International Cooperative Biodiversity Groups (ICBG). These multi-institutional partnerships combine the resources of technologically advanced institutions in the United States with biologically diversity rich countries.[34]

In 1993, a group led by Dr. David Kingston from VPISU (Virginia Polytechnic Institute and State University) was funded by NIH to work in Suriname. The group included the Missouri Botanical Garden, Conservation International, Bristol-Myers Squibb, and Bedrijf Geneesmiddelen Voorziening Suriname. The Suriname project was successful in collecting and analyzing plant samples, and in isolating bioactive compounds. However, the project was discontinued due to the relatively limited biodiversity in Suriname, with an estimated 4000 plant species. A parallel ICBG program was initiated in Madagascar in 1998, and the project moved completely to Madagascar in 2003.

Madagascar is the world's third largest island and is the home of an estimated 13,000 plant species.[35] More than 90% of the species cannot be found anywhere else in the world. Deforestation since the last century or so has reduced the forest cover to less than 10% of the original vegetations, and much of the remaining forest has been seriously degraded.[36] From 1998 to 2003, the collection of plant samples was carried out near the

Zahamena National Park in the wet forests to the south west of the capital of Antananarivo. After 2003, the collection moved to the endangered dry forest in northern Madagascar.[34] Northern Madagascar is the center of distribution of various species within the country due to the special geology, soil types, and climate in the region. Except for the existing protected areas, the remaining forests in northern Madagascar are being significantly reduced. This is mainly caused by the rapid increase of the human population. The increasing population and natural disasters like fire and landslides are both important factors in the loss of the remaining forests.[34]

Work in Madagascar from 1998 to 2008 was focused on the collection of plant samples. Since 2008, the focus shifted to the collection of microbial and marine samples. The current program goals include several aspects.[34] First, to collect microbial and marine samples. The microbial samples are processed in Madagascar to isolate pure cultures, and these are grown and extracted to yield crude microbial extracts. Marine samples are also extracted in Madagascar, while botanical inventory continues to guide analysis of species distribution. This analysis can contribute to the determination of the priority of the areas that need protection and conservation in northern Madagascar; Furthermore, based on the results of the new conservation analysis, some guidance can be obtained for the status of the existing protected areas in northern Madagascar; Additionally, this process will promote the development of a phytochemical research community in Madagascar, including the improvement of institutional facilities and the professional level of Madagascar scientists.

This dissertation reports results from searching for novel antiproliferative and antiplasmodial agents from the extracts from Madagascar rain forests and South Africa.

The research focuses on the isolation and structure elucidation of bioactive compounds from various plant extracts. The research involves bioassay-guided fractionation and a series of analytical techniques, including 1D and 2D-NMR, LC-MS/GC-MS/MS, UV, IR, optical rotation, and electronic circular dichroism (ECD). In addition, chemical conversions were also involved for some structure determinations. The A2780 human ovarian cancer cell line was the most frequently used antiproliferative bioassay, in addition to some other anticancer cell lines. The Dd2 drug-resistant strain of *Plasmodium falciparum* was used for the antimalarial assay. The research work is discussed in detail in the following chapters.

1.6 References

1. Cragg, G. M.; Newman, D. J. Natural products: a continuing source of novel drug leads. *Biochim. Biophys. Acta.* **2013,** *1830*, 3670-3695.

2. Cragg, G. M.; Kingston, D. G. I.; Newman, D. J. Anticancer agents from natural products. CRC press. **2012**.

3. Kingston, D. G.; Newman, D. J. Mother nature's combinatorial libraries; their influence on the synthesis of drugs. *Curr. Opin. Drug Discov. Devel.* **2002,** *5*, 304-316.

4. Stewart, B. W., Wild, C. P. *World cancer report 2014*. IARC Nonserial **2014**.

5. Global cancer facts and figures. *Am. Cancer Soc. Atlanta* **2007**.

6. Habner, B. A. *The pharmacological basis of therapeutics*. 11th ed.; New York, p 1315-1403.

7. Newman, D. J.; Cragg, G. M. Natural products as sources of new drugs over the 30 years from 1981 to 2010. *J. Nat. Prod.* **2012,** *75*, 311-335.

8. Butler, M. S. Natural products to drugs: natural product-derived compounds in clinical trials. *Nat. Prod. Rep.* **2008,** *25*, 475-516.

9. Noble, R. L.; Beer, C. T.; Cutts, J. H. Role of chance observations in chemotherapy: *Vinca rosea*. *Ann. N. Y. Acad. Sci.* **1958,** *76*, 882-894.

10. Svoboda, G. H.; Johnson, I. S.; Gorman, M.; Neuss, N. Current status of research on the alkaloids of *Vinca rosea* Linn. (*Catharanthus roseus* G. Don). *J. Pharm. Sci.* **1962,** *51*, 707-720.

11. Barnett, C. J.; Cullinan, G. J.; Gerzon, K.; Hoying, R. C.; Jones, W. E.; Newlon, W. M.; Poore, G. A.; Robison, R. L.; Sweeney, M. J. Structure-activity relationships of dimeric *Catharanthus* alkaloids. 1. Deacetyl vinblastine amide (vindesine) sulfate. *J.*

Med. Chem. **1978,** *21*, 88-96.

12. Mangeney, P.; Andriamialisoa, R. Z.; Lallemand, J. Y.; Langlois, N.; Langlois, Y.; Potier, P. 5'-Nor anhydrovinblastine-prototype of a new class of vinblastine derivatives. *Tetrahedron* **1979,** *35*, 2175-2179.

13. Fahy, J.; Duflos, A.; Ribet, J.-P.; Jacquesy, J.-C.; Berrier, C.; Jouannetaud, M.-P.; Zunino, F. Vinca alkaloids in superacidic media: A method for creating a new family of antitumor derivatives. *J. Am. Chem. Soc.* **1997,** *119*, 8576-8577.

14. Wani, M. C.; Taylor, H. L.; Wall, M. E.; Coggon, P.; McPhail, A. T. Plant antitumor agents. VI. Isolation and structure of taxol, a novel antileukemic and antitumor agent from *Taxus brevifolia*. *J. Am. Chem. Soc.* **1971,** *93*, 2325-2327.

15. Schiff, P. B.; Fant, J.; Horwitz, S. B. Promotion of microtubule assembly in vitro by taxol. *Nature* **1979,** *277*, 665-667.

16. Holmes, F. A.; Walters, R. S.; Theriault, R. L.; Forman, A. D.; Newton, L. K.; Raber, M. N.; Buzdar, A. U.; Frye, D. K.; Hortobagyi, G. N. Phase II trial of taxol, an active drug in the treatment of metastatic breast cancer. *J. Natl. Cancer Inst.* **1991,** *83*, 1797-1805.

17. Bissery, M.-C.; Nohynek, G.; Sanderink, G.-J.; Lavelie, F. Docetaxel (Taxotere(R)) a review of preclinical and clinical experience. Part I: preclinical experience. *Anti-Cancer Drugs* **1995,** *6*, 339-355.

18. Galsky, M. D.; Dritselis, A.; Kirkpatrick, P.; Oh, W. K. Cabazitaxel. *Nat. Rev. Drug Discov.* **2010,** *9*, 677-678.

19. Canel, C.; Moraes, R. M.; Dayan, F. E.; Ferreira, D. Podophyllotoxin. *Phytochemistry* **2000,** *54*, 115-120.

20. Stähelin, H., von Wartburg, A. The chemical and biological route from podophyllotoxin. *J. Am. Chem. Soc.* **1962,** *84*, 1748-1749.

21. Schlitzer, M. Malaria chemotherapeutics part I: History of antimalarial drug development, currently used therapeutics, and drugs in clinical development. *Chem. Med. Chem.* **2007,** *2*, 944-986.

22. Watt, G.; Long, G. W.; Padre, L. P.; Alban, P.; Sangalang, R.; Ranoa, C. P. Chloroquine and quinine: A randomized, double-blind comparison of efficacy and side effects in the treatment of *Plasmodium falciparum* malaria in the Philippines. *Trans. R. Soc. Trop. Med. Hyg.* **1988,** *82*, 205-208.

23. Chaturvedi, D.; Goswami, A.; Pratim Saikia, P.; Barua, N. C.; Rao, P. G. Artemisinin and its derivatives: A novel class of anti-malarial and anti-cancer agents. *Chem. Soc. Rev.* **2010,** *39*, 435-454.

24. Haynes, R. K. From artemisinin to new artemisinin antimalarials: biosynthesis, extraction, old and new derivatives, stereochemistry and medicinal chemistry requirements. *Curr. Top. Med. Chem.* **2006,** *6*, 509-537.

25. Crespo-Ortiz, M. P.; Wei, M. Q. Antitumor activity of artemisinin and its derivatives: From a well-known antimalarial agent to a potential anticancer drug. *J. Biomed. Biotechnol.* **2012,** *2012*, 247597.

26. Lang, G.; Mayhudin, N. A.; Mitova, M. I.; Sun, L.; van der Sar, S.; Blunt, J. W.; Cole, A. L.; Ellis, G.; Laatsch, H.; Munro, M. H. Evolving trends in the dereplication of natural product extracts: New methodology for rapid, small-scale investigation of natural product extracts. *J. Nat. Prod.* **2008,** *71*, 1595-1599.

27. Wolfender, J. L.; Ndjoko, K.; Hostettmann, K. The potential of LC-NMR in

phytochemical analysis. *Phytochem. Anal.* **2001,** *12*, 2-22.

28. Aguilar, M. I. HPLC of peptides and proteins. In *HPLC of Peptides and Proteins*, Springer New York: 2004; Vol. 251, pp 3-8.

29. Konishi, Y.; Kiyota, T.; Draghici, C.; Gao, J.-M.; Yeboah, F.; Acoca, S.; Jarussophon, S.; Purisima, E. Molecular formula analysis by an MS/MS/MS technique to expedite dereplication of natural products. *Analyt. Chem.* **2007,** *79*, 1187-1197.

30. Cordell, G. A.; Shin, Y. G. Finding the needle in the haystack. The dereplication of natural product extracts. *Pure Appl. Chem.* **1999,** *71*, 1089-1094.

31. Lang, G.; Mayhudin, N. A.; Mitova, M. I.; Sun, L.; van der Sar, S.; Blunt, J. W.; Cole, A. L. J.; Ellis, G.; Laatsch, H.; Munro, M. H. G. Evolving trends in the dereplication of natural product extracts: new methodology for rapid, small-scale investigation of natural product extracts. *J. Nat. Prod.* **2008,** *71*, 1595-1599.

32. Spraul, M.; Hofmann, M.; Lindon, J. C.; Nicholson, J. K.; Wilson, I. D. Liquid chromatography coupled with high-field proton nuclear magnetic resonance spectroscopy: Current status and future prospects. *Anal. Proc.* **1993,** *30*, 390-392.

33. Wolfender, J. L.; Queiroz, E. F.; Hostettmann, K. Phytochemistry in the microgram domain - a LC-NMR perspective. *Magn. Reson. Chem.* **2005,** *43*, 697-709.

34. Miller, J. S.; Birkinshaw, C.; Callmander, M. The Madagascar International Cooperative Biodiversity Group (ICBG): Using natural products research to build science capacity. http://hdl.handle.net/10125/181

35. Goodman, S. M.; Benstead, J. P. Updated estimates of biotic diversity and endemism for Madagascar. *Oryx* **2005,** *39*, 73-77.

36. Myers, N.; Mittermeier, R. A.; Mittermeier, C. G.; Da Fonseca, G. A. B.; Kent, J.

Biodiversity hotspots for conservation priorities. *Nature* **2000,** *403*, 853-858.

2 Antimalarial 5,6-Dihydro-α-pyrones from *Cryptocarya rigidifolia*: Related Bicyclic Tetrahydro-α-Pyrones are Artifacts

This chapter is a slightly expanded version of a submitted article to the *Journal of Natural Products.* Attributions from co-authors of the articles are described as follows in the order of the names listed. The author of this dissertation (Yixi Liu) conducted the isolation and structural elucidation part of the titled compounds, and drafted the manuscript. Dr. Harinantenaina was a mentor for this work, provided invaluable advice and hints for the structural elucidation of the compounds, and also proofread the manuscript before submission. Mrs. Peggy Brodie performed the A2780 bioassay on the isolated fractions and compounds. Dr. Jessica D. Wiley and Dr. Maria B. Cassera performed the Dd2 bioassay. Dr. James S. Miller and Dr. F. Ratovoson from Missouri Botanical Garden collected and identified the plant. Dr. Etienne Rakotobe and Dr. Vincent E. Rasamison from Madagascar carried out the initial plant extraction. Dr. David G. I. Kingston was a mentor for this work and the corresponding author for the published article. He provided critical suggestions for this work and crucial revisions to the manuscript.

2.1 Introduction

As a part of the Madagascar International Cooperative Biodiversity Group (ICBG) program,[1] an ethanol extract of the root wood of *Cryptocarya rigidifolia* (Lauraceae) was selected for bioassay-directed fractionation because of its reproducible activity against *Plasmodium falciparum* Dd2 (IC_{50} ~5 μg/mL). The genus *Cryptocarya* is distributed throughout the tropic, subtropic, and temperate regions of the world, and its members

produce an array of secondary metabolites including flavonoids such as cryptochinones,[2] which have recently been shown to act as farnesoid X receptor agonists,[3] alkaloids,[4] and a variety of 5,6-dihydro-α-pyrones,[5-10] some of which have the ability to stabilize the tumor suppressor PDCD4.[11] Other *Cryptocarya* derived α-pyrones display antiparasitic,[12] antimycobacterial,[12] antitumor,[13] and anticancer activities.[11, 14, 15]

A combination of liquid-liquid partition, open column chromatography, solid phase extraction (SPE), HPLC, and preparative TLC afforded a series of new 5,6-dihydro-α-pyrones (**2.1**–**2.5**) and bicyclic tetrahydro-α-pyrone derivatives (**2.6**–**2.11**) from the root wood of *C. rigidifolia*.(Figure 2.1) As explained below, compounds **2.6**–**2.11** were shown to be produced by cyclization of 5,6-dihydro-α-pyrones during the isolation process. 5,6-Dihydro-α-pyrones have been isolated from several members of the genus *Cryptocarya*, while the bicyclic pyrones have only been isolated from *C. latifolia*,[7] *C. myrtifolia*,[6] *Polyalthia parviflora*, and the Chinese medicinal ants, *Polyrhacis lamellidens*.[16] All of the reported isolation and purification procedures that yielded the bicyclic pyrones involved chromatography on silica gel at some stage, and our studies suggest that these bicyclic pyrones may also be artifacts.[6, 7, 16, 17]

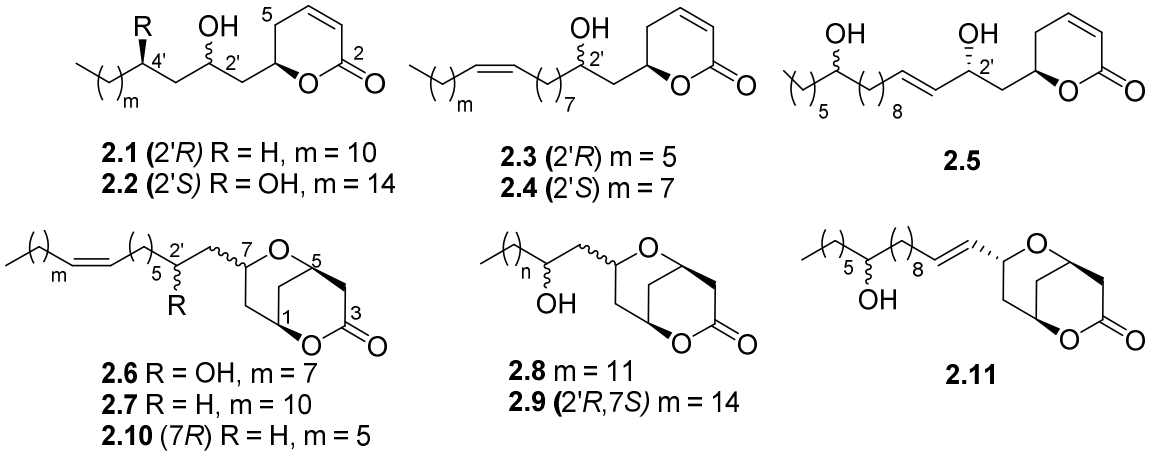

Figure 2.1 Structures of Compounds **2.1**–**2.11**

2.2 Results and Discussion

2.2.1 Isolation of active compounds

The EtOAc-soluble fraction obtained from a liquid-liquid partition of the ethanol extract (100 mg) showed antiplasmodial activity. Dereplication as previously described[18] indicated that the extract contained at least one new bioactive compound, and so a larger sample was investigated. Fractionation of the EtOAc-soluble fraction of this sample by chromatography on Sephadex LH-20, reverse phase SPE, normal phase silica gel column chromatography, and C18 HPLC yielded compounds **2.1** and **2.6** – **2.8**, together with fractions that were mixtures of 5,6-dihydro-α-pyrones and bicyclic tetrahydro-α-pyrones. Purification of these fractions was effected by diol PTLC or HPLC to yield compounds **2.2**, **2.3**, **2.5**, and **2.9**–**2.11**. Similar fractionation of the antiplasmodial hexanes fraction yielded compounds **2.4** and **2.7**. (Scheme 2.1)

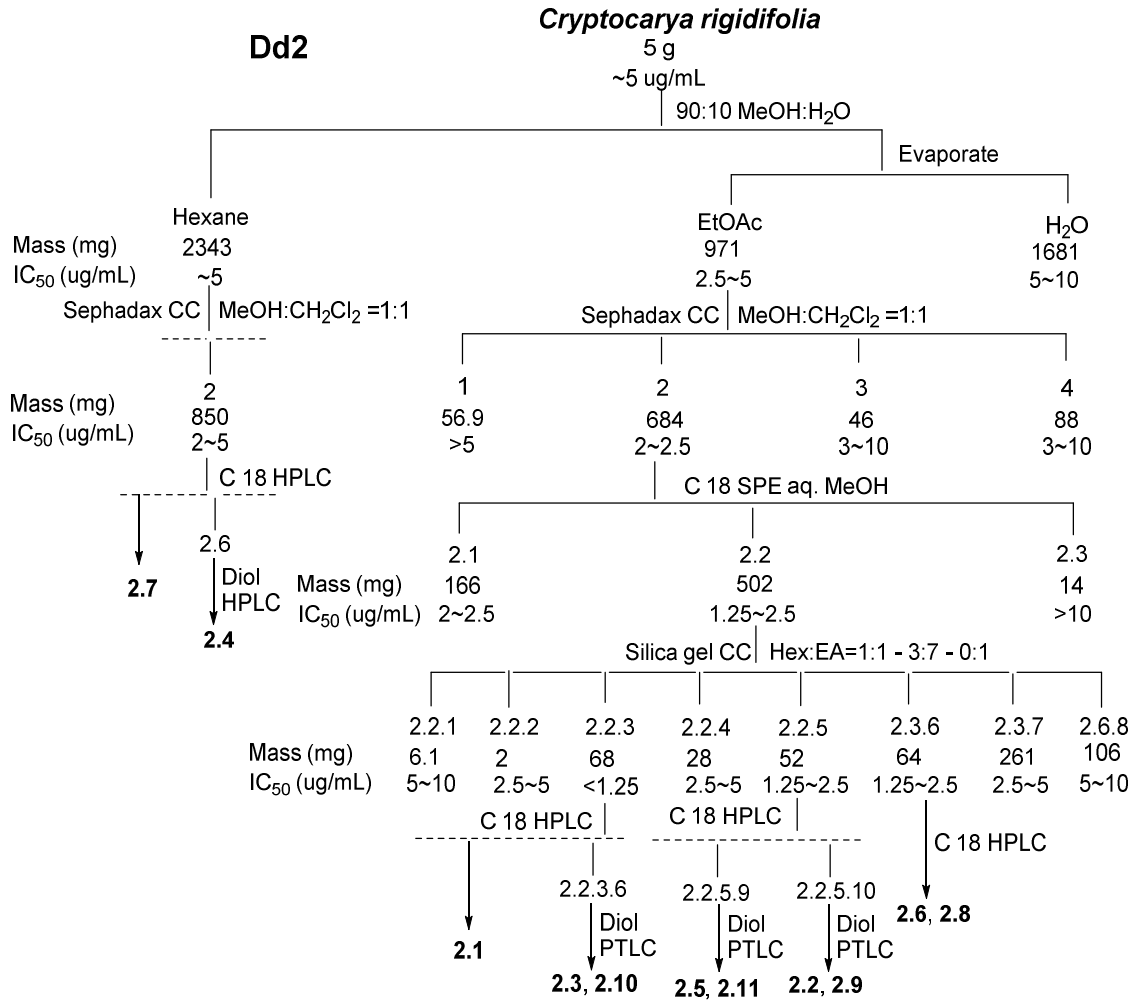

Scheme 2.1 Bioassay-guided Separation of *Cryptocarya rigidifolia*

2.2.2 Structure elucidation of compound **2.1**

Compound **2.1** was isolated as a clear oil, and its molecular formula was established as $C_{20}H_{36}O_3$ by HRESIMS (*m/z* 325.2753 $[M+H]^+$). Its IR spectrum showed absorptions at 3340, and 1719 and 1613 cm^{-1} assigned to a hydroxyl group and an α,β-unsaturated δ-lactone, respectively. Its ^1H NMR spectroscopic data had signals for a conjugated olefin at δ_H 6.90 (m, 1H, H-4) and δ_H 6.03 (dt, J = 9.8, 1.7 Hz, 1H, H-3), two oxymethine groups at δ_H 4.75 (m, 1H, H-6) and δ_H 4.00 (brs, 1H, H-2'), a terminal primary methyl group (δ_H 0.88, t, J = 7.0 Hz, 3H, CH_3-15') in the upfield region, and a

multiplet at δ_H 2.36 (2H, H-5), representing a deshielded methylene group. In the HMBC spectrum the methylene protons at δ_H 2.36 (H-5) showed correlations both to an olefin group (δ_C 121.3, C-3 and δ_C 145.0, C-4) and to the oxymethine resonance at δ_H 4.75 and δ_C 74.8 (C-6). In addition, both the olefinic protons (δ_H 6.90, H-4 and δ_H 6.03, H-3) and the oxymethine at δ_H 4.75 (H-6) correlated with a carbonyl carbon at δ_C 164.6 (C-2) (Figure 1). These data indicated a 6-substituted-5,6-dihydro-α-pyrone, a common ring system of secondary metabolites found in *Cryptocarya* species.[19] The remaining oxymethine group at δ_H 4.00 (1H, H-2') was assigned to C-2', which was flanked by two methylenes (C-1' and C-3') as indicated by HMBC correlations (Figure 2.2) from the methylene protons at δ_H 1.92 (ddd, J = 14.5, 9.6, 2.2 Hz, H-1') and δ_H 1.65 (m, H-1') to δ_C 30.1 (C-5); from δ_H 4.00 (H-2') to the oxymethine carbon at δ_C 74.8 (C-6); and from H-2' to the two neighboring methylene carbons at δ_C 41.2 (C-1') and δ_C 38.2 (C-3'). The absolute configuration at C-6 was determined to be *R* by the positive Cotton effects at 256 nm observed in its ECD spectrum in MeOH, arising from the n→π* transitions of the lactone ring.[13, 20-22] The ^{1}H NMR spectra of the (*R*) and (*S*) Mosher ester derivatives of **2.1**[23] revealed slight differences in the ^{1}H chemical shifts of C-6 and adjacent protons that allowed the assignment of the *R* configuration to C-2' of **2.1** (Figure 2.3). The complete assignment of all protons and carbons of **2.1** (Table 2.1) was accomplished by further interpretation of its HMBC and HSQC spectra. Compound **2.1** was thus assigned as 6*R*-(2'*R*-hydroxypentadecyl)-5,6-dihydro-*2H*-pyran-2-one, and named cryptorigidifoliol A.[21, 22]

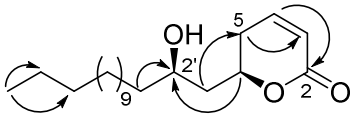

Figure 2.2 Key HMBC Correlations of **2.1**

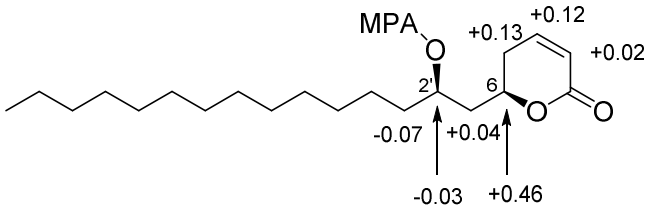

Figure 2.3 $\Delta\delta(H) = \delta_S - \delta_R$ Data of *R* and *S*-MPA Derivatives of Compound **2.1**

2.2.1 Structure elucidation of compound **2.2**

Compound **2.2** was obtained as an oil with the molecular formula $C_{24}H_{44}O_4$ based on its HRESIMS spectrum (*m/z* 397.3317 $[M+H]^+$). The UV, IR and ^1H NMR spectroscopic data of **2.2** were comparable to those of **2.1**, suggesting that **2.2** is also a 6-substituted-5,6-dihydro-α-pyrone. The major difference between the ^1H NMR spectroscopic data of **2.1** and **2.2** was the presence of an additional signal for an oxymethine proton at δ_H 3.89 (m, 1H, H-4') in **2.2**. The HMBC correlation between the oxymethine proton and the carbon signal at δ_C 69.8 (C-2') assigned the additional hydroxyl group to C-4', and this assignment is supported by the HMBC cross peaks between the two adjacent methylene protons (δ_H 1.61, m, 2H, H-3'; δ_H 1.47, m, 2H, H-5') and the oxymethine carbon at δ_C 74.0. Similarly to **2.1**, the complete assignments of all protons and carbons of **2.2** (Table 2.1) were accomplished by interpretation of its HMBC and HSQC spectra. ECD and the Mosher ester method were used to assign the configurations of C-6, C-2', and C-4' as *R*, *S*, *R*, respectively. (Figure 2.4) Compound **2.2** awas thus assigned as 6*R*-(2'*S*,4'*R*-dihydroxynonadecyl)-5,6-dihydro-*2H*-pyran-2-

Table 2.1 ^{1}H and ^{13}C NMR Spectroscopic Data for Compounds **2.1**– **2.5**.

one and has been named cryptorigidifoliol B.

	2.1 [a]		**2.2** [a]		**2.3** [a]		**2.4** [a]		**2.5** [a]
posn	δ_H [b]	δ_c [c]	δ_H [b]	δ_c [c]	δ_H [b]	δ_c [c]	δ_H [b]	δ_c [c]	δ_H [b]	δ_c [c]
2		164.6 (C)		163.5 (C)		164.2 (CH_2)		164.2 (CH_2)		163.5 (C)
3	6.03 dt (9.8, 1.7)	121.3 (CH)	6.03 dt (9.8, 1.7)	121.3 (CH)	6.03 dt (9.8, 1.7)	121.3 (CH)	6.04 dt (9.8, 1.7)	121.3 (CH)	6.03 brd (9.8)	121.3 (CH)
4	6.90 m	145.0 (CH)	6.90 m	145.0 (CH)	6.90 m	145.0 (CH)	6.90 m	145.0 (CH)	6.90 m	145.0 (CH)
5	2.36 m	30.1 (CH_2)	2.44 m	29.2 (CH_2)	2.36 m	30.3 (CH_2)	2.42 m	30.2 (CH_2)	2.44 m	29.2 (CH_2)
6	4.75 m	74.8 (CH)	4.69 m	76.4 (CH)	4.75 m	74.7 (CH)	4.66 m	74.8 (CH)	4.69 m	72.5 (CH)
1'	1.92 ddd (14.5, 9.6, 2.2)	41.2 (CH_2)	2.04 m	39.6 (CH_2)	1.92 ddd (14.5, 9.6, 2.2)	42.3 (CH_2)	1.96 ddd (14.5, 9.6, 2.2)	42.1 (CH_2)	1.79 m	43.8 (CH_2)
	1.65 m		1.79 ddd (14.3, 5.6, 3.9)		1.64 ddd (14.5, 10.2, 2.9)		1.81 ddd (14.5, 10.2, 2.9)		1.73 m	
2'	4.00 brs	67.3 (CH)	4.15 m	69.8 (CH)	4.00 m	67.1 (CH)	3.86 m	67.4 (CH)	4.63 m	63.3 (CH)
3'	1.49-1.41 m	38.2 (CH_2)	1.66-1.53 m	42.9 (CH_2)	1.45 m	38.2 (CH_2)	1.50 m	38.5 (CH_2)	5.49 dd (15.3, 7.0)	131.4 (CH)
4'	1.49-1.41 m	25.7 (CH_2)	3.89 m	74.0 (CH)	1.37-1.31 m	25.0 (CH_2)	1.38-1.27 m	25.3 (CH_2)	5.68 m	132.6 (CH)
5'	1.35-1.22 m	29.6 (CH_2)	1.66-1.53 m	38.2 (CH_2)	1.35-1.22 m	29.6 (CH_2)	1.28-1.21 m	29.6 (CH_2)	2.03 m	32.9 (CH_2)
6'	1.35-1.22 m	29.6 (CH_2)	1.47 m	25.4 (CH_2)	1.35-1.22 m	29.6 (CH_2)	1.28-1.21 m	29.6 (CH_2)	1.49-1.61 m	28.0 (CH_2)
7'	1.35-1.22 m	29.6 (CH_2)	1.35-1.22 m	29.6 (CH_2)	1.35-1.22 m	29.6 (CH_2)	1.28-1.21 m	29.6 (CH_2)	1.33-1.22 m	29.6 (CH_2)
8'	1.35-1.22 m	29.6 (CH_2)	1.35-1.22 m	29.6 (CH_2)	1.37-1.31 m	27.0 (CH_2)	1.38-1.27 m	27.0 (CH_2)	1.33-1.22 m	29.6 (CH_2)
9'	1.35-1.22 m	29.6 (CH_2)	1.35-1.22 m	29.6 (CH_2)	2.05-1.99 m	29.4 (CH_2)	2.00 m	29.6 (CH_2)	1.33-1.22 m	29.6 (CH_2)
10'	1.35-1.22 m	29.6 (CH_2)	1.35-1.22 m	29.6 (CH_2)	5.34 m	130.0 (CH)	5.35 m	131.2 (CH)	1.33-1.22 m	29.6 (CH_2)
11'	1.35-1.22 m	29.6 (CH_2)	1.35-1.22 m	29.6 (CH_2)	5.34 m	130.0 (CH)	5.35 m	131.2 (CH)	1.42-1.32 m	29.6 (CH_2)
12'	1.35-1.22 m	29.6 (CH_2)	1.35-1.22 m	29.6 (CH_2)	2.05-1.99 m	29.4 (CH_2)	2.00 m	29.6 (CH_2)	1.49-1.61 m	42.1 (CH_2)
13'	1.35-1.22 m	32.0 (CH_2)	1.35-1.22 m	29.6 (CH_2)	1.37-1.31 m	27.0 (CH_2)	1.38-1.27 m	27.0 (CH_2)	4.15 m	64.4 (CH_2)
14'	1.35-1.22 m	22.8 (CH_2)	1.35-1.22 m	29.6 (CH_2)	1.35-1.22 m	29.6 (CH2)	1.28-1.21 m	29.6 (CH2)	1.49-1.61 m	42.1 (CH_2)
15'	0.88 t (7.0)	14.2 (CH_3)	1.35-1.22 m	29.6 (CH_2)	1.35-1.22 m	32.0 (CH_2)	1.28-1.21 m	29.6 (CH_2)	1.42-1.32 m	29.6 (CH_2)
16'			1.35-1.22 m	29.6 (CH_2)	1.35-1.22 m	22.8 (CH_2)	1.28-1.21 m	29.6 (CH_2)	1.33-1.22 m	29.6 (CH_2)
17'			1.35-1.22 m	32.0 (CH_2)	0.88 t (7.0)	14.2 (CH_3)	1.28-1.21 m	32.0 (CH_2)	1.33-1.22 m	32.0 (CH_2)
18'			1.35-1.22 m	22.8 (CH_2)			1.28-1.21 m	22.8 (CH_2)	1.33-1.22 m	22.8 (CH_2)
19'			0.88 t (7.0)	14.2 (CH_3)			0.88 t (7.0)	14.2 (CH_3)	0.88 t (7.0)	14.2 (CH_3)

[a] Spectra obtained in $CDCl_3$; assignments based on analysis of 2D NMR spectra.
[b] Data (δ) measured at 500 MHz; brs = broad singlet, brd = broad doublet, t = triplet, ddd = doublet of doublets of doublets, dt = doublet of triplets, m = multiplet. *J* values are in Hz and are omitted if the signals overlapped as multiplets. The overlapped signals were assigned from HSQC and HMBC spectra without designating multiplicity.
[c] Data (δ) measured at 125 MHz; CH_3, CH_2, CH, and C multiplicities were determined by an HSQC experiment.

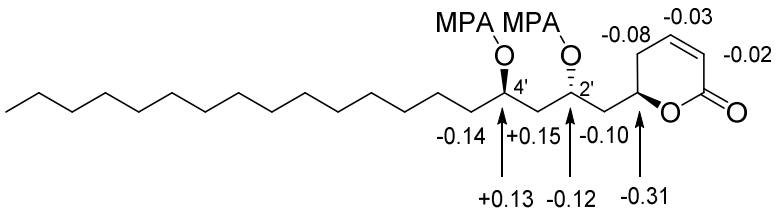

Figure 2.4 $\Delta\delta(H) = \delta_S - \delta_R$ Data of *R* and *S*-MPA Derivatives of Compound **2.2**

2.2.2 Structure elucidation of compound **2.3**

The molecular formula of compound **2.3** ($C_{22}H_{38}O_3$; HRESIMS *m/z* 351.2902 $[M+H]^+$) and its ^1H NMR spectrum (δ_H 5.34, m, 2H, H-10' and H-11') indicated that it had an additional disubstituted olefin moiety as compared with compound **2.1**. Its UV, IR and ^1H NMR spectroscopic data indicated the presence of the same α-pyrone ring as **2.1** and **2.2**, and HMBC correlations from δ_H 5.34 (H-10' and H-11') to δ_C 27.0 indicated that the additional olefin group must be located between two methylene groups. Long range correlation from both δ_H 2.05 - 1.99 (m, 4H, H-9' and H-12') and δ_H 1.37 - 1.31 (m, 4H, H-8' and 13') to the carbons at δ_C 130 (C-10' and 11') in the HMBC spectrum assigned the olefin group to C-10' and 11'. The geometry of the double bond was assigned as *Z* based on the upfield ^{13}C chemical shift of the methylenes connected to the double bond (δ_C 29.4).[13, 24] The position of the double bond within the alkyl chain was determined unambiguously by analysis of the GC-EIMS fragmentation of the dimethyldisulfide (DMDS) derivative of **2.3**,[25, 26] which showed a major ion at *m/z* 299 attributable to fragmentation between the two CH_3S groups located at the original site of unsaturation. Fragment ions at *m/z* 281 and 145 were also observed to support the assigned structure (Figure 2.5). The relative stereochemistry of **3** and the assignment of its ^1H and ^{13}C NMR were determined by the same methods as for **2.1** and **2.2**.(Table 2.1) Compound **2.3** was

assigned as 6*R*-(2'*R*-hydroxy-10'*Z*-heptadecenyl)-5,6-dihydro-*2H*-pyran-2-one,[23,26] and is named cryptorigidifoliol C.

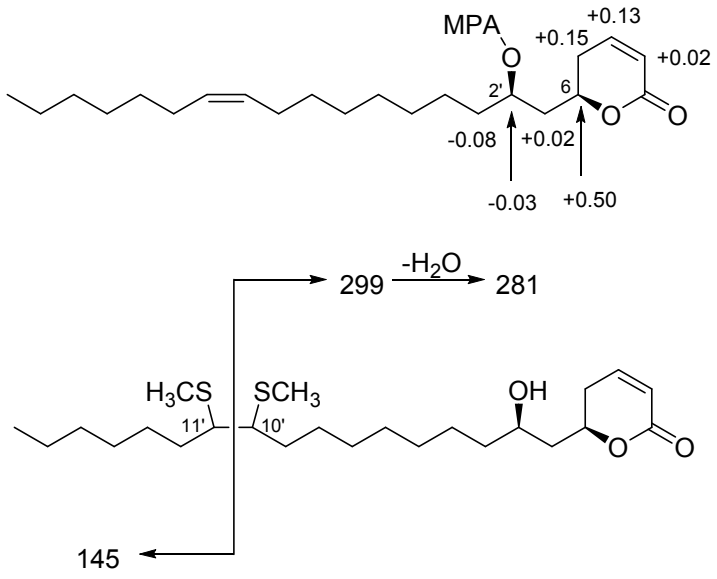

Figure 2.5 $\Delta\delta(H) = \delta_S - \delta_R$ Data of *R* and *S*-MPA Derivative and EI-MS Fragmentations of the DMDS Adduct of Compound **2.3**

2.2.3 Structure elucidation of compound **2.4**

The molecular formula of **2.4** ($C_{24}H_{42}O_3$, HRESIMS *m/z*: 396.3489 $[M+NH_4]^+$) differed from the molecular formula of **2.3** ($C_{22}H_{38}O_3$) only by a C_2H_4 unit. Inspection of the ^{1}H NMR spectra of **2.3** and **2.4** demonstrated that **2.4** possessed a very similar structure with **2.3**, but with two additional carbons in the alkenyl chain. The intense fragment ions at *m/z* 299 and 173, and the additional ion peak at *m/z* 281 in the EIMS spectrum of the DMDS adduct of **2.5** indicated that the position of the double bond was between C-10' and C-11' (Figure 2.6). The complete NMR data and stereochemistry of all chiral centers in **2.4** were assigned by the same methods as for **2.1**–**2.3**. (Table 2.1) Compound **2.4** was assigned as 6*R*-(2'*S*-hydroxy-10'*Z*-nonadecenyl)-5,6-dihydro-*2H*-pyran-2-one[21, 22] and is named cryptorigidifoliol D.

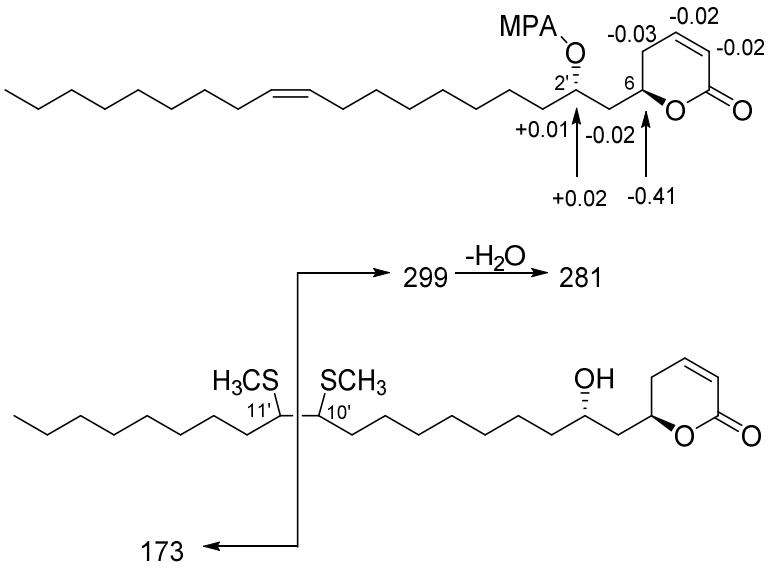

Figure 2.6 $\Delta\delta(H) = \delta_S - \delta_R$ Data of *R* and *S*-MPA Derivative and EI-MS Fragmentations of the DMDS Adduct of Compound **2.4**

2.2.4 Structure elucidation of compound **2.5**

The ^{1}H NMR spectrum of compound **2.5** ($C_{24}H_{42}O_4$, HRESIMS *m/z*: 377.3060 [M-OH]$^+$) showed the presence of two oxymethine groups (δ_H 4.63, m, 1H, H-2'; δ_H 4.15, m, 1H, H-12') and a double bond (δ_H 5.68, m, 1H, H-4'; δ_H 5.49, dd, *J* = 15.3, 7.0, 1H, H-3') on the alkyl chain, besides the α-pyrone ring signals at δ_H 6.9, 6.03, 4.69, and 2.44. The large coupling constant (15.3 Hz) observed for H-3' indicated the *E* geometry of the double bond. In the HMBC spectrum, correlations were observed between the protons at δ_H 1.79 and 1.73 (each m, 1H, H-1') and δ_C 131.4 (C-3'), and between the proton at δ_H 4.63 (m, 1H, H-2') and δ_C 132.6 (C-4'). These observations suggested the connection of the olefin group with the oxymethine at C-2'. The ESIMS of **2.5** showed significant ions at *m/z* 265 and 247, together with a less intense ion at *m/z* 111, consistent with assignment of the second hydroxyl group to C-12' (Figure 2.7). The configurations at C-6 and C-2' were assigned to be *R* and *S*, respectively by interpretation of the ECD

spectroscopic data and by the Mosher method. An attempt was made to determine the configuration at C-12' by using the Mosher method, but it did not lead to any firm conclusion, since we could not distinguish the chemical shifts of the protons of the two methylene groups attached to C-12'. Compound **2.5** was assigned as 6*R*-(2'*R*,12'-dihydroxy-3'*E*-nonadecenyl)-5,6-dihydro-*2H*-pyran-2-one, and named cryptorigidifoliol E.

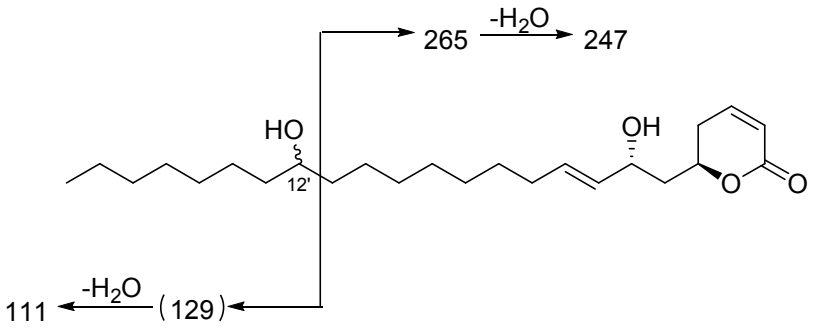

Figure 2.7 ESI-MS Fragmentations of Compound **2.5**

2.2.5 Structure elucidation of compound **2.6**

Compound **2.6** had the molecular formula of $C_{24}H_{42}O_4$ based on its HRESIMS (*m/z* 395.3149 $[M+H]^+$). Its IR spectrum showed the absorptions characteristic of a δ-lactone ring (1719 and 1073 cm^{-1}). Its ^1H NMR spectrum lacked the signals for the vinyl protons of an α,β-unsaturated lactone, and the IR absorption at 1615 cm^{-1} found in compounds **2.1**–**2.5** was absent. A new methylene signal was observed at δ_H 2.89 (brd, J = 19.3 Hz, 1H, H-4a) and 2.78 (dd, J = 19.3, 4.5 Hz, 1H, H-4b), which showed HMBC correlations with a carbonyl carbon at δ_C 169.7 (C-3) (Figure 2.8). A signal for a vinyl proton was observed in the ^1H NMR spectrum at δ_H 5.33 (m, 2H, H-8' and H-9'), and the four degrees of unsaturation of **2.6** thus required a second ring in addition to the lactone and the double bond. The ^1H NMR spectrum showed the presence of four oxymethine protons

[δ_H 4.89 (m, 1H, H-1), δ_H 4.36 (t, J = 4.5 Hz, 1H, H-5), δ_H 4.10 (m, 1H, H-7), and δ_H 3.81 (m, 1H, H-2')] directly attached to δ_C 73.1 (C-1), δ_C 66.0 (C-5), δ_C 63.6 (C-6), and δ_C 68.3 (C-2') respectively, which assignments were confirmed by HSQC. In the HMBC spectrum, cross-peaks were observed from the two oxymethine protons at δ_H 4.89 (H-1) and δ_H 4.36 (H-5) to the carbonyl carbon at δ_C 169.7 (C-3) and the oxymethine at C-7 (δ_C 63.6), and correlations between the two oxymethine protons H-1 and H-5 and carbons at C-5 (δ_C 66.0) and C-1 (δ_C 73.1), respectively; and a long-range correlation between the oxymethine proton at δ_H 4.10 (H-7) and the carbon at δ_C 68.3 (C-2') bearing the oxymethine at δ_H 3.81 (m, 1H, H-2') (Figure 2) allowed us to assign the bicyclic ring system, the alkyl chain substituted at C-7, and a hydroxyl group at C-2' of **2.6**

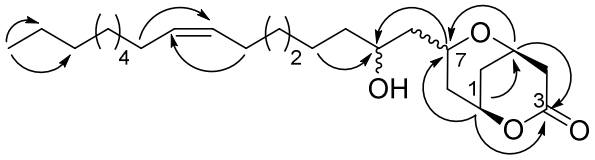

Figure 2.8 Key HMBC Correlations of **2.6**

The long range cross peaks observed between δ_H 5.33 (m, 2H, H-8', H-9') and δ_C 29.6 in the HMBC spectrum indicated that the allylic methylene groups resonated at δ_C 29.6 (C-7' and C-10'), and indicated the *Z* geometry of the sole double bond in the alkyl chain. The position of this double bond was assigned to C-8'/9' based on the EIMS fragmentation of the DMDS adduct, which had an intense peak at *m/z* 173 and a peak at *m/z* 297 corresponding to loss of water from the lactone-containing fragment ion (Figure 2.9).

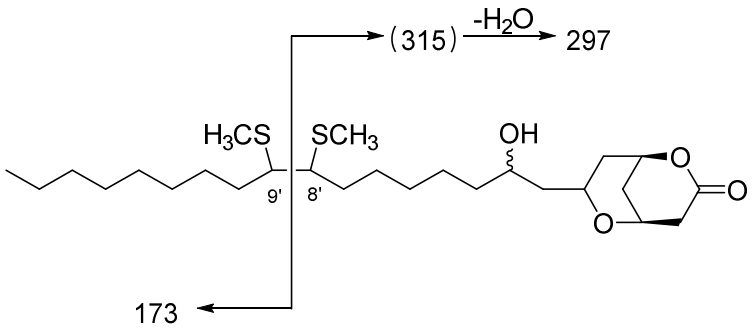

Figure 2.9 EI-MS Fragmentations of the DMDS Adduct of Compound **2.6**

An attempt to assign the stereochemistry at C-2' of **2.6** by the Mosher ester method was not successful, since there was no significant Δδ (H) difference between its *R*- and *S*-MPA derivatives. Since the bicyclic tetrahydro-α-pyrones in this work such as **2.6** are formed from the corresponding 5,6-dihydro-α-pyrones, as explained below, and all of these 5,6-dihydro-α-pyrones have the *R* configuration at C-6, it is proposed that the configuration of **6** at C-1 (corresponding to C-6 in the putative monocyclic precursor) must be the same. Because of a change in group priorities this makes this configuration *S.* The configuration at C-5 can also be assigned as *R* to give a *cis* fused ring, because the *S* configuration would give a much more strained *trans* fused molecule, and the conversion takes place readily at room temperature. The same *cis* fused configuration was demonstrated for some related bicyclic tetrahydro-α-pyrones by x-ray crystallography.[17, 27] The configuration of **2.6** at C-7 could not be assigned, because its 5,6-dihydro-α-pyrone precursor was not isolated. The complete NMR assignments of **6** (Table 2.2) were determined by further interpretation of its HMBC and HSQC spectra. Compound **2.6** was assigned as (1*R*,5*R*)-7-(2'-hydroxy-8'*Z*-heptadecenyl)-2,6-dioxabicyclo[3.3.1]nonan-3-one and has been named cryptorigidifoliol F.

Table 2.2 ^{1}H and ^{13}C NMR Spectroscopic Data for Compounds **2.6**– **2.8**, and ^{1}H NMR Spectroscopic Data for Compounds **2.9**–**2.11**

	2.6 [a]		**2.7** [a]	**2.8**		**2.9**	**2.10** [a]		**2.11** [a]
posn	δ_H [b]	δ_c [c]	δ_H [b]	δ_c [c]	δ_H [b]	δ_c [c]	δ_H [b]	δ_H [b]	δ_H [b]
1	4.89 m	73.1 (CH)	4.89 m	73.1 (CH)	4.89 m	73.1 ((CH)	4.89 m	4.90 m	4.89 m
3		169.7 (C)		169.7 (C)		169.7 (C)			
4	2.89 brd (19.3) 2.78 dd (19.3, 4.5)	36.4 (CH_2)	2.89 brd (19.3) 2.78 dd (19.3, 4.5)	36.4 (CH_2)	2.89 brd (19.3) 2.78 dd (19.3, 4.5)	36.4 (CH_2)	2.91 brd (19.3) 2.81 dd (19.3, 5.3)	2.85 brd (19.3) 2.78 dd (19.3, 4.5)	2.87 brd (19.3) 2.79 dd (19.3, 5.2)
5	4.36 t (4.5)	66.0 (CH)	4.35 brs	66.0 (CH)	4.36 t (4.5)	66.0 (CH)	4.41 brs	4.34 brs	4.40 brs
6	1.41 m	29.4 (CH_2)	1.51 m	29.4 (CH_2)	1.41 m	29.4 (CH_2)	1.38 m	1.51 m	1.30 m
7	4.10 m	63.6 (CH)	3.73 brs	73.6 (CH)	4.12 m	63.6 (CH)	4.02 m	3.73 brs	4.27 m
8	1.92 m	37.8 (CH_2)	1.95 m	37.6 (CH_2)	1.98 m	37.8 (CH_2)	2.04 m	1.96 m	1.94 m
1'	1.58 ddd (14.5, 8.7, 3.4) 1.62 m	42.2 (CH_2)	1.57 m	35.6 (CH_2)	1.63 m	42.2 (CH_2)	1.64 m	1.57 m	1.78 m 5.41 ddt (15.3, 7.0, 1.4)
2'	3.81 m	68.3 (CH)	1.35-1.22 m	29.6 (CH_2)	3.81 m	68.3 (CH)	3.79 m	1.35-1.22 m	5.67 m
3'	1.67 m	36.8 (CH_2)	1.35-1.22 m	29.6 (CH_2)	1.67 m	36.8 (CH_2)	1.64 m	1.35-1.22 m	2.03 m
4'	1.35-1.22 m	25.8 (CH_2)	1.35-1.22 m	29.6 (CH_2)	1.35-1.22 m	25.8 (CH_2)	1.35-1.22 m	1.35-1.22 m	1.36 m
5'	1.35-1.22 m	29.6 (CH_2)	1.35-1.22 m	29.6 (CH_2)	1.35-1.22 m	29.6 (CH_2)	1.35-1.22 m	1.35-1.22 m	1.29-1.19 m
6'	1.38-1.28 m	27.3 (CH_2)	1.46-1.38 m	27.3 (CH_2)	1.35-1.22 m	29.6 (CH_2)	1.35-1.22 m	1.45-1.38 m	1.29-1.19 m
7'	2.03-1.98 m	29.6 (CH_2)	2.07-1.97 m	29.6 (CH_2)	1.35-1.22 m	29.6 (CH_2)	1.35-1.22 m	2.08-1.97 m	1.29-1.19 m
8'	5.33 m	130.2 (CH)	5.34 m	130.2 (CH)	1.35-1.22 m	29.6 (CH_2)	1.35-1.22 m	5.36 m	1.29-1.19 m
9'	5.33 m	130.2 (CH)	5.34 m	130.2 (CH)	1.35-1.22 m	29.6 (CH_2)	1.35-1.22 m	5.36 m	1.29-1.19 m
10'	2.03-1.98 m	29.6 (CH_2)	2.07-1.97 m	29.6 (CH_2)	1.35-1.22 m	29.6 (CH_2)	1.35-1.22 m	2.07-1.98 m	1.63 m
11'	1.38-1.28 m	27.3 (CH_2)	1.46-1.38 m	27.3 (CH_2)	1.35-1.22 m	29.6 (CH_2)	1.35-1.22 m	1.46-1.38 m	3.89 m
12'	1.35-1.22 m	29.6 (CH_2)	1.35-1.22 m	29.6 (CH_2)	1.35-1.22 m	32.0 (CH_2)	1.35-1.22 m	1.35-1.22 m	1.63 m
13'	1.35-1.22 m	29.6 (CH_2)	1.35-1.22 m	29.6 (CH_2)	1.35-1.22 m	22.8 (CH_2)	1.35-1.22 m	1.35-1.22 m	1.29-1.19 m
14'	1.35-1.22 m	29.6 (CH_2)	1.35-1.22 m	29.6 (CH_2)	0.88 t (7.0)	14.2 (CH_3)	1.35-1.22 m	1.35-1.22 m	1.29-1.19 m
15'	1.35-1.22 m	32.0 (CH_2)	1.35-1.22 m	29.6 (CH_2)			1.35-1.22 m	0.88 t (7.0)	1.29-1.19 m
16'	1.35-1.22 m	22.8 (CH_2)	1.35-1.22 m	29.6 (CH_2)			1.35-1.22 m		1.29-1.19 m
17'	0.88 t (7.0)	14.2 (CH_3)	1.35-1.22 m	29.6 (CH_2)			0.88 t (7.0)		0.88 t (7.0)
18'			1.35-1.22 m	32.0 (CH_2)					
19'	1.35-1.22 m	22.8 (CH_2)							
20'	0.88 t (7.0)	14.2 (CH_3)							

[a] Spectra obtained in $CDCl_3$; assignments based on analysis of 2D NMR spectra.
[b] Data (δ) measured at 500 MHz; s = singlet, br d = broad doublet, dd = doublet of doublets, ddd = doublet of doublets of doublets, m = multiplet. *J* values are in Hz and are omitted if the signals overlapped as multiplets. The overlapped signals were assigned from HSQC and HMBC spectra without designating multiplicity.
[c] Data (δ) measured at 125 MHz; CH_3, CH_2, CH, and C multiplicities were determined by an HSQC experiment.

2.2.6 Structure elucidation of compound **2.7** and **2.8**

Compounds **2.7** (*m/z* 421.3662 $[M+H]^+$) and **2.8** (*m/z* 355.2831 $[M+H]^+$) also contained a bicyclic tetrahydro-α-pyrone ring. Comparison of their molecular weights and ^1H NMR spectra with those of cryptorigidifoliol F (**2.6**) revealed that the only structural differences were in the alkyl chain length and the absence or presence of a double bond or hydroxyl group on the alkyl chain. Cryptorigidifoliol G (**2.7**), with a molecular formula of $C_{27}H_{48}O_3$, was a similar bicyclic tetrahydro-α-pyrone to **2.6** but lacked the C-2' hydroxy group and had a 20 carbon alkenyl chain at C-7. Preparation of its DMDS derivative allowed us to assign the double bond to be at C-8' (*m/z* at 299 and 215) (Figure 2.10). Its configuration at C-7 could not be determined because its presumed monocyclic precursor was not isolated. Cryptorigidifoliol H (**2.8**), as also a similar bicyclic tetrahydro-α-pyrone to **2.6** but with a saturated alkyl chain at C-7; the chain length was determined to be 14 based on its molecular formula of $C_{21}H_{38}O_4$. As in the case of **2.7**, its configuration at C-7 could not be determined.

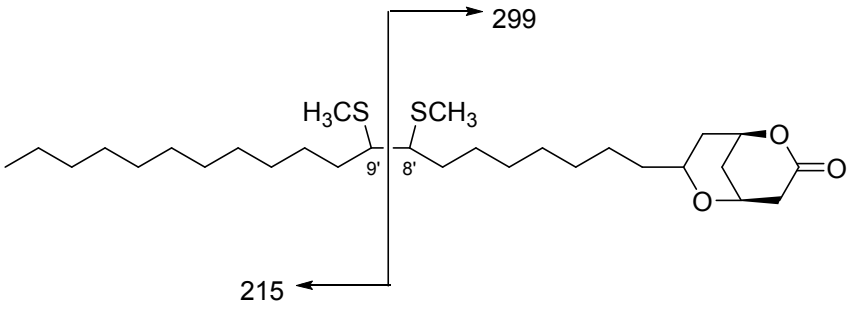

Figure 2.10 EI-MS Fragmentations of the DMDS Adduct of Compound **2.7**

2.2.7 Structure elucidation of compound **2.9**–**2.11**

Compounds **2.9**–**2.11** (cryptorigidifoliols I–K) are the bicyclic derivatives of **2.2**, **2.3**, and **2.5**, as determined by the conversions described below and by comparison of their IR, ^{1}H NMR and HRESIMS data with those of their 5,6-dihydro-α-pyrone precursors and those of compounds **2.6**–**2.8**. Since the configurations of the 2'-hydroxyl group of precursors **2.2**, **2.3**, and **2.5** have been established, the corresponding configurations at C-7 of **2.9**, **2.10**, and **2.11** were assigned as (*S*), (*R*), and (*R*), respectively. Surprisingly, compounds **2.7** and **2.10** showed no detectable optical activity. Since it is unlikely that they are racemic, given their formation from non-racemic precursors, the lack of measurable optical activity may be due to the nearly symmetrical structures of these compounds. Compounds **2.6**, **2.8**, **2.9**, and **2.11** had no significant Δδ (H) difference between their *R*- and *S*-MPA derivatives, so their configurations at these positions could not be determined.

2.2.8 Evidence that bicyclic tetrahydropyrones **2.6** – **2.11** are artifacts

The initial purification of the bioactive EtOAc fraction involved Sephadex LH-20 column chromatography, reverse phase SPE, normal phase silica gel column chromatography, and C_{18} HPLC. This procedure yielded fractions that in most cases were mixtures of 5,6-dihydro-α-pyrones and bicyclic tetrahydropyrones. In addition, it was noted that the early eluting fractions from the open silica gel column contained either pure 5,6-dihydro-α-pyrone **2.1**, or mixtures of 5,6-dihydro-α-pyrones **2.2**, **2.3**, and **2.5** and bicyclic tetrahydropyrones **2.9**–**2.11**. The later-eluting fractions, however, yielded only the bicyclic tetrahydropyrones **2.6**, **2.7**, and **2.8**. This suggested that the 5,6-dihydro-

α-pyrones were cyclized during their exposure to silica gel, with the more polar later-eluting compounds that were exposed for a longer time to silica gel becoming completely converted to cyclized product. Pure 5,6-dihydro-α-pyrone **2.2** and related compounds were thus prepared by purification by PTLC on diol silica gel, which did not induce intramolecular cyclization. It is worth noting that Grovic and coworkers isolated only 5,6-dihydro-α-pyrones, without artifacts, by using diol column chromatography during their bioassay-guided fractionation of a Papua New Guinea species of *Cryptocarya* in order to find compounds that can rescue Pdcd4 from TPA-induced degradation.[13]

To verify the cyclization hypothesis, silica gel was mixed with compound **2.2** in MeOH/hexanes/EtOAc and the resulting suspension was allowed to stand for 3 h at room temperature. Examination of the resulting solution showed that only compound **2.9** was present, confirming that silica gel catalyzed the cyclization of the 5,6-dihydro-α-pyrone **2.2** to the bicyclic tetrahydropyrone **2.9** (Scheme 2.2). Compounds **2.3** and **2.5** were also treated in the same way, leading to the formation of the corresponding bicyclic tetrahydropyrone derivatives **2.10** and **2.11**.

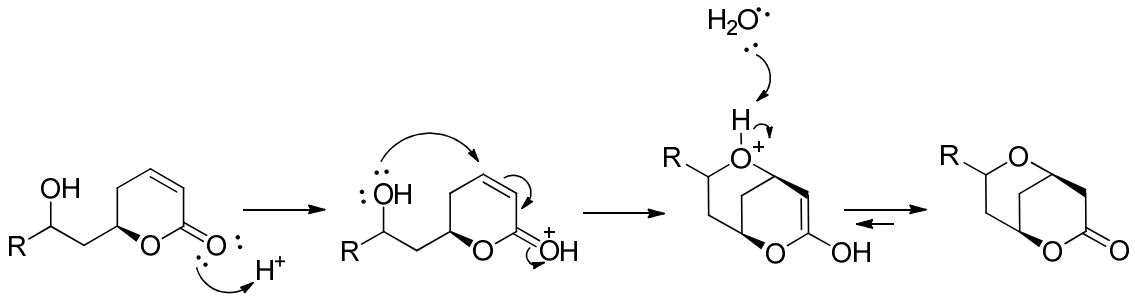

Scheme 2.2 Proposed Mechanism of Formation of Tetrahydro-α-pyrone Derivatives

Those observations supported the hypothesis that the bicyclic tetrahydropyrones are formed by intramolecular cyclization of C-2'-hydroxylated 5,6-dihydro-α-pyrones.

This does not however rule out the possibility that at least some bicyclic tetrahydropyrones are formed in the plant, and examination of the crude extract by ^{1}H NMR spectroscopy indicated that it did contain signals consistent with the presence of bicyclic tetrahydropyrones. This result could either be due to the presence of the cyclized compounds in the plant or to intramolecular cyclization during the extraction of the plant and the processing of the extract in Madagascar prior to analysis. Regrettably we did not have access to fresh plant material to test these alternate hypotheses, but the fact that chromatography over silica gel was used in every case where the cyclized compounds are reported strongly suggests that these compounds are indeed formed during the purification process.

2.2.9 Biological activities

Compounds **2.1**–**2.11** were evaluated for their antiparasitic activity against the chloroquine/mefloquine-resistant Dd2 strain of *Plasmodium falciparum*. Compounds **2.1–2.7** exhibited moderate antimalarial activity, with IC_{50} values of 9.2 ± 0.9, 5.8 ± 1.4, 5.5 ± 0.7, 9.0 ± 3.0, 4 ± 2, 7.4 ± 0.6, and 6.0 ± 0.5 μM, respectively. Compounds **2.8**–**2.11** were all less active, with IC_{50} values > 10 μM (Tables 2.3 and 2.4). These data indicate that the presence of the α,β-unsaturated ketone is not essential for antimalarial activity, since the bicyclic compounds **2.6** and **2.7** have comparable activity to the α,β-unsaturated compounds **2.1**–**2.5**.

All of the compounds were also evaluated for their antiproliferative activity against A2780 human ovarian cancer cells, but only compound **2.3** had an IC_{50} value less than 10 μM (Tables 2.3 and 2.4). Since these compounds have only moderate antiparasitic

activities, significant improvement in their potency and therapeutic index will be necessary before they can be used as lead compounds for the development of new antiplasmodial drugs.

Table 2.3 Bioactivities of 5,6-Dihydro-α-pyrones **2.1–2.5**

	2.1	**2.2**	**2.3**	**2.4**	**2.5**	Artemisinin	Taxol
Dd2[a] IC_{50} (μM)	9.2 ± 0.9	5.8 ± 1.4	5.5 ± 0.7	7.4 ± 0.6	9.0 ± 3.0	0.007 ± 0.001	N/A
A2780[b] IC_{50} (μM)	> 10	> 10	8.6	> 10	> 10	N/A	0.028 ± 0.002

[a] Antimalrial activity against the Dd2 strain of *Plasmodium falciparum*
[b] Antiproliferative activity against human ovarian cancer cells

Table 2.4 Bioactivities of Bicyclic Tetrahydro-α-pyrone Derivatives **2.6–2.11**

	2.6	**2.7**	**2.8**	**2.9**	**2.10**	**2.11**	Artemisinin	Taxol
Dd2[a] IC_{50} (μM)	4.0 ± 2.0	6.0 ± 0.5	> 10	> 10	> 10	> 10	0.007 ± 0.001	N/A
A2780[b] IC_{50} (μM)	> 10	> 10	> 10	> 10	> 10	> 10	N/A	0.028 ± 0.002

[a] Antimalrial activity against the Dd2 strain of *Plasmodium falciparum*
[b] Antiproliferative activity against human ovarian cancer cells

2.3 Conclusion

The formation of compounds **2.6**−**2.11** serves to highlight the fact that 5,6-dihydro-α-pyrones containing hydroxyl groups at the C-2' position in the side chain are susceptible to cyclization in the presence of silica gel at room temperature. It is thus possible that the bicyclic tetrahydropyrones previously reported[6, 7, 16, 17] were also formed by cyclization of the corresponding 5,6-dihydro-α-pyrones during the isolation process. This finding also provides support for the general belief that silica gel should be avoided for the isolation of most natural products, since it will not in general be known whether or not the unknown compounds might be susceptible to similar unwanted reactions. In place of silica gel, diol and C18 media are suitable for acid-sensitive compounds such as 5,6-dihydro-α-pyrones.

2.4 Experimental Section

2.4.1 General experimental procedures

IR and UV spectra were measured on MIDAC M-series FTIR and Shimadzu UV-1201 spectrophotometers, respectively. 1D and 2D NMR spectra were recorded on a Bruker Avance 500 spectrometer in $CDCl_3$ or pyridine-d_5 (with $CDCl_3$ or pyridine- d_5 as reference). High resolution ESI mass spectra were obtained on an Agilent 6220 mass spectrometer. ECD spectra were obtained on a JASCO J-815 circular dichroism spectrometer. Open column chromatography was performed using Sephadex LH-20 and silica gel (230-400 mesh, Silicycle Co. USA). Semi-preparative HPLC was performed using Shimadzu LC-10AT pumps coupled with a semipreparative Phenomenex C_{18} column (5 μm, 250 × 10 mm) and semipreparative Varian diol column (250 x 10.0 mm), a Shimadzu SPD M10A diode array detector, and a SCL-10A system controller. Preparative HPLC was performed using Shimadzu LC-8A pumps coupled with a preparative Varian Phenomenex C18 column (250 × 21.4 mm), a Shimadzu SPD M10A diode array detector, and a SCL-10A system controller. Preparative TLC was performed using diol plates (~ 500 m^2/g, SorbTec Co. USA). All isolated compounds were purified to 95% purity or better, as judged by HPLC (both UV and ELSD detection) before determining bioactivity.

2.4.2 Plant material

Plant parts of *Cryptocarya rigidifolia* van der Werff (Lauraceae) were collected by Fidy Ratovoson et al. at an elevation of about 1000 m from a 13 m tall tree with a diameter of 13 cm at breast height. The tree had round green fruit, with the remains of

brown calyx above. Collection was made near the towns of Imerimandroso and Antanandava in the district of Ambatondrazaka, north of the Zahamena National Park, at coordinates 17°28'45"S 048°44'10"E. The tree was growing in medium altitude rainforest, on the edge of an old area of slash and burn agriculture. Duplicate voucher specimens (Ratovoson 250) were deposited at the Centre National d'Application des Recherches Pharmaceutiques (CNARP), the Herbarium of the Department of Forestry and Fishery Research (TEF), and the Missouri Botanical Garden, St. Louis, Missouri (MO).

2.4.3 Extraction and isolation

A ground sample of *C. rigidifolia* root wood (310 g) was extracted with EtOH at room temperature to yield 16.3 g of crude EtOH extract designated MG 0441, and a portion of this extract was made available to Virginia Tech for bioassay-guided isolation. The crude EtOH extract (5.0 g) of the wood root of *C. rigidifolia* was dissolved in 90% aq. MeOH and extracted with hexanes. The 90% aq. MeOH layer was then evaporated, suspended in H_2O, and extracted with EtOAc. The antimalarial activities were concentrated in the EtOAc (IC_{50} 2.5~5 μg/mL) and hexanes fractions (IC_{50} ~5 μg/mL). The EtOAc fraction (971 mg) was subjected to Sephadex LH-20 size chromatography to give four fractions, and the most active fraction Fr-2 (IC_{50} 2.5~5 μg/mL) was fractionated by C_{18} SPE using 70% aq. MeOH, 100% MeOH, and CH_2Cl_2 separately. The 100% MeOH fraction (IC_{50} 1.25~2.5 μg/mL) was then divided into 8 sub-fractions by silica gel column chromatography (hexanes:EtOAc from 1:1 to 3:7 to 1:9, and a final elution with MeOH). The third sub-fraction (IC_{50} <1.25 μg/mL) was subjected to C18 HPLC with a

solvent gradient from H_2O:CH_3CN, 20:80 to 10:90 from 0.01 to10 min, to 0:100 from 10 to 15 min, and ending with 100% CH_3CN to 30 min, furnishing compound **2.1** (t_R 20.2 min, 1.1 mg, IC_{50} 2.98 μg/mL) and an active fraction (t_R 20.8 min). Further purification of the active fraction by diol PTLC yielded **2.3** (1.4 mg, IC_{50} 1.93 μg/mL) and **2.10** (0.4 mg, IC_{50} 5.74 μg/mL). The fourth sub-fraction from silica gel column chromatography was subjected to C18 HPLC with a solvent gradient from H_2O:CH_3CN, 30:70 to 20:80 from 0.01 to15 min, to 10:90 from 15 to 35 min, to 0:100 from 35 to 50 min, and ending with 100% CH_3CN to 60 min. Purification by diol PTLC of the mixtures with t_R 37.5 min and t_R 40.2 min obtained from this process gave compounds **2.5** (0.9 mg, IC_{50} 3.55 μg/mL), **2.11** (3.1 mg, IC_{50} >20 μg/mL), **2.2** (1.3 mg, IC_{50} 2.30 μg/mL) and **2.9** (0.5 mg, IC_{50} 6.57 μg/mL). The fifth sub-fraction from silica gel column chromatography was further purified by C 18 HPLC by using the same profile as the fourth sub-fraction, to give pure compounds **2.8** (4.2 mg, t_R 38 min, IC_{50} 13.6 μg/mL) and **2.6** (9.6 mg, t_R 40.8 min, IC_{50} 1.58 μg/mL).

The hexanes fraction was subjected to Sephadex LH-20 size chromatography to give three fractions, and the most active fraction Fr-2 (IC_{50} 2.5~5 μg/mL) was fractionated by preparative C18 HPLC with a solvent gradient from H_2O:CH_3CN, 30:70 to 0:100 from 0.01 to 30 min, and ending with 100% CH_3CN to 45 min. This process yielded compound **2.7** (1.6 mg, t_R 39 min, IC_{50} 2.50 μg/mL) and an active fraction (t_R 32.5 min). Further purification of the fraction by diol HPLC with a solvent gradient from hexanes:EtOAc, 90:10 to 80:20 from 0.01 to 10 min, to 70:30 from 10 to 15 min, to 60:40 from 15 to 20 min, to 0:100 from 20 to 25 min, and ending with 100% EtOAc wash to 35 min, furnished compound **2.4** (0.9 mg, IC_{50} 2.76 μg/mL).

2.4.4 Cryptorigidifoliol A (**2.1**)

Colorless oil; $[\alpha]^{21}_{D}$ +5.6 (*c* 0.54, MeOH); UV (MeOH) λ_{max} (log ε): 204 (3.63) nm; IR ν_{max} 3340, 2922, 2849, 1719, 1613, 1089 cm^{-1}; ECD (*c* 0.031 mM, MeOH) λ_{max} ($\Delta\varepsilon$) 203 (+8.5), 235 (+2.4), 256 (+3.8); ^{1}H and ^{13}C NMR data, see Table 2.1; HRESIMS *m/z* $[M+H]^+$ 325.2753 (calcd for $C_{20}H_{37}O_3^+$, 325.2737).

2.4.5 Cryptorigidifoliol B (**2.2**)

Colorless oil; $[\alpha]^{21}_{D}$ +9.1 (*c* 0.11, MeOH); UV (MeOH) λ_{max} (log ε): 204 (3.83) nm; IR ν_{max} 3343, 2922, 2850, 1714, 1615, 1092 cm^{-1}; ECD (*c* 0.031 mM, MeOH) λ_{max} ($\Delta\varepsilon$) 209 (+9.7), 235 (+1.9), 256 (+3.5); ^{1}H and ^{13}C NMR data, see Table 2.1; HRESIMS *m/z* $[M+H]^+$: 397.3317 (calcd for $C_{24}H_{45}O_4^+$, 397.3312).

2.4.6 Cryptorigidifoliol C (**2.3**)

Colorless oil; $[\alpha]^{21}_{D}$ +18.8 (*c* 0.96, MeOH); UV (MeOH) λ_{max} (log ε): 204 (3.91) nm; IR ν_{max} 3439, 2924, 2855, 1728, 1623, 1044 cm^{-1}; ECD (*c* 0.031 mM, MeOH) λ_{max} ($\Delta\varepsilon$) 207 (+9.3), 235 (+1.2), 255 (+3.1); ^{1}H and ^{13}C NMR data, see Table 2.1; HRESIMS *m/z* $[M+H]^+$ 351.2902 (calcd for $C_{22}H_{39}O_3^+$, 351.2894).

2.4.7 Cryptorigidifoliol D (**2.4**)

Colorless oil; $[\alpha]^{21}_{D}$ 0 (*c* 1.98, MeOH); UV (MeOH) λ_{max} (log ε): 204 (3.50) nm; IR ν_{max} 3444, 2922, 2855, 1724, 1625, 1034 cm^{-1}; ECD (*c* 0.031 mM, MeOH) λ_{max} ($\Delta\varepsilon$) 208 (+10.6), 235 (+1.6), 256 (+3.0); ^{1}H and ^{13}C NMR data, see Table 2.1; HRESIMS *m/z* $[M+NH_4]^+$ 396.3489 (calcd for $C_{24}H_{46}NO_3^+$, 396.3472).

2.4.8 Cryptorigidifoliol E (**2.5**)

Colorless oil; $[\alpha]^{21}_{D}$ -25 (*c* 0.4, MeOH); UV (MeOH) λ_{max} (log ε): 204 (3.24) nm; IR ν_{max}: 3382, 2922, 2845, 1729, 1625, 1077 cm^{-1}; ECD (*c* 0.031 mM, MeOH) λ_{max} ($\Delta\varepsilon$) 207 (+11.0), 234 (+2.3), 256 (+3.2); ^{1}H and ^{13}C NMR data, see Table 2.1; HRESIMS *m/z* $[M\text{-}OH]^{+}$ 377.3060 (calcd for $C_{24}H_{41}O_3^{+}$, 377.3050).

2.4.9 Cryptorigidifoliol F (**2.6**)

Colorless oil; $[\alpha]^{21}_{D}$ -14.3 (*c* 4.25, MeOH); UV (MeOH) λ_{max} (log ε): 204 (3.14) nm; IR ν_{max} 3450, 2932, 2855, 1719, 1073 cm^{-1}; ^{1}H and ^{13}C NMR data, see Table 2.2; HRESIMS *m/z* $[M+H]^{+}$ 395.3149 (calcd for $C_{24}H_{43}O_4^{+}$, 396.3156).

2.4.10 Cryptorigidifoliol G (**2.7**)

Colorless oil; $[\alpha]^{21}_{D}$ 0 (*c* 1.57, MeOH); UV (MeOH) λ_{max} (log ε): 204 (3.14) nm; IR ν_{max} 3450, 2932, 2855, 1719, 1073 cm^{-1}; ^{1}H and ^{13}C NMR data, see Table 2.2; HRESIMS *m/z* $[M+H]^{+}$ 421.3662 (calcd for $C_{27}H_{49}O_3^{+}$, 421.3676).

2.4.11 Cryptorigidifoliol H (**2.8**)

Colorless oil; $[\alpha]^{21}_{D}$ -10.6 (*c* 0.66, MeOH); UV (MeOH) λ_{max} (log ε): 204 (2.66) nm; IR ν_{max} 3540, 2917, 2845, 1719, 1070 cm^{-1}; ^{1}H and ^{13}C NMR data, see Table 2.2; HRESIMS *m/z* $[M+H]^{+}$355.2831 (calcd for $C_{21}H_{39}O_4^{+}$, 355.2843).

2.4.12 Cryptorigidifoliol I (**2.9**)

Colorless oil; $[\alpha]^{21}_{D}$ -7.5 (*c* 0.4, MeOH); UV (MeOH) λ_{max} (log ε): 204 (3.43) nm; IR ν_{max} 3340, 2943, 2846, 1727, 1068 cm^{-1}; ^{1}H and ^{13}C NMR data, see Table 2.2; HRESIMS *m/z* $[M+H]^+$ 397.3317 (calcd for $C_{24}H_{45}O_4^+$, 397.3312).

2.4.13 Cryptorigidifoliol J (**2.10**)

Colorless oil; $[\alpha]^{21}_{D}$ 0 (*c* 1.21, MeOH); UV (MeOH) λ_{max} (log ε): 204 (3.62) nm; IR ν_{max} 3345, 2939, 2844, 1739, 1056 cm^{-1}; ^{1}H and ^{13}C NMR data, see Table 2.2; HRESIMS *m/z* $[M+H]^+$351.2902 (calcd for $C_{22}H_{39}O_3^+$, 351.2894).

2.4.14 Cryptorigidifoliol K (**2.11**)

Colorless oil; $[\alpha]^{21}_{D}$ -9.5 (*c* 3.06, MeOH); UV (MeOH) λ_{max} (log ε): 204 (3.10) nm; IR ν_{max} 3431, 2956, 2867, 1732, 1036 cm^{-1}; ^{1}H and ^{13}C NMR data, see Table 2.2; HRESIMS *m/z* $[M+H]^+$ 377.3060 (calcd for $C_{24}H_{41}O_3^+$, 377.3050).

2.4.15 Dimethyldisulfide derivatization.

Pure samples (~200 μg) dissolved in 200 μL of hexanes were treated with dimethyldisulfide (400 μL) and 1–2 drops of iodine solution (6% w/v in ether) in a 6 dram vial at 40°C for 30 h. The mixture was then cooled and diluted with hexanes (1 mL), and iodine was removed by extracting with thiosulphate (1 mL, 5% w/v). The organic layer was removed, and the water layer was re-extracted with hexanes:CH_2Cl_2 (1:1). The combined organic layers were dried and subjected to analysis by GC-EIMS.[25, 26]

2.4.16 Preparation of the *R* and *S*-MPA ester derivatives of 5,6-dihydro-α-pyrones

The in-NMR-tube reaction[28] was carried out to prepare the MPA ester derivatives. The selected 5,6-dihydro-α-pyrone (0.2 mg) was dissolved in pyridine-d_5 in a clean NMR tube, and *R*-(−)-α-methoxyphenylacetyl (MPA) chloride (0.5 mg) was added to the NMR tube under an N_2 gas flow, and the NMR tube was gently shaken. The reaction NMR tube was kept at room temperature overnight and was then analyzed by ^{1}H NMR spectroscopy. The *S*-MPA esters of the 5,6-dihydro-α-pyrones were prepared from *S*-MPA chloride by the same method.

2.4.17 Preparation of bicyclic tetrahydropyrones

Compound **2.2** (0.2 mg) was dissolved in a mixture of MeOH (2 mL), EtOAc (0.5 mL) and hexanes (0.5 mL). Enough silica gel powder was added to the solution to absorb it, and the mixture was kept at room temperature for 3 h. The resulting damp powder was eluted by MeOH, and the eluate concentrated on a rotavapor. The product was identified as **2.9** by ^{1}H NMR spectroscopy. Compounds **2.3** and **2.5** (each 0.2 mg) were also treated separately and worked up under the same conditions. The products were identified as **2.10** and **2.11**, respectively, by ^{1}H NMR spectroscopy.

2.4.18 Antiproliferative bioassay

The A2780 ovarian cancer cell line antiproliferative bioassay was performed at Virginia Tech as previously reported.[29, 30] The A2780 cell line is a drug-sensitive ovarian cancer cell line.[31] Paclitaxel was used as the positive control; it had an IC_{50} value of 73 $\pm$ 15 nM.

2.4.19 Antimalarial bioassay

The effect of each compound on parasite growth of the Dd2 strain of *P. falciparum* was measured in a 72 h treatment using the malaria SYBR green I-based fluorescence assay as described previously.[32, 33] Artemisinin was used as the positive control; it had an IC_{50} value of 7 ± 1 nM.

2.5 References

1. Kingston, D. G. I. A natural love of natural products. *J. Org. Chem.* **2008,** *73*, 3975-3984.

2. Chou, T. H.; Chen, J. J.; Lee, S. J.; Chiang, M. Y.; Yang, C. W.; Chen, I. S. Cytotoxic flavonoids from the leaves of *Cryptocarya chinensis*. *J. Nat. Prod.* **2010,** *73*, 1470-1475.

3. Lin, H. R.; Chou, T. H.; Huang, D. W.; Chen, I. S. Cryptochinones from *Cryptocarya chinensis* act as farnesoid X receptor agonists. *Bioorg. Med. Chem. Lett.* **2014,** *24*, 4181-4186.

4. Wu, T. S.; Lin, F. W. Alkaloids of the wood of *Cryptocarya chinensis*. *J. Nat. Prod.* **2001,** *64*, 1404-1407.

5. Fu, X.; Sevenet, T.; Hamid, A.; Hadi, A.; Remy, F.; Pais, M. Kurzilactone from *Cryptocarya kurzii*. *Phytochemistry* **1993,** *33*, 1272-1274.

6. Drewes, S. E.; Horn, M. M.; Shaw, R. S. α-Pyrones and their derivatives from two *Cryptocarya species*. *Phytochemistry* **1995,** *40*, 321-323.

7. Drewes, S. E.; Sehlapelo, B. M.; Horn, M. M.; Scott-Shaw, R.; Sandor, P. 5,6-Dihydro-α-pyrones and two bicyclic tetrahydro-α-pyrone derivatives from *Cryptocarya latifolia*. *Phytochemistry* **1995,** *38*, 1427-1430.

8. Toneto Novaes, L. F.; Drekener, R. L.; Avila, C. M.; Pilli, R. A. Total synthesis of cryptomoscatones D1 and D2: Stereochemical assignment of cryptomoscatone D1. *Tetrahedron* **2014,** *70*, 6467-6473.

9. Deschamps, J. R.; George, C.; Flippen-Anderson, J. L.; Spencer, G. A new Cryptocarya lactone. *Acta Crystallogr., Sect. E: Struct. Rep. Online* **2001,** *57*, o648-o649.

10. Rali, T.; Wossa, S. W.; Leach, D. N. Comparative chemical analysis of the essential oil constituents in the bark, heartwood and fruits of *Cryptocarya massoy* (Oken) Kosterm. (Lauraceae) from Papua New Guinea. *Molecules* **2007,** *12*, 149-154.

11. Cuccarese, M. F.; Wang, Y.; Beuning, P. J.; O'Doherty, G. A. Cryptocaryol structure-activity relationship study of cancer cell cytotoxicity and ability to stabilize PDCD4. *ACS Med. Chem. Lett.* **2014,** *5*, 522-526.

12. Cardona, W.; Quinones, W.; Robledo, S.; Velez, I. D.; Murga, J.; Garcia-Fortanet, J.; Carda, M.; Cardona, D.; Echeverri, F. Antiparasite and antimycobacterial activity of passifloricin analogs. *Tetrahedron* **2006,** *62*, 4086-4092.

13. Grkovic, T.; Blees, J. S.; Colburn, N. H.; Schmid, T.; Thomas, C. L.; Henrich, C. J.; McMahon, J. B.; Gustafson, K. R. Cryptocaryols A-H, α-pyrone-containing 1,3-polyols from *Cryptocarya sp*. Implicated in stabilizing the tumor suppressor Pdcd4. *J. Nat. Prod.* **2011,** *74*, 1015-1020.

14. Meragelman, T. L.; Scudiero, D. A.; Davis, R. E.; Staudt, L. M.; McCloud, T. G.; Cardellina, J. H.; Shoemaker, R. H. Inhibitors of the NF-κB Activation Pathway from Cryptocarya rugulosa. *J. Nat. Prod.* **2009,** *72*, 336-339.

15. Sturgeon, C. M.; Cinel, B.; Diaz-Marrero, A. R.; McHardy, L. M.; Ngo, M.; Andersen, R. J.; Roberge, M. Abrogation of ionizing radiation-induced G2 checkpoint and inhibition of nuclear export by *Cryptocarya* pyrones. *Cancer Chemother. Pharmacol.* **2008,** *61*, 407-413.

16. Jiang, Z. H.; Yang, Q. X.; Tanaka, T.; Kouno, I. Bicyclic polyketide lactones from Chinese medicinal ats, *Polyrhacis lamellidens*. *J. Nat. Prod.* **2008,** *71*, 724-727.

17. Liou, J. R.; Wu, T. Y.; Thang, T. D.; Hwang, T. L.; Wu, C. C.; Cheng, Y. B.;

Chiang, M. Y.; Lan, Y. H.; El-Shazly, M.; Wu, S. L.; Beerhues, L.; Yuan, S. S.; Hou, M. F.; Chen, S. L.; Chang, F. R.; Wu, Y. C. Bioactive 6S-styryllactone constituents of *Polyalthia parviflora*. *J. Nat. Prod.* **2014,** *77*, 2626-2632.

18. Liu, Y.; Rakotondraibe, H.; Brodie, P. J.; Wiley, J. D.; Cassera, M. B.; Goetz, M.; Kingston, D. G. I. Antiproliferative and antimalarial sesquiterpene lactones from *Piptocoma antillana* from Puerto Rico. *Nat. Prod. Commun.* **2014,** *9*, 1403-1406.

19. Davies-Coleman, M. T.; Rivett, D. E. A. Naturally occurring 6-substituted 5,6-dihydro-α-pyrones. *Prog. Chem. Org. Nat. Prod.* **1989,** *55*, 1-35.

20. Snatzke, G. Circular dichroism and optical rotatory dispersion. Principles and application to the investigation of the stereochemistry of natural products. *Angew. Chem., Int. Ed. Engl.* **1968,** *7*, 14-25.

21. Raoelison, G. E.; Terreaux, C.; Queiroz, E. F.; Zsila, F.; Simonyi, M.; Antus, S.; Randriantsoa, A.; Hostettmann, K. Absolute configuration of two new 6-alkylated α-pyrones (=2H-pyran-2-ones) from *Ravensara crassifolia*. *Helv. Chim. Acta* **2001,** *84*, 3470-3476.

22. Costa, V. C. d. O.; Tavares, J. F.; Silva, A. B.; Duarte, M. C.; Agra, M. d. F.; Barbosa-Filho, J. M.; de Souza, I. L. L.; da Silva, B. A.; Silva, M. S. Hyptenolide, a new α-pyrone with spasmolytic activity from *Hyptis macrostachys*. *Phytochem. Lett.* **2014,** *8*, 32-37.

23. Dale, J. A.; Mosher, H. S. Nuclear magnetic resonance enantiomer regents. Configurational correlations via nuclear magnetic resonance chemical shifts of diastereomeric mandelate, O-methylmandelate, and α-methoxy-α-trifluoromethylphenylacetate (MTPA) esters. *J. Am. Chem. Soc.* **1973,** *95*, 512-519.

24. Jie, M. S. F. L. K.; Pasha, M. K.; Alam, M. S. Synthesis and nuclear magnetic resonance properties of all geometrical isomers of conjugated linoleic acids. *Lipids* **1997,** *32*, 1041-1044.

25. Nichols, P. D.; Guckert, J. B.; White, D. C. Determination of monounsaturated fatty acid double-bond position and geometry for microbial monocultures and complex consortia by capillary GC-MS of their dimethyl disulfide adducts. *J. Microbiol. Methods* **1986,** *5*, 49-55.

26. Mansour, M. P.; Holdsworth, D. G.; Forbes, S. E.; Macleod, C. K.; Volkman, J. K. High contents of 24:6(n-3) and 20:1(n-13) fatty acids in the brittle star *Amphiura elandiformis* from Tasmanian coastal sediments. *Biochem. Syst. Ecol.* **2005,** *33*, 659-674.

27. Drewes, S. E.; Horn, M. M.; Ramesar, N. S.; Ferreira, D.; Nel, R. J. J.; Hutchings, A. Absolute configurations of all four stereoisomers of cryptocaryalactone and deacetyl cryptocaryalactone. *Phytochemistry* **1998,** *49*, 1683-1687.

28. Su, B. N.; Park, E. J.; Mbwambo, Z. H.; Santarsiero, B. D.; Mesecar, A. D.; Fong, H. H. S.; Pezzuto, J. M.; Kinghorn, A. D. New chemical constituents of *Euphorbia quinquecostata* and absolute configuration assignment by a convenient Mosher ester procedure carried out in NMR tubes. *J. Nat. Prod.* **2002,** *65*, 1278-1282.

29. Cao, S.; Brodie, P. J.; Miller, J. S.; Randrianaivo, R.; Ratovoson, F.; Birkinshaw, C.; Andriantsiferana, R.; Rasamison, V. E.; Kingston, D. G. I. Antiproliferative xanthones of terminalia calcicola from the Madagascar rain forest. *J. Nat. Prod.* **2007,** *70*, 679-681.

30. Pan, E.; Harinantenaina, L.; Brodie, P., J.; Miller, J. S.; Callmander, M. W.; Rakotonandrasana, S.; Rakotobe, E.; Rasamison, V. E.; Kingston, D. G. I. Four Diphenylpropanes and a Cycloheptadibenzofuran from *Bussea sakalava* from the

Madagascar Dry Forest. *J. Nat. Prod.* **2010,** *73*, 1792-1795.

31. Louie, K. G.; Behrens, B. C.; Kinsella, T. J.; Hamilton, T. C.; Grotzinger, K. R.; McKoy, W. M.; Winker, M. A.; Ozols, R. F. Radiation survival parameters of antineoplastic drug-sensitive and -resistant human ovarian cancer cell lines and their modification by buthionine sulfoximine. *Cancer Res.* **1985,** *45*, 2110-2115.

32. Bennett, T. N.; Paguio, M.; Gligorijevic, B.; Seudieu, C.; Kosar, A. D.; Davidson, E.; Roepe, P. D. Novel, rapid, and inexpensive cell-based quantification of antimalarial drug efficacy. *Antimicrob. Agents Chemother.* **2004,** *48*, 1807-1810.

33. Smilkstein, M.; Sriwilaijaroen, N.; Kelly, J. X.; Wilairat, P.; Riscoe, M. Simple and inexpensive fluorescence-based technique for high-throughput antimalarial drug screening. *Antimicrob. Agents Chemother.* **2004,** *48*, 1803-1806.

3 Antiproliferative Compounds from *Cleistanthus boivinianus* from the Madagascar Dry Forest

This chapter is a slightly expanded version of a submitted article to the *Journal of Natural Product*, which is waiting for the final decision after revision. Attributions from co-authors of the articles are described as follows in the order of the names listed. The author of this dissertation (Yixi Liu) mentored the undergraduate student (Kelly Young) with the initial isolation with two compounds and finished up with isolating five more compounds, and elucidated the structures for all compounds, and drafted the manuscript. Dr. Harinantenaina was a mentor for this work, provided invaluable advice and hints for the structural elucidation of the compounds, and also proofread the manuscript before submission. Mrs. Peggy Brodie performed the A2780 bioassay on the isolated fractions and compounds. Dr. Jessica D. Wiley and Dr. Maria B. Cassera performed the Dd2 bioassay. Dr. Martin W. Callmander, and Dr. Richard Randrianaivo from Missouri Botanical Garden collected and identified the plant. Dr. Etienne Rakotobe and Dr. Vincent E. Rasamison from Madagascar carried out the initial plant extraction. Dr. Karen TenDyke and Dr. Yongchun Shen from Eisai Inc. performed the A2058, HCT-116 and MES-SA bioassays on the compounds isolated. Dr. David G. I. Kingston was a mentor for this work and the corresponding author for the published article. He provided critical suggestions for this work and crucial revisions to the manuscript.

3.1 Introduction

As a part of the Madagascar International Cooperative Biodiversity Group (ICBG) program,[1, 2] an ethanol extract of the stems of *Cleistanthus boivinianus* (Baill.) Müll. Arg. (Phyllanthaceae) was found to have moderate antiproliferative activity against the A2780 ovarian cancer cell line (IC_{50} 4.5 μg/ml), and it was thus selected for evaluation for the presence of novel antiproliferative agents. The genus *Cleistanthus* is native to Africa, India, and across to Australia,[3] and comprises approximately 140 species, but only five of these have been investigated chemically: *C. collinus*, *C. patulus*, *C. schlechteri var. schlechteri*, *C. gracilis,*[3] and *C. indochinensis*.[4] Arylnaphthalide lignans are major constituents of the genus, while arytetralin, furofuranoid, and dibenzylbutane lignans and terpenoids have also been isolated from it and are known for their toxic properties.[3-11]

Bioassay-guided isolation of the stems of *Cleistanthus boivinianus* furnished the new bioactive aryltetralin lignan **3.1** as the most potent antiproliferative (A2780) component with IC_{50} values at nanomolar level. It is an analogue of the cytotoxic natural product podophyllotoxin, with a substitution at C-3 instead of the C-4 position. This is the first report on this compound with this unique structure. Its strong activity suggested that analogues of podophyllotoxin-type compounds with substitution at C-3 instead of C-4 display more potent activity than those substituted C-4 with no substitution at C-3. In addition, the new arylnaphthalide lignan **3.2** together with the five known aryltetralin lignans deoxypicropodophyllotoxin (**3.3**),[12] (±)-*β*-apopicropodophyllin (**3.4**),[13-15] (-)-desoxypodophyllotoxin (**3.5**),[16] (-)-yatein (**3.6**),[17] and *β*-peltatin-5-*O*-*β*-D-glucopyranoside (**3.7**)[18] were also isolated. (Figure 3.1) The structures of the known

compounds **3.3**–**3.7** were determined by comparison of their ^{1}H NMR, mass spectra, and optical rotation values with the data reported in the literature, except for the case of **3.4** which had no optical rotation. The isolation of racemic *β*-apopicropodophyllin is noteworthy, since all previous isolates have been of the dextrorotatory isomer.

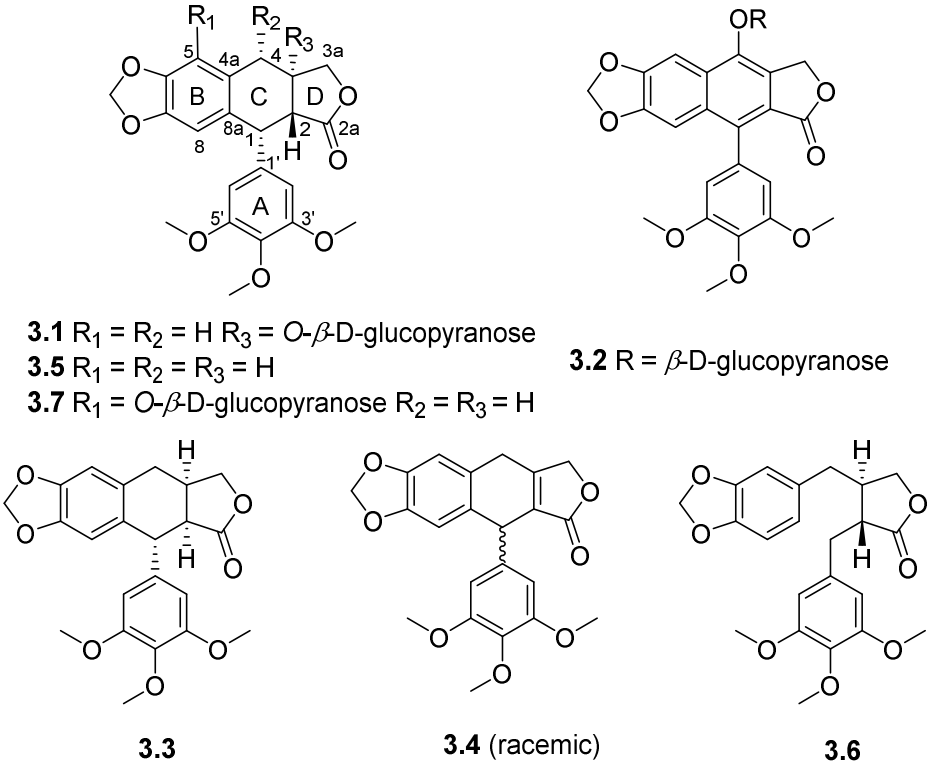

Figure 3.1 Structures of Compounds **3.1–3.7**

3.2 Results And Discussion

3.2.1 Isolation of active compounds

Dereplication of an active EtOAc-soluble fraction obtained from liquid-liquid partition of the extract (100 mg) as previously described[19] indicated that it contained at least one new bioactive compound, and so a larger sample was investigated. Fractionation of this extract yielded an antiproliferative EtOAc fraction which was further subjected to

size-exclusion column chromatography on Sephadex LH-20 followed by reversed phase Solid Phase Extraction (SPE). The most active fractions from the C18 SPE were subjected to C18 HPLC to yield compounds **3.3**, **3.5**, and **3.6** and three semi-pure active fractions. Further purification of these fractions by silica gel or diol HPLC furnished compounds **3.1**, **3.2**, **3.4**, and **3.7**. (Scheme 3.1)

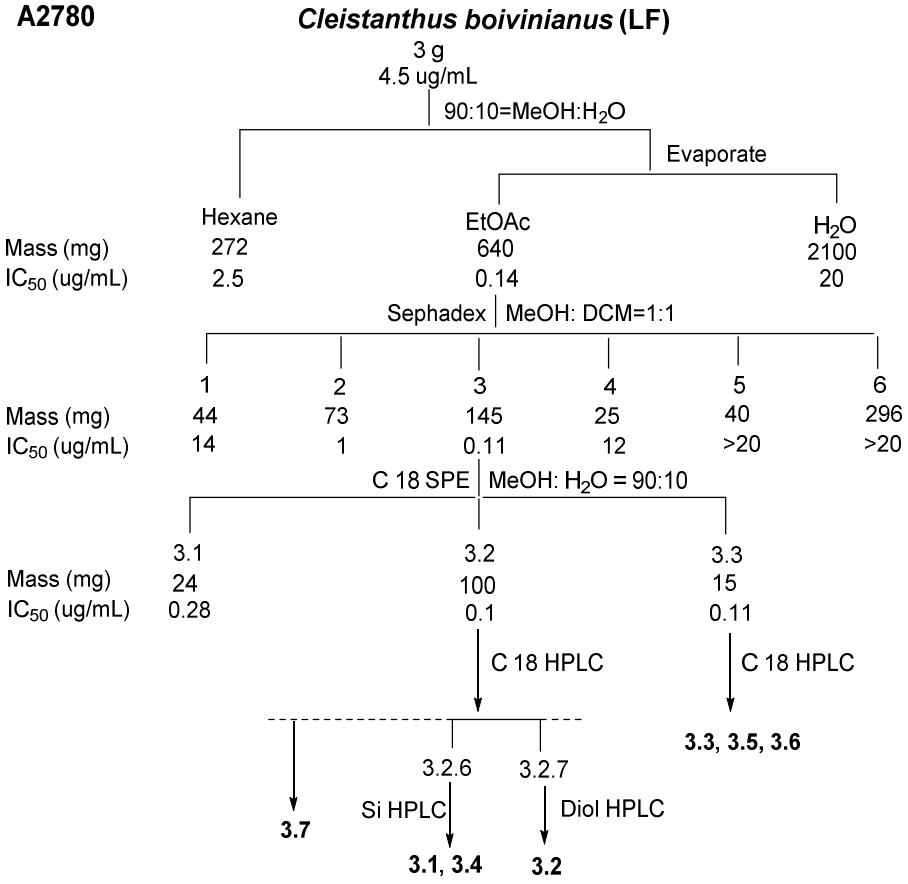

Scheme 3.1 Bioassay-guided Separation of *Cleistanthus boivinianus*

3.2.2 Structure elucidation of compound **3.1**

Compound **3.1** was isolated as a white solid with the molecular formula $C_{28}H_{32}O_{13}$ based its HRESIMS. Its IR spectrum showed absorption bands at 3402, 1760, 1590, and 1053 cm^{-1} ascribable to hydroxyl, ester carbonyl, aromatic methines, and ether groups, respectively. The UV spectrum of **3.1** showed absorption maxima at 291, 245 and 208 nm. Its ^1H NMR spectrum contained three singlet aromatic signals at δ_H 6.78 (1H, H-5), δ_H 6.72 (1H, H-8), and δ_H 6.55 (2H, H-2' and H-6'), together with a methylenedioxy group, indicated by the proton signal at δ_H 5.49 (s, 2H, OCH_2O). The presence of three aromatic methoxyl groups in **3.1** was shown by signals at δ_H 3.75 (MeO-3' and MeO-5', 6H) and δ_H 3.79 (MeO-4', 3H), and signals for 13 protons were observed in the aliphatic region. A single signal for a β-anomeric proton at δ_H 4.18 (J = 7.7 Hz, 1H, H-1") revealed that **3.1** contained one sugar unit. Analysis of COSY, HSQC, and HMBC spectra assigned the sugar proton signals as δ_H 4.18 (J = 7.7 Hz, 1H), δ_H 3.14–3.09 (1H), δ_H 3.24–3.17 (2H), δ_H 3.02 (ddd, J = 9.2, 8.5, 2.4 Hz, 1H), δ_H 3.59 (J = 11.8 Hz, 1H), and δ_H 3.79 (dd, J = 11.8, 2.4 Hz, 1H). The remaining aliphatic protons were assigned by HSQC to the protons of two methylene groups at δ_H 4.58 and 3.98 (J = 10.2 Hz, each 1H, H_2-3a), and δ_H 3.35 and 2.91 (J = 5.1 Hz, each 1H, H_2-4), respectively, and to two methine protons at δ_H 4.47 (J = 2.3 Hz, 1H, H-1) and δ_H 3.76 (J = 2.3 Hz, 1H, H-2). These assignments were confirmed by analysis of the ^1H–^1H COSY spectrum, which contained correlations between δ_H 4.47 (J = 2.3, 1H, H-1) and δ_H 3.76 (J = 2.3, 1H, H-2). All of the above data indicated that **3.1** had an aryltetralin lignan skeleton.[4] This was also supported by the HMBC spectrum, with cross-peaks from H-1 (δ_H 4.47) to δ_C 105.7 (C-8) and to δ_C 104.9 (C-2' and C-6'), supporting the linkage of C-1 to both the A- and B-rings. HMBC

cross peaks between H-5 (δ_H 6.78) and C-4 (δ_C 37.0) and between H-4 (δ_H 3.35 and δ_H 2.91) and C-8a (δ_C 130.5) assigned the C-4a and C-4 connection, and the presence of the lactone ring was confirmed by cross-peaks between the methylene protons at δ_H 4.58 and δ_H 3.98 (H_2-3a) and the ester carbonyl carbon C-2a (δ_C 178.4). The three-bond correlation between the methylenedioxy protons at δ_H 5.94 and C-6 and C-7 (δ_C 147.3) indicated the position of the methylenedioxy group at C-6 and C-7 of the B-ring. Finally, the positions of the methoxyl groups at C-3', C-5', and C-4' were assigned from the cross peaks from the methoxy signals at δ_H 3.75 to C-3' and C-5', and the signal at δ_H 3.79 to C-4'. (Figure 3.2)

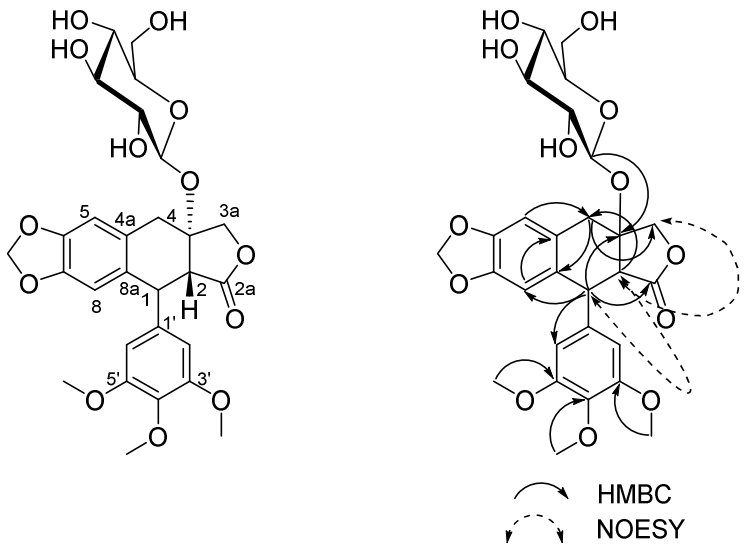

Figure 3.2 Key HMBC and NOESY Correlations of **3.1**

The signals for H-1 and H-2 were each observed as a doublet in the ^{1}H NMR spectrum with a gauche (J = 2.3 Hz) coupling constant. This indicated that H-1 and H-2 were pseudoequatorial and *cis* to each other.[4] This observation was confirmed by a NOESY experiment, in which the interaction of H-1 and H-2 was observed. The *trans*-configuration of the D-ring was determined by the NOESY correlation between H-2 and

H-3a at δ_H 4.58 d (10.2). The 1*R* absolute configuration was established by the electronic circular dichroism (ECD) spectrum of **3.1**, which gave a positive Cotton effect at 288 nm ($\Delta\varepsilon$ +1.02), consistent with the positive effect for other 1*R* lignans.[4, 20-25] These data combined with the relative configuration determined above allowed the *R* and *S* configurations to be assigned for the C-2 and C-3 chiral centers, respectively.

Mild acid hydrolysis of **3.1** gave (+)-*β*-apopicropodophyllin (**3.4a**) and a sugar that was identified as D-glucose by TLC and optical rotation comparison with a standard sample. (Figure 3.3) The placement of glucose at C-3 was evident from the HMBC correlation between the anomeric proton at δ_H 4.18 and the quaternary carbon at δ_C 83.6 (C-3). The configuration of the glucose unit was assigned as *β* on the basis of the coupling constant (J = 7.7 Hz) of the anomeric proton. The complete assignment of all protons and carbons of **3.1** (Table 3.1) was accomplished by analysis of the COSY, HSQC, HMBC, and NOESY spectra. Thus, compound **3.1** was assigned as (1*R*,2*R*,3*S*)-3-*O*-(*β*-D-glucopyranosyl)-3',4',5'-trimethoxy-6,7-methylenedioxy-1,9-cyclolignan-11,12-olide, and named cleistanolide A.

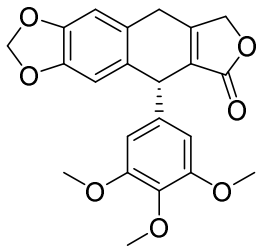

Figure 3.3 Structure of Compound **3.4a**

Table 3.1 ^{1}H NMR (500 MHz, CD_3OD) and ^{13}C NMR (125 MHz, CD_3OD) Chemical Shift Data (δ, ppm) for Compounds **3.1** and **3.2**

	3.1		**3.2**	
posn	δ_H	δ_C (DEPT)	δ_H	δ_C (DEPT)
1	4.47 d (2.3)	47.1 (CH)		128.6 (C)
2	3.76 d (2.3)	52.8 (CH)		119.7 (C)
2a		178.4 (C)		170.4 (C)
3a	4.58 d (10.2) 3.98 d (10.2)	76.9 (CH_2)	5.75 d (15.3) 5.53 d (15.3)	67.3 (CH_2)
3		83.6 (C)		130.4 (C)
4	3.35 d (5.1) 2.91 d (5.1)	37.0 (CH_2)		144.3 (C)
4a		127.3 (C)		136.5 (C)
5	6.78 s	108.9 (CH)	8.04 s	98.6 (CH)
6		147.3 (C)		149.6 (C)
7		147.3 (C)		149.6 (C)
8	6.72 s	105.7 (CH)	6.95 s	102.8 (CH)
8a		130.5 (C)		131.7 (C)
1'		130.5 (C)		131.1 (C)
2'	6.55 s	104.9 (CH)	6.59 s	107.6 (CH)
3'		154.4 (C)		152.9 (C)
4'		136.2 (C)		137.2 (C)
5'		154.4 (C)	6.59 s	152.9 (C)
6'	6.55 s	104.9 (CH)		107.6 (CH)
OCH_2O	5.94 s	101.1 (CH_2)	6.11 s	101.6 (CH_2)
OMe-3’	3.79 s	59.8	3.82 s	55.4
OMe-4’	3.75 s	55.3	3.88 s	59.9
OMe-5’	3.79 s	59.8	3.82 s	55.4
Glu				
1"	4.18 d (7.7)	99.2 (CH)	4.89[a]	104.8 (CH)
2"	3.14-3.09	73.6 (CH)	3.63 dd (9.0, 7.8)	74.2 (CH)
3"	3.24-3.17	76.4 (CH)	3.48 t (9.0)	76.7 (CH)
4"	3.24-3.17	69.8 (CH)	3.44 m	70.1 (CH)
5"	3.02 ddd (9.2, 8.5, 2.4)	76.7 (CH)	3.33[a]	77.0 (CH)
6"	3.79 dd (11.8, 2.4) 3.59 dd (11.8, 2.4)	61.3 (CH_2)	3.90[b] 3.71 dd (11.9, 6.0)	61.3 (CH_2)

[a]Peaks covered by the CH_3OH peak; chemical shift assigned from HSQC and HMBC spectra.
[b]Peak covered by an OMe peak.

As indicated by the experiment described above, cleistanolide A is sensitive to conversion to its α,β-unsaturated derivative **3.4 a**, and a sample of **3.1** left in MeOH/$CHCl_3$ for a few days underwent decomposition, most likely caused by traces of HCl in the $CHCl_3$. Attempted enzymatic hydrolysis of **3.1** did not proceed under normal conditions, so the aglycone could not be isolated.

3.2.3 Structure elucidation of compound **3.2**

Compound **3.2** had the molecular formula of $C_{28}H_{29}O_{13}$, based on its HRESIMS data. Its IR spectrum showed absorptions for OH and ester carbonyl groups at 3400 and 1734 cm^{-1}, respectively. Its ^1H NMR spectrum was similar to that obtained for **3.1**, and its UV absorption maxima at 260, 315, and 351 nm indicated the presence of a naphthalene nucleus,[13] suggesting that **3.2** was an arylnaphthalide lignan. The ^1H NMR spectrum of **3.2** exhibited signals for two aromatic protons at δ_H 8.04 and 6.95 (s, each 1H, H-5 and H-8) and for an oxymethylene group at δ_H 5.75 and 5.53 (J = 15.4 Hz, each 1H, H_2-3a), but lacked the signals for the two methine protons at C-1 and C-2 and the methylene protons at C-4 observed in **3.1**. These facts confirmed the presence of a naphthalene unit in **3.2**. In the HMBC spectrum, the correlation from H-5 (δ_H 8.04) and H_2-3a (δ_H 5.75 and 5.53) to δ_C 144.3 (C-4) confirmed the linkage of C-4 to both the B- and D-rings, while the correlations of δ_H 6.59 (s, 1H, H-2' or/and H-6') and δ_H 6.95 (H-8) to δ_C 128.6 (C-1) connected the A- and B-rings to C-1. A comparison of the NMR spectra of **3.2** with those of dehydropodophyllotoxin (**3.2a**) suggested that compound **3.2** is a glycosylated derivative of **3.2a**.[26] The HMBC correlation between the anomeric proton signal at δ_H 4.89 (H-1") and δ_C 144.3 (C-4) confirmed that the sugar was located at C-4 of the

aglycone. Acid hydrolysis of **3.2** gave dehydropodophyllotoxin (**3.2a**) as the aglycon, and a sugar that was identified as a *β*-D-glucose by ^{1}H NMR, TLC, and optical rotation comparison with a standard sample. The complete assignments of all protons and carbons of **3.2** (Table 1) were accomplished by analysis of the HSQC and HMBC spectra. Compound **3.2** was thus assigned as 4-*O*-(*β*-D-glucopyranosyl)-dehydropodophyllotoxin.

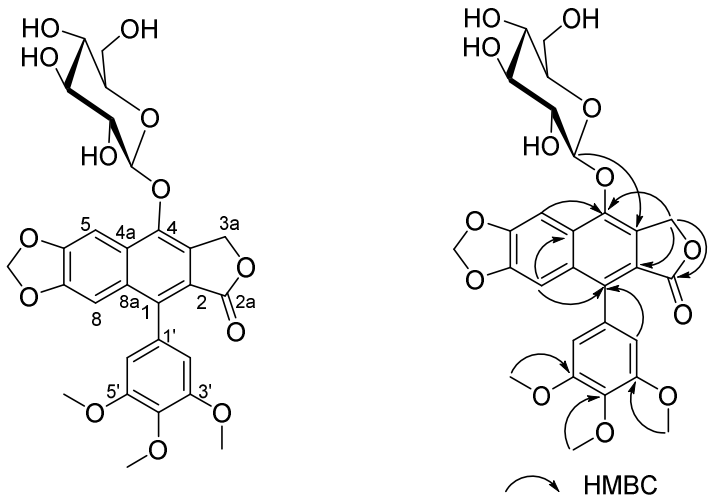

Figure 3.4 Key HMBC and NOESY Correlations of **3.2**

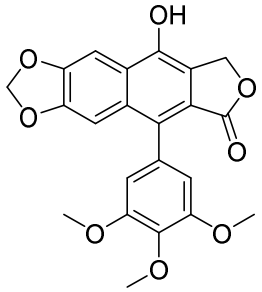

Figure 3.5 Structure of Compound **3.2a**

3.2.4 Biological activities

All isolated compounds were evaluated for their antiproliferative activity against the A2780 human ovarian cancer cell line, and some were evaluated in other cell lines

and for antimalarial activity (Table 3.2). Compound **3.1** showed the highest antiproliferative activity (IC_{50} 33.0 ± 3.6 nM) against the A2780 cell line, followed by **3.4** (63.1 ± 6.7 nM) and **3.5** (230 ± 1 nM). The potency of **3.1** is similar to that of the anticancer drug paclitaxel, which has an IC_{50} value of 73 nM in this assay. Compounds **3.2** and **3.7** showed only modest antiproliferative activities, with IC_{50} values of 2.1 ± 0.3 and 4.9 ± 0.1 μM, respectively. Glycosylation with the *β*-D-glucose moiety in **3.1** improves activity slightly compared with the racemic unglycosylated and eliminated compound **3.4**. The unsaturated D-ring of **3.4** increased the activity about 4 fold compared with the *trans* dihydro D-ring analog **3.5**, while the *cis* D-ring analog **3.3** was much less potent than **3.4**, consistent with previous studies indicating the significance of the trans fused lactone for activity.[27, 28] A glucose moiety at C-5 or C-4 and the aromatization of the C-ring reduced activity, as shown by the fact that compounds **3.2** and **3.7** were about 10 and 20-fold less potent than **3.5**, respectively. Furthermore, although good antiproliferative activity has been observed in other cell lines for (-)-yatein (**3.6**),[13] it was only weakly active against the A2780 cell line. Compound **3.1** also displayed potent antiproliferative activity against the HCT-116 human colon carcinoma cell line with an IC_{50} value of 20.5 nM, and weak antimalarial activity against *Plasmodium falciparum* with an IC_{50} value of 12.6 ± 3.2 μM. Compound **3.4** displayed moderate antiproliferative activity against A2058 human caucasian metastatic melanoma and MES-SA human uterine sarcoma cells, with IC_{50} values of 4.6 and 4.0 μM, respectively.

Table 3.2 Antiproliferative and Antimalarial Activities (IC_{50} Values, μM)

cell line	paclitaxel	**3.1**	**3.2**	**3.3**	**3.4**	**3.5**	**3.6**	**3.7**
A2780	0.073 ± 0.015	0.033 ± 0.0036	2.1 ± 0.3	35 ± 5	0.063 ± 0.007	0.23 ± 0.001	34.2 ± 1.4	4.9 ± 0.1
HCT-116	NT	0.0205	NT	NT	NT	NT	NT	NT
A2058	NT	NT	NT	NT	4.6	NT	NT	NT
MES-SA	NT	NT	NT	NT	4.0	NT	NT	NT
P. falciparum	NT	12.6 ± 3.2	NT	NT	NT	NT	NT	NT

Podophyllotoxin is an important starting material for the development of new therapeutic agents because of its remarkable biological activity.[29] In order to obtain more active but less toxic antitumor agents, extensive structural modifications of podophyllotoxin have been undertaken, including different substitutions and configurations at C-4, a methylenedioxy group on ring A, an aromatized ring C, and a trans-fusion between the tetralin system and the lactone.[29-34] Among all the SAR studies, most efforts were focused on exploring different 4-substituted podophyllotoxin derivatives,[29] since the 4-position proved to be very important for antimitotic activity.[35, 36] However, some SAR studies on aryltetralin lignans suggested that 4-substitution may not be essential for antiproliferative activity in podophyllotoxin-type compounds. In a study by Kellog et al., deoxypodophyllotoxin showed stronger antiproliferative activity than podophyllotoxin against the GLC4 cell line,[30] while Sun and coworkers showed that podophyllotoxin analogues with a 4α oxygenated group exhibited significantly lower activity against HeLa and KB cancer cell lines than analogues without 4-substitutions.[21]

In summary, compound **3.1** is a new podophyllotoxin analogue with potent antiproliferative activity against the A2780 cell line. It is also the first reported C-3 substituted podophyllotoxin analogue. It would be an attractive substrate for further studies to explore its mechanism of action were it not for its lability to acidic conditions, which suggests that it would not be stable enough for drug use.

3.3 Experimental Section

3.3.1 General experimental procedures

IR and UV spectra were measured on MIDAC M-series FTIR and Shimadzu UV-1201 spectrophotometers, respectively. ^{1}H and ^{13}C NMR spectra were recorded on a Bruker Avance 500 spectrometer in CD_3OD (with CD_3OD as reference) and $CDCl_3$ (with $CDCl_3$ as reference). Mass spectra were obtained on an Agilent 6220 mass spectrometer. Open column chromatography was performed using Sephadex LH-20, and solid phase extraction was performed using C18 cartridges. Semi-preparative HPLC was performed using Shimadzu LC-10AT pumps coupled with a semi-preparative Phenomenex C18 column (5 μm, 250 × 10 mm), a Shimadzu SPD M10A diode array detector, and a SCL-10A system controller. All isolated compounds were purified to 95% purity or better, as judged by HPLC (both UV and ELSD detection) before determining bioactivity.

3.3.2 Plant material

Leaves of *Cleistanthus boivinianus* (Baill.) Müll. Arg. (collection: Stéphan Rakotonandrasana et al. 1036) were collected at an elevation of 51 m from a 3 m tall tree with yellow flowers. Collection was made 5 km north-east of the village of Marivorahona, PK 123, Andohanantsohihy, in a mosaic of dry forest and savanna trees; coordinates 13°06'37"S 049°09'39"E. Collection was made by Stéphan Rakotonandrasana with assistance from R. Randrianaivo, R. Rakotonandrasana, C. Claude, V. Benjara, and M. Modeste. Duplicate voucher specimens are deposited at the Centre National d'Application des Recherches Pharmaceutiques (CNARP), the Herbarium of the Parc Botanique et Zoologique de Tsimbazaza, Antananarivo, Madagascar (TAN), the Missouri

Botanical Garden, St. Louis, Missouri (MO), and the Museum National d'Histoire Naturelle in Paris, France (P).

3.3.3 Extraction and isolation

A ground sample of *Cleistanthus boivinianus* leaves (250 g) was extracted with EtOH at room temperature to yield 33.4 g of crude EtOH extract designated MG4031. A total of 5.88 g of this extract was made available to Virginia Tech. An active EtOAc-soluble fraction obtained from liquid-liquid partition of the extract (100 mg) was subjected to dereplication studies using size-exclusion chromatography, reverse phase HPLC coupled with bioassay, high-resolution ESIMS, ^{1}H NMR, and a database search using the online Dictionary of Natural Product (DNP). The results indicated that the extract contained at least one new bioactive compound, and so a 3.0 g sample was investigated. The crude EtOH extract was dissolved in 90% aq. MeOH (300 mL), and extracted with hexanes (3 × 200 mL)., and extracted with hexanes (3 × 200 mL). Evaporation of the hexane-soluble fraction afforded 271 mg of residue. The 90% aq. MeOH layer was then evaporated, suspended in H_2O (300 mL), and extracted with EtOAc (3 × 200 mL) to yield 640 mg of an EtOAc-soluble fraction with an IC_{50} value of 0.19 µg/mL. The EtOAc fraction was subjected to Sephadex LH-20 open column chromatography (CH_2Cl_2:MeOH, 1:1) to give 6 fractions. The most active fraction Fr 3 (IC_{50} 0.11 µg/mL) was then divided into 3 sub-fractions by C18 solid phase extraction by using 40% aq. MeOH (Fr 3-1), 70% Aq. MeOH (Fr 3-2), and 100% MeOH (Fr 3-3). Further purification of the most active sub-fraction Fr 3-3 (IC_{50} 0.11 µg/mL) by HPLC on a C18 column with a solvent gradient from H_2O:CH_3CN, 60:40 to 50:50 from 0 to 17 min, to 40:60 from 17 to 22 min, to 40:60 from 22 to 27 min and ending with 100%

CH_3CN from 27 to 35 min yielded compounds **3.3** (1.2 mg, t_R 23.5 min), **3.5** (1.5 mg, t_R 24.5 min), and **3.6** (2.1 mg, t_R 26.5 min). Purification of the sub-fraction Fr 3-2 (IC_{50} 0.1 µg/mL) by C18 HPLC furnished 8 fractions (solvent gradient from H_2O:CH_3CN, 70:30 to 62:38 from 0 to 15 min, and ending with 100% CH_3CN from 15 to 24 min), among which the 3rd (t_R 12 min), 6th (t_R 14.5 min), and 7th (t_R 15.5 min) fractions were active with IC_{50} value of 1.5, 0.1, and 1.2 µg/mL, respectively. Further purification of the 3rd fraction by HPLC on a silica gel column with a solvent gradient from $CHCl_3$:MeOH, 95:5 to 90:10 from 0 to 5 min, to 88:12 from 5 to 12 min, and ending with a 100% MeOH wash from 13 to 20 min, yielded compound **3.7** (2.8 mg, t_R 13.5 min). Further purification of the 6th fraction by HPLC on a silica gel column with a solvent gradient from $CHCl_3$:MeOH, 95:5 to 90:10 from 0 to 5 min, to 80:20 from 5 to 10 min, to 70:30 from 10 to 15 min, and ending with a 100% MeOH wash from 16 to 25 min, yielded compound **3.4** (5 mg, t_R 6 min) and **3.1** (19 mg, t_R 14 min). Further purification of the 7th fraction by HPLC on a diol column with a solvent gradient from $CHCl_3$:MeOH, 100:0 to 95:5 from 0 to 5 min, to 90:10 from 5 to 15 min, to 87.5:12.5 from 15 to 20 min, and ending with a 100% MeOH wash from 20 to 25 min, yielded compound **3.2** (3 mg, t_R 22.5 min).

3.3.4 Cleisthanolide A (**3.1**)

Amorphous powder; $[\alpha]^{21}_D$ +120 (*c* 0.1, MeOH); CD (*c* 0.031, MeOH) λ_{max} ($\Delta\varepsilon$): 210 (+22.59), 234 (+5.98), 248 (-1.33), 288 (+1.02) nm; UV (MeOH) λ_{max}(log ε): 291 (3.19), 245 (3.7), 208 (4.4) nm; IR (film) ν_{max} 3402, 2912, 1760, 1590, 1053 cm^{-1}; ^{1}H and ^{13}C NMR data, see Table 3.1; HRESIMS *m/z* $[M+Na]^+$ 599.1741 (calcd for $C_{28}H_{32}NaO_{13}^+$, 599.1735)

3.3.5 4-*O*-(β-D-Glucopyranosyl)-dehydropodophyllotoxin (**3.2**)

Amorphous powder, $[\alpha]^{21}_{D}$ -14 (*c* 0.22, MeOH); UV (MeOH) λ_{max} (log ε): 351 (3.69), 315 (4.0), 260 (4.7) nm; IR (film) ν_{max}: 3400, 2920, 1734, 1645, 1070 cm^{-1}; ^{1}H and ^{13}C NMR data, see Table 3.1; HRESIMS *m/z* $[M+H]^{+}$ 573.1635 (calcd for $C_{28}H_{29}O_{13}^{+}$, 599.1603)

3.3.6 (±)-β-Apopicropodophyllin (**3.4**)

Amorphous powder, $[\alpha]^{21}_{D}$ 0 (*c* 0.5, $CHCl_3$). Its ^{1}H and ^{13}C NMR spectra were identical with literature data.[13-15]

3.3.7 Antiproliferative bioassay

The A2780 ovarian cancer cell line antiproliferative bioassay was performed at Virginia Tech as previously reported.[37, 38] The A2780 cell line is a drug-sensitive ovarian cancer cell line.[39] Paclitaxel was used as the positive control; it had an IC_{50} value of 0.073 ± 0.015 μM.

3.3.8 Antimalarial bioassay

The effect of each compound on parasite growth of the Dd2 strain of *P. falciparum* was measured in a 72 h growth assay in the presence of compound as described previously.[40-42]

3.3.9 Acid hydrolysis of compounds **3.1** and **3.2**

Compound **3.1** (2 mg) was dissolved in dilute citrate/phosphate buffer (pH 7.0, 4 mL) and *β*-D-glucosidase (4 mg) was added. The mixture was incubated for 2 weeks at

37 °C; no reaction was observed. The reaction mixture was then adjusted to pH 5.0 with dilute HCl and stirred at 37°C overnight. The mixture was then briefly heated to boiling, extracted with EtOAc (3x10 mL) and both the organic and the water layers were evaporated to dryness under reduced pressure. The structure of the white powder (1.2 mg) derived from the organic layer was determined to be **3.4a** by its ^{1}H NMR spectrum and optical rotation ($[\alpha]^{21}_D$: +86, *c* 1.2, $CHCl_3$; lit. +96.8[13]). The semi-solid carbohydrate from the water layer (0.5 mg) was dissolved in 2 mL of water and kept overnight before determination of its optical rotation. Compound **3.2** (1 mg) was dissolved in dilute HCl (pH 5.0, 2 mL) and stirred at 37 °C overnight. The reaction mixture was extracted with EtOAc (3x10 mL) and both the organic and the water layers were evaporated to dryness under reduced pressure. The structure of the dried powder from the organic layer was determined to be **3.2a** by its ^{1}H NMR spectrum. TLC of the sugar from both **3.1** and **3.2** on a silica gel plate with $CHCl_3$:MeOH:H_2O = 15:6:1 showed that it had an identical R_f value (0.23) to glucose. The isolated glucose had $[\alpha]^{21}_D$ (*c* 0.5, H_2O) values of +41.9 and +43.2, respectively.

3.4 References

1. Rakotondraibe, H. L.; Graupner, P. R.; Xiong, Q.; Olson, M.; Wiley, J. D.; Krai, P.; Brodie, P., J.; Callmander, M. W.; Rakotobe, E.; Ratovoson, F.; Rasamison, V. E.; Cassera, M. B.; Hahn, D. R.; Kingston, D. G. I.; Fotso, S. Neolignans and Other Metabolites from *Ocotea cymosa* from the Madagascar Rain Forest and their Biological Activities. *J. Nat. Prod.* **2015,** *78*, doi: 10.1021/np5008153.

2. Kingston, D. G. I. A natural love of natural products. *J. Org. Chem.* **2008,** *73*, 3975-3984.

3. Pinho, P. M. M.; Kijjoa, A. Chemical constitutents of the plants of the genus *Cleistanthus* and their biological activity. *Phytochem. Rev.* **2007,** *6*, 175-182.

4. Thanh, V. T. T.; Pham, V. C.; Mai, H. D. T.; Litaudon, M.; Gueritte, F.; Retailleau, P.; Nguyen, V. H.; Chau, V. M. Cytotoxic lignans from fruits of *Cleistanthus indochinensis*: Synthesis of cleistantoxin derivatives. *J. Nat. Prod.* **2012,** *75*, 1578-1583.

5. Trinh, T. T. V.; Pham, V. C.; Doan, T. M. H.; Nguyen, V. H.; Chau, V. M.; Litaudon, M.; Gueritte, F. Cytotoxic aryltetralin lignans from fruits of Cleistanthus indochinensis. *Planta Med.* **2014,** *80*, 695-702.

6. Thanh, V. T. T.; Pham, V. C.; Nguyen, H. H.; Mai, H. D. T.; Minh, H. N. T.; Nguyen, V. H.; Litaudon, M.; Gueritte, F.; Chau, V. M. Cleistanone: A triterpenoid from *Cleistanthus indochinensis* with a new carbon skeleton. *Eur. J. Org. Chem.* **2011,** *2011*, 4108-4111.

7. Parasuraman, S.; Raveendran, R. Effect of cleistanthin A and B on adrenergic and cholinergic receptors. *Pharmacogn. Mag.* **2011,** *7*, 243-247.

8. Pinho, P. M.; Naengchomnong, W.; Kijjoa, A.; Nazareth, N.; Silva, A. M. S.;

Eaton, G.; Herz, W. An unusual glucoside from *Cleistanthus gracilis*. *Phytochemistry* **2006,** *67*, 1789-1792.

9. Ramesh, C.; Ravindranath, N.; Ram, T. S.; Das, B. Studies on phytochemicals - 42. Arylnaphthalide lignans from *Cleistanthus collinus*. *Chem. Pharm. Bull.* **2003,** *51*, 1299-1300.

10. Sastry, K. V.; Rao, E. V.; Buchanan, J. G.; Sturgeon, R. J. Cleistanthoside B, a diphyllin glycoside from *Cleistanthus patulus* heartwood. *Phytochemistry* **1987,** *26*, 1153-1154.

11. Pradheepkumar, C. P.; Shanmugam, G. Anticancer potential of cleistanthin A isolated from the tropical plant *Cleistanthus collinus*. *Oncol. Res.* **1999,** *11*, 225-232.

12. Broomhead, A. J.; Dewick, P. M. Aryltetralin lignans from *Linum flavum* and *Linum capitatum*. *Phytochemistry* **1990,** *29*, 3839-3844.

13. Novelo, M.; Cruz, J. G.; Hernandez, L.; Pereda-Miranda, R.; Chai, H.; Mar, W.; Pezzuto, J. M. Chemical studies on Mexican Hyptis species. VI. Biologically active natural products from Mexican medicinal plants. II. Cytotoxic constituents from *Hyptis verticillata*. *J. Nat. Prod.* **1993,** *56*, 1728-1736.

14. Pelter, A.; Ward, R. S.; Li, Q.; Pis, J. An asymmetric synthesis of isopodophyllotoxin. *Tetrahedron: Asymmetry* **1994,** *5*, 909-910.

15. Andrews, R. C.; Teague, S. J.; Meyers, A. I. Asymmetric Total Synthesis of (-)-Podophyllotoxin+. *J. Am. Chem. Soc.* **1988,** *110*, 7854-7858.

16. San Feliciano, A.; Medarde, M.; Lopez, J. L.; Puebla, P.; Miguel del Corral, J. M.; Barrero, A. F. Lignans from *Juniperus thurifera*. *Phytochemistry* **1989,** *28*, 2863-2866.

17. Carpenter, C. D.; O'Neill, T.; Picot, N.; Johnson, J. A.; Robichaud, G. A.; Webster,

D.; Gray, C. A. Anti-mycobacterial natural products from the Canadian medicinal plant *Juniperus communis*. *J. Ethnopharmacol.* **2012,** *143*, 695-700.

18. Tanoguchi, M.; Arimoto, M.; Saika, H.; Yamaguchi, H. Studies on the constituents of the seeds of *Hernandia ovigera* L. VI. Isolation and structural determination of three lignans. *Chem. Pharm. Bull.* **1987,** *35*, 4162-4168.

19. Liu, Y.; Rakotondraibe, H.; Brodie, P. J.; Wiley, J. D.; Cassera, M. B.; Goetz, M.; Kingston, D. G. I. Antiproliferative and antimalarial sesquiterpene lactones from *Piptocoma antillana* from Puerto Rico. *Nat. Prod. Commun.* **2014,** *9*, 1403-1406.

20. Yamaguchi, H.; Arimoto, M.; Tanoguchi, M.; Ishida, T.; Inoue, M. Studies on the constituents of the seeds of *Hernandia ovigera* L. III. Structures of two new lignans. *Chem. Pharm. Bull.* **1982,** *30*, 3212-3218.

21. Sun, Y. J.; Li, Z. L.; Chen, H.; Liu, X. Q.; Zhou, W.; Hua, H. M. Three new cytotoxic aryltetralin lignans from *Sinopodophyllum emodi*. *Bioorg. Med. Chem. Lett.* **2011,** *21*, 3794-3797.

22. Zhao, C.; Nagatsu, A.; Hatano, K.; Shirai, N.; Kato, S.; Ogihara, Y. New lignan glycosides from Chinese medicinal plant, *Sinopodophillum emodi*. *Chem. Pharm. Bull.* **2003,** *51*, 255-261.

23. Gu, J. Q.; Park, E. J.; Totura, S.; Riswan, S.; Fong, H. H. S.; Pezzuto, J. M.; Kinghorn, A. D. Constituents of the twigs of *Hernandia ovigera* that inhibit the transformation of JB6 murine epidermal cells. *J. Nat. Prod.* **2002,** *65*, 1065-1068.

24. Klyne, W.; Stevenson, R.; Swan, R. J. Optical rotatory dispersion. XXVIII. Absolute configuration of otobain and derivatives. *J. Chem. Soc. C* **1966**, 893-896.

25. Swan, R. J.; Klyne, W.; MacLean, H. Optical rotatory dispersion studies. XLI.

The absolute configuration of plicatic acid. *Can. J. Chem.* **1967,** *45*, 319-324.

26. Atta-ur-Rahman.; Ashraf, M.; Choudhary, M. I.; Habib-ur-Rehman.; Kazmi, M. H. Antifungal aryltetralin lignans from leaves of *Podophyllum hexandrum*. *Phytochemistry* **1995,** *40*, 427-431.

27. Rai, K. M. L.; Basavaraju, Y. B.; Sadashivamurthy, B. Biological assay and antimitotic activity of novel analogues of β-apopicropodophyllin. *Indian J. Pharm. Sci.* **2007,** *69*, 116-118.

28. Gensler, W. J.; Gatsonis, C. D. The podophyllotoxin—picropodophyllin equilibrium. *J. Org. Chem.* **1966,** *31*, 3224-3227.

29. Liu, Y. Q.; Yang, L.; Tian, X. Podophyllotoxin: current perspectives. *Curr. Bioact. Compd.* **2007,** *3*, 37-66.

30. Middel, O.; Woerdenbag, H. J.; van Uden, W.; van Oeveren, A.; Jansen, J. F. G. A.; Feringa, B. L.; Konings, A. W. T.; Pras, N.; Kellogg, R. M. Synthesis and cytotoxicity of novel lignans. *J. Med. Chem.* **1995,** *38*, 2112-2118.

31. Lee, K. H.; Beers, S. A.; Mori, M.; Wang, Z. Q.; Kuo, Y. H.; Li, L.; Liu, S. Y.; Chang, J. Y.; Han, F. S.; Cheng, Y. C. Antitumor agents. 111. New 4-hydroxylated and 4-halogenated anilino derivatives of 4'-demethylepipodophyllotoxin as potent inhibitors of human DNA topoisomerase II. *J. Med. Chem.* **1990,** *33*, 1364-1368.

32. Dantzig, A.; LaLonde, R. T.; Ramdayal, F.; Shepard, R. L.; Yanai, K.; Zhang, M. Cytotoxic responses to aromatic ring and configurational variations in α-conidendrin, podophyllotoxin, and sikkimotoxin derivatives. *J. Med. Chem.* **2001,** *44*, 180-185.

33. Lee, K. H. Current developments in the discovery and deign of nw dug cndidates from pant natural product leads. *J. Nat. Prod.* **2004,** *67*, 273-283.

34. Srivastava, V.; Negi, A. S.; Kumar, J. K.; Gupta, M. M.; Khanuja, S. P. S. Plant-based anticancer molecules: A chemical and biological profile of some important leads. *Bioorg. Med. Chem.* **2005,** *13*, 5892-5908.

35. Liu, Y. Q.; Tian, J.; Qian, K.; Zhao, X. B.; Morris-Natschke, S. L.; Yang, L.; Nan, X.; Tian, X.; Lee, K. H. Recent progress on C-4-modified podophyllotoxin analogs as potent antitumor agents. *Med. Res. Rev.* **2015,** *35*, 1-62.

36. Gordaliza, M.; Castro, M. A.; Miguel Del Corral, J. M.; San Feliciano, A. Antitumor properties of podophyllotoxin and related compounds. *Curr. Pharm. Des.* **2000,** *6*, 1811-1839.

37. Cao, S.; Brodie, P. J.; Miller, J. S.; Randrianaivo, R.; Ratovoson, F.; Birkinshaw, C.; Andriantsiferana, R.; Rasamison, V. E.; Kingston, D. G. I. Antiproliferative xanthones of terminalia calcicola from the Madagascar rain forest. *J. Nat. Prod.* **2007,** *70*, 679-681.

38. Pan, E.; Harinantenaina, L.; Brodie, P., J.; Miller, J. S.; Callmander, M. W.; Rakotonandrasana, S.; Rakotobe, E.; Rasamison, V. E.; Kingston, D. G. I. Four Diphenylpropanes and a Cycloheptadibenzofuran from *Bussea sakalava* from the Madagascar Dry Forest. *J. Nat. Prod.* **2010,** *73*, 1792-1795.

39. Louie, K. G.; Behrens, B. C.; Kinsella, T. J.; Hamilton, T. C.; Grotzinger, K. R.; McKoy, W. M.; Winker, M. A.; Ozols, R. F. Radiation survival parameters of antineoplastic drug-sensitive and -resistant human ovarian cancer cell lines and their modification by buthionine sulfoximine. *Cancer Res.* **1985,** *45*, 2110-2115.

40. Bennett, T. N.; Paguio, M.; Gligorijevic, B.; Seudieu, C.; Kosar, A. D.; Davidson, E.; Roepe, P. D. Novel, rapid, and inexpensive cell-based quantification of antimalarial drug efficacy. *Antimicrob. Agents Chemother.* **2004,** *48*, 1807-1810.

41. Smilkstein, M.; Sriwilaijaroen, N.; Kelly, J. X.; Wilairat, P.; Riscoe, M. Simple and inexpensive fluorescence-based technique for high-throughput antimalarial drug screening. *Antimicrob. Agents Chemother.* **2004,** *48*, 1803-1806.

42. Rakotondraibe, L. H.; Graupner, P. R.; Xiong, Q.; Olson, M.; Wiley, J. D.; Krai, P.; Brodie, P. J.; Callmander, M. W.; Rakotobe, E.; Ratovoson, F.; Rasamison, V. E.; Cassera, M. B.; Hahn, D. R.; Kingston, D. G. I.; Fotso, S. Neolignans and other metabolites from *Ocotea cymosa* from the Madagascar rain forest and their biological activities. *J. Nat. Prod.* **2015**, Ahead of Print.

4 Antiproliferative and Antimalarial Sesquiterpene Lactones from *Piptocoma antillana* from Puerto Rico

This chapter is a slightly expanded version of a published article.[1] Attributions from co-authors of the articles are described as follows in the order of the names listed. The author of this disseration (Yixi Liu) conducted the isolation and structural elucidation part of the titled compounds, and drafted the manuscript. Dr. Harinantenaina was a mentor for this work, provided invaluable advice and hints for the structural elucidation of the compounds, and also proofread the manuscript before submission. Mrs. Peggy Brodie performed the A2780 bioassay on the isolated fractions and compounds. Dr. Jessica D. Wiley and Dr. Maria B. Cassera performed the Dd2 bioassay. Dr. Michael Goetz from Natural Products Discovery Institute provided the plant extract. Dr. David G. I. Kingston was a mentor for this work and the corresponding author for the published article. He provided critical suggestions for this work and crucial revisions to the manuscript.

4.1 Introduction

The genus *Piptocoma*, a member of the Asteraceae family, was first discovered in the West Indies, and consisted initially of only three species. The genus was expanded in 2000, when Pruski described the Central and South American plant species from the genus *Pollalesta* as cogeneric with *Piptocoma*, and this raised the number of *Piptocoma* species to eighteen.[2] A literature search demonstrated that the only reports on the chemical constituents of the genus *Piptocoma* were in the last two years, describing the isolation of cytotoxic sesquiterpene lactones, phenylpropanol coumarates, and flavonoids from *P. rufescens*.[3, 4]

Our ongoing screening of extracts from the Natural Products Discovery Institute collection as part of a collaborative research program to explore the potential of the former Merck collection of extracts[5] indicated that a CH_2Cl_2 extract of the leaves and twigs of *P. antillana* exhibited significant antiproliferative activity against the A2780 human ovarian cancer cell line. We report herein the bioassay-guided isolation and structure identification of the components responsible for the antiproliferative activity, as well as the antiplasmodial activity of the same compounds. (Figure 4.1)

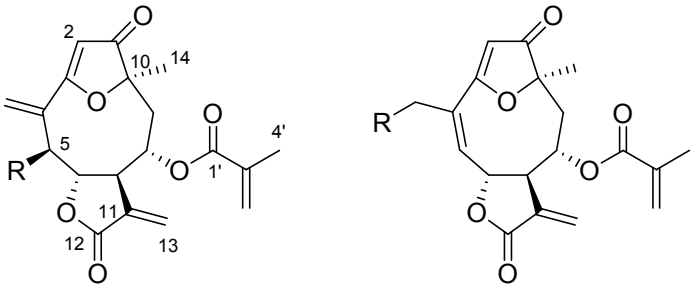

Figure 4.1 Structures of Compounds **4.1–4.4**

4.2 Results and discussion

4.2.1 Isolation of active compounds

An active CH_2Cl_2-soluble fraction obtained from liquid-liquid partition of the extract (100 mg) was subjected to dereplication studies using size-exclusion chromatography, reverse phase HPLC coupled with bioassay, high-resolution ESIMS (HRESIMS), ^{1}HNMR, and a database search using the online Dictionary of Natural Product (DNP). The results indicated that the extract contained at least one new bioactive

compound, and so a 2.0 g sample was investigated. Fractionation of this extract yielded an antiproliferative CH_2Cl_2 fraction which was further subjected to size-exclusion column chromatography on Sephadex LH-20 followed by normal phase silica gel column chromatography. The most active fractions from the silica gel column were subjected to C18 HPLC to yield two known (**4.1**, **4.2**) and two new (**4.3**, **4.4**) bioactive sesquiterpene lactones.

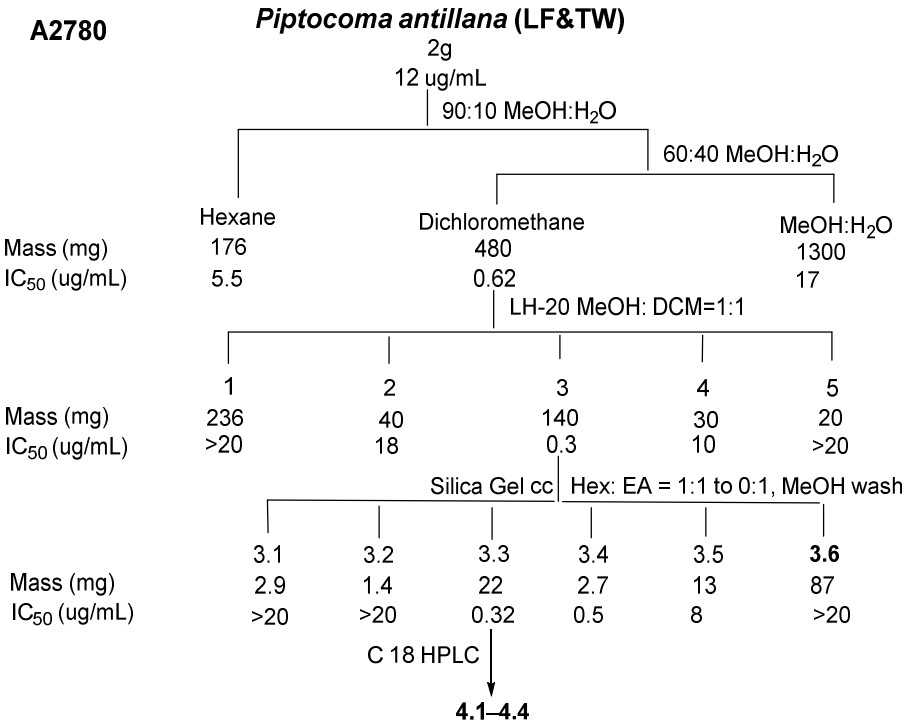

Scheme 4.1 Bioassay-guided Separation of *Piptocoma antillana*

4.2.2 Structure elucidation of compounds **4.1** and **4.2**

Compound **4.1** had the molecular formula $C_{19}H_{20}O_7$ as determined by high resolution electrospray ionization mass spectroscopy (HRESIMS) analysis. It was determined to be 5-epiisogoyazensolide (**4.1**) by searching its molecular formula and key

^{1}H NMR spectroscopic features in the DNP database and comparison of its full ^{1}H NMR spectrum with reported literature data.[6-8] Compound **4.2** was identified as 1-oxo-3,10-epoxy-8-(2-methylacryloxy)-15-acetoxy-germacra-2,4,11(13)-trien-6(12)-olide (15-acetylgoyazensolide) by comparison of its spectroscopic data with values reported in the literature.[9-11]

4.2.3 Structure elucidation of compound **4.3**

Compound **4.3** was obtained as an amorphous white powder and had the molecular formula $C_{20}H_{22}O_7$ as indicated by HRESIMS analysis (*m/z*: 375.1461 $[M+H]^+$, calcd. for $C_{20}H_{23}O_7^+$, 375.1438). Its IR spectrum showed absorptions characteristic of an α,β-unsaturated γ-lactone (1765 and 1640 cm^{-1}), γ-lactones typically have IR absorptions at about 1765 cm^{-1} due to the carbonyl resonance, and at 1640 cm^{-1} from the C=C stretch; an α,β-unsaturated ester (1710 and 1645 cm^{-1}), the appearance of the ester carbonyl stretch at 1710 cm^{-1} is due to the normal ester carbonyl resonance at 1740 cm^{-1} reduced to 1710 cm^{-1} by conjugation with the double bond; as well as a dihydrofuran-3-one ring (1709 and 1582 cm^{-1}), the appearance of the carbonyl stretch at 1709 cm^{-1} is due to the normal cyclopentanone carbonyl stretch at 1740 cm^{-1} reduced to 1709 by conjugation with the double bond.[3, 8, 9, 12] The similarity of the IR spectroscopic data of **4.3** with those of **4.1**, in conjunction with the UV absorption characteristics at λ_{max} 208 and 270 nm, suggested that **4.3** was also a furan ring-containing germacranolide similar to goyazensolide or furanoheliangolide.[8, 9, 12] Its ^{1}H NMR spectrum displayed signals for a methyl group at δ_H1.53 (s, 3H, CH_3-14), two exocyclic methylene groups as two doublets at δ_H 6.21 (*J*= 3.3 Hz, 1H) and 5.46 (*J*=2.9 Hz, 1H) and two singlets at δ_H6.00 and 5.78

(each 1H), representing (H_2-13 and H_2-15), and an olefinic proton at δ_H5.82 (s, 1H, H-2). These signals are all very similar to those in the goyazensolide skeleton of **4.1**. In the ^{13}C NMR spectrum, the presence of signals attributable to a conjugated ketone carbonyl at δ_C 204.4 ppm (C-1), a lactone carbonyl at δ_C 169.1(C-12), the carbons of an oxygen bearing alkene at δ_C 106.8 (C-2) and 185.9 (C-3) and of two exocyclic alkenes at δ_C 133.9 (C-11), 123.8 (C-13), 134.5 (C-4), and 127.1 (C-15), and three oxygen bearing methines at δ_C 84.5 (C-5), 85.1 (C-6), and 72.3 (C-8), supported the preliminary structural assignment.[11] In the HMBC experiment, protons at δ_H 6.00 and 5.78 correlated with both C-3 (δ_C 185.9) and C-5 (δ_C 84.5), which allowed us to assign the two olefinic protons to be those of H_2-15 (Fig. 2). In the same manner, the other pair of the exocyclic methylene protons at δ_H 6.21 and 5.46 were determined to be those of H_2-13 due to their correlations with δ_C 169.1(C-12) and δ_C 44.8(C-7). The ^1H and ^{13}C NMR spectra of **4.1** also revealed the expected signals from the goyazensolide methacrylate side chain, namely for a methyl group at δ_H1.82 (s, 3H, H-4'), two olefinic proton signals at δ_H 5.95 and 5.53 (m, 1H for each, H-3'), and four carbon resonances at δ_C 166.9 (C-1'), 135.4 (C-2'), 126.4 (C-3'), and 18.0 (C-4').[11] This assignment was confirmed by the HMBC correlations (Figure 4.2) between the proton signals of H-4' with both C-1' and C-3'. The acyl group was located at C-8 by the long range HMBC cross peak observed between the signals at δ_H 4.31 (ddd, *J* =11.8, 1.4, 1.3 Hz, 1H, H-8) and δ_C 166.9 (C-1'). The^1H spectrum of **4.3** contained an additional proton signal at δ_H3.73 (s, 3H) as compared with the spectrum of **4.1**. A carbon signal at δ_C 57.2 and a deshielded proton signal at δ_H 4.23 (H-5) confirmed the presence of a methoxyl group at C-5 in **4.3** as compared with the hydroxyl group of **4.1**. The HMBC correlation between δ_H3.73 (s, 3H) and δ_C 84.5 (C-5) substantiated the placement

of the methoxyl group at the C-5 position in **4.3**. The complete assignments of all protons and carbons of **4.3** (Table 4.1) were accomplished by further interpretation of the HMBC and NOESY spectra. The relative configurations at C-5, C-6, C-7, C-8, and C-10 of **4.3** were suggested by the analysis of a NOESY experiment (Figure 4.2).

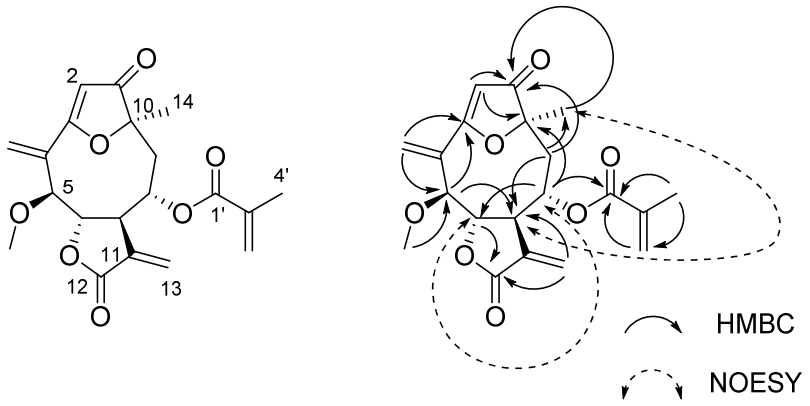

Figure 4.2 Key HMBC and NOESY Correlations of **4.3**

The absolute configuration at C-7 was determined to be *R* by the negative Cotton effects at 225 and 268 nm observed in its CD spectrum. This is consistent with previous studies demonstrating that sesquiterpene lactones with a C-7, C-6 trans-fused α-methylene-γ-lactone moiety display negative Cotton effects in the range of 216–225 and 252–271 nm in their CD spectra, arising from the π→π* and n→π* transitions of the lactone ring, respectively.[13-15] Compound **4.3** was thus assigned as (5*S*,6*S*,7*R*,8*S*,10*R*)-1-oxo-3,10-epoxy-5-methoxy-8-(2-methylacryloxy) germacra-2,4(15),11(13)-trien-6,12-olide,[16] or 5-*O*-methyl-5-epiisogoyazensolide.

4.2.4 Structure elucidation of compound **4.4**

Compound **4.4** was isolated as an amorphous white powder with a molecular formula of $C_{20}H_{22}O_7$ based on its HRESIMS spectrum. The close similarity of the UV, IR,

^{1}H and ^{13}C NMR spectroscopic data of **4.4** with those of **4.1** and **4.3** demonstrated that all three compounds contain the same goyazensolide skeleton with a methacrylate side chain at the C-8 position. Comparison of the ^{1}H NMR spectroscopic data of **4.4** with those of **4.2** indicated that the major differences between them were the lack of signals for the 15-

Table 4.1 ^{1}H and ^{13}C NMR Data (δ, ppm) for Compounds **4.3** and **4.4**

	4.3		**4.4**	
posn	δ_H[b]	δ_C[c]	δ_H[b]	δ_C[c]
1		204.4 C		204.6 C
2	5.82 s	106.8 CH	5.77 brs	106.4 CH
3		185.9 C		184.4 C
4		134.5 C		131.8 C
5	4.23 s	84.5 CH	6.27 dt (2.9, 1.4)	137.3 CH
6	4.74 d (5.2)	85.1 CH	5.33 ddt (5.5, 2.9, 1.4)	81.3 CH
7	4.21 m	44.8 CH	3.80 ddd (5.5, 3.2, 2.7)	50.9 CH
8	4.31 ddd (11.8, 1.4, 1.3)	72.3 CH	4.54 dt (11.8, 2.2)	73.2 CH
9	2.52 dd (13.7, 11.8)	44.6 CH_2	2.49 dd (13.9, 11.8)	43.9 CH_2
	2.33 dd (13.7, 1.4)		2.32 dd(13.9, 2.2)	
10		90.4 C		89.8 C
11		133.9 C		133.1 C
12		169.1 C		168.6 C
13	6.21 d (3.3)	123.8 CH_2	6.23 d (3.2)	124.6 CH_2
	5.46 d (2.9)		5.47 d (2.7)	
14	1.53 s	21.2 CH_3	1.54 s	20.7 CH_3
15	6.00 s	127.1 CH_2	4.16 ddd (12.8, 1.4, 1.3)	72.7 CH_2
	5.78 s		4.12 ddd (12.8,1.4, 1.3)	
1'		166.9 C		166.8 C
2'		135.4 C		135.3 C
3'	5.95 m	126.4 CH_2	6.01 brs	126.6 CH_2
	5.53 m		5.55 m	
4'	1.82 s	18.0 CH_3	1.83 s	18.0 CH_3
5-OMe	3.73 s	57.2 CH_3		
15-OMe			3.40 s	58.5 CH_3

acetyl group in **4.2** and the addition of signals at δ_H 3.40 (s, 3H) and δ_C 58.5 (15-OMe) for an *O*-methyl group. HMBC correlations from the H-15 with the methoxy carbon at δ_C 58.5 and from the methoxy protons δ_H 3.40 (s, 3H) with the deshielded oxygen bearing methylene carbon at δ_C 72.7 (C-15) confirmed that the methoxy group was at C-15 (Figure 4.3). As in the case of **4.3**, all proton and carbon signals of **4.4** were assigned by interpretation of the data obtained from HMBC and NOESY experiments (Table 4.1). In addition, comparison of the CD and NOESY spectrum of **4.4** with **4.3** indicated that both compounds have the same absolute configurations at their C6, C7, C8, and C10 stereogenic centers. Therefore, compound **4.4** was determined to be (6*S*,7*R*,8*S*,10*R*)-1-

oxo-3,10-epoxy-15-methoxy-8-(2-methylacryloxy)germacra-2,4(5),11(13)-trien-6,12-olide,[9] or 15-*O*-methylgoyazensolide.

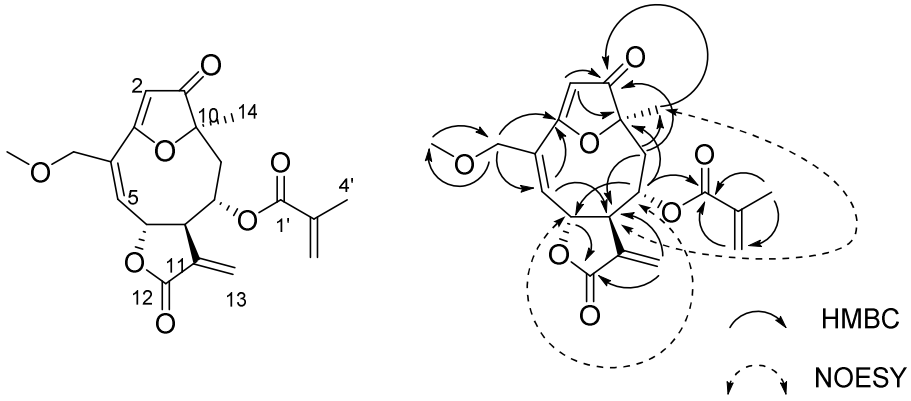

Figure 4.3 Key HMBC and NOESY Correlations of **4.4**

4.2.5 Bioactivities

Compounds **4.1**–**4.4** were evaluated for their antiproliferative activity against the A2780 human ovarian cancer cell line. They showed micromolar activities with half-maximum inhibitory concentration (IC_{50}) values of 1.56 ± 0.04, 1.62 ± 0.05, 1.5 ± 0.5, and 0.6 ± 0.3 μM, respectively. All the compounds were further evaluated for their antimalarial activity against *P. falciparum* Dd2 (a chloroquine/mefloquine-resistant strain), and showed IC_{50} values of 9.0 ± 0.6, 8.0 ± 0.4, 6.2 ± 0.5, and 2.2 ± 0.5 μM, respectively.

4.3 Experimental Section

4.3.1 General experimental procedures

IR and UV spectra were measured on MIDAC M-series FTIR and Shimadzu UV-1201 spectrophotometers, respectively. ^{1}H and ^{13}C NMR spectra were recorded on a Bruker Avance 500 spectrometer in $CDCl_3$, with $CDCl_3$ as reference. Mass spectra were

obtained on an Agilent 6220 mass spectrometer. Open column chromatography was performed using Sephadex LH-20 and silica gel (230-400 mesh, Silicycle Co. USA). Semi-preparative HPLC was performed using Shimadzu LC-10AT pumps coupled with a semipreparative Phenomenex C18 column (5 μm, 250 × 10 mm), a Shimadzu SPD M10A diode array detector, and a SCL-10A system controller. All isolated compounds were purified to 95% purity or better, as judged by HPLC (both UV and ELSD detection) before determining bioactivity.

4.3.2 Plant material

Leaves and twigs of *P. antillana* Urb were collected by Hannah Stevens of the New York Botanical Garden near Manatí, Puerto Rico (18º4.385 N, 66º54.382 W). A voucher specimen is on deposit at the NYBG under the accession number HS 00246a.

4.3.3 Extraction and isolation

The dried and powdered leaves and twigs of *P. antillana* were exhaustively extracted with ethanol in two 24-hour percolation steps; successive partition of the concentrated extract with hexane and methylene chloride gave an active methylene chloride extract. For purposes of fractionation and purification, 2.0 g of the original ethanol extract designated 1000892-7G (IC_{50} 12 μg/mL) was suspended in 90% aq. MeOH (300 mL), and extracted with hexanes (3 × 200 mL). Evaporation of the hexane-soluble fraction afforded 176 mg of residue. The 90% aq. MeOH layer was then diluted to 60% and extracted with CH_2Cl_2 (3 × 200 mL) to yield 479 mg of CH_2Cl_2-soluble fraction. The aqueous MeOH layer was concentrated to give 1.3 g of brown residue. The CH_2Cl_2 fraction was found to have antiproliferative activity with an IC_{50} value of 0.62

µg/mL, and was subjected to Sephadex LH-20 open column chromatography (CH_2Cl_2:MeOH, 1:1) to give 5 fractions. The most active fraction Fr 3 (IC_{50} 0.5 µg/mL) was then divided into six sub-fractions by silica gel column chromatography (hexanes:EtOAc, 1:1). Further purification of the most active sub-fraction Fr 3-4 (IC_{50}0.3 µg/mL) was done by using HPLC on a C-18 column with a solvent gradient from H_2O:CH_3CN, 70:30 to 68:32 from 0 to 30 min, to 58:42 from 30 to 60 min, and ending with 100% $CH_3CN$from 60 to 80 min. This process yielded compounds **4.1** (2.5 mg, t_R31 min), **4.4** (1.5 mg, t_R60 min), **4.3** (1.1 mg, t_R 64.5 min), and **4.2** (1.2 mg, t_R66 min).

4.3.4 5-*O*-Methyl-5-epiisogoyazensolide (**4.1**)

Amorphous powder; $[\alpha]^{21}_D$ -95.6 (*c* 0.27, MeOH); UV (MeOH) λ_{max} (log ε): 270 (2.20), 208 (3.89) nm; IR (film) ν_{max} 1765, 1710, 1709, 1645, 1640, 1582, 1454 cm^{-1}; ECD (*c* 0.031, MeOH) λ_{max} (Δε) 206 (+10), 225 (-4.0), 268 (-4.2), 320 (+2.5); ^1H and ^{13}C NMR data, see Table 4.1; HRESIMS *m/z* $[M+H]^+$ 375.1461 (calcd for $C_{20}H_{23}O_7^+$ 375.1438)

4.3.5 5-*O*-Methylgoyazensolide (**4.2**)

Amorphous powder; $[\alpha]^{21}_D$ -121.8 (*c* 0.27, MeOH); UV (MeOH) λ_{max} (log ε) : 267 (2.67), 207 (4.01) nm; IR (film) ν_{max} 1769, 1710, 1709, 1653, 1587, 1456 cm^{-1}; ECD (*c* 0.031, MeOH) λ_{max} (Δε) 203 (+5.7), 216 (-1.8), 276 (-2.3), 318 (+2.9); ^1H and ^{13}C NMR data, see Table 4.1. HRESIMS *m/z* $[M+H]^+$ 374.1459 (calcd for $C_{20}H_{23}O_7^+$, 375.1438)

4.3.6 Antiproliferative bioassay

The A2780 ovarian cancer cell line antiproliferative bioassay was performed at Virginia Tech as previously reported.[17] The A2780 cell line is a drug-sensitive ovarian cancer cell line.[18] Paclitaxel was used as the positive control; it had an IC_{50} value of 0.024 μM.

4.3.7 Antimalarial bioassay

The effect of each compound on parasite growth of the Dd2 strain of *P. falciparum* was measured in a 72 h growth assay in the presence of compound as described previously with minor modifications.[19, 20] Briefly, ring stage parasite cultures (1% hematocrit and 1% parasitemia) were grown for 72 h in the presence of increasing concentrations of the drug in a 5.05% CO_2, 4.93% O_2, and 90.2% N_2 gas mixture at 37 °C. After 72 h in culture, parasite growth was determined by DNA quantitation using SYBR Green I.[31] The half-maximal inhibitory concentration (IC_{50}) calculation was performed with GraFit software using a nonlinear regression curve fitting. IC_{50} values are the average of three independent determinations with each determination in duplicate and are expressed ± SD. Artemisinin was used as the positive control; it had an IC_{50} value of 7 nM.

4.4 References

1. Liu, Y.; Rakotondraibe, H.; Brodie, P. J.; Wiley, J. D.; Cassera, M. B.; Goetz, M.; Kingston, D. G. I. Antiproliferative and antimalarial sesquiterpene lactones from Piptocoma antillana from Puerto Rico. *Nat. Prod. Commun.* **2014,** *9*, 1403-1406.

2. Pruski, J. F. Compositae of the Guayana highland—X. Reduction of Pollalesta to Piptocoma (Vernonieae: Piptocarphinae) and consequent nomenclatral adjustments *Noron* **1996,** *6*, 96-102.

3. Ren, Y.; Acuna, U. M.; Jimenez, F.; Garcia, R.; Mejia, M.; Chai, H.; Gallucci, J. C.; Farnsworth, N. R.; Soejarto, D. D.; Carcache, d. B. E. J.; Kinghorn, A. D. Cytotoxic and NF-κB inhibitory sesquiterpene lactones from *Piptocoma rufescens*. *Tetrahedron* **2012,** *68*, 2671-2678.

4. Ren, Y.; Jimenez, F.; Garcia, R.; Mejia, M.; Chai, H.; Farnsworth, N. R.; Soejarto, D. D.; Kinghorn, A. D. A cytotoxic dimeric furanoheliangolide from *Piptocoma rufescens*. *Tetrahedron Lett.* **2013,** *54*, 5457-5460.

5. Trinh, T. T. V.; Pham, V. C.; Doan, T. M. H.; Nguyen, V. H.; Chau, V. M.; Litaudon, M.; Gueritte, F. Cytotoxic aryltetralin lignans from fruits of Cleistanthus indochinensis. *Planta Med.* **2014,** *80*, 695-702.

6. Devi, J. C.; Pai, K. V. K. Chemical examination of fruits of Cleistanthus collinus. *Pharma Chem.* **2011,** *3*, 160-164.

7. Wolfender, J. L.; Ndjoko, K.; Hostettmann, K. The potential of LC-NMR in phytochemical analysis. *Phytochem. Anal.* **2001,** *12*, 2-22.

8. Delgado, G.; Romo, d. V. A.; Herz, W. Sesquiterpene lactones from *Viguiera species*. *Phytochemistry* **1982,** *21*, 1305-1308.

9. Batistada, C. F.; Dias, D. A.; Lopes, J. L. C.; Vichnewski, W. Flavonoids and heliangolides from *Lychnophora diamantinana*. *Phytochemistry* **1993,** *34*, 261-263.

10. Soares, A. C. F.; Silva, A. N.; Matos, P. M.; Henrique, d. s. E.; Heleno, V. C. G.; Lopes, N. P.; Lopes, J. L. C.; Sass, D. C. Complete 1H and 13C NMR structural assignments for a group of four goyazensolide-type furanoheliangolides. *Quim. Nova* **2012,** *35*, 2205-2209.

11. Lunardello, M. A.; Tomaz, J. C.; Vichnewski, W.; Lopes, J. L. C. Sesquiterpene lactones and flavonoids from *Eremanthus mattogrossensis* and *Eremanthus eriopus*. *J. Braz. Chem. Soc.* **1995,** *6*, 307-3011.

12. Herz, W.; Kumar, N. Sesquiterpene lactones of Calea zacatechichi and C. urticifolia. *Phytochemistry* **1980,** *19*, 593-597.

13. Youssef, D.; Frahm, A. W. Circular dichroism of C-7, C-6 trans-fused guaianolides of *Centaurea scoparia*. *Phytochemistry* **1996,** *41*, 1107-1111.

14. Stoecklin, W.; Waddell, T. G.; Geissman, T. A. Circular dichroism and optical rotatory dispersion of sesquiterpene lactones. *Tetrahedron* **1970,** *26*, 2397-2409.

15. Waddell, T. G.; Stoecklin, W.; Geissman, T. A. Circular dichroism of sesquiterpene lactones. *Tetrahedron Lett.* **1969**, 1313-1316.

16. Valdes, D. A.; Bardon, A.; Catalan, C. A. N.; Gedris, T. E.; Herz, W. Goyazensolides and isogoyazensolides from Argentine *Centratherum punctatum ssp. punctatum*. *Biochem. Syst. Ecol.* **1998,** *26*, 805-808.

17. Parasuraman, S.; Raveendran, R. Diuretic effects of cleistanthin A and cleistanthin B from the leaves of *Cleistanthus collinus* in wistar rats. *J. Young Pharm.* **2012,** *4*, 73-77.

18. Kovendan, K.; Arivoli, S.; Maheshwaran, R.; Baskar, K.; Vincent, S. Larvicidal

efficacy of *Sphaeranthus indicus*, *Cleistanthus collinus* and *Murraya koenigii* leaf extracts against filarial vector, Culex quinquefasciatus Say (Diptera: Culicidae). *Parasitol Res* **2012,** *111*, 1025-1035.

19. Thanh, V. T. T.; Pham, V. C.; Nguyen, H. H.; Mai, H. D. T.; Minh, H. N. T.; Nguyen, V. H.; Litaudon, M.; Gueritte, F.; Chau, V. M. Cleistanone: A triterpenoid from *Cleistanthus indochinensis* with a new carbon skeleton. *Eur. J. Org. Chem.* **2011,** *2011*, 4108-4111.

20. Parasuraman, S.; Raveendran, R. Effect of cleistanthin A and B on adrenergic and cholinergic receptors. *Pharmacogn. Mag.* **2011,** *7*, 243-247.

5 Bioactive Compounds from *Stuhlmannia moavi* from the Madagascar Dry Forest

This chapter is a slightly expanded version of a s a published article.[1] Attributions from co-authors of the articles are described as follows in the order of the names listed. The author of this dissertation (Yixi Liu) conducted the isolation and structural elucidation part of the titled compounds, and drafted the manuscript. Dr. Harinantenaina was a mentor for this work, provided invaluable advice and hints for the structural elucidation of the compounds, and also proofread the manuscript before submission. Mrs. Peggy Brodie performed the A2780 bioassay on the isolated fractions and compounds. Dr. Jessica D. Wiley and Dr. Maria B. Cassera performed the Dd2 bioassay. Dr. Carla Slebodnick screened the X-ray crystal sample. Dr. Martin W. Callmander and Dr. Richard Randrianaivo from Missouri Botanical Garden collected the plant, and Dr. Chris Birkinshawand and Dr. Wendy Applequist provided clarification of a confused taxonomy. Dr. Etienne Rakotobe and Dr. Vincent E. Rasamison from Madagascar carried out the initial plant extraction. Dr. David G. I. Kingston was a mentor for this work and the corresponding author for the published article. He provided critical suggestions for this work and crucial revisions to the manuscript.

5.1 Introduction

As a part of the Madagascar International Cooperative Biodiversity Group (ICBG) program,[2, 3] an ethanol extract of the leaves of a plant initially identified as an *Eligmocarpus* sp. was selected for evaluation as a possible source of new antiproliferative agents based on its activity against the A2780 ovarian cancer cell line. The final identification of the plant proved to be a botanical challenge. Although it was initially

identified in the field as a species of *Eligmocarpus*, it was then reidentified as *Bussea sakalava* Du Puy & R. Rabev., and was finally classified as *Stuhlmannia moavi* Taub. (synonym: *Caesalpinia insolita* (Harms) Brenan & J.B. Gillett) (Leguminosae).[4]

The largely tropical genus *Caesalpinia,* a member of the informal Caesalpinia group[5] in the Leguminoseae family, traditionally comprises up to 150 species, although *Caesalpinia* sensu stricto is now considered to comprise only about a dozen species.[6] Seventeen species of the genus *Caesalpinia*, as circumscribed in its broadest sense, have been found in China, and some of them have been used for the treatment of rheumatism and inflammatory diseases in Chinese traditional medicine.[7] Triterpenes, flavonoids and other compounds have been isolated from plants of the genus *Caesalpinia* sensu lato,[8, 9] and 5-hydroxy-1,4-naphthoquinone has been isolated from the Asian species *C. sappan*.[10] The genus is also a rich source of cassane-type diterpenes,[11, 12] which have been reported to have significant antimalarial,[13] antibacterial,[14] antihelmintic,[15] antiproliferative and antineoplasmic activities.[16, 17] *Caesalpinia* is one of 21 genera included in the Caesalpinia group of legumes,[5] a group of genera that includes the East African and Madagascan monospecifc genus *Stuhlmannia.*[5, 18] The only previous chemical studies on the genus *Stuhlmannia* led to the isolation of some antimicrobial furanoid diterpenes.[19]

We describe herein the isolation and structure elucidation of the new bioactive 1,4-naphthoquinone stuhlmoavin (**5.1**) and several other bioactive compounds (Fig. 5.1).

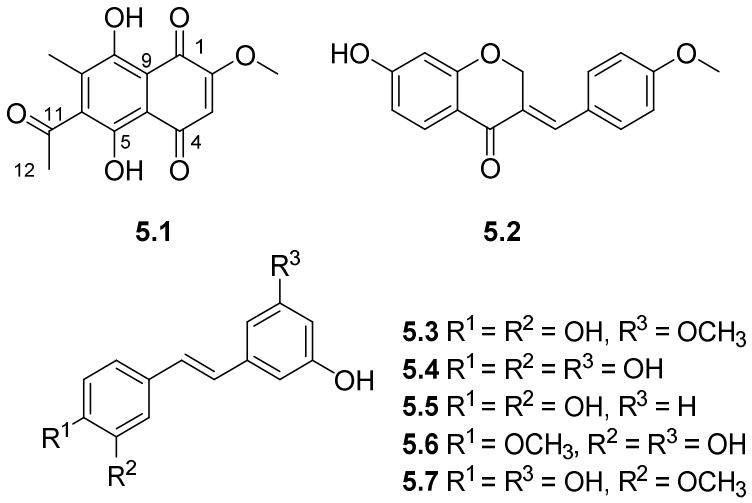

Figure 5.1 Structures of Compounds from *Stuhlmannia moav.*

5.2 Results and Discussion

5.2.1 Isolation of active compounds

Bioassay-guided isolation of the root extract of *S. moavi* furnished the known isoflavonoid bonducellin (**5.2**), together with the five known stilbenoids 3,4,5'-trihydroxy-3'-methoxy-trans-stilbene (**5.3**),[20] piceatannol (**5.4**),[21, 22] resveratrol (**5.5**),[23] rhapontigenin (**5.6**),[24] and isorhapontigenin (**5.7**).[24] The structures of compounds **5.2**–**5.7** were determined by comparison of their ^{1}H NMR and mass spectra with literature data. Compound **5.1** showed moderate A2780 activity, compounds **5.2**–**5.5** showed weak A2780 activities, and compounds **5.1**– **5.3** also showed weak antimalarial activities against the Dd2 drug-resistant strain of *Plasmodium falciparum*. (Scheme 5.1)

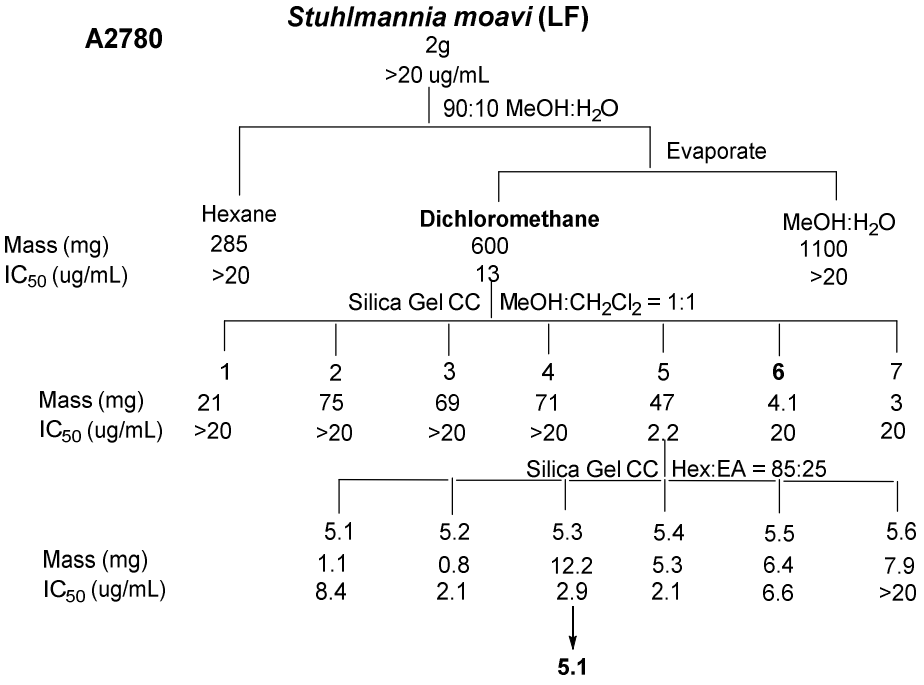

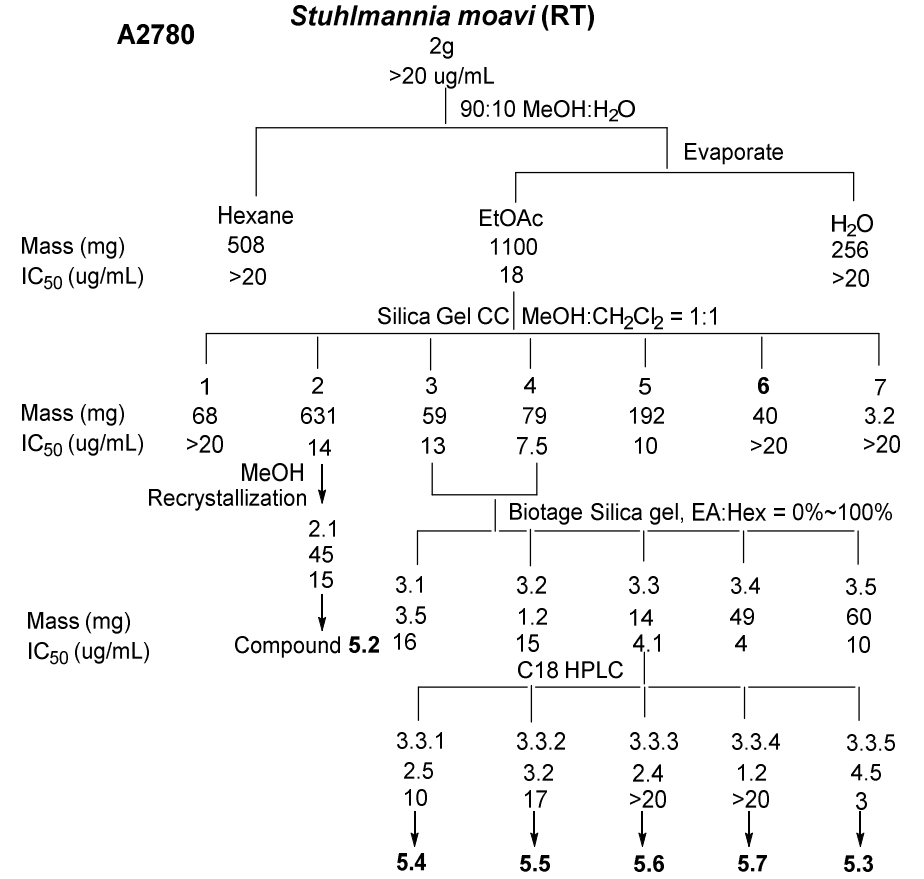

Scheme 5.1 Bioassay-guided Separation of *Stuhlmannia moavi*

5.2.2 Structure elucidation of compound **5.1**

Compound **5.1** (red needles) had the molecular formula $C_{14}H_{12}O_6$, as indicated by high-resolution ESIMS analysis (*m/z* 277.0729 [M+H]+, calcd. 277.0712). The IR spectrum showed absorptions characteristic of ketone (1708 cm^{-1}) and chelated hydroxyl (3384 cm^{-1}) functions as well as quinone carbonyl groups (1609 and 1564 cm^{-1}).[25, 26] The ^1H NMR data (Table 5.1) displayed resonances due to aromatic methyl (δ_H 2.22, s, 3H), acetyl methyl (δ_H 2.57, s, 3H), methoxy (δ_H 3.95, s, 3H), and aromatic methine (δ_H 6.19, s, 1H) groups. Two additional deshielded broad singlets at δ_H 12.63 (s, 1H) and δ_H 12.90 (s, 1H) indicated the presence of two hydrogen bonded hydroxyl groups in **5.1**. The ^1H NMR signals, taken in conjunction with the UV absorption spectrum, suggested that **5.1** had a 1,4-naphthoquinone skeleton with two peri-substituted hydroxyl groups.[26, 27] The ^{13}C NMR spectrum of **5.1** (Table 5.1) exhibited 14 carbon signals, and the ^{13}C DEPT NMR spectrum showed signals due to two methyl groups (δ_C 12.7, δ_C 31.8), one methoxy group (δ_C 56.9), and one methine (δ_C 110.7).

The 10 remaining quaternary carbon signals in the ^{13}C NMR spectrum corresponded to an acetyl carbonyl group (δ_C 202.0), two quinone carbonyl groups (δ_C 186.7 and 181.3), three oxygen bearing aromatic carbons at δ_C 158.9, 154.5, and 160.8, and four signals for more shielded carbons at δ_C 110.3, 135.5, 108.9, and 110.7, corresponding to an aromatic methine, a methylated aromatic carbon, and the two bridgehead carbons of the naphthoquinone skeleton. In the HMBC experiment (Figure 5.2), the correlations between δ_H 12.63 (OH-8) and δ_C 158.9, and δ_H 12.90 (OH-5) and δ_C 154.5, suggested that the two carbons were at the 8 and 5 positions, respectively.

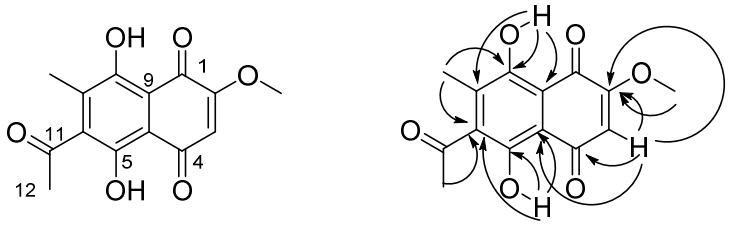

Figure 5.2 Key HMBC correlations of **5.1**

The HMBC correlations between the proton signals of the methyl group at δ_H 2.57 (CH_3-12) and both the carbonyl carbon at δ_C 202.0 (C-11) and the aromatic carbon at δ_C 142.1 (C-6), together with the long range HMBC correlation between δ_H 12.90 (OH-5) and δ_C 142.1 (C-6), indicated the attachment of an acetyl group at the C-6 position. In addition, the methyl group was assigned to C-7 based on the long-range correlations (Fig. 5.2) observed between the signal at δ_H 2.22 and δ_C 142.1 (C-6), δ_C 135.5 (C-7), and δ_C 158.9 (C-8). Furthermore, the signals for the deshielded hydroxyl groups OH-1 and OH-4 also correlated with carbon signals at δ_C 110.7 and δ_C 108.9, which were assigned to the two bridgehead carbons at C-9 and C-10, respectively. In the same manner, the methine group at the C-3 position was confirmed by observation of the HMBC long range correlation between δ_H 6.19 (H-3) and C-10 (δ_C 108.9). Moreover, the signal at H-3 correlated with both of the two quinone carbonyl groups at δ_C 181.3 and δ_C 186.7, which were assigned to C-4 and C-1. The methoxy group was assigned to C-2 (δ_C 160.8), which agrees with the correlation between δ_H 3.95 and δ_C 160.8 in the HMBC experiment. Compound **5.1** was thus deduced to be 6-acetyl-2-methoxy-7-methyl-1,4-naphthoquinone and has been named stuhlmoavin.

Table 5.1 ^{1}H and ^{13}C NMR Data (δ, ppm) for Compound **5.1** (500 and 125 MHz)

position	δ_H[a]	δ_C (DEPT)[a]
1		186.7 (C)[b]
2		160.8 (C)
3	6.19 s	110.3 (CH)
4		181.3 (C)[b]
5		154.5 (C)
6		142.1 (C)
7		135.5 (C)
8		158.9 (C)
9		110.7 (C)
10		108.9 (C)
11		202.0 (C)
12	2.57 s	31.8 (CH_3)
2-OCH_3	3.95 s	56.9 (CH_3)
7-CH_3	2.22 s	12.7 (CH_3)
5-OH	12.90 s	
8-OH	12.63 s	

[a]In $CDCl_3$. Assignments based on HMBC
[b]These signals may be exchanged

The proposed structure of **5.1** was confirmed by single-crystal X-ray diffraction analysis (Fig. 5.3).

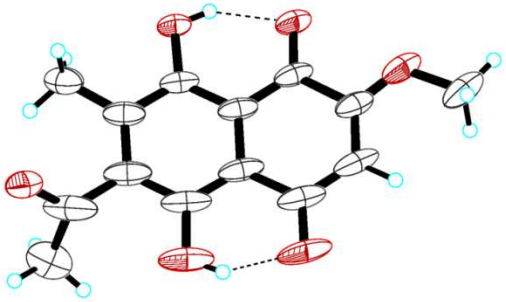

Figure 5.3 Anisotropic Displacement Ellipsoid Drawing of Compound **5.1**.

5.2.3 Biological activities

Compounds **5.1**–**5.5** showed antiproliferative activity against the A2780 human ovarian cancer cell line. Among the seven compounds isolated, **5.1** showed moderate activity with an IC_{50} value of 8.1 ± 0.4 μM. Compounds **5.2**–**5.5** showed weaker

activities with IC_{50} values of 10.6 ± 0.4 μM, 54 ± 1 μM, 41 ± 1 μM, and 74 ± 1 μM, respectively. Compounds **5.1**–**5.5** were also evaluated for antimalarial activity against *Plasmodium falciparum* Dd2 (a chloroquine/mefloquine-resistant strain), and compounds **5.1**–**5.3** showed moderate activities with IC_{50} values of 24 ± 7, 26 ± 3, and 27 ± 2 μM, respectively.

5.3 Experimental

5.3.1 General experimental procedures

IR and UV spectra were measured on MIDAC M-series FTIR and Shimadzu UV-1201 spectrophotometers, respectively. ^{1}H and ^{13}C NMR spectra were recorded on a Bruker Avance 500 spectrometer in $CDCl_3$ with TMS as internal standard. Mass spectra were obtained on an Agilent 6220 mass spectrometer. Open column chromatography was performed using Sephadex LH-20 and silica gel (230-400 mesh, Silicycle Co. USA). Flash chromatography was performed on a Biotage Horizon flash chromatograph using a C18 column (Phenomenex, 150 x 12 mm, 11 g). Semi-preparative HPLC was performed using Shimadzu LC-10AT pumps coupled with a semipreparative Phenomenex C18 column (5 μm, 250 × 10 mm), a Shimadzu SPD M10A diode array detector, and a SCL-10A system controller. All isolated compounds were purified to 95% purity or better, as judged by HPLC and by NMR (both UV and ELSD detection) before determining bioactivity. The HPLC chromatograms and NMR spectra can be found in the Supplementary Data.

5.3.2 Plant material

Leaves and roots of *Stuhlmannia moavi* Taub.[4] Brenan and Gillett[3] collected in dry forest 3 km north of Tsaratanana in the Sava locality, Daraina, in northern Madagascar The sample was from a tree 12 m high, 30 cm DBH, with yellow flowers and orange anthers. The tree is common in this location. It was identified as *Stuhlmannia moavi* Taub. (synonyms: C. insolita (Harms) Brenan & J.B. Gillett, from Madagascar and *Caesalpinia dalei* Brenan & J.B. Gillett, from East Africa) by comparison with the literature,[3,4] and by matching photographs taken in the field with herbarium specimens housed in the collections of the Royal Botanic Gardens, Kew.

5.3.3 Extraction and isolation

A ground sample of *Stuhlmannia moavi* leaves (309 g) was extracted with EtOH at room temperature to yield 27.9 g of crude EtOH extract designated MG 4425. A total of 5.64 g of this extract was made available to Virginia Tech. The crude EtOH extract (2.0 g) was dissolved in 90% aq. MeOH (300 mL), and extracted with hexanes (3 × 200 mL). Evaporation of the hexane-soluble fraction afforded 285 mg of residue. The 90% aq. MeOH layer was then evaporated, suspended in H_2O (300 mL), and extracted with EtOAc (3 × 200 mL) to yield 600 mg of EtOAc-soluble fraction. The aqueous layer was concentrated to give 1.1 g of brown residue. The hexanes fraction was found to be cytotoxic with an IC_{50} value of 13 µg/mL and was subjected to Sephadex LH-20 open column chromatography (CH_2Cl_2:MeOH, 1:1) to give 7 fractions. Further purification of the most active fraction (IC_{50} 3.2 µg/mL) furnished the major and most active compound **5.1** (5.8 mg) with an IC_{50} of 2.6 µg/mL.

A ground sample of *S. moavi* roots (335 g) was extracted with EtOH at room temperature to yield 19.6 g of crude EtOH extract designated MG 4423. A total of 4.36 g of this extract was made available to Virginia Tech. A part of the crude EtOH extract (2.0 g) was dissolved in 90% aq. MeOH (300 mL) and extracted with hexanes (3 × 200 mL). Evaporation of the hexanes-soluble fraction yielded 508 mg of residue. The 90% aq. MeOH layer was then evaporated, suspended in H_2O (300 mL), and extracted with EtOAc (3 × 200 mL) to yield 1.106 mg of EtOAc-soluble fraction. The aqueous layer was concentrated to give 256 mg of brown residue. The EtOAc fraction was found to be weakly cytotoxic with an IC_{50} value of 18 µg/mL and was subjected to Sephadex LH-20 open column chromatography (CH_2Cl_2: MeOH = 1:1) to give 7 fractions. Compound **5.2** (10.1 mg) was crystallized from MeOH from the second fraction. The third fraction from the Sephadex column (IC_{50} 13 µg/mL) was further fractionated using a C18 flash chromatograph column to yield 5 fractions. The third subfraction was subjected to HPLC on a C18 column with a solvent gradient from H_2O:MeOH, 55:45 (for 30 min), to 40:60 from 30 to 35 min, to 0:100 from 35 to 40 min, and ending with 100% MeOH to 55 min. This process yielded compounds **5.4** (2.5 mg, t_R 14 min), **5.5** (3.2 mg, t_R 23.8 min), **5.6** (2.4 mg, t_R 26.5 min), **5.7** (1.2 mg, t_R 32 min) and **5.3** (4.5 mg, t_R 41.5 min).

5.3.4 Stuhlmoavin (**5.1**)

Red crystals; mp 185 °C; UV λ_{max} (MeOH) (log ε): 217 (4.11), 296 (3.54), 492 (3.27) nm; IR ν_{max} 3384, 1708, 1609 and 1564 cm^{-1}; ^1H and ^{13}C NMR data, see Table 5.1; HRESIMS *m/z* $[M+H]^+$ 277.0729 (calcd for $C_{14}H_{14}O_6^+$, 277.0712).

5.3.5 X-ray crystallography of **5.1**

A red needle (0.01 x 0.04 x 0.62 mm^3) was centered on the goniometer of an Agilent SuperNova A diffractometer operating with CuKα radiation. The data collection routine, unit cell refinement, and data processing were carried out with the program CrysAlisPro.[28] The Laue symmetry and systematic absences were consistent with the monoclinic space group *P2₁/n.* The structure was solved using SHELXS-97[29] and refined using SHELXL-97 via OLEX2.[30] The final refinement model involved anisotropic displacement parameters for non-hydrogen atoms and a riding model for all hydrogen atoms. A 2-position disorder model was used for the ketone oxygen with relative occupancies that refined to 0.490(13) and 0.510(13). The relatively poor refinement statistics and elongated displacement parameters are attributed to the small size and high mosaicity of the crystal. Crystal data: $C_{14}H_{12}O_6$, M_r =276.24, monoclinic, *P2₁/n,* a = 4.9896(3) Å, b = 23.446(3) Å, c = 10.5394(7) Å, α = 90°, β = 100.893(6)°, γ = 90°, V = 1210.73(18) $Å^3$, 9071 reflections, 196 parameters; crystal size 0.62 x 0.04 x 0.01 mm^3. The final indices were R_1 = 0.0803, wR_2 = 0.2080 [I>2σ(I)]. Crystallographic data for compound 1 have been deposited as Supporting Information at the Cambridge Crystallographic Data Centre (deposition no. CCDC 919140).[31]

5.3.6 Antiproliferative bioassay

A2780 ovarian cancer cell line antiproliferative bioassay was performed at Virginia Tech as previously reported.[32] The A2780 cell line is a drug-sensitive ovarian cancer cell line.[33] Paclitaxel was used as the positive control; it had an IC_{50} value of 0.024 μM.

5.3.7 Antimalarial bioassay

The effect of each compound on parasite growth of the Dd2 strain of *P. falciparum* was measured in a 72 h growth assay in the presence of compound as described previously with minor modifications.[34, 35] Briefly, ring stage parasite cultures (200 μL per well, with 1% hematocrit and 1% parasitemia) were grown for 72 h in the presence of increasing concentrations of the drug in a 5.05% CO_2, 4.93% O_2, and 90.2% N_2 gas mixture at 37 °C. After 72 h in culture, parasite viability was determined by DNA quantitation using SYBR Green I (50 μL of SYBR Green I in lysis buffer at 0.4 μL of SYBR Green I/mL of lysis buffer).[31] The half-maximum inhibitory concentration (IC_{50}) calculation was performed with GraFit software using a nonlinear regression curve fitting. IC_{50} values are the average of three independent determinations with each determination in duplicate and are expressed ± SEM. Artemisinin was used as the positive control; it had an IC_{50} value of 7 nM.

5.4 References

1. Liu, Y.; Harinantenaina, L.; Brodie, P. J.; Bowman, J. D.; Cassera, M. B.; Slebodnick, C.; Callmander, M. W.; Randrianaivo, R.; Rakotobe, E.; Rasamison, V. E.; Applequist, W.; Birkinshaw, C.; Lewis, G. P.; Kingston, D. G. I. Bioactive compounds from *Stuhlmannia moavi* from the Madagascar dry forest. *Bioorg. Med. Chem.* **2013,** *21*, 7591-7594.

2. Cao, S.; Kingston, D. G. I. Biodiversity conservation and drug discovery: Can they be combined? The Suriname and Madagascar experiences. *Pharm. Biol.* **2009,** *47*, 809 – 823.

3. Kingston, D. G. I. Modern natural products drug discovery and its relevance to biodiversity conservation. *J. Nat. Prod.* **2011,** *74*, 496-511.

4. Brenan, J. P. M. Notes on African Caesalpinioïdeae. *Kew Bull.* **1963,** *17*, 197-218.

5. Lewis, G. In *Legumes of the World*, Lewis, G.; Schrire, B.; Mackinder , B.; Lock, M., Eds. Royal Botanic Gardens: Kew, UK, 2005; pp 127-161.

6. Gagnon, E.; Lewis, G. P.; Solange Sotuyo, J.; Hughes, C. E.; Bruneau, A. A molecular phylogeny of *Caesalpinia* sensu lato: Increased sampling reveals new insights and more genera than expected. *S. Afr. J. Bot.* **2013**, in press.

7. Wu, M.; Wang, Y. F.; Zhang, M. L.; Huo, C. H.; Dong, M.; Shi, Q. W.; Kiyota, H. Chemical constituents of plants from the genus *Caesalpinia*. *Chem. Biodivers* **2011,** *8*, 1370-1399.

8. Woldemichael, G. M.; Singh, M. P.; Maiese, W. M.; Timmermann, B. N. Constituents of antibacterial extract of *Caesalpinia paraguariensis* Burk. *Z. Naturforsch. (C)* **2003,** *58*, 70-75.

9. Srinivas, K. V. N. S.; Koteswara, R. Y.; Mahender, I.; Das, B.; Rama, K. K. V. S.; Hara, K. K.; Murty, U. S. N. Flavanoids from *Caesalpinia pulcherrima*. *Phytochemistry* **2003,** *63*, 789-793.

10. Lim, M. Y.; Jeon, J. H.; Jeong, E. Y.; Lee, C. H.; Lee, H. S. Antimicrobial activity of 5-hydroxy-1,4-naphthoquinone isolated from *Caesalpinia sappan* toward intestinal bacteria. *Food Chem.* **2006,** *100*, 1254-1258.

11. Cheng, J.; Roach, J. S.; McLean, S.; Reynolds, W. F.; Tinto, W. F. Three new cassane diterpenes from *Caesalpinia pulcherrima*. *Nat. Prod. Commun.* **2008,** *3*, 1751-1754.

12. Pranithanchai, W.; Karalai, C.; Ponglimanont, C.; Subhadhirasakul, S.; Chantrapromma, K. Cassane diterpenoids from the stem of *Caesalpinia pulcherrima*. *Phytochemistry* **2009,** *70*, 300-304.

13. Kalauni, S. K.; Awale, S.; Tezuka, Y.; Banskota, A. H.; Linn, T. Z.; Asih, P. B. S.; Syafruddin, D.; Kadota, S. Antimalarial activity of cassane- and norcassane-type diterpenes from *Caesalpinia crista* and their structure-activity relationship. *Biol. Pharm. Bull.* **2006,** *29*, 1050-1052.

14. Dickson, R. A.; Houghton, P. J.; Hylands, P. J. Antibacterial and antioxidant cassane diterpenoids from *Caesalpinia benthamiana*. *Phytochemistry* **2007,** *68*, 1436-1441.

15. Jabbar, A.; Zaman, M. A.; Iqbal, Z.; Yaseen, M.; Shamim, A. Anthelmintic activity of *Chenopodium album* (L.) and *Caesalpinia crista* (L.) against trichostrongylid nematodes of sheep. *J. Ethnopharmacol.* **2007,** *114*, 86-91.

16. Hou, Y.; Cao, S.; Brodie, P.; Miller, J. S.; Birkinshaw, C.; Ratovoson, F.;

Rakotondrajaona, R.; Andriantsiferana, R.; Rasamison, V. E.; Kingston, D. G. I. Antiproliferative cassane diterpenoids of *Cordyla madagascariensis ssp.* madagascariensis from the Madagascar rainforest. *J. Nat. Prod.* **2008,** *71*, 150-152.

17. Yadav, P. P.; Maurya, R.; Sarkar, J.; Arora, A.; Kanojiya, S.; Sinha, S.; Srivastava, M. N.; Raghubir, R. Cassane Diterpenes from *Caesalpinia bonduc*. *Phytochemistry* **2009,** *70*, 256-261.

18. Lewis, G. P. Notes on *Stuhlmannia* Taub. and the correct placement of *Caesalpinia insolita* (Harms) Brenan & Gillett (Leguminosae: Caesalpinioideae: Casalpinieae). . *Kew Bull.* **1996,** *51*, 377-379.

19. Odalo, J. O.; Joseph, C. C.; Nkunya, M. H. H.; Sattler, I.; Lange, C.; Dahse, H.-M.; Moellman, U. Cytotoxic, anti-proliferative and antimicrobial furanoditerpenoids from *Stuhlmannia moavi*. *Phytochemistry* **2009,** *70*, 2047-2052.

20. Prakash, S.; Khan, M. A.; Khan, K. Z.; Zaman, A. Stilbenes of Gnetum-Ula. *Phytochemistry* **1985,** *24*, 622-624.

21. Hart, J. H. Role of phytostilbenes in decay and disease resistance. *Ann. Rev. Phytopathol.* **1981,** *19*, 437-58.

22. Cardona, M. L.; Fernandez, M. I.; Garcia, M. B.; Pedro, J. R. Synthesis of natural polyhydroxystilbenes. *Tetrahedron* **1986,** *42*, 2725-30.

23. Nakajima, K.; Taguchi, H.; Endo, T.; Yosioka, I. The constituents of *Scirpus fluviatilis* (Torr.) A. Gray. I. The structures of two new hydroxystilbene dimers, scirpusin A and B. *Chem. Pharm. Bull.* **1978,** *26*, 3050-7.

24. Silayo, A.; Ngadjui, B. T.; Abegaz, B. M. Homoisoflavonoids and stilbenes from the bulbs of *Scilla nervosa subsp. rigidifolia*. *Phytochemistry* **1999,** *52*, 947-955.

25. Gerber, N. N.; Wieclawek, B. The structures of two naphthoquinone pigments from an actinomycete. *J. Org. Chem.* **1966,** *5*, 1496-8.

26. Hanumaiah, T.; Rao, B. K.; Rao, C. P.; Rao, G. S. R.; Rao, J. U. M.; Rao, K. V. J.; Marshall, D. S.; Thomson, R. H. Naphthalenes and naphthoquinones from *Ventilago species*. *Phytochemistry* **1985,** *24*, 1811-1815.

27. Natori, S.; Kumada, Y.; Nishikawa, H. The structure of mompain, a naphthoquinone from *Helicobasidium mompa* Tanaka, and its relation to spinochrome A (M). *Chem. Pharm. Bull.* **1965,** *13*, 633-5.

28. Kingston, D. G. I.; Newman, D. J. Mother nature's combinatorial libraries; Their influence on the synthesis of drugs. *Curr. Opin. Drug Disc.* **2002,** *5*, 304-316.

29. Sheldrick, G. M. A short history of SHELX. *Acta Crystallogr., Sect. A: Found. Crystallogr.* **2008,** *A64*, 112-122.

30. Dolomanov, O. V.; Bourhis, L. J.; Gildea, R. J.; Howard, J. A. K.; Puschmann, H. OLEX2: a complete structure solution, refinement and analysis program. *J. Appl. Crystallogr.* **2009,** *42*, 339-341.

31. Fahy, J.; Duflos, A.; Ribet, J. P.; Jacquesy, J. C.; Berrier, C.; Jouannetaud, M. P.; Zunino, F. Vinca alkaloids in superacidic media: A method for creating a new family of antitumor derivatives. *J. Am. Chem. Soc.* **1997,** *119*, 8576-8577.

32. Cao, S.; Brodie, P. J.; Miller, J. S.; Randrianaivo, R.; Ratovoson, F.; Birkinshaw, C.; Andriantsiferana, R.; Rasamison, V. E.; Kingston, D. G. I. Antiproliferative xanthones of terminalia calcicola from the Madagascar rain forest. *J. Nat. Prod.* **2007,** *70*, 679-681.

33. Louie, K. G.; Behrens, B. C.; Kinsella, T. J.; Hamilton, T. C.; Grotzinger, K. R.; McKoy, W. M.; Winker, M. A.; Ozols, R. F. Radiation survival parameters of

antineoplastic drug-sensitive and -resistant human ovarian cancer cell lines and their modification by buthionine sulfoximine. *Cancer Res.* **1985,** *45*, 2110-2115.

34. Bennett, T. N.; Paguio, M.; Gligorijevic, B.; Seudieu, C.; Kosar, A. D.; Davidson, E.; Roepe, P. D. Novel, rapid, and inexpensive cell-based quantification of antimalarial drug efficacy. *Antimicrob. Agents Chemother.* **2004,** *48*, 1807-1810.

35. Smilkstein, M.; Sriwilaijaroen, N.; Kelly, J. X.; Wilairat, P.; Riscoe, M. Simple and inexpensive fluorescence-based technique for high-throughput antimalarial drug screening. *Antimicrob. Agents Chemother.* **2004,** *48*, 1803-1806.

6 Structure Elucidation of Antiproliferative Bisbenzylisoquinoline Alkaloids from *Anisocycla grandidieri* from the Madagascar Dry Forest

This chapter is a slightly expanded version of a published article.[1] Attributions from co-authors of the articles are described as follows in the order of the names listed. The author of this disseration (Yixi Liu) conducted the isolation and structural elucidation part of the titled compounds, and drafted the manuscript. Dr. Harinantenaina was a mentor for this work, provided invaluable advice and hints for the structural elucidation of the compounds, and also proofread the manuscript before submission. Mrs. Peggy Brodie performed the A2780 bioassay on the isolated fractions and compounds. Dr. Carla Slebodnick screened the single crystal samples. Dr. Martin W. Callmander, and Dr. Richard Randrianaivo from Missouri Botanical Garden collected and identified the plant. Dr. Etienne Rakotobe and Dr. Vincent E. Rasamison from Madagascar carried out the initial plant extraction. Dr. Karen TenDyke and Dr. Yongchun Shen from Eisai Inc. performed the H460, MCF-7, and UACC-257 bioassays on the compounds isolated. Dr. David G. I. Kingston was a mentor for this work and the corresponding author for the published article. He provided critical suggestions for this work and crucial revisions to the manuscript.

6.1 Introduction

As a part of the Madagascar International Cooperative Biodiversity Group (ICBG) program, an ethanol extract of the stems of *Anisocycla grandidieri* Baill. (Menispermaceae) was found to have moderate activity against the A2780 ovarian cancer cell line (IC_{50} 9.4 μg/mL). It was thus selected for evaluation for the presence of novel

anticancer agents. Plant species belonging to the genus *Anisocycla* are rich sources of unique bisbenzylisoquinoline (BBIQ) alkaloids,[2-5] which are known to have antibacterial,[6] cytotoxic,[7-9] antimalarial,[7, 8] anticancer,[10] hypotensive,[10] and antiplasmodial[11, 12] activities. In 1972, Schlittler and coworkers[13] reported the isolation and structure characterization of the four BBIQ alkaloids stebisimine (**6.1**), (+)-2'-norcocsuline (**6.2**), trilobine (**6.3**) and (-)-epistephanine (**6.4**) from *A. grandidieri*, while (+)-1,2-dehydrotelobine (**6.5**) was first isolated from *Daphnandra apatela* in 1978.[14] Because of the lack of full NMR spectroscopic data in previous reports, we describe herein the NMR assignments of all carbons and protons of stebisimine (**6.1**),[13, 15] (+)-1,2-dehydrotelobine (**6.5**),[14] and (+)-2'-norcocsuline (**6.2**).[13, 16] The structures and stereochemistries of **6.1** and **6.2** were confirmed by single crystal X-ray crystallography. The results of antiproliferative evaluation of all isolated compounds against the A2780 (human ovarian cancer), H460 (large cell lung cancer), MCF-7 (breast ductal carcinoma), and UACC-257 (melanoma) cell lines are also reported in this study. (Figure 6.1)

6.2 Results and Discussion

6.2.1 Isolation of bioactive compounds

Bioassay-guided separation including liquid-liquid partition, LH-20 size-exclusive and silica gel column chromatography, was used to obtain the four pure compounds stebisimine (**6.1**), (+)-2'-norcocsuline (**6.2**), (+)-1,2-dehydrotelobine (**6.5**), and puetogaline B (**6.6**). Herein, we report the structural elucidation and antiproliferative properties of the four compounds. (Scheme 6.1)

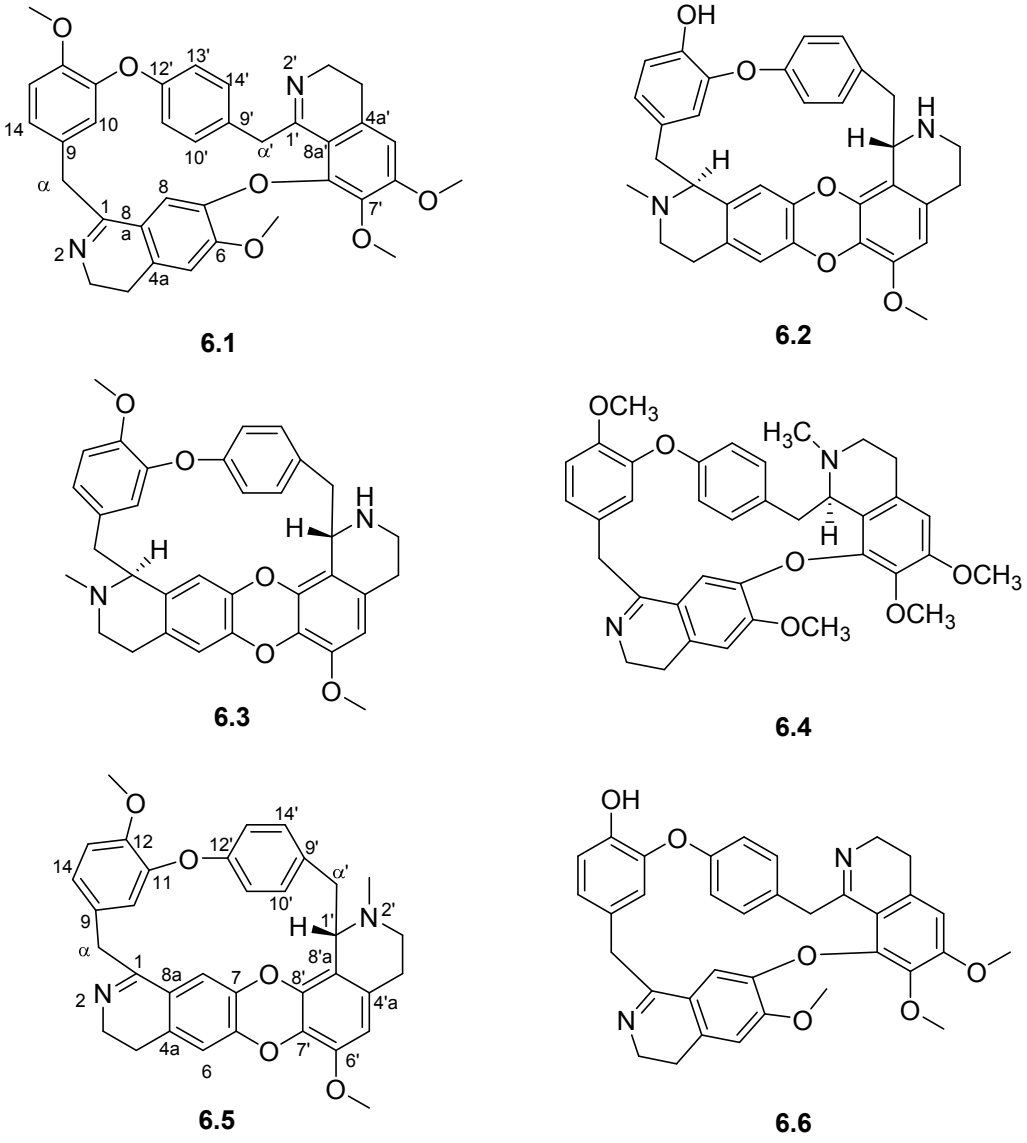

Figure 6.1 Structures of Compounds **6.1**–**6.6**

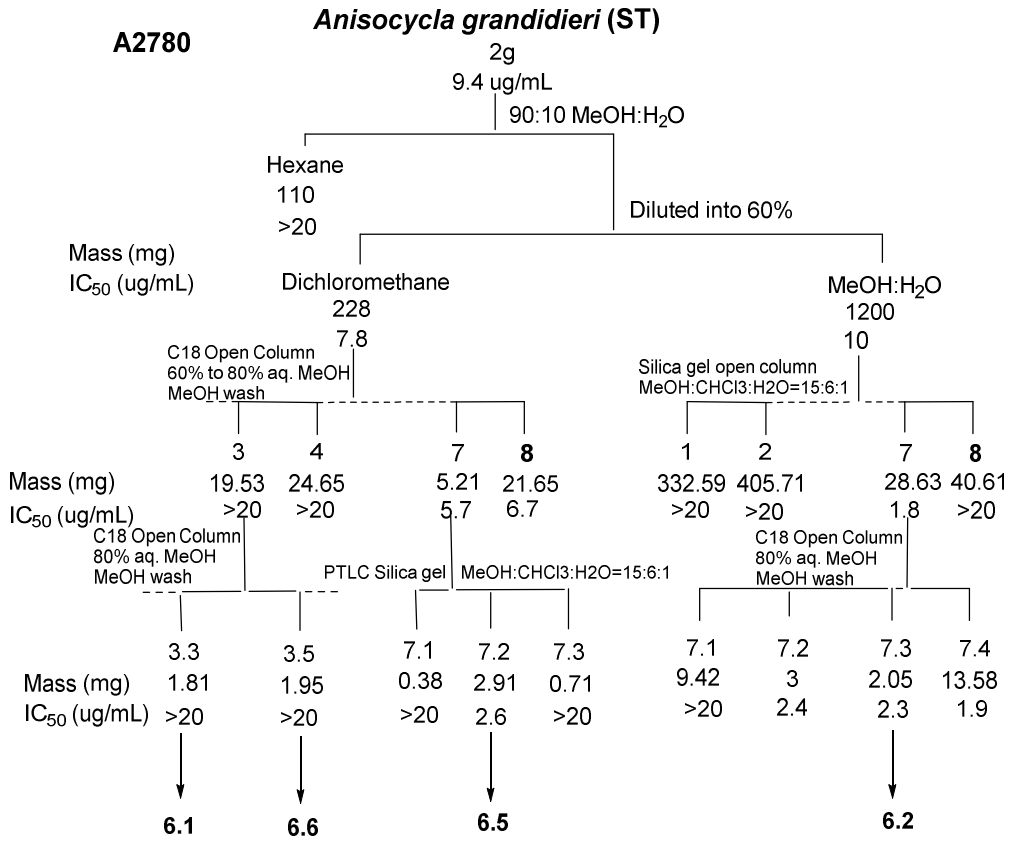

Scheme 6.1 Bioassay-guided Separation of *Anisocycla grandidieri*

6.2.2 Structure elucidation of compound **6.1**

Stebisimine (**6.1**) was isolated as a white solid. A molecular formula of $C_{36}H_{34}N_2O_6$ was assigned to **6.1** as determined by High Resolution Electrospray Ionization Mass Spectrometry (HRESIMS) (*m/z* 591.2486 $[M+H]^+$, calcd. 591.2490). The low intensity of the molecular ion peak, the lack of benzylic cleavage fragments,[17] and the characteristic UV absorptions with maxima at 203, 236, and 278 nm were all indicative of a conjugated BBIQ alkaloid structure for **6.1**.[18] In the ^1H NMR spectrum, there were 10 aromatic proton resonances: three singlets assignable to H-5, H-5' and H-8 (δ_H 6.71, δ_H 6.53 and δ_H 6.72), three proton signals (δ_H 5.87, 1H, d, *J*=2.1; δ_H 6.80, 1H, d, *J*=8.3; δ_H 6.88, 1H, dd, *J*=8.3, 2.1) corresponding to one AMX system and four signals

(δ_H 6.40, 1H, dd, *J*=8.3, 2.6; δ_H 6.79, 1H, dd, *J*=8.3, 2.2; δ_H 6.98, 1H, dd, *J*=8.3, 2.6; δ_H 7.35, 1H, brd, *J*=8.6) ascribable to a *para*-substituted benzyl group presents in the BBIQ alkaloid with at least two diaryl ether bridges.[17] The proton coupling patterns as well as the ^{13}C NMR data of **6.1** were very similar to those of puetogaline B (**6.6**) suggesting that **6.1** also possessed a tail-to-tail BBIQ alkaloid skeleton. The ^{13}C NMR spectrum (Table 6.2) showed two signals at δ_C 164.2 and δ_C 166.5, indicating the presence of two imine functions which were confirmed by the IR absorption at 1600 cm^{-1}.[19] The ^{13}C NMR chemical shifts at δ_C 143.6 (C-7), δ_C 147.2 (C-8'), δ_C 150.0 (C-11), and δ_C 153.4 (C-12') suggested the presence of two diaryl ether bridges between C-7 and C-8' and between C-11 and C-12'.[19] The above conclusions were all in good agreement with the data from the HMBC experiment (Figure 6.2). In addition, The ^{1}H NMR spectrum displayed signals for three aromatic methoxy groups (δ_H 3.86, δ_H 3.89, δ_H 3.95, each 3-proton singlets) together with a shielded methoxy group (δ_H 3.24, 3H, s). The four methoxy groups present in the molecule were respectively assigned to be attached at C-6, C-6', C-12, and C-7' by interpretation of the HMQC and HMBC experiments. The long-range correlations between the methoxy protons at δ_H 3.95 and the carbon at δ_C 147.0 (C-12) on one hand and the shielded methoxy protons at δ_H 3.24 and the carbon signal at δ_C 137.6 (C-7') on the other hand allowed us to assign the methoxy groups to C-12 and C-7'. Furthermore, the HMBC experiment showed that the 6- and 6'-methoxy proton signals were correlated with the carbon signals at δ_C 151.6 (C-6) and δ_C 155.2 (C-6'), respectively. A NOESY experiment was carried out to confirm the locations of the methoxy groups, and these data (Fig. 6.2) indicated correlations between the following protons: H-5 (δ_H 6.71) and the methoxy proton signal at δ_H 3.89 (6-OMe); H-5' (δ_H 6.53)

and the methoxy signal at δ_H 3.86 (6'-OMe); the methoxy signal at δ_H 3.24 (7'-OMe) and the methoxy signal at δ_H 3.86 (6'-OMe); and H-13 (δ_H 6.80) and the methoxy signal at δ_H 3.95 (12-OMe). The complete assignments of all protons and carbons of **6.1** (Tables 6.1 and 2) were accomplished by further analysis of the HMQC, HMBC, and NOESY spectra. The structure of **6.1** was thus elucidated as stebisimine, and this was confirmed by X-ray crystallographic analysis of a single crystal obtained by crystallization from MeOH (Fig. 6.3).

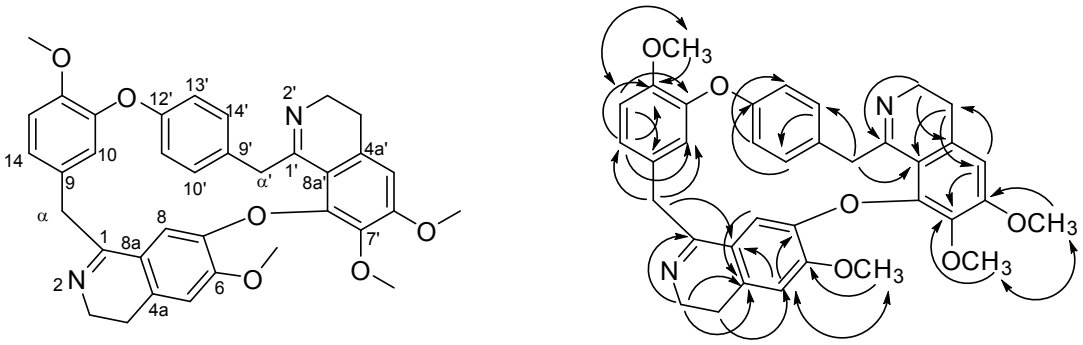

Figure 6.2 Key HMBC (Single Headed Arrows) and NOESY (Double Headed Arrows) Correlations of **6.1**

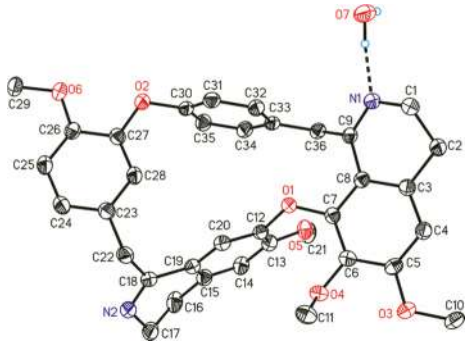

Figure 6.3 Anisotropic Displacement Ellipsoid Drawing of Compound **6.1**

Table 6.1 ^{1}H NMR (500 MHz) Chemical Shift Data (δ, ppm) for Compounds **6.1**–**6.4**

posn	**6.1**	**6.2**	**6.3**	**6.4**	posn	**6.1**	**6.2**	**6.3**	**6.4**
1			3.23 m		1'		3.99 d (9.4)	4.35 br s	
3	3.20 m	3.31 m	2.67 m	3.22 m	3'	3.66 m	2.89 dd (12.1, 9.0)	2.86 m	3.58 ddd (14.2, 10.7, 6.4)
	3.87 m	3.83 dt (15.3, 4.8)		3.88 m		3.80 m	3.27 m	3.17 m	3.89 m
4	2.49 m	2.39 overlapped	2.67 m	2.49 m	4'	2.71 m	2.75 overlapped	2.57 m	2.71 m
		2.41 dd (11.5, 4.8)					2.95 dt (17.2, 9.0)	2.86 m	
5	6.71 s	6.63 s	6.62 s	6.70 s	5'	6.53 s	6.41 s	6.31 s	6.51 s
8	6.72 s	6.56 s	6.15 s	6.71 s	α'	3.98 d (14.4)	2.71 dd (12.8, 9.4)	2.62 m	3.99 d (14.5)
α	3.34 d (12.9)	3.57 d (13.1)	2.67 m	3.38 d (12.9)		4.51 d (14.4)	3.23 d (12.8)	3.32 dd (15.0, 2.3)	4.45 d (14.5)
	3.84 m	3.85 m	2.95 dd (14.2, 2.0)	3.84 dd (12.7, 2.1)	10'	6.79 dd (8.3, 2.2)	6.93 brd (8.1)	7.19 d (8.2)	6.80 brd (8.3)
10	5.87 d (2.1)	6.6 d (1.8)	6.52 brs	5.92 brs	11'	6.4 dd (8.3, 2.6)	6.75 dd (8.2, 2.0)	7.00 dd (8.2, 2.4)	6.38 dd (8.3, 2.6)
13	6.80 d (8.3)	6.85 d (8.3)	6.91 d (8.1)	6.83 d (8.3)	13'	6.98 dd (8.3, 2.6)	7.20 dd (8.3, 2.0)	7.21 d (8.0)	6.99 dd (8.3, 2.6)
14	6.88 dd (8.3, 2.1)	6.97 dd (8.3, 1.8)	6.82 dd (8.1, 1.6)	6.84 dd (8.3, 1.6)	14'	7.35 brd (8.6)	7.39 brd (8.4)	7.66 brd (8.4)	7.40 brd (8.5)
2-NCH_3			2.44 s		2'-NCH_3		2.57 s		
6-OCH_3	3.89 s			3.93 s	6'-OCH_3	3.86 s	3.88 s	3.86 s	3.86 s
12-OCH_3	3.95 s	3.90 s			7'-OCH_3	3.24 s			3.21 s

Table 6.2 ^{13}C-NMR (125 MHz) Chemical Shift Data (δ, ppm) for Compounds **6.1**–**6.4**

posn	**6.1**	**6.2**	**6.3**	**6.4**	posn	**6.1**	**6.2**	**6.3**	**6.4**
1	166.5 (C)	165.4 (C)	67.5 (CH)	166.5 (C)	1'	164.2 (C)	58.8 (CH)	54.2 (CH)	164.3 (C)
3	50.9 (CH_2)	46.8 (CH_2)	49.6 (CH_2)	46.8 (CH_2)	3'	46.8 (CH_2)	44.6 (CH_2)	44.9 (CH_2)	46.8 (CH_2)
4	26.2 (CH_2)	25.4 (CH_2)	27.7 (CH_2)	26.2 (CH_2)	4'	27.6 (CH_2)	24.7 (CH_2)	28.3 (CH_2)	27.6 (CH_2)
4a	121.0 (C)	134.8 (C)	134.8 (C)	135.1 (C)	4a'	136.7 (C)	128.5 (C)	129.8 (C)	136.4 (C)
5	110.4 (CH)	115.3 (CH)	115.5 (CH)	110.4 (CH)	5'	105.5 (CH)	107.6 (CH)	106.7 (CH)	105.2 (CH)
6	151.6 (C)	142.6 (C)	139.5 (C)	151.7 (C)	6'	155.2 (C)	146.1 (C)	146.1 (C)	155.3 (C)
7	143.6 (C)	138.8 (C)	139.7 (C)	143.7 (C)	7'	137.6 (C)	138.3 (C)	135.7 (C)	136.7 (C)
8	115.8 (CH)	114.2 (CH)	114.1 (CH)	116.4 (CH)	8'	147.2 (C)	128.6 (C)	140.6 (C)	147.5 (C)
8a	134.8 (C)	123.3 (C)	133.8 (CH_2)	121.0 (C)	8a'	115.1 (C)	119.8 (C)	122.0 (C)	115.0 (C)
α	41.8 (CH_2)	42.6 (CH_2)	41.3 (CH_2)	42.0 (CH_2)	α'	45.2 (CH_2)	40.3 (CH_2)	38.7 (CH_2)	45.0 (CH_2)
9	130.7 (C)	129.4 (C)	129.6 (C)	129.5 (C)	9'	135.9 (C)	136.6 (C)	138.9 (C)	136.4 (C)
10	116.4 (CH)	117.6 (CH)	116.6 (CH)	116.5 (CH)	10'	130.4 (CH)	131.4 (CH)	131.3 (CH)	130.8 (CH)
11	150.0 (C)	148.8 (C)	143.7 (C)	147.8 (C)	11'	122.1 (CH)	121.4 (CH)	121.3 (CH)	121.9 (CH)
12	147.0 (C)	147.4 (C)	148.1 (C)	143.5 (C)	12'	153.4 (C)	154 (C)	153.9 (C)	153.3 (C)
13	111.9 (CH)	112.3 (CH)	115.8 (CH)	115.3 (CH)	13	122.1 (CH)	122.8 (CH)	122.5 (CH)	121.8 (CH)
14	121.8 (CH)	122.5 (CH)	122.2 (CH)	122.7 (CH)	14'	127.8 (CH)	130.1 (CH)	128.2 (CH)	127.7 (CH)
2-NCH_3			43.0 (CH_3)		2'-NCH_3		42.4 (CH_3)		
6-OCH_3	56.0 (CH_3)			56.1 (CH_3)	6'-OCH_3	56.0 (CH_3)	56.0 (CH_3)	56.3 (CH_3)	56.1 (CH_3)
12-OCH_3	56.0 (CH_3)	56.3 (CH_3)			7'-OCH_3	60.2 (CH_3)			60.2 (CH_3)

6.2.3 Structure elucidation of compound **6.5**

(+)-1,2-Dehydrotelobine (**6.5**) showed UV absorptions at 203, 235, 263, and 336 nm that also agreed with the reported data.[14] Its molecular formula was assigned as $C_{35}H_{32}N_2O_5$ based on its HRESIMS (*m/z* 561.2381 $[M+H]^+$, calcd. 561.2389). The ^1H NMR spectrum displayed ten aromatic signals with same coupling patterns to those of compound **6.1**, suggesting that compound **6.5** possessed the same aromatic substitution patterns as **6.1**. Furthermore, the ^{13}C NMR spectrum displayed only one carbon signal at δ_C 165.4 (C-1), with an additional typical *N*-methyl proton signal at δ_H 2.57 (3H, s) and a deshielded signal for a methine (δ_H 3.99, d, J = 9.4; δ_C 58.8), suggesting that one of the imine groups which were present in **6.1** was replaced with a tertiary amine bearing a methyl group. The long range HMBC correlations from the methyl at δ_H 2.57 (2'-NMe) to the methine at C-1' (δ_C 58.8), and to the methylene at C-3' (δ_C 44.6) corroborated the location of the methyl group at the 2' position. By comparison with **6.1**, the absence of the shielded methoxy proton signal at δ_H 3.24 (7'-OMe 3H, s) and of one of the three aromatic methoxy proton signals in **6.5**, together with the number of the degrees of unsaturation (Ω=21), suggested the presence of a new diaryl ether bridge between C-6 and C-7' instead of an imine function in **6.5**. The above conclusion was supported by the results of the HMBC experiment (Figure 6.4). All proton and carbon signals of **6.5** were assigned by interpretation of the data obtained from HMQC and HMBC experiments. The stereochemistry at C-1' was assigned as *S* based on the comparison of its optical rotation value with the reported data in the literature.[20] The structure of **6.5** was thus assigned as (+)-1,2-dehydrotelobine.

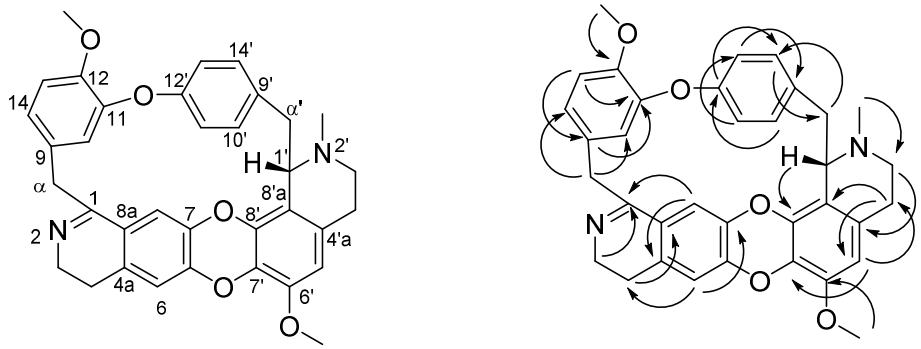

Figure 6.4 Key HMBC (Single Headed Arrows) and NOESY (Double Headed Arrows) Correlations of **6.5**

6.2.4 Structure elucidation of compound **6.2**

Compound **6.2** was assigned as (+)-2'-norcocsuline based on the similarities of its spectroscopic data with those of (+)-cocsuline (**6.7**).[21] The molecular formula was determined to be $C_{34}H_{32}N_2O_5$ by HRESIMS (*m/z* 549.2365 $[M+H]^+$, calcd. 549.2389). The ten aromatic protons with the same coupling patterns as those of **6.1** and **6.5** showed that compound **6.2** was also a BBIQ alkaloid. The ^{13}C NMR spectroscopic data of **6.2** compared with those of **6.5** revealed the absence of carbon signals above 160 ppm. Its ^1H NMR spectrum differed from that of **6.5** in having only one methoxy signal at δ_H 3.86 (6'-OMe, 3H, s), a deshielded proton signal of H-1' (δ_H 4.35, H-1', 1H, brs), an additional methine signal (δ_H 3.23, H-1, m; δ_C 67.5, C-1), and a signal ascribable to an *N*-methyl group at δ_H 2.44 (2-NCH_3, 3H, s). The above data indicated the presence of two secondary amine groups in **6.2** compared to one in **6.5**. Furthermore, the twenty degrees of unsaturation together with the absence of the imine group in **6.2** suggested that compounds **6.5** and **6.2** shared the same ring system. The assignments of all proton and carbon signals of **6.2** were substantiated by comparison of its NMR spectroscopic data

with those of **6.7**.[21] The configurations at C-1 and C-1' were assigned as *anti* since the signal of H-10 appeared as a broad singlet at δ_H 6.52.[17] The structure of compound **6.2** was assigned as (+)-2'-norcocsuline by comparison of its optical rotation value with the reported data for (+)-2'-norcocsuline and (+)-cocsuline.[16, 22] The complete structure was confirmed by single crystal X-ray crystallographic analysis, and an anisotropic displacement ellipsoid drawing of **6.2** is shown in Figure 6.5.

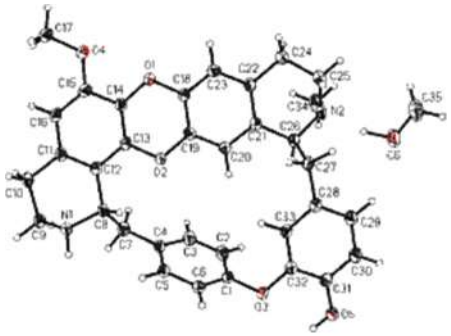

Figure 6.5 Anisotropic Displacement Ellipsoid Drawing of Compound **6.2**.

6.2.5 Structure elucidation of compound **6.6**

Compound **6.6** was identified as puetogaline B by its physical and spectroscopic data (Table 6.1 and 6.2), which were in good agreement with the published data.[23]

6.2.6 Antiproliferative bioactivities

Compounds **6.1**, **6.2**, **6.5**, and **6.6** were evaluated for their antiproliferative activities in four different cell (Table 6.3). Both (+)-1,2-dehydrotelobine (**6.5**) and (+)-2'-norcocsuline (**6.2**) showed moderate antiproliferative activity to the ovarian cancer (A2780), large cell lung cancer (H460), breast ductal carcinoma (MCF-7), and melanoma (UACC-257) cell lines, with IC_{50} values in the 1 – 6 μM range. Compounds **6.1** and **6.6** had IC_{50} values >10 μM to all four cell lines.

Table 6.3 Antiproliferative Activities (μM) of Compounds **6.1**, **6.2**, **6.5**, and **6.6**.

	Cell line IC_{50}			
compound	A2780	H460	MCF-7	UACC-257
6.1	>20	>10	>10	>10
6.5	2.7±0.3	>3.33, <10	>1.11, <3.33	6.37±1.91
6.2	4.1±0.3	2.18±0.65	4.23±1.27	3.37±1.01
6.6	>20	>10	>10	>10

6.3 Experimental

6.3.1 General experimental procedures

Optical rotations were recorded on a JASCO P-2000 polarimeter. IR and UV spectra were measured on MIDAC M-series FTIR and Shimadzu UV-1201 spectrophotometers, respectively. ^{1}H and ^{13}C NMR spectra were recorded on a Bruker Avance 500 spectrometer in $CDCl_3$ with TMS as internal standard. The chemical shifts are given in δ (ppm), and apparent coupling constants (*J*) are reported in Hz. Mass spectra were obtained on an Agilent 6220 LC-TOF-MS in the positive ion mode. Open column chromatography and preparative TLC were performed using silica gel (230-400 mesh, Silicycle Co. USA) and silica gel plates (60 F254, Silicycle Co. USA), respectively.

6.3.2 Plant material

Stems of *A. grandidieri* were collected in the dry semi-deciduous forest of Sahafary, 15 km from the village of Saharenana, in the northern part of Madagascar (12°34′48″S 049°26′31″E). Voucher specimens with collection number *Rakotondrajaona et al. 391* have been deposited in herbaria at the Parc Botanique and Zoologique de Tsimbazaza (TAN), the Centre National d'Application des Recherches Pharmaceutiques (CNARP), the Missouri Botanical Garden in St. Louis, Missouri (MO), and at the Muséum National d'Histoire Naturelle in Paris, France (P).

6.3.3 Extraction and isolation

A ground sample of *A. grandidieri* stems (250 g) was extracted with EtOH at room temperature to yield 12.2 g of crude EtOH extract designated MG 4002. A total of 4.84 g of this extract was made available to Virginia Tech. The crude EtOH extract (2.0 g) was dissolved in 90% aq. MeOH (300 mL) and extracted with hexanes (3 × 200 mL) to afford 110 mg of residue after evaporation of the hexanes-soluble fraction. The 90% aq. MeOH layer was then diluted to 60% and extracted with CH_2Cl_2 (3×300 mL) to yield 228 mg of CH_2Cl_2-soluble fraction. The 60% aq. MeOH layer was concentrated to give 1190 mg of brown residue. The CH_2Cl_2 and 60% aq. MeOH fractions were found to have antiproliferative activity with IC_{50} values of 6.2 μg/mL and 11 μg/mL, respectively. The CH_2Cl_2 fraction was then divided into 11 fractions by an open silica gel column ($CHCl_3$:MeOH:H_2O=15:6:1 as eluent). Preparative TLC on silica gel of the most active fraction (Fr-7, 5.7 μg/mL) yielded compound **6.5** (2.9 mg). The third fraction (Fr-3) was subjected to an open C-18 column to furnish compounds **6.1** (1.8 mg) and **6.6** (2.0 mg) in the CH_2Cl_2 fraction. The 60% aq. MeOH fraction was applied to an open silica gel column (solvent system: $CHCl_3$:MeOH:H_2O=15:6:1) to give 8 fractions. Further purification of the most active fraction (Fr-7, 3.7 μg/mL) by an open C18 column (solvent systems: 80% aq. MeOH and MeOH) gave compound **6.2** (2.1 mg).

6.3.4 NMR spectroscopy

The NMR spectra were recorded on a Bruker Advance II 500-MHz spectrometer (Bruker Biospin Corporation, Billerica, Massachusetts, USA). All samples were dissolved in $CDCl_3$, and NMR experiments were recorded at 298 K. Chemical shifts (δ)

in ppm are referenced to TMS at 0.00 ppm for ^{1}H and ^{13}C. Coupling constants (*J*) are given in Hertz. The pulse conditions of 1D NMR were as follows for **6.1**: for ^{1}H, spectrometer frequency (SF)=500.16 MHz, acquisition time (AQ) = 3.6372 s, relaxation delay (RD) = 1.000 s, spectral width (SW) = 9009.0 Hz, FT data size = 32 K, digital resolution = 0.137 Hz, line broadening (LB) = 1.0 Hz, number of dummy scans (DS) = 2; for ^{13}C, SF = 125.77 MHz, AQ = 1.0420 s, RD=1.000 s, SW = 31446.5 Hz, FT data size = 32K, digital resolution = 0.48 Hz, LB = 1.0 Hz,. The 2D spectra used 1024-256 (HMQC), 1024-189 (HMBC), 1024-128 (NOESY) data point matrices, which were zero filled to 1024-1024 (HMQC), 1024-378 (HMBC), 1024-1024 (NOESY), after sinebell weighting applied to both dimensions. For HMQC, SF = 500.16 MHz (^{1}H), 125.77 MHz (^{13}C), AQ=0.1364 s, RD = 1.5000 s, NS = 86, DS = 16, pre-scan delay (DE) = 6.50 ms, dwell time (DW) = 97.000 ms, receiver gain (RG) = 30, SW = 7507.5 Hz (^{1}H), 31446.5 Hz (^{13}C); for HMBC, AQ = 0.1364 s, RD = 1.5000 s, NS = 80, DS = 16, DE = 6.50 ms, DW = 76.800 ms, RG = 30, SW = 7500.2 Hz (^{1}H), 31466.5 Hz (^{13}C); for NEOSY, AQ = 0.1600 s, RD = 1.000s, NS = 32, DS = 32, DE = 6.50ms, DW = 100 ms, RG = 20, SW = 6399.5 Hz (^{1}H), 6399.5 Hz (^{13}C). The pulse conditions were as follows for **6.5**: for ^{1}H, SF = 500.16 MHz, AQ = 3.6372s, RD = 1.0000 s, SW = 9009.0Hz, FT data size = 32K, digital resolution = 0.137 Hz, LB = 1.0 Hz; for ^{13}C, SF = 125.77 MHz, AQ = 1.0420 s, RD = 1.0000 s, SW = 31446.5 Hz, FT data size = 32 K, digital resolution = 0.48 Hz, LB = 1.0 Hz. The 2D spectra used 1024-84 (HMQC), 1024-239 (HMBC) data point matrices, which were zero filled to 102-512 (HMQC), 1024-1024 (HMBC), after sinebell weighting applied to both dimensions. For HMQC, SF = 500.16 MHz (^{1}H), 125.77 MHz (^{13}C), AQ = 0.1364 s, RD = 1.5000 s, NS = 160, DS = 16, DE = 6.00 ms, DW = 97.000

ms, RG = 23, SW = 7507.5 Hz (^{1}H), 31446.5 Hz (^{13}C); for HMBC, SF = 500.16 MHz (^{1}H), 125.770MHz (^{13}C), AQ = 0.1364 s, RD = 1.5000 s, NS = 120, DS = 16, DE = 6.50 ms, DW = 76.800 ms, RG = 30, SW = 7507.5 Hz (^{1}H), 31446.5 Hz (^{13}C); The pulse conditions were as follows for **6.2**: for ^{1}H, SF = 500.16 MHz, AQ = 3.6372 s, RD = 1.0000 s, SW = 9009.0 Hz, FT data size = 32 K, digital resolution = 0.147 Hz, LB = 1.0 Hz; for ^{13}C, SF = 125.77 MHz, AQ = 1.0420 s, RD = 1.0000 s, SW = 31446.5 Hz, FT data size = 32K, digital resolution = 0.48 Hz, LB = 1.00 Hz. The pulse conditions were as follows for **6.6**: for ^{1}H, SF = 500.16 MHz, AQ = 3.6372 s, RD = 1.0000 s, SW = 9009.0 Hz, FT data size = 32K, digital resolution = 0.147 Hz, LB = 1.0 Hz; for ^{13}C, SF = 125.77 MHz, AQ = 1.0420 s, RD = 1.0000 s, SW = 31446.5 Hz, FT data size = 32 K, digital resolution = 0.48 Hz, LB = 1.00 Hz. The 2D spectra use 1024-256 (HMQC), 1024-256 (HMBC) data point matrices, which were zero filled to 102-1024(HMQC), 1024-516 (HMBC), after sinebell weighting applied to both dimensions. For HMQC, SF = 500.16 MHz (^{1}H), 125.77 MHz (^{13}C), AQ = 0.1364 s, RD = 1.5000 s, NS = 85, DS = 16, DE = 6.50 ms, DW = 97.000 ms, RG = 30, SW = 7507.5 Hz (^{1}H), 31446.5 Hz (^{13}C); for HMBC, SF = 500.16 MHz (^{1}H), 125.770 MHz (^{13}C), AQ = 0.2047 s, RD = 1.5000 s, NS = 120, DS = 32, DE = 6.50 ms, DW = 100 ms, RG = 30, SW = 4997.6 Hz (^{1}H), 31446.5 Hz (^{13}C)

6.3.5 Stebisimine (**6.1**)

White crystals from MeOH; UV λ_{max} (MeOH) (log ε): 203 (2.42), 236 (1.77), 278 (0.84), 315 nm; IR ν_{max} 3000, 1600, 1502, 1278, 1098, 1013 cm^{-1}; ^{1}H and ^{13}C NMR data, see Tables 6.1 and 6.2. HRESIMS *m/z* $[M+H]^{+}$ 591.2486 (calcd for $C_{36}H_{35}N_2O_6^{+}$, 591.2490).

6.3.6 (+)-1, 2-Dehydrotelobine (**6.5**)

Amorphous powder, $[\alpha]^{21}D$ +125.2° (*c* 0.7, MeOH); UV λ_{max} (MeOH) (log ε): 203(2.11), 235 (0.6), 263 (0.35), 336 (0.17) nm; IR ν_{max} 2925, 1599, 1501, 1279, 1098 cm^{-1}; ^{1}H and ^{13}C NMR data, see Tables 6.1 and 6.2; HRESIMS *m/z*: 561.2381 $[M+H]^+$ (calcd $C_{35}H_{33}N_2O_6^+$, 561.2389)

6.3.7 (+)-2'-Norcocsuline (**6.2**)

White crystals from MeOH, $[\alpha]^{21}D$ +250° (*c* 0.1, MeOH); UV λ_{max} (MeOH) (log ε): 203 (1.25), 240 (0.75), 293 (0.16) nm; IR ν_{max} 3420, 2925, 1501, 1279, 1098 cm^{-1}; ^{1}H and ^{13}C NMR data, see Tables 6.1 and 6.2; HRESIMS *m/z*: 549.2365 $[M+H]^+$ (calcd for $C_{35}H_{33}N_2O_6^+$, 549.2389).

6.3.8 Puetogaline B (**6.6**)

Amorphous powder; UV λ_{max} (MeOH) (log ε): 205 (1.41), 234 (0.95), 278 (0.48) nm; IR ν_{max} 2925, 1599, 1505, 1279, 1098, 1013 cm^{-1}; ^{1}H and ^{13}C NMR data, see Tables 6.1 and 6.2; HRESIMS *m/z*: 577.2338 $[M+H]^+$ [calcd for $C_{35}H_{33}N_2O_6^+$, 577.2389

6.3.9 X-ray Crystallography

*6.3.9.1 Stebisimine (**6.1**)*

A colorless plate (0.007 x 0.147 x 0.149 mm^3) was centered on the goniometer of an Oxford Diffraction Nova diffractometer. The data collection routine, unit cell refinement, and data processing were carried out with the program CrysAlisPro.[24] The Laue symmetry was consistent with the triclinic space groups P1 and P-1. As the

molecule is not chiral, the centric space group, P-1, was chosen. The structure was solved by direct methods and refined using SHELXTL NT.[25] The final refinement model involved anisotropic displacement parameters for non-hydrogen atoms. A riding model was used for the aromatic and alkyl hydrogens. Hydrogen atom positions of the water molecule were located from the residual electron density map and refined independently; the displacement parameters were fixed at Uiso(H) = 1.5 Ueq(O). Cryatal data: $C_{36}H_{34}N_2O_6 \bullet H_2O$, M_r =608.67, triclinic, *P*-1, *a*= 11.4221(12) Å, *b*= 11.4745(10) Å, *c*= 13.2216(14) Å, α= 102.650(8)°, β= 105.377(9)°, γ = 107.547(9)°, *V*=1506.5(3) Å^3, 9585 reflections, 416 parameters; crystal size 0.149 x 0.147 x 0.007 mm^3. The final indices were R_1 = 0.0464, wR_2 = 0.1085 [$I>2\sigma(I)$]. Crystallographic data for compound **1** have been deposited as Supporting Information at the Cambridge Crystallographic Data Centre (deposition no. CCDC 919139).[26]

*6.3.9.2 (+)-2'-Norcocsuline (**6.2**)*

A colorless rod (0.8 x 0.12 x 0.30 mm^3) was centered on the goniometer of an Oxford Diffraction SuperNova diffractometer operating with CuKα radiation. The data collection routine, unit cell refinement, and data processing were carried out with the program CrysAlisPro.[24] The Laue symmetry and systematic absences were consistent with the orthorhombic space group $P2_12_12_1$. The structure was solved using SHELXS-97[26] and refined using SHELXL-97[26] via the OLEX2 Program System.[27] The final refinement model involved anisotropic displacement parameters for non-hydrogen atoms. A riding model was used for the aromatic and alkyl hydrogens. Hydrogen atom positions for the hydroxyl and amine groups were located from the residual electron density peaks and refined independently; the displacement parameters were fixed at U_{iso}(H) = 1.5

U_{eq}(O). The absolute configuration was established from anomalous dispersion effects (99% Friedel mates measured; Flack x = 0.00(15);[28] Hooft P2(true) = 1.000, P3(true) = 1.000, P3(rac-twin) = $0.7x10^{-37}$; P3(false) = $0.2x10^{-139}$, y = 0.-0.03(4)).[29] Cryatal data: $C_{34}H_{32}N_2O_5 \bullet CH_3OH$, M_r =580.66, orthorhombic, $P2_12_12_1$, a = 7.25361(9) Å, b = 13.36293(14) Å, c = 30.1627(3) Å, α=β=γ=90°, V=2923.65(6) Å^3, 31248 reflections, 401 parameters; crystal size 0.30 x 0.12 x 0.08 mm^3. The final indices were R_1 = 0.0327, wR_2 = 0.0854 [$I>2\sigma(I)$]. Crystallographic data for compound **6.3** have been deposited as Supporting Information at the Cambridge Crystallographic Data Centre (deposition no. CCDC 919138).[26]

6.3.10 Antiproliferative bioassays

Antiproliferative Bioassay. The A2780 ovarian cancer cell line assay was performed at Virginia Tech as previously reported.[30] The A2780 cell line is a drug-sensitive ovarian cancer cell line.[31]

6.4 References

1. Liu, Y.; Harinantenaina, L.; Brodie, P. J.; Slebodnick, C.; Callmander, M. W.; Rakotondrajaona, R.; Rakotobe, E.; Rasamison, V. E.; TenDyke, K.; Shen, Y.; Kingston, D. G. I. Structure elucidation of antiproliferative bisbenzylisoquinoline alkaloids from *Anisocycla grandidieri* from the Madagascar dry forest. *Magn. Reson. Chem.* **2013,** *51*, 574-579.

2. Kanyinda, B.; Vanhaelen-Fastre, R.; Vanhaelen, M. Benzylisoquinoline alkaloids from *Anisocycla jollyana* leaves. *J. Nat. Prod.* **1995,** *58*, 1587-1589.

3. Kanyinda, B.; Vanhaelen-Fastre, R.; Vanhaelen, M.; Ottinger, R. Bisbenzylisoquinoline alkaloids from *Anisocycla cymosa* roots. *J. Nat. Prod.* **1993,** *56*, 957-960.

4. Kanyinda, B.; Vanhaelen-Fastre, R.; Vanhaelen, M.; Ottinger, R. Identification by two-dimensional NMR spectroscopy of two new benzylisoquinoline alkaloids from leaves of *Anisocycla cymosa*. *J. Nat. Prod.* **1992,** *55*, 607-612.

5. Kanyinda, B.; Vanhaelen-Fastre, R.; Vanhaelen, M. A new bisbenzylisoquinoline-N-oxide alkaloid from seeds of *Anisocycla cymosa*. *J. Nat. Prod.* **1993,** *56*, 618-620.

6. Sedmera, P.; Nguyen, T. N.; Valka, I.; Cave, A.; Cortes, D.; Simanek, V. A new bisbenzylisoquinoline alkaloid from *Phaeanthus vietnamensis* and its antibacterial activity. *Heterocycles* **1990,** *30*, 205-209.

7. Lin, L. Z.; Shieh, H. L.; Angerhofer, C. K.; Pezzuto, J. M.; Cordell, G. A.; Xue, L.; Johnson, M. E.; Ruangrungsi, N. Traditional medicinal plants of Thailand. XIX. Cytotoxic and antimalarial bisbenzylisoquinoline alkaloids from *Cyclea barbata*. *J. Nat. Prod.* **1993,** *56*, 22-29.

8. Likhitwitayawuid, K.; Angerhofer, C. K.; Cordell, G. A.; Pezzuto, J. M. Traditional medicinal plants of Thailand. XX. Cytotoxic and antimalarial bisbenzylisoquinoline alkaloids from *Stephania erecta*. *J. Nat. Prod.* **1993,** *56*, 30-38.

9. Klausmeyer, P.; McCloud, T. G.; Scudiero, D. A.; Currens, M. J.; Cardellina, J. H., II; Shoemaker, R. H. Discovery and preliminary SAR of bisbenzylisoquinoline alkaloids as inducers of C/EBPα. *Bioorg. Med. Chem.* **2012,** *20*, 4646-4652.

10. Hussain, S. F.; Khan, L.; Guinaudeau, H.; Leet, J. E.; Freyer, A. J.; Shamma, M. The alkaloidal profile of *Cocculus pendulus*. *Tetrahedron* **1984,** *40*, 2513-2517.

11. Steele, J. C. P.; Simmonds, M. S. J.; Veitch, N. C.; Warhurst, D. C. Evaluation of the anti-plasmodial activity of bisbenzylisoquinoline alkaloids from *Abuta grandifolia*. *Planta Med.* **1999,** *65*, 413-416.

12. Mambu, L.; Martin, M.-T.; Razafimahefa, D.; Ramanitrahasimbola, D.; Rasoanaivo, P.; Frappier, F. Spectral characterization and antiplasmodial activity of bisbenzylisoquinolines from *Isolona ghesquiereina*. *Planta Med.* **2000,** *66*, 537-540.

13. Schlittler, E.; Weber, N. Alkaloids of *Anisocyclea grandidieri* (Menispermaceae). *Helv. Chim. Acta* **1972,** *55*, 2061-2064.

14. Bick, I. R. C.; Sotheeswaran, S. Alkaloids of *Daphnandra apatela*. *Aust. J. Chem.* **1978,** *31*, 2077-2083.

15. Barton, D. H. R.; Kirby, G. W.; Wiechers, A. Phenol oxidation and biosynthesis. XI. The structure of stebisimine and the biosynthesis of epistephanine. *J. Chem. Soc. C* **1966**, 2313-2319.

16. Lavault, M.; Bruneton, J.; Cave, A.; Chan, K. C.; Deverre, J. R.; Sevenet, T.; Guinaudeau, H. Bis(benzylisoquinoline) alkaloids from *Albertisia cf.* A. papuana. *Can. J.*

Chem. **1987,** *65*, 343-347.

17. Guinaudeau, H.; Freyer, A. J.; Shamma, M. Spectral characteristics of the bisbenzylisoquinoline alkaloids. *Nat. Prod. Rep.* **1986,** *3*, 477-488.

18. Guha, K. P.; Mukherjee, B.; Mukherjee, R. Bis(benzylisoquinoline) alkaloids - a review. *J. Nat. Prod.* **1979,** *42*, 1-84.

19. Zhang, H.; Yue, J.-M. New bisbenzylisoquinoline alkaloids from *Cocculus laurifolius*. *Nat. Prod. Res.* **2006,** *20*, 553-557.

20. Likhitwitayawuid, K.; Angerhofer, C. K.; Cordell, G. A.; Pezzuto, J. M. Traditional medicinal plants of Thailand. XX. Cytotoxic and antimalarial bisbenzylisoquinoline alkaloids from Stephania erecta. *J. Nat. Prod.* **1993,** *56*, 30-8.

21. Atta-ur-Rahman; Atia-Tul-Wahab; Nawaz, S. A.; Choudhary, M. I. New cholinesterase inhibiting bisbenzylisoquinoline alkaloids from *Cocculus pendulus*. *Chem. Pharm. Bull.* **2004,** *52*, 802-806.

22. Bhakuni, D. S.; Joshi, P. P. Alkaloids of *Cocculus pendulus*. *Tetrahedron* **1975,** *31*, 2575-2579.

23. Mahiou, V.; Roblot, F.; Fournet, A.; Hocquemiller, R. Bisbenzylisoquinoline alkaloids from *Guatteria boliviana* (Annonaceae). *Phytochemistry* **2000,** *54*, 709-716.

24. Gordaliza, M.; Castro, M. A.; del Corral, J. M. M.; San Feliciano, A. Antitumor properties of podophyllotoxin and related compounds. *Curr. Pharm. Design* **2000,** *6*, 1811-1839.

25. Sheldrick, G. M. A short history of SHELX. *Acta Crystallogr., Sect. A: Found. Crystallogr.* **2008,** *A64*, 112-122.

26. Kingston, D. G. I.; Newman, D. J. Mother nature's combinatorial libraries; Their

influence on the synthesis of drugs. *Curr. Opin. Drug Disc.* **2002,** *5*, 304-316.

27. Dolomanov, O. V.; Bourhis, L. J.; Gildea, R. J.; Howard, J. A. K.; Puschmann, H. OLEX2: a complete structure solution, refinement and analysis program. *J. Appl. Crystallogr.* **2009,** *42*, 339-341.

28. Flack, H. D. On enantiomorph-polarity estimation. *Acta Crystallogr., Sect. A: Found. Crystallogr.* **1983,** *A39*, 876-881.

29. Hooft, R. W. W.; Straver, L. H.; Spek, A. L. Determination of absolute structure using Bayesian statistics on Bijvoet differences. *J. Appl. Crystallogr.* **2008,** *41*, 96-103.

30. Cao, S.; Brodie, P. J.; Miller, J. S.; Randrianaivo, R.; Ratovoson, F.; Birkinshaw, C.; Andriantsiferana, R.; Rasamison, V. E.; Kingston, D. G. I. Antiproliferative xanthones of terminalia calcicola from the Madagascar rain forest. *J. Nat. Prod.* **2007,** *70*, 679-681.

31. Louie, K. G.; Behrens, B. C.; Kinsella, T. J.; Hamilton, T. C.; Grotzinger, K. R.; McKoy, W. M.; Winker, M. A.; Ozols, R. F. Radiation survival parameters of antineoplastic drug-sensitive and -resistant human ovarian cancer cell lines and their modification by buthionine sulfoximine. *Cancer Res.* **1985,** *45*, 2110-2115.

7 Antiproliferative Compounds from *Ocotea macrocarpa* from the Madagascar Dry Forest

This chapter is a slightly expanded version of a published article.[1] Attributions from co-authors of the articles are described as follows in the order of the names listed. The author of this dissertation (Yixi Liu) mentored the undergraduate student (Emily Cheng) with the initial isolation of two compounds and isolated three more compounds, elucidated the structures of all compounds, and drafted the manuscript. Dr. Harinantenaina was a mentor for this work, provided invaluable advice and hints for the structural elucidation of the compounds, and he also proofread the manuscript before submission. Mrs. Peggy Brodie performed the A2780 bioassay on the isolated fractions and compounds. Dr. Jessica D. Wiley and Dr. Maria B. Cassera performed the Dd2 bioassay. Dr. Wendy Applequist from Missouri Botanical Garden supervised the collection of the plant and Dr. Andriamalala Rakotondrafara made the actual plant collection. Dr. Michel Ratsimbason and Vincent E. Rasamison from Madagascar carried out the initial plant extraction. Dr. David G. I. Kingston was a mentor for this work and the corresponding author for the published article. He provided critical suggestions for this work and crucial revisions to the manuscript.

7.1 Introduction

As a part of the Madagascar International Cooperative Biodiversity Group (ICBG) program,[2, 3] an ethanol extract of the roots of *Ocotea macrocarpa* was found to have moderate activity against the A2780 ovarian cancer cell line (IC_{50} 3.9 μg/ml). This extract was thus selected for further evaluation for the presence of novel anticancer

agents. The plant genus *Ocotea*, the largest member of the Lauraceae family, comprises approximately 350 species that are distributed throughout tropical and subtropical climates. Most species are found in the Americas from Mexico to Argentina, seven species are found in Africa, one specie is found in the Canary Islands, and about 34 recognized species are found in Madagascar.[4, 5] Some species are used in traditional medicine, including for treatment of fever and malaria.[6] Chemical investigations on various *Ocotea* species have led to the isolation of a wide range of secondary metabolites including alkaloids, flavonoids, lignans, and terpenoids, many of which exhibited interesting antiproliferative, antifungal, antiherpetic, anti-inflammatory, and antimicrobial activities.[7-13]

7.2 Results and Discussion

7.2.1 Isolation of active compounds

Bioassay-guided isolation (Scheme 7.1) of an extract of the roots of *Ocotea macrocarpa* produced five bioactive compounds (Figure 7.1): one new butanolide (**7.1**), two new secobutanolides (**7.2** and **7.3**), and two known butanolides, linderanolide B (**7.4**)[14] and isolinderanolide (**7.5**).[15] The structures of the known compounds were determined by a comparison of their ^{1}H NMR and mass spectra data with literature data, together with a comparison of their optical rotation values with the literature values.

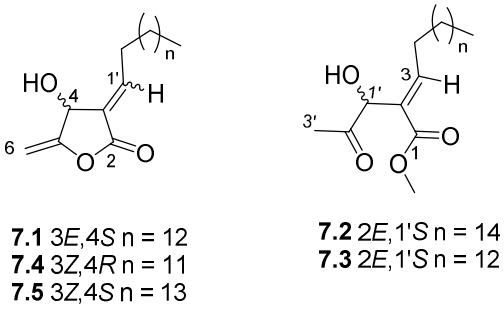

7.1 3*E*,4*S* n = 12
7.4 3*Z*,4*R* n = 11
7.5 3*Z*,4*S* n = 13

7.2 2*E*,1'*S* n = 14
7.3 2*E*,1'*S* n = 12

Figure 7.1 Structures of Compounds **7.1**–**7.5**.

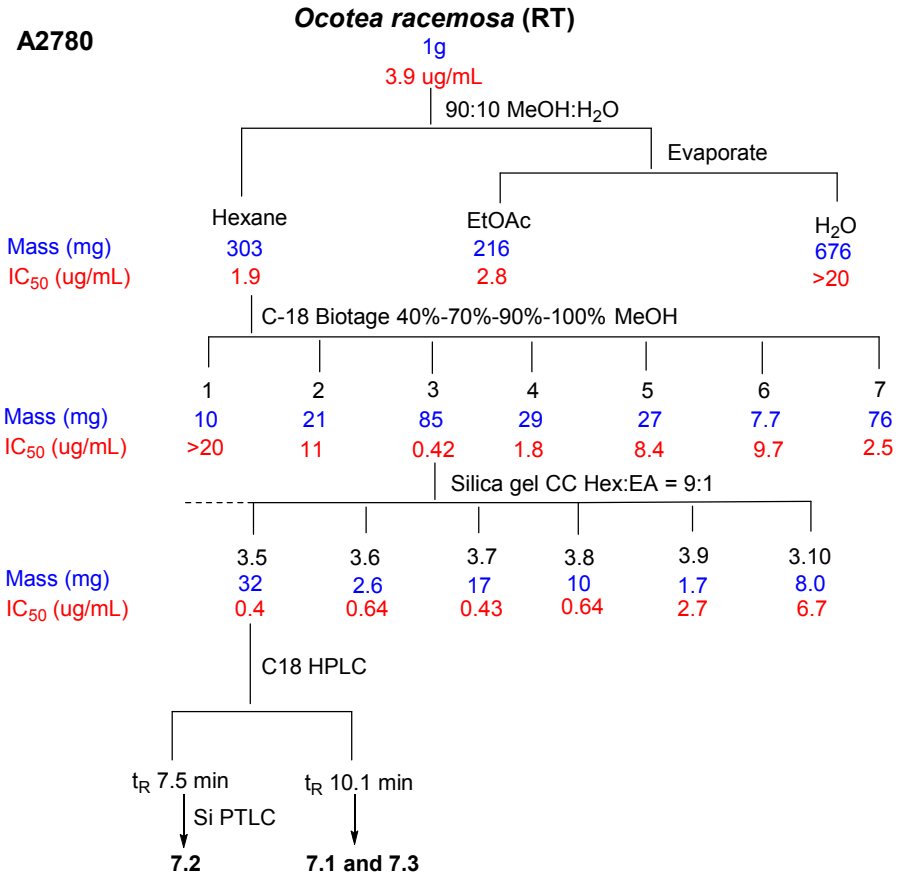

Scheme 7.1 Bioassay-guided Separation of *Ocotea macrocarpa*

7.2.2 Structure elucidation of compound **7.1**

Compound **7.1** was isolated as a colorless oil. The molecular formula was determined to be $C_{20}H_{34}O_3$ by HRESIMS ($[M + H]^+$, *m/z* 323.2586, cal. for $C_{20}H_{35}O_3^+$

323.2581). The IR exhibited the characteristic absorption bands at 3450 cm^{-1} for a hydroxyl group, and 1760 and 1700 cm^{-1} for an α,β-unsaturated-γ-lactone.[16] The UV spectrum of **7.1** had an absorption maximum at 226 nm. The IR, UV and ^1H NMR spectroscopic data of **7.1** were comparable to those of **7.4** and **7.5**, suggesting that **7.1** had the same β-hydroxy-γ-methylene-α,β-unsaturated γ-lactone skeleton. The proton signal at δ_H 7.10 (dt, J = 7.8, 2.0 Hz, 1H, H-1′) in **7.1** differed significantly from the corresponding signals in **7.4** and **7.5** at δ_H 6.68 (td, J= 7.8, 2.0 Hz, 1H, H-1′), suggesting the *E* configuration for $\Delta^{3(1')}$ in **7.1**.[16, 17] The ^1H NMR spectrum of **7.1** also displayed resonances assignable to two exomethylene protons appearing at δ_H 4.96 and δ_H 4.72 (dd, J = 2.8, 1.4 Hz, each 1H, H_2-6), one oxymethine at δ_H 5.26 (brs, 1H, H-4), and two deshielded methylene protons at δ_H 2.50 and δ_H 2.43 (dt, J = 14.8, 7.2 Hz, each 1H, H_2-2′). The positions of these protons were assigned from HMBC experimentation (Fig. 7.2). The exocyclic olefinic signals at δ_H 4.96 and δ_H 4.72 (H_2-6) were correlated with both a quaternary carbon at δ_C 157.8 (C-5) and a methine carbon at δ_C 66.7 (C-4). Carbon 5 also correlated with the oxymethine signal at δ_H 5.26 (H-4). Furthermore, clear long range correlations between both the oxymethine proton at δ_H 5.26 (H-4) and the olefinic proton at δ_H 7.10 (H-1′) to the carbonyl carbon at δ_C 166.1 (C-2) were observed in the HMBC spectrum.

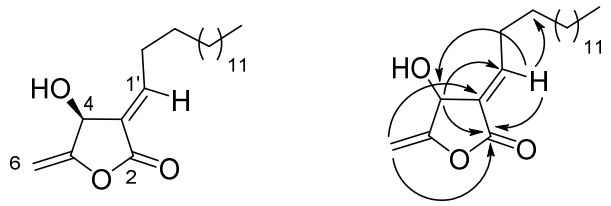

Figure 7.2 Key HMBC Correlations of **7.1**

In addition, a broad peak at δ_H 1.25−1.31 (28H, H-3′−14′) and a triplet at δ_H 0.88 (*J* = 7.0 Hz, H-15′) were attributed to the methylene protons in a long alkyl chain and the terminal methyl group in **7.1**, respectively. Compound **7.1** showed an $[\alpha]^{21}_D$ value of –11.11 (*c* 0.27, MeOH), indicating the *S* configuration at C-4 as described for previously reported butanolides.[17-19] The complete assignments of all protons and carbons of **7.1** (Table 7.1) were accomplished by further interpretation of its HMBC and HSQC spectra. Thus, the structure of **7.1** was elucidated as (3*E*,4*S*)-4-hydroxy-5-methylene-3-pentadecylidene-dihydro-furan-2-one, and named macrocarpolide A.

Table 7.1 ^{1}H and ^{13}C NMR Data for Compound **7.1**

posn	δ_H	δ_c
2		166.1 (C)
3		127.4 (C)
4	5.26 brs	66.7 (CH)
5		157.8 (C)
6	4.96 dd (2.8, 1.4) 4.72 dd (2.8, 1.4)	91.5 (CH_2)
1′	7.10 dt (7.8, 2.0)	150.3 (CH)
2′	2.50 dt (14.6, 7.7) 2.43 dt (14.6, 7.7)	29.8 (CH_2)
3′	1.25-1.31	28.3 (CH_2)
4′	1.25-1.31	29.8-29.5 (CH_2)
5′	1.25-1.31	29.8-29.5 (CH_2)
6′	1.25-1.31	29.8-29.5 (CH_2)
7′	1.25-1.31	29.8-29.5 (CH_2)
8′	1.25-1.31	29.8-29.5 (CH_2)
9′	1.25-1.31	29.8-29.5 (CH_2)
10′	1.25-1.31	29.8-29.5 (CH_2)
11’	1.25-1.31	29.8-29.5 (CH_2)
12′	1.25-1.31	29.8-29.5 (CH_2)
13′	1.25-1.31	32.1 (CH_2)
14′	1.25-1.31	22.8 (CH_2)
15′	0.88 t (7.0)	14.3 (CH_3)

Compound **7.2**, a colorless oil, had a molecular formula of $C_{23}H_{42}O_4$, as deduced from its HRESIMS spectrum (*m/z* 383.3157 $[M+H]^+$, calcd. for $C_{23}H_{43}O_4^+$, 383.3156). The IR spectrum of **7.2** showed absorption bands characteristic of hydroxyl (3458 cm^{-1}), ester (1734 cm^{-1}), and ketone (1715 cm^{-1}) groups. The UV absorption at 222 nm together with its IR and ^{1}H NMR spectroscopic data indicated a secobutanolide skeleton.[17, 19]

Comparison of the ^{1}H NMR spectroscopic data of **7.2** with those of **7.1** revealed that the ^{1}H NMR spectrum of **7.2** exhibited additional signals at δ_H 3.73 (s, 3H, 1-OMe) and δ_H 2.15 (s, 3H, H-3′), but lacked the signals at δ_H 4.96 and δ_H 4.72 in **7.1**. This fact confirmed the presence of a methoxy and an acetyl group, and the absence of the *α,β*-unsaturated-*γ*-lactone ring in **7.2**. In its HMBC spectrum, protons of the acetyl group at δ_H 2.15 (H-3′) showed correlations to an oxymethine group at δ_C 73.5 (C-1′).(Figure 7.3) The methoxy protons at δ_H 3.73 (1-OMe) correlated with a carbonyl carbon at δ_C 166.7 (C-1), and the olefinic proton at δ_H 7.08 (t, *J*= 7.7 Hz, H-3) exhibited cross peaks with both the oxymethine carbon (δ_C 73.5, C-1′) and the carbonyl carbon (δ_C 166.7, C-1). Those correlations confirmed the assignment of a secobutanolide skeleton to **7.2**. By the same analysis used to characterize compound **7.1**, the deshielded methylene group of **7.2** was assigned at C-4 by the HMBC correlation between δ_H 2.35 (q, *J* = 7.6 Hz, 2H, H-4) and the quaternary olefinic carbon at δ_C 129.9 (C-2). Furthermore, the presence of an *E* trisubstituted double bond was evident from the characteristic chemical shift of the olefinic proton at δ_H 7.08 (H-3), compared to that of known compounds with a *Z* conformation (δ_H 6.69).[17, 19]

The positive optical activity (+2.23, *c* 2.24, MeOH) of **7.2** indicated that C-1′ possessed the *S* configuration.[20-22] Similarly to **7.1**, the complete assignments of all

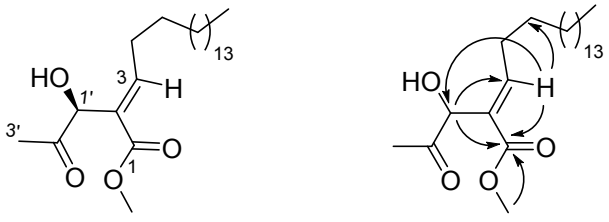

Figure 7.3 Key HMBC Correlations of **7.2**

protons and carbons of **7.2** (Table 7.2) were accomplished by further interpretation of its HMBC and HSQC spectra. From the above data, compound **7.2** was assigned as (2*E*)-2-[(1*S*)-1-hydroxy-2-oxo-propyl]-nonadec-2-enoic acid methyl ester, and named macrocarpolide B.

Table 7.2 ^{1}H and ^{13}C NMR Data for Compounds **7.2** and **7.3**.

		7.2		**7.3**
posn	δ_H	δ_c	δ_H	δ_c
1		166.7 (C)		166.7 (C)
2		129.9 (C)		129.9 (C)
3	7.08 t (7.7)	149.3 (CH)	7.08 t (7.0)	149.3 (CH)
4	2.35 q (7.6)	28.9 (CH_2)	2.35 q (7.6)	28.9 (CH_2)
5	1.25-1.31	28.4 (CH_2)	1.26 br s	28.4 (CH_2)
6	1.25-1.31	29.8-29.5 (CH_2)	1.26 br s	29.8-29.5 (CH_2)
7	1.25-1.31	29.8-29.5 (CH_2)	1.26 br s	29.8-29.5 (CH_2)
8	1.25-1.31	29.8-29.5 (CH_2)	1.26 br s	29.8-29.5 (CH_2)
9	1.25-1.31	29.8-29.5 (CH_2)	1.26 br s	29.8-29.5 (CH_2)
10	1.25-1.31	29.8-29.5 (CH_2)	1.26 br s	29.8-29.5 (CH_2)
11	1.25-1.31	29.8-29.5 (CH_2)	1.26 br s	29.8-29.5 (CH_2)
12	1.25-1.31	29.8-29.5 (CH_2)	1.26 br s	29.8-29.5 (CH_2)
13	1.25-1.31	29.8-29.5 (CH_2)	1.26 br s	29.8-29.5 (CH_2)
14	1.25-1.31	29.8-29.5 (CH_2)	1.26 br s	29.8-29.5 (CH_2)
15	1.25-1.31	29.8-29.5 (CH_2)	1.26 br s	32.1 (CH_2)
16	1.25-1.31	29.8-29.5 (CH_2)	1.26 br s	29.8-29.5 (CH_2)
17	1.25-1.31	32.1 (CH_2)	0.88 t (7.0)	14.3 (CH_3)
18	1.25-1.31	22.8 (CH_2)		
19	0.88 t (7.0)	14.3 (CH_3)		
1′	4.90 brd (4.9)	73.5 (CH)	4.90 brs	73.5 (CH)
2′		206.2 (C)		206.2 (C)
3′	2.15 s	25.0 (CH_3)	2.15 s	25.0 (CH_3)
1-OMe	3.73 s	52.2 (CH_3)	3.73 s	52.2 (CH_3)

The molecular formula of compound **7.3** ($C_{21}H_{38}O_4$, HRESIMS *m/z*: 355.2856 $[M+H]^+$, calcd. for $C_{21}H_{39}O_4^+$, 355.2843) differed from that of **7.2** by C_2H_4, suggesting a two-carbon deletion in the side chain. Analysis of the UV, IR and ^{1}H NMR spectra revealed **7.3** to be a similar secobutanolide to **7.2**, with the same *E* geometry of the

trisubstituted double bond [δ_H 7.08 (t, J = 7.0 Hz, 1H, H-3)], but with two carbons less in the alkyl chain. Similarly to **7.2**, the *S* configuration at C-1′ was deduced by the positive optical rotation value of +2.27 (*c* 0.88, MeOH).[20-22] The complete assignments of all protons and carbons of **7.3** (Table 7.2) were accomplished by interpretation of its HMBC and HSQC spectra. Therefore, compound **7.3** was assigned as (2*E*)-2-[(1*S*)-1-hydroxy-2-oxo-propyl]-heptadec-2-enoic acid methyl ester, and named macrocarpolide C.

7.2.3 Antiproliferative Activities

Compounds **7.1–7.5** showed good antiproliferative activities against the drug-sensitive A2780 ovarian cell line[23] as previously described[24] using paclitaxel (IC_{50} 0.073 ± 0.015 μM) as the positive control. Their IC_{50} values were 2.57 ± 0.12 (**7.1**), 1.98 ± 0.23 (**7.2**), 1.67 ± 0.05 (**7.3**), 2.43 ± 0.41 (**7.4**), and 1.65 ± 0.44 μM (**7.5**). The similar IC_{50} values for the five compounds suggests that they have a similar mechanism of action, possibly as Michael acceptors.

7.3 Experimental section

7.3.1 General experimental procedures

IR and UV spectra were measured on MIDAC M-series FTIR and Shimadzu UV-1201 spectrophotometers, respectively. ^1H and ^{13}C NMR spectra were recorded on a Bruker Avance 500 spectrometer in $CDCl_3$ (with $CDCl_3$ as reference). Mass spectra were obtained on an Agilent 6220 mass spectrometer. Open column chromatography and preparative TLC was performed using silica gel (230–400 mesh, Silicycle Co. USA) and silica gel plates (60 F254, Silicycle Co. USA), respectively. Flash chromatography was

performed on a Biotage Horizon flash chromatograph using a C18 column (Phenomenex, 150 × 12 mm, 11 g). Semi-preparative HPLC was performed using Shimadzu LC-10AT pumps coupled with a semipreparative Phenomenex C18 column (5 μm, 250 × 10 mm), a Shimadzu SPD M10A diode array detector, and a SCL-10A system controller.

7.3.2 Plant material

Plant parts of *Ocotea macrocarpa* Kosterm. (Lauraceae) were collected by Andriamalala Rakotondrafara et al. on 23 March 2011. The collection was made in the district of Ankazobe in the Analamanga region of Madagascar, in the Analamaitso forest near the village of Tsaramandroso. The coordinates were 17°57'32"S 047°07'33"E, and the elevation was 1478 m. The tree was 14 m tall with a diameter at breast height of 25 cm. It had cream-yellow petals and yellow inflorescences. Duplicate voucher specimens (Rakotondrafara 989) have been deposited at the Centre National d'Application des Recherches Pharmaceutiques (CNARP), Parc Botanique and Zoologique de Tsimbazaza (TAN), the Missouri Botanical Garden, St. Louis, Missouri (MO), and the herbarium of the National Museum of Natural History, Paris (P).

7.3.3 Extraction and isolation

A ground sample of *Ocotea macrocarpa* roots (250 g) was extracted with EtOH at room temperature to yield 8.3 g of crude EtOH extract designated MG4725. A total of 1.85 g of this extract was made available to Virginia Tech. The crude EtOH extract (1.0 g) was dissolved in 90% aq. MeOH (300 mL), and extracted with hexanes (3 × 200 mL). Evaporation of the hexanes-soluble fraction afforded 302.7 mg of residue. The 90% aq. MeOH layer was then evaporated, suspended in H_2O (300 mL), and extracted with

EtOAc (3 × 200 mL) to yield 215.5 mg of EtOAc-soluble fraction. The aqueous layer was concentrated to give 476.6 mg of brown residue. The hexanes fraction was found to be cytotoxic with an IC_{50} value of 1.9 μg/mL and was subjected to C 18 flash column chromatography (aq. MeOH, 40% to 70% to 90% to 100%) to give 7 new fractions. The most active fraction Fr 3 (85.4 mg, IC_{50} 0.42 μg/mL) was then divided into 10 sub-fractions by silica gel open column chromatography (Hex:EtOAc = 9:1). Further purification of one the most active sub-fractions Fr 3-5 (IC_{50} 0.4 μg/mL) was done by using HPLC on a C18 column with a solvent gradient from H_2O:MeOH, 10:90 to 0:100 from 0 to 10 min and ending with 100% MeOH from 10 to 30 min. This process yielded two active fractions with retention time of 7.5 min and 10.1 min respectively. Preparative silica gel TLC (Hex:EtOAc= 9:1) purification of the two fractions yielded compounds **7.2** (0.76 μg/mL), and compounds **7.1** (0.91 μg/mL) and **7.3** (0.83 μg/mL), respectively. Further purification of the other active sub-fraction from silica gel open column Fr 3-6 by C18 HPLC, with a solvent gradient from H_2O:MeOH, 30:70 to 20:80 from 0 to 15 min, to 10:90 from 15 to 25 min, to 0:100 from 25 to 35 min, and ending with 100% MeOH furnished compounds **7.4** (t_R 23.1 min, 0.75 μg/mL) and **7.5** (t_R 27.6 min, 0.55 μg/mL).

7.3.4 Macrocarpolide A (**7.1**)

Colorless oil, $[\alpha]^{21}_D$ -11.11 (*c* 0.27, MeOH); UV (MeOH) λ_{max} (log ε) : 226 (3.35) nm; IR (film) ν_{max} 3450, 1760, 1700, 1049 cm^{-1}; ^1H and ^{13}C NMR data, see Table 7.1; HRESIMS *m/z* $[M+H]^+$ 323.2586 (calcd for $C_{20}H_{35}O_3^+$, 323.2581)

7.3.5 Macrocarpolide B (**7.2**)

Colorless oil, $[\alpha]^{21}_{D}$ +2.23 (*c* 2.24, MeOH); UV (MeOH) λ_{max} (log ε) : 222 (3.26) nm; IR (film) ν_{max} 3458, 1734, 1715, 1040 cm^{-1}; ^{1}H and ^{13}C NMR data, see Table 7.1; HRESIMS *m/z* $[M+H]^+$ 383.3157 (calcd for $C_{23}H_{43}O_4^+$, 383.3156)

7.3.6 Macrocarpolide C (**7.3**)

Colorless oil, $[\alpha]^{21}_{D}$ +2.27 (*c* 0.88, MeOH); UV (MeOH) λ_{max} (log ε) : 222 (3.43) nm; IR (film) ν_{max} 3455, 1736, 1710, 1060 cm^{-1}; ^{1}H and ^{13}C NMR data, see Table 7.1; HRESIMS *m/z* $[M+H]^+$ 355.2856 (calcd for $C_{21}H_{39}O_4^+$, 355.2843)

7.3.7 Antiproliferative bioassay

The A2780 ovarian cancer cell line antiproliferative bioassay was performed at Virginia Tech as previously reported.[24] The A2780 cell line is a drug-sensitive ovarian cancer cell line.[23] Paclitaxel was used as the positive control; it had an IC_{50} value of 0.073 ± 0.015 μM.

7.4 References

1. Liu, Y.; Cheng, E.; Rakotondraibe, L. H.; Brodie, P. J.; Applequist, W.; Randrianaivo, R.; Rakotondrafara, A.; Ratsimbason, M.; Rasamison, V. E.; Kingston, D. G. I. Antiproliferative compounds from *Ocotea macrocarpa* from the Madagascar dry forest. *Tetrahedron Lett.* **2015**, Ahead of Print.

2. Harinantenaina, L.; Brodie, P. J.; Maharavo, J.; Bakary, G.; TenDyke, K.; Shen, Y.; Kingston, D. G. I. Antiproliferative homoscalarane sesterterpenes from two Madagascan sponges. *Bioorg. Med. Chem.* **2013,** *21*, 2912-2917.

3. Murphy, B. T.; Brodie, P.; Slebodnick, C.; Miller, J. S.; Birkinshaw, C.; Randrianjanaka, L. M.; Andriantsiferana, R.; Rasamison, V. E.; TenDyke, K.; Suh, E. M.; Kingston, D. G. I. Antiproliferative limonoids of a *Malleastrum* sp. from the Madagascar rainforest. *J. Nat. Prod.* **2008,** *71*, 325-329.

4. Rohwer, J. G. Toward a phylogenetic classification of the lauraceae: Evidence from matK sequences. *Syst. Bot.* **2000,** *25*, 60-71.

5. van der Werff, H. A revision of the genus *Ocotea* Aubl. (Lauraceae) in Madagascar and the Comoro Islands. *Adansonia, sér. 3,* **2013,** *35*, 235-279.

6. Coelho de Souza, G.; Haas, A. P. S.; von Poser, G. L.; Schapoval, E. E. S.; Elisabetsky, E. Ethnopharmacological studies of antimicrobial remedies in the south of Brazil. *J. Ethnopharmacol.* **2004,** *90*, 135-143.

7. Destryana, R. A.; Young, D. G.; Woolley, C. L.; Huang, T. C.; Wu, H. Y.; Shih, W. L. Antioxidant and anti-inflammation activities of *Ocotea*, *Copaiba* and blue cypress essential oils in vitro and in vivo. *J. Am. Oil Chem. Soc.* **2014,** *91*, 1531-1542.

8. Jose de Camargo, M.; Miranda, M. L. D.; Kagamida, C. M.; Rodrigues, E. D.;

Garcez, F. R.; Garcez, W. S. Sesquiterpenes of *Ocotea lancifolia* (Lauraceae). *Quim. Nova* **2013,** *36*, 1008-1013.

9. Garett, R.; Romanos, M. T. V.; Borges, R. M.; Santos, M. G.; Rocha, L.; da Silva, A. J. R. Antiherpetic activity of a flavonoid fraction from *Ocotea notata* leaves. *Rev. Bras. Farmacogn.* **2012,** *22*, 306-313.

10. Yamaguchi, M. U.; Garcia, F. P.; Cortez, D. A. G.; Ueda-Nakamura, T.; Filho, B. P. D.; Nakamura, C. V. Antifungal effects of Ellagitannin isolated from leaves of *Ocotea odorifera* (Lauraceae). *Antonie Van Leeuwenhoek* **2011,** *99*, 507-514.

11. Garcez, F. R.; da Silva, A. F. G.; Garcez, W. S.; Linck, G.; Matos, M. d. F. C.; Santos, E. C. S.; Queiroz, L. M. M. Cytotoxic aporphine alkaloids from *Ocotea acutifolia*. *Planta Med.* **2011,** *77*, 383-387.

12. Castro, R. D.; Lima, E. O. Antifungal activity of Brazilian sassafras (*Ocotea odorifera* Vell.) and rosemary (*Rosmarinus officinalis* L.) essential oils against genus Candida. *Rev. Bras. Plant. Med.* **2011,** *13*, 203-208.

13. Cuca, L. E.; Leon, P.; Coy, E. D. A bicyclo[3.2.1]octanoid neolignan and toxicity of the ethanol extract from the fruit of *Ocotea heterochroma*. *Chem. Nat. Compd.* **2009,** *45*, 179-181.

14. Seki, K.; Sasaki, T.; Wano, S.; Haga, K.; Kaneko, R. Linderanolides and isolinderanolides, ten butanolides from *Lindera glauca*. *Phytochemistry* **1995,** *40*, 1175-1181.

15. Anderson, J. E.; Ma, W.; Smith, D. L.; Chang, C. J.; McLaughlin, J. L. Biologically active γ-lactones and methylketoalkenes from *Lindera benzoin*. *J. Nat. Prod.* **1992,** *55*, 71-83.

16. Cheng, H. I.; Lin, W. Y.; Duh, C. Y.; Lee, K. H.; Tsai, I. L.; Chen, I. S. New cytotoxic butanolides from *Litsea acutivena*. *J. Nat. Prod.* **2001,** *64*, 1502-1505.

17. Cheng, M. J.; Tsai, I. L.; Lee, S. J.; Jayaprakasam, B.; Chen, I. S. Steryl epoxide, secobutanolide and butanolides from the stem wood of *Machilus zuihoensis*. *Phytochemistry (Elsevier)* **2005,** *66*, 1180-1185.

18. Martinez V, J. C.; Yoshida, M.; Gottlieb, O. R. The chemistry of Brazilian lauraceae. Part LXI. ω-Ethyl, ω-ethenyl and ω-ethynyl-α-alkylidene-γ-lactones from *Clinostemon mahuba*. *Phytochemistry* **1981,** *20*, 459-464.

19. Tsai, I. L.; Hung, C. H.; Duh, C. Y.; Chen, I. S. Cytotoxic butanolides and secobutanolides from the stem wood of formosan *Lindera communis*. *Planta Med.* **2002,** *68*, 142-145.

20. Chen, C. Y.; Chen, C. H.; Wong, C. H.; Liu, Y. W.; Lin, Y. S.; Wang, Y. D.; Hsui, Y. R. Cytotoxic constituents of the stems of *Cinnamomum subavenium*. *J. Nat. Prod.* **2007,** *70*, 103-106.

21. Kuo, S. Y.; Hsieh, T. J.; Wang, Y. D.; Lo, W. L.; Hsui, Y. R.; Chen, C. Y. Cytotoxic constituents from the leaves of *Cinnamomum subavenium*. *Chem. Pharm. Bull.* **2008,** *56*, 97-101.

22. Tanaka, H.; Nakamura, T.; Ichino, K.; Ito, K. Secoisolancifolide and secoisoobtusilactone in *Actinodaphne longifolia*. *Phytochemistry* **1989,** *28*, 1905-1907.

23. Louie, K. G.; Behrens, B. C.; Kinsella, T. J.; Hamilton, T. C.; Grotzinger, K. R.; McKoy, W. M.; Winker, M. A.; Ozols, R. F. Radiation survival parameters of antineoplastic drug-sensitive and -resistant human ovarian cancer cell lines and their modification by buthionine sulfoximine. *Cancer Res.* **1985,** *45*, 2110-2115.

24. Cao, S.; Brodie, P. J.; Miller, J. S.; Randrianaivo, R.; Ratovoson, F.; Birkinshaw, C.; Andriantsiferana, R.; Rasamison, V. E.; Kingston, D. G. I. Antiproliferative xanthones of terminalia calcicola from the Madagascar rain forest. *J. Nat. Prod.* **2007,** *70*, 679-681.

8 Antiproliferative Compounds from *Malleastrum* sp. from the Madagascar Dry Forest

This chapter is a slightly expanded version of an article submitted to the journal *Natural Product Communications.* Attributions from co-authors of the articles are described as follows in the order of the names listed. The author of this dissertation (Yixi Liu) mentored the undergraduate student (Houston Wiedle Jr.) with the compounds isolation, and elucidated the structures of all compounds, and drafted the manuscript. Mrs. Peggy Brodie performed the A2780 bioassay on the isolated fractions and compounds. Dr. Martin Callmander and Dr. Robert Rakotondrajaona from Missouri Botanical Garden collected and identified the plant. Dr. Etienne Rakotobe and Dr. Vincent E. Rasamison from Madagascar carried out the initial plant extraction. Dr. David G. I. Kingston was a mentor for this work and the corresponding author for the published article. He provided critical suggestions for this work and crucial revisions to the manuscript.

8.1 Introduction

As a part of the Madagascar International Cooperative Biodiversity Group (ICBG) program,[1, 2] an ethanol extract of the leaves of a *Malleastrum* sp. (Meliceae) was selected for evaluation as a possible source of new antiproliferative agents based on its activity against the A2780 ovarian cancer cell line. The Meliceae family has its origins in the western Gondwanan region of Pangea and played an important part in the dispersal of the mahogany biota. The dispersal was most likely an “out-of-Africa” scenario with dispersal across Eurasia and North America due to a land bridge. With multiple fossil findings, it has been confirmed that the entry of Meliceae into southern continents from Oligocene to

Pliocene must be considered as important in establishing a pantropical distribution for the family.[3] This family has been known to produce structurally unique, highly oxygenated, and biologically active liminoids.[4] Liminoids have been shown to inhibit the growth of estrogen receptor negative and positive human breast cancer cells in culture. There has also been success in inhibiting cancer cell lines of leukemia, ovary, cervix, stomach, and liver. Prevalent in many known antioxidant foods, rings in the limonoid nucleus play a critical role in antineoplastic activity.[5] Therefore, plants in the Meliceae family may hold compounds that can be utilized in conjunction with radiation therapies of certain cancers.[6]

As a member of the Meliceae family, the genus *Malleastrum* was first segregated from the genus *Cipadessa* and has been found to contain eleven species. Recent chemical work on the genus *Malleastrum* has afforded new limonoids with tetranortriterpenoid skeletons.[7] These compounds have also been found in other plants such as *Carapa guianensis* and have been used in popular medicine to treat inflammation and infection. Compounds in the plant material such as 6α-acetoxygedunin, 7-deacetoxy-7-oxogedunin, andirobin, gedunin and methyl-angolensate impair the production of inflammatory mediators that trigger leukocyte infiltration into the inflammatory site as well as the inflammatory cytokines tumor necrosis factor (TNF)-α and IL-1β.[8]

A bioassay-guided isolation of compounds from the leaves of the plant, *Malleastrum rakotozafyi,* afforded a new clerodane diterpene, 18-oxo-cleroda-3,13-dien-16,15-olide (**8.1**), together with three known clerodane diterpenes: 16,18-dihydroxykolavenic acid lactone (**8.2**),[9] solidagolactone (**8.3**),[10] and (-)-kolavenol (**8.4**),[11] and one known labdane diterpene: 3-oxo-ent-Iabda-8(17),13-dien-15,16-olide (**8.5**).[12]

(Figure 8.1)

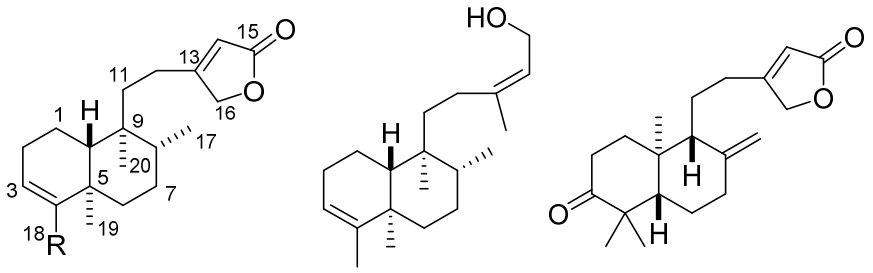

8.1 R=CHO
8.2 R=CH_2OH
8.3 R=CH_3

8.4 **8.5**

Figure 8.1 Structures of Compounds **8.1–8.5**.

8.2 Results and Discussion

8.2.1 Isolation of active compounds

An active CH_2Cl_2-soluble fraction obtained from liquid-liquid partition of the extract (100 mg) was subjected to dereplication studies using size-exclusion chromatography, reverse phase HPLC coupled with bioassay, high-resolution ESIMS (HRESIMS), ^{1}HNMR, and a database search using the online Dictionary of Natural Product (DNP). The results indicated that the extract contained a possible new bioactive compound, therefore a larger scale sample (1.0 g) was investigated. Fractionation of this extract yielded an antiproliferative CH_2Cl_2 fraction which was further subjected to Sephadex LH-20 column chromatography followed by normal phase solid phase extract (SPE). The most active fractions from the silica gel SPE were subjected to C18 HPLC to yield one new (**8.1**) and four known (**8.2**–**8.5**) bioactive diterpenes. (Scheme 8.1)

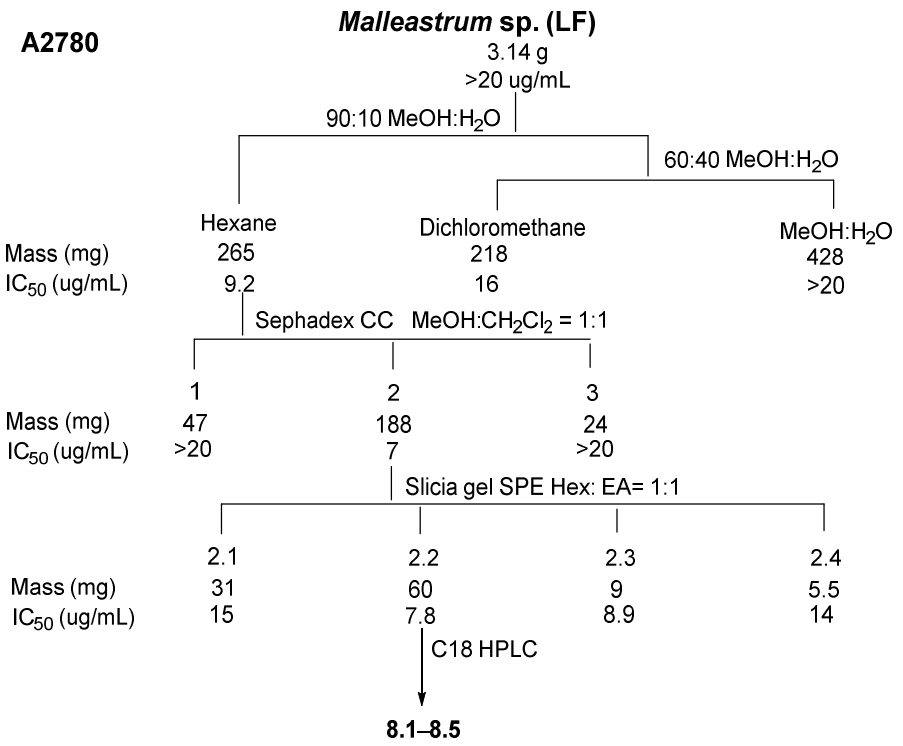

Scheme 8.1 Bioassay-guided Separation of *Malleastrum* sp.

The structures of the known compounds **8.2**–**8.5** were determined by searching their molecular formula and key ^{1}H NMR spectroscopic features in the DNP database and comparison of their full ^{1}H NMR spectrum and optical rotation values with reported literature data.

8.2.2 Structure elucidation of compound **8.1**

Compound **8.1** was isolated as a colorless oil with a molecular formula of $C_{20}H_{28}O_3$, as established from HRESIMS (*m/z* $[M+H]^+$ 317.2111, calc. for 317.2112). The UV spectrum exhibited an absorbance compatible with an α,β-unsaturated γ-lactone moiety (213 nm).[9] The IR spectrum showed absorptions characteristic of a β-substituted butenolide moiety at 1779, 1747, and 1634 cm^{-1}, and a β-unsaturated aldehyde carbonyl

at 1683 cm^{-1}.[13] The IR, UV and ^1H NMR spectroscopic data of **8.1** were comparable to those of **8.2**–**8.4**, suggesting the same clerodane-type diterpene skeleton for **8.1**. Further examination of the ^1H NMR spectra indicated that **8.1** was most similar to **8.2**, differing by the presence of an additional aldehyde signal at δ_H 9.31 (s, 1H, H-18) in **8.1**, the absence of the oxymethylene at δ_H 4.10 (brs, 2H, H_2-18) in **8.2**, and the more deshielded olefinic proton at δ_H 6.58 (dd, *J*= 4.7, 2.7 Hz, 1H, H-3) in **8.1** instead of that at δ_H 5.57 (brs, 1H, H-3) in **8.2**. These differences could be accounted for by the oxidation of the allylic alcohol group found in **8.2** to an aldehyde group in **8.1**. The ^1H NMR spectrum of **8.1** also displayed resonances assignable to an olefinic proton at δ_H 5.85 (m, 1H, H-14), one oxymethylene group at δ_H 4.75 (brd, *J*= 1.7 Hz, 2H, H_2-16), and 14 protons in the region of 1.25–2.70 ppm. The presence of three methyl groups in **8.1** was suggested by the two singlets at δ_H 1.17 and δ_H 0.81 (each 3H, H_3-19 and H_3-20) and a doublet at δ_H 0.83 (d, *J*= 6.3 Hz, 3H, H_3-17), which were attached to two quaternary carbons and a tertiary carbon, respectively.

All the above data supported a clerodane-type skeleton for **8.1**.[14-16] The structure was confirmed as the C-18 aldehyde analog of **8.2** by HMBC experiment (Fig. 8.2). The correlations between the olefinic proton at δ_H 5.85 (H-14) and the oxymethylene carbon at δ_C 72.5 (C-16), and between the oxymethylene protons at δ_H 4.75 (H_2-16) and the carbonyl carbon at δ_C 173.1 (C-15) confirmed the presence of the α,β-unsaturated γ-lactone ring. The lactone ring was connected at the β position with C-12 due to the cross peaks between H_2-11 (δ_H 1.71 and 1.61) and C-13 (δ_C 169.5), and between H_2-12 (δ_H 2.33 and 2.16) and both C-14 (δ_C 114.9) and C-16 (δ_C 72.5). In addition, the correlations

between the aldehyde proton at δ_H 9.31 (H-18) and both the olefinic carbon C-3 (δ_C 153.1) and the quaternary carbon C-5 (δ_C 37.6) allowed us to place the aldehyde group at C-4. In the same manner, the three methyl groups were located at C-5, C-8, and C-9 based on long range HMBC correlations between δ_H 1.17 (H_3-19) and both δ_C 151.5 (C-4) and δ_C 34.6 (C-6), between δ_H 0.83 (H_3-17) and both C-7 (δ_C 27.7) and C-9 (δ_C 37.5), and between H_3-20 and both C-8 (δ_C 35.9) and C-10 (δ_C 46.4).

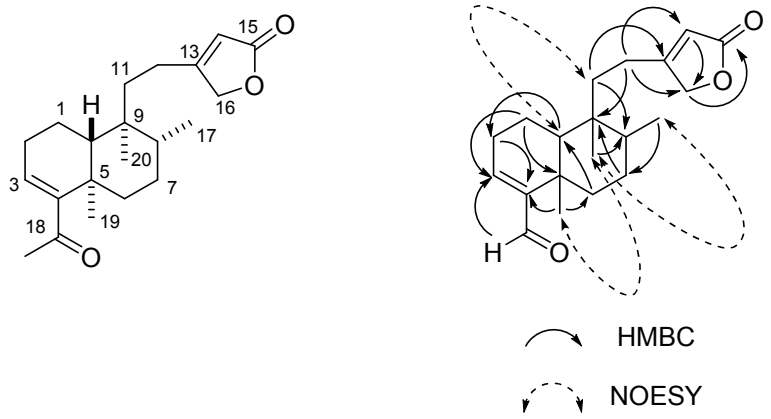

Figure 8.2 Key HMBC and NOESY Correlations of **8.1**.

Furthermore, the relative configuration of **8.1** was determined by a NOESY experiment (Fig. 8.2). Observation of clear NOE correlations between δ_H 0.81 (H_3-20) and both δ_H 0.83 (H_3-17) and δ_H 1.17 (H_3-19), indicated the *cis* relationships between the three methyl groups. At the same time, the NOE correlation between δ_H 1.27 (H-10) and δ_H 1.61 (H-11a) suggested the *cis* relationships between C-10 and the C-11–C-12 side chain bearing the lactone ring, and a *trans* A/B ring junction of **8.1**. The complete assignments of all protons and carbons of **8.1** (Table 8.1) were accomplished by further interpretation of its HMBC and HSQC spectra. Thus, the structure of compound **8.1** was elucidated as 18-oxo-cleroda-3,13-dien-16,15-olide.

Table 8.1 ^{1}H and ^{13}C NMR Data for Compound **8.1**

posn	δ_H[b]	δ_C[c]
1	1.65[d]	17.3 CH_2
	1.51 m	
2	2.51 dt (20.4, 5.1)	29.0 CH_2
	2.88 m	
3	6.58 dd (4.7, 2.7)	151.3 CH
4		151.5 C
5		37.6 C
6	2.68 dt (13.4, 2.7)	34.6 CH_2
	1.12 m	
7	1.67[d]	27.7 CH_2
	1.49[d]	
8	1.48[d]	35.9 CH
9		37.5 C
10	1.27 m	46.4 CH
11	1.71[d]	34.4 CH_2
	1.61[d]	
12	2.33 m	22.4 CH_2
	2.16 m	
13		169.5 C
14	5.85 m	114.9 CH
15		173.1 C
16	4.75 brd (1.7)	72.5 CH_2
17	0.83 d (6.3)	15.4 CH_3
18	9.31 s	194.2 C
19	1.17 s	19.7 CH_3
20	0.81 s	17.6 CH_3

8.2.3 Antiproliferative activities

Compounds **8.1**–**8.5** were evaluated for their antiproliferative activity against the A2780 human ovarian cancer cell line. Compounds **8.1**, **8.3**, and **8.4** showed micromolar A2780 activities with IC_{50} value of 3.0 ± 0.8, 7.8 ± 0.2, and 17.9 ± 3 μM, respectively.

8.3 Experimental section

8.3.1 General experimental procedures

IR and UV spectra were measured on MIDAC M-series FTIR and Shimadzu UV-1201 spectrophotometers, respectively. ^{1}H and ^{13}C NMR spectra were recorded on a Bruker Avance 500 spectrometer in $CDCl_3$, with $CDCl_3$ as reference. Mass spectra were obtained on an Agilent 6220 mass spectrometer. Open column chromatography was

performed using Sephadex LH-20. Solid phase extract was performed using silica gel (230-400 mesh, Silicycle Co. USA). Semi-preparative HPLC was performed using Shimadzu LC-10AT pumps coupled with a semipreparative Phenomenex C-18 column (5 μm, 250 × 10 mm), a Shimadzu SPD M10A diode array detector, and a SCL-10A system controller.

8.3.2 Plant material

8.3.3 Extraction and isolation

A ground sample of *M.* sp. leaves g was extracted with EtOH at room temperature to yield g of crude EtOH extract designated MG 3652. A total of 3.14 g of this extract was made available to Virginia Tech. A part of the crude EtOH extract (1.0 g) was dissolved in 90% aq. MeOH (300 mL) and extracted with hexanes (3 × 200 mL). Evaporation of the hexanes-soluble fraction yielded 265.1 mg of residue. The 90% aq. MeOH layer was then evaporated, suspended in H_2O (300 mL), and extracted with dichloromethane (3 × 200 mL) to yield 218.3 mg of CH_2Cl_2-soluble fraction. The aqueous layer was concentrated to give 428 mg of green residue. The hexanes fraction was found to be weakly cytotoxic with an IC_{50} value of 9.2 μg/mL and was subjected to Sephadex LH-20 open column chromatography (CH_2Cl_2: MeOH = 1:1) to give 3 fractions. The most active fraction Fr-2 (IC_{50} 7 μg/mL) was fractionated by silica gel SPE using hexanes/EtOAc (70:30 to 50:50 to 30:70 to 0:100, MeOH wash) to give 4 sub-fractions. The second sub-fraction Fr-2-2 (IC_{50} 6.8 μg/mL) was then subjected to C18 HPLC with a solvent gradient from H_2O:CH_3CN, 30:70 to 20:80 from 0.01 to10 min, to 10:90 from 10 to 15 min, to 0:100 from 15 to 20 min, and ending with 100% CH_3CN to

35 min, furnishing compounds **8.1** (t_R 13.5 min, IC_{50} 0.97 μg/mL), **8.2** (t_R 9.5 min, IC_{50} >20 μg/mL), **8.3** (t_R 23.8 min, IC_{50} 2.37 μg/mL), **8.4** (t_R 28.6 min, IC_{50} 5.2 μg/mL), and **8.5** (t_R 12 min, IC_{50} >20 μg/mL).

8.3.4 18-Oxo-cleroda-3,13-dien-16,15-olide (**8.1**)

Amorphous powder, $[\alpha]^{21}_D$ -60.2 (*c* 0.68, MeOH); UV (MeOH) λ_{max} (log ε): 213 (3.96) nm; IR (film) ν_{max} 2922, 2864, 1779, 1747, 1715, 1683, 1559 cm^{-1}; ^1H and ^{13}C NMR data, see Table 8.1; HRESIMS: *m/z* $[M+H]^+$ 317.2112 (calcd. for $C_{20}H_{29}O_3^+$: 317.2111)

8.3.5 Antiproliferative bioassay

The A2780 ovarian cancer cell line antiproliferative bioassay was performed at Virginia Tech as previously reported.[17] The A2780 cell line is a drug-sensitive ovarian cancer cell line.[6] Paclitaxel was used as the positive control; it had an IC_{50} value of 0.073 ± 0.015 μM.

8.4 References

1. Kingston, D. G. I. Modern natural products drug discovery and its relevance to biodiversity conservation. *J. Nat. Prod.* **2011,** *74*, 496-511.

2. Murphy, B. T.; Brodie, P.; Slebodnick, C.; Miller, J. S.; Birkinshaw, C.; Randrianjanaka, L. M.; Andriantsiferana, R.; Rasamison, V. E.; TenDyke, K.; Suh, E. M.; Kingston, D. G. I. Antiproliferative limonoids of a *Malleastrum* sp. from the Madagascar rainforest. *J. Nat. Prod.* **2008,** *71*, 325-329.

3. Muellner, A. N.; Savolainen, V.; Samuel, R.; Chase, M. W. The mahogany family "out-of-Africa": Divergence time estimation, global biogeographic patterns inferred from plastid *rbcL* DNA sequences, extant, and fossil distribution of diversity. *Mol. Phylogenet. Evol.* **2006,** *40*, 236-250.

4. Coombes, P. H.; Mulholland, D. A.; Randrianarivelojosia, M. Vilasinin limonoids from *Malleastrum antsingyense* J.F. Leroy (Meliodeae: Meliaceae). *Biochem. Syst. Ecol.* **2008,** *36*, 74-76.

5. Miller, E. G.; Porter, J. L.; Binnie, W. H.; Guo, I. Y.; Hasegawa, S. Further studies on the anticancer activity of citrus limonoids. *J. Agric. Food Chem.* **2004,** *52*, 4908-4912.

6. Louie, K. G.; Behrens, B. C.; Kinsella, T. J.; Hamilton, T. C.; Grotzinger, K. R.; McKoy, W. M.; Winker, M. A.; Ozols, R. F. Radiation survival parameters of antineoplastic drug-sensitive and -resistant human ovarian cancer cell lines and their modification by buthionine sulfoximine. *Cancer Res.* **1985,** *45*, 2110-2115.

7. Murphy, B. T.; Brodie, P.; Slebodnick, C.; Miller, J. S.; Birkinshaw, C.; Randrianjanaka, L. M.; Andriantsiferana, R.; Rasamison, V. E.; TenDyke, K.; Suh, E. M.; Kingston, D. G. I. Antiproliferative limonoids of a *Malleastrum sp.* from the Madagascar

rain forest. *J. Nat. Prod.* **2008,** *71*, 325-329.

8. das Gracas Henriques, M.; Penido, C. The therapeutic properties of *Carapa guianensis*. *Curr. Pharm. Des.* **2014,** *20*, 850-856.

9. Cao, S.; Hou, Y.; Brodie, P.; Miller, J. S.; Randrianaivo, R.; Rakotobe, E.; Rasamison, V. E.; Kingston, D. G. I. Antiproliferative compounds of *Cyphostemma greveana* from a Madagascar dry forest. *Chem. Biodiversity* **2011,** *8*, 643-650.

10. Hara, N.; Asaki, H.; Fujimoto, Y.; Gupta, Y. K.; Singh, A. K.; Sahai, M. Clerodane and ent-halimane diterpenes from *Polyalthia longifolia*. *Phytochemistry* **1995,** *38*, 189-194.

11. Monti, H.; Tiliacos, N.; Faure, R. Copaiba oil: isolation and characterization of a new diterpenoid with the dinorlabdane skeleton. *Phytochemistry* **1999,** *51*, 1013-1015.

12. Zdero, C.; Bohlmann, F.; Mungai, G. M. Carvotacetone derivatives and other constituents from representatives of the *Sphaeranthus* group. *Phytochemistry* **1991,** *30*, 3297-303.

13. Gao, F.; Mabry, T. J. Ten cis-clerodane-type diterpene lactones from *Gutierrezia texana*. *Phytochemistry* **1986,** *26*, 209-216.

14. Bohlmann, F.; Zdero, C. Naturally occurring terpene derivatives. Part 132. Diterpenes with a new carbon skeleton from *Printzia laxa*. *Phytochemistry* **1978,** *17*, 487-489.

15. Henderson, M. S.; McCrindle, R.; McMaster, D. Constituents of Solidago species. V. Nonacidic diterpenoids from *Solidago gigantea* var serotina. *Can. J. Chem.* **1973,** *51*, 1346-1358.

16. Wagner, H.; Seitz, R.; Lotter, H.; Herz, W. New furanoid ent-clerodanes from

Baccharis tricuneata. *J. Org. Chem.* **1978,** *43*, 3339-3345.

17. Cao, S.; Brodie, P. J.; Miller, J. S.; Randrianaivo, R.; Ratovoson, F.; Birkinshaw, C.; Andriantsiferana, R.; Rasamison, V. E.; Kingston, D. G. I. Antiproliferative xanthones of terminalia calcicola from the Madagascar rain forest. *J. Nat. Prod.* **2007,** *70*, 679-681.

9 Miscellaneous Natural Products Studied

9.1 Introduction

During the search for novel anticancer and antimalarial agents, some extracts yielded only known compounds. These known compounds isolated from various plants are reported in this chapter, in order to provide a complete record of the work that has been done, and also to document the botanical sources of the isolated compounds

9.2 Anticancer Extracts

9.2.1 *Monoporus sp.* (Myrsinaceae) MG 0596 (LF)

Liquid/liquid partition of the EtOH extract of *Monoporus sp*. afforded an active aqueous methanol (IC_{50} 9.9 μg/mL) fraction. Diaion HP-20 column chromatography of the MeOH fraction gave five fractions with a most active one with an IC_{50} value of 1.8 μg/mL. This active fraction (Fr. 5) was subjected to silica gel column chromatography to give ten fractions. Compound **9.1** (Sakuraso-saponin, IC_{50} 1.84 μM) was obtained from sub-fractions 5−8,as the only active compound that could be isolated.

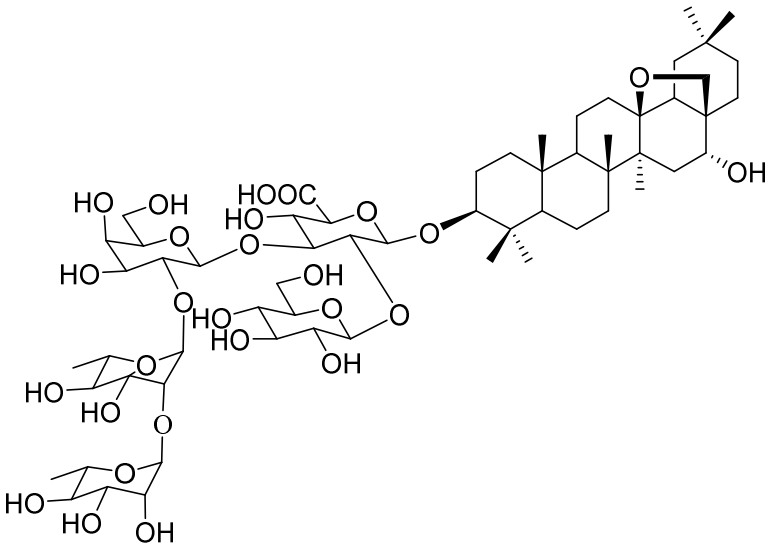

9.1

9.2.2 *Premna corymbosa* (Verbenaceae) MG 4508 (RT)

Liquid/liquid partition of the EtOH extract of *Premna corymbosa* afforded an active hexanes (IC_{50} 8.1 μg/mL) fraction. Two successive separations on a silica gel column gave two known compounds 9-phenanthrenol (**9.2**) and (3β,7β,22E) stigmasta-5,22-diene-3,7-diol (**9.3**) with IC_{50} values of 38 μM and 30 μM, respectively

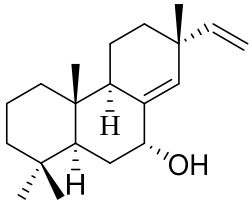

9.2

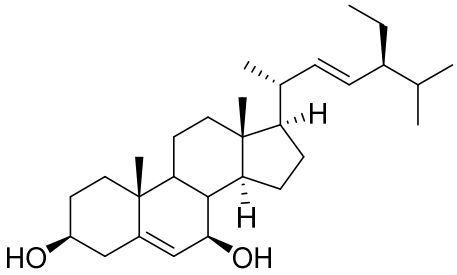

9.3

9.2.3 *Premna perplexans* (Verbenaceae) MG 2860 (RT) + MG 2862 (WD) + MG 2863 (LF+FR)

Liquid/liquid partition of the EtOH extract of *Premna perplexanes* (three parts) afforded an active aqueous MeOH (IC_{50} 13 μg/mL) fraction. Diaion HP-20 column chromatagrphy of the MeOH fraction gave seven fractions with the most active one (Fr. 5) with an IC_{50} of 6.5 μg/mL. This active fraction was subjected to silica gel column chromatography to give two known triterpenoid saponins Mi-Saponin A (**9.4**) and (**9.5**) with IC_{50} values of 4.9 μM and 4.7 μM, respectively, together with an active subfraction. Further purified on C18 column chromatography of the active sub-fraction (Fr. 5.12) furnished the known compound **9.6** (2.2 μM)

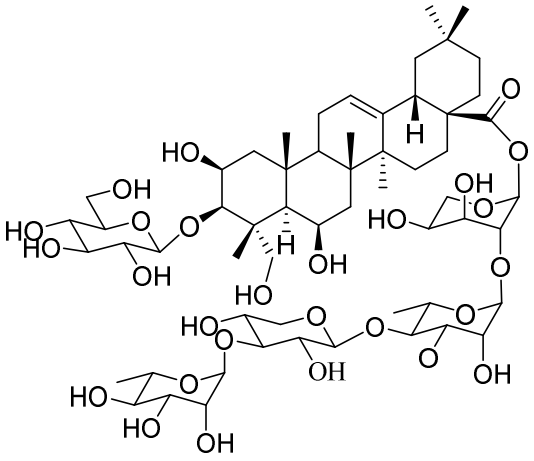

9.4

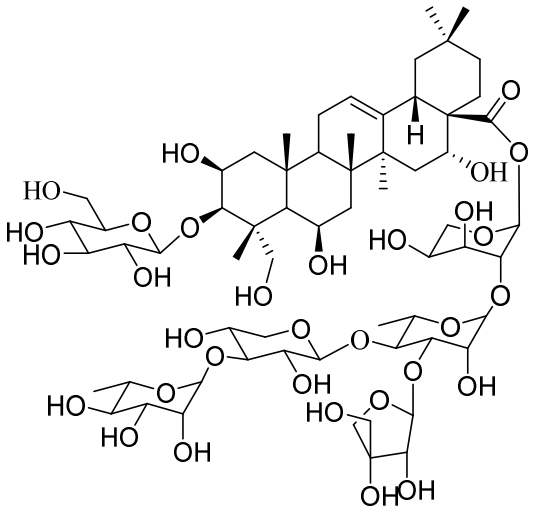

9.5

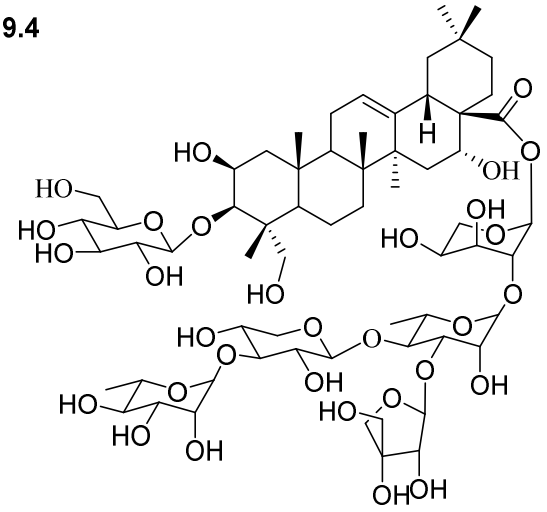

9.6

9.2.4 *Epallage longipes* (Asteraceae), MG 4849 (RT)

Liquid/Liquid partition of the EtOH extract of *Epallage longipe* (IC_{50} 1.7 μg/mL) furnished an active EtOAc fraction with an IC_{50} value of 0.76 μg/mL. Successive Sephadex LH-20 column chromatography and C18 HPLC of the EtOAc fraction gave two known sesquiterpene lactones kingiolide (**9.7**) and helenalin-(2-hydroxyethyl-3-methyl)acrylate (**9.8**) with IC_{50} values of 0.64 μM and 0.75 μM, respectively

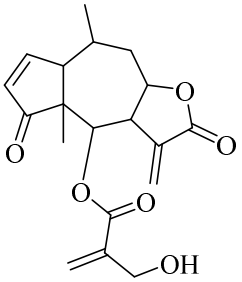

9.7

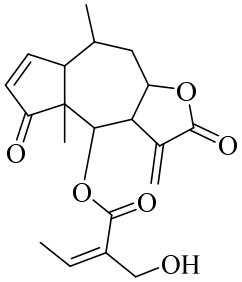

9.8

9.2.5 *Cinnamosma fragrans* (Canellaceae), MG 2360 (RT)

Liquid/Liquid partition of the EtOH extract of *Cinnamosma fragrans* (IC_{50} 4 μg/mL) furnished an active EtOAc fraction with an IC_{50} value of 2.5 μg/mL. Successive sephadex LH-20 column chromatography of the EtOAc fraction gave six fractions. Solid phase extraction on the second and third fractions furnished the two known terpenoids cinnafragrin (**9.9**) and cinnamosmolide (**9.10**) with IC_{50} values of 0.68 μM and 2.82 μM, respectively.

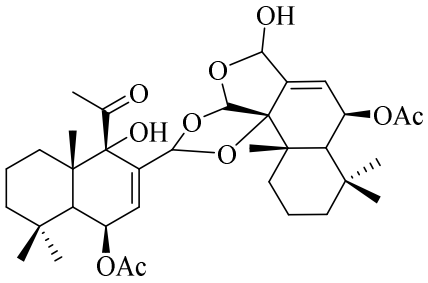

9.9

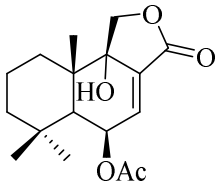

9.10

10 Summary and General Conclusions

10.1 Isolation of Bioactive Natural Products

In our continuing search for biologically active natural products from Madagascar rainforests as part of International Cooperative Biodiversity Group (ICBG) program and a collaborative research project established between Virginia Tech and the Institute for Hepatitis and Virus Research (IHVR), more than 16 plants were selected for initial inspection. Thirteen of them were fractionated to yield 9 new and 42 known compounds, guided by antiproliferative bioassay against the A2780 human ovarian cancer cell line. One antimalarial extract was selected for fractionation to yield 11 new compounds, guided by antiplasmodial bioassay against the Dd2 strain of *Plasmodium falciparum*.

10.2 Antiproliferative Extracts

Investigation of the Madagascan plant *Cleistanthus boivinianus* for antiproliferative activity against the A2780 ovarian cancer cell line led to the isolation of one new aryltetralin lignan named cleistanolide A, and two known arylnaphthalide lignans (±)-*β*-apopicropodophyllin and (-)-desoxypodophyllotoxin, with potent antiproliferative activity with IC_{50} value of 33.0 ± 3.6, 63.1 ± 6.7, and 230 ± 1 nM, respectively. Cleistanolide A also displayed potent antiproliferative activity against the HCT-116 human colon carcinoma cell line with an IC_{50} value of 20.5 nM, and weak antimalarial activity against *Plasmodium falciparum* with an IC_{50} value of 12.6 ± 3.2 μM. (±)-*β*-apopicropodophyllin also displayed moderate antiproliferative activity against A2058 human caucasian metastatic melanoma and MES-SA human uterine sarcoma

cells, with IC_{50} values of 4.6 and 4.0 μM, respectively. A new arylnaphthalide lignan named 4-*O*-(*β*-D-glucopyranosyl)-dehydropodophyllotoxin and a known arylnaphthalide lignan with moderate antiproliferative activity with IC_{50} values of 2.1 ± 0.3 μM and 4.9 ± 0.1 μM, respectively. In addition, two known arylnaphthalide lignans deoxypicropodophyllotoxin and (-)-yatein were isolated with IC_{50} values more than 10 μM.

Investigation of the Puerto Rico plant *Piptocoma antillana* (Asteraceae) for antiproliferative activity against the A2780 ovarian cancer cell line led to the isolation of two new antiproliferative goyazensolide type sesquiterpenes lactones named 5-*O*-methyl-5-epiisogoyazensolide and 15-*O*-methylgoyazensolide, together with the two known sesquiterpene lactones 5-epiisogoyazensolide and 15-acetylgoyazensolide. The isolated compounds showed micromolar activities with half-maximum inhibitory concentration (IC_{50}) values of 1.56 ± 0.04, 1.62 ± 0.05, 1.5 ± 0.5, and 0.6 ± 0.3 μM, respectively.

Investigation of the Madagascan plant *Stuhlmannia moavi* (Leguminosae) for antiproliferative activity against the A2780 ovarian cancer cell line led to the isolation of one new 1,4-naphthoquinone named stuhlmoavin with moderate activity with an IC_{50} value of 8.1 ± 0.4 μM, together with the known isoflavonoid bonducellin and the five known stilbenoids 3,4,5'-trihydroxy-3'-methoxy-trans-stilbene, piceatannol, resveratrol, rhapontigenin, and isorhapontigenin, with weak activities with IC_{50} values of 10.6 ± 0.4 μM, 54 ± 1 μM, 41 ± 1 μM, and 74 ± 1 μM, respectively. Stuhlmoavin, bonducellin, and 3,4,5'-trihydroxy-3'-methoxy-trans-stilbene also showed moderate antimalarial activity against *Plasmodium falciparum* Dd2 with IC_{50} values of 24 ± 7, 26 ± 3, and 27 ± 2 μM,

respectively. The structure of stuhlmoavin was confirmed by single-crystal X-ray diffraction analysis.

Investigation of the Madagascan plant *Anisocycla grandidieri* (Menispermaceae) for antiproliferative activity against the A2780 ovarian cancer cell line led to the isolation of the two known bisbenzylisoquinoline alkaloids (+)-1,2-dehydrotelobine and (+)-2'-norcocsuline with moderate antiproliferative activity with IC_{50} values of 2.7±0.3 and 4.1 ±0.3 μM, respectively, together with two known inactive alkaloids stebisimine and puetogaline B. The structures and stereochemistries of stebisimine and (+)-2'-norcocsuline were confirmed by single crystal X-ray crystallography. Because of the lack of full NMR spectroscopic data in previous reports, the NMR assignments of all carbons and protons of stebisimine, (+)-1,2-dehydrotelobine, and (+)-2'-norcocsuline were reported.

Investigation of the Madagascan plant *Ocotea macrocarpa* (Lauraceae) for antiproliferative activity against the A2780 ovarian cancer cell line led to the isolation of one new butanolide named macrocarpolide A and two new secobutanolides macrocarpolide B and C, with good activity with IC_{50} values of 2.57 ± 0.12, 1.98 ± 0.23, 1.67 ± 0.05, 2.43 ± 0.41, and 1.65 ± 0.44 μM, respectively.

Investigation of the Madagascan plant *Malleastrum rakotozafyi* (Meliceae) for antiproliferative activity against the A2780 ovarian cancer cell line led to the isolation of one new clerodane type diterpene named 18-oxo-cleroda-3,13-dien-16,15-olide, together with three known clerodane diterpenes 16,18-dihydroxykolavenic acid lactone, solidagolactone, and (-)-kolavenol, and one known labdane diterpene 3-oxo-ent-labda-8(17),13-dien-15,16-olide. 18-Oxo-cleroda-3,13-dien-16,15-olide, 6,18-dihydroxy-

kolavenic acid lactone, and solidagolactone showed micromolar A2780 activities with IC_{50} value of 3.01 ± 0.8, 7.84 ± 0.2, and 17.9 ± 3 μM, respectively.

10.3 Antimalarial extract

Bioassay-guided separation of the Madagascar plant *Cryptocarya rigidifolia* for antiplasmodial activity led to the isolation of five new 5,6-dihydro-α-pyrones named cryptorigidifoliol A–E and six bicyclic tetrahydro-α-pyrone derivatives named cryptorigidifoliol F–K. Cryptorigidifoliol A–G exhibited moderate antimalarial activity, with IC_{50} values of 9.2 ± 0.9, 5.8 ± 1.4, 5.5 ± 0.7, 9 ± 3, 4.0 ± 2, 7.4 ± 0.6, and 6.0 ± 0.5 μM, respectively. Cryptorigidifoliol H–K were all less active, with IC_{50} values > 10 μM. The bicyclic tetrahydro-α-pyrones were shown to be produced by cyclization of 5,6-dihydro-α-pyrones during the isolation process involved by silica gel.

10.4 Conclusions

The complex structures and biological importance of the substances found in nature are very fascinating. In the six-year research period, more than twenty crude extracts were studied, leading to the isolation of twenty new compounds and thirty-four known compounds. Among these compounds, (1*R*,2*R*,3*S*)-3-*O*-(*β*-D-glucopyranosyl)-3',4',5'-trimethoxy-6,7-methylenedioxy-1,9-cyclolignan-11,12-olide (cleistanolide A, **3.1**) isolated from the stems of *Cleistanthus boivinianus*, showed the most potent antiproliferative activity against the A2780 cell line with an IC_{50} value of 33.0 ± 3.6 nM. This compound is the first example of a new class of podophyllotoxin analogs with substitution at C-3. The potent activity of this compound suggests that C-3 substituted

derivatives are interesting lead structures. Unfortunately, the instability of an oxygenated substituent at C-3 indicates that cleistanolide A is not a good lead compound for drug discovery, but would still be useful to study its antitumor mechanism. However, it might be possible to change the substituent at C-3 to obtain more stable derivatives, which might then have both improved bioactivity and improved stability compared with podophyllotoxin.

The study of *Cryptocarya rigidifolia* showed that the isolated bicyclic pyrones were artificial derivatives of 5,6-dihydro-α-pyrones with C-2' hydroxyl groups, formed during the isolation process using silica gel for chromatography. This finding emphasizes the need for great care in the use of silica gel for the purification of natural product extracts. Whenever possible, alternate chromatographic media such as diol or C18 derivatized silica gel should be used.

The work reported in this dissertation has shown that novel bioactive compounds continue to be isolated from plant extracts. However, many known compounds were isolated and in some cases were the only bioactive compounds found in specific plant extracts. Thus indicates that careful dereplication methods should decrease the time spent in reisolating know compounds and allow work to focus on extracts with novel compounds. Such dereplication approaches can be based on the combined application of chromatography and structure-determination facilities, to shorten the isolation time of traditional methods. Methods involving HPLC-NMR and HPLC-MS are particularly powerful. Improved dereplication procedures will allow more efficient identification of novel lead compounds.

11 Appendix

^{1}H NMR spectrum of **2.1** in $CDCl_3$ (500 Hz)

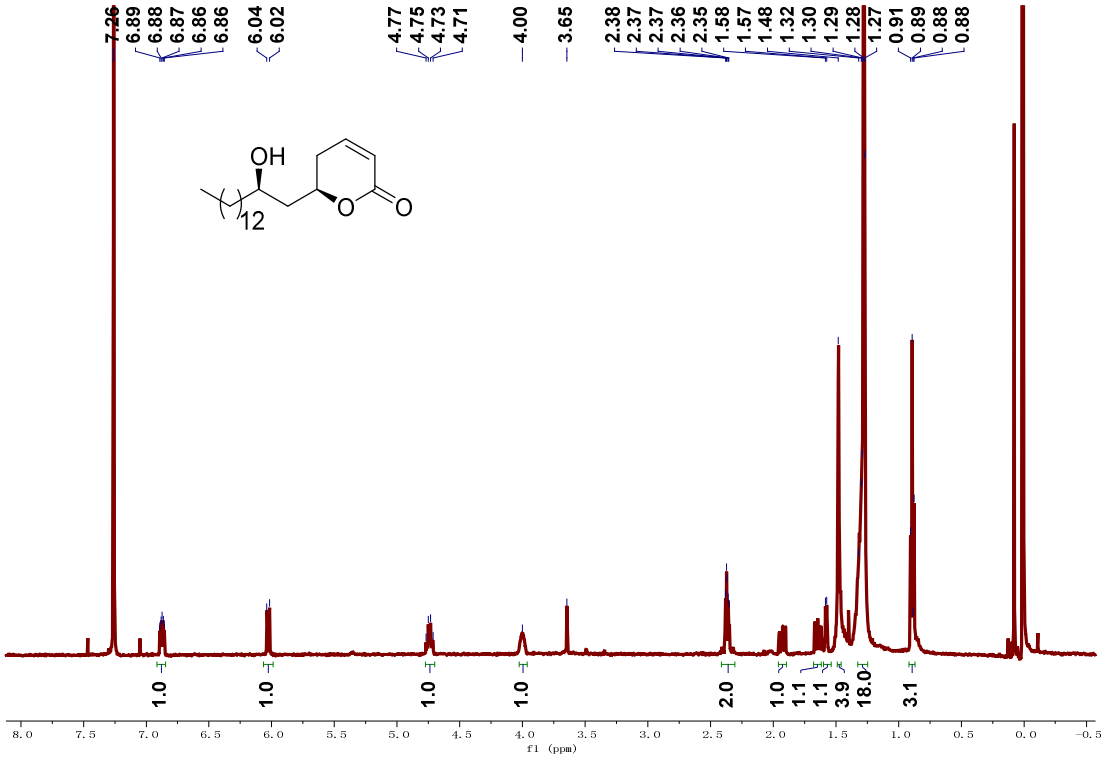

^{1}H NMR spectrum of **2.2** in $CDCl_3$ (500 Hz)

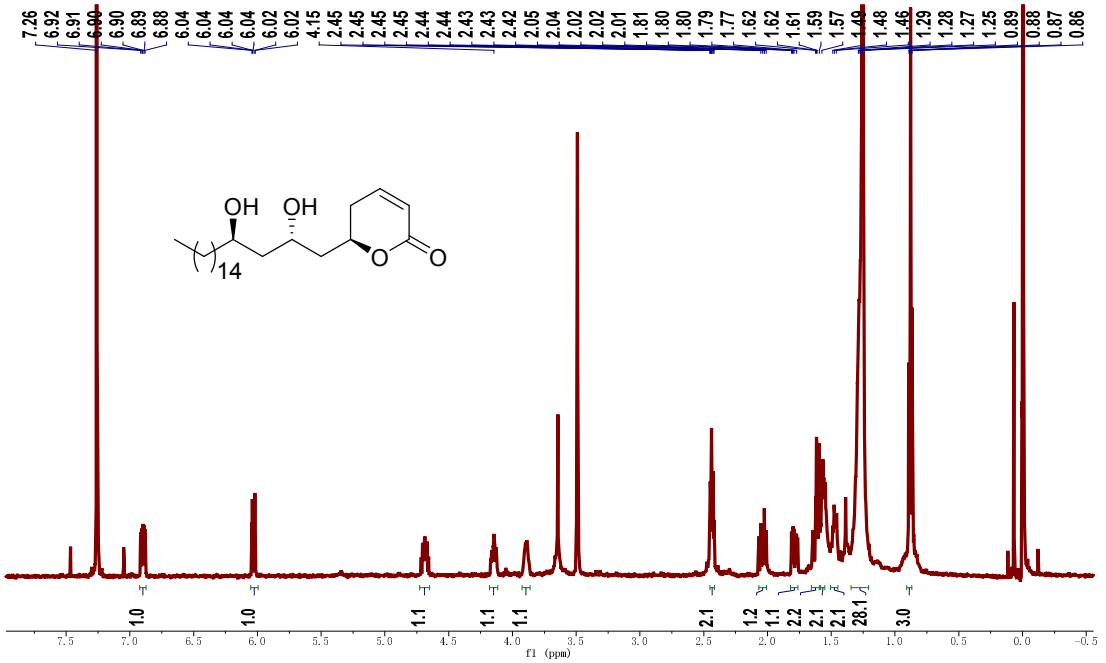

^{1}H NMR spectrum of **2.3** in $CDCl_3$ (500 Hz)

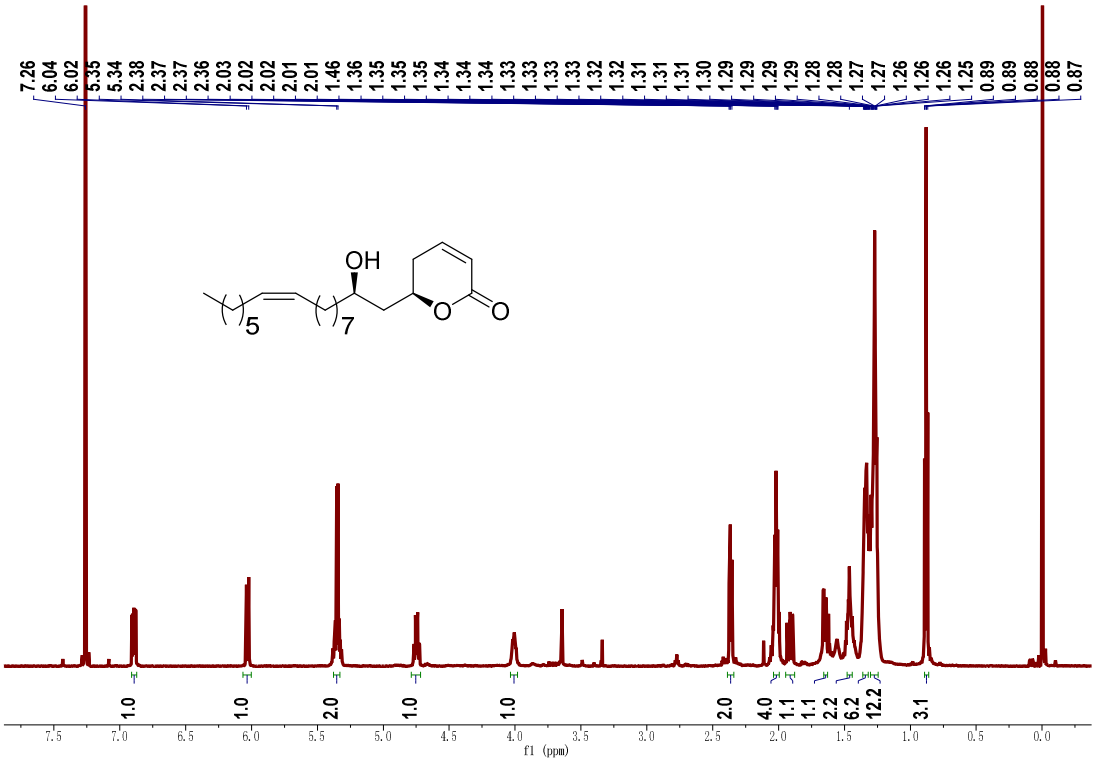

^{1}H NMR spectrum of **2.4** in $CDCl_3$ (500 Hz)

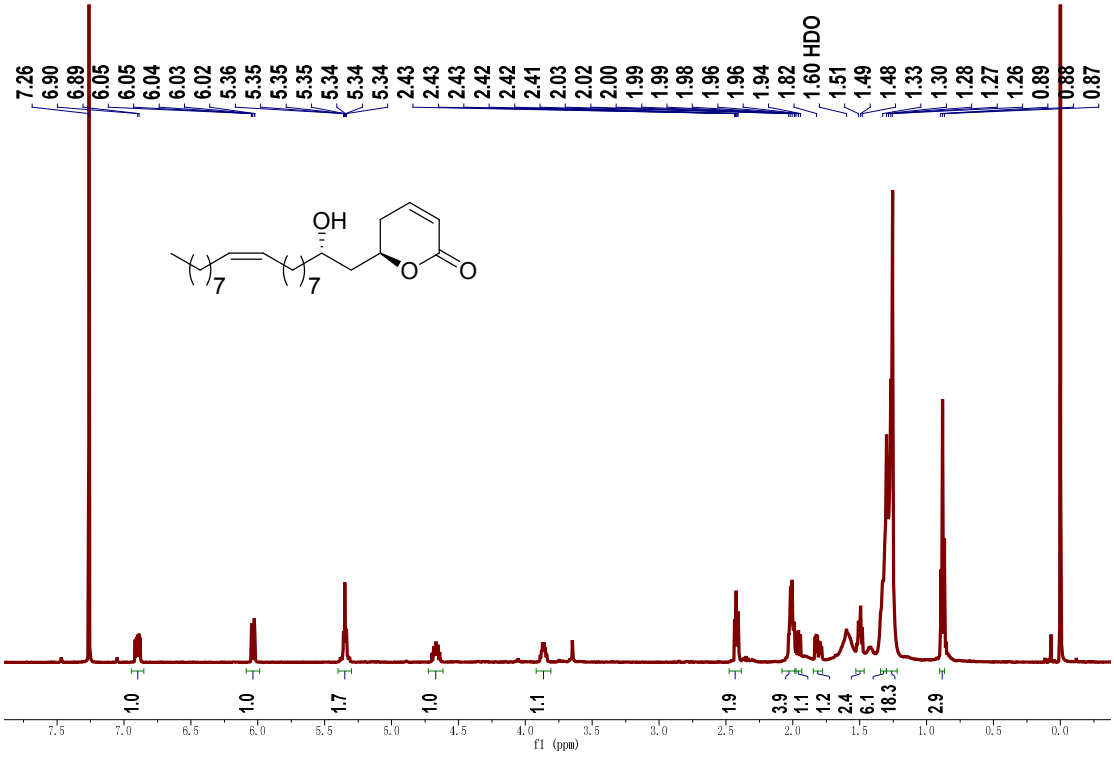

^{1}H NMR spectrum of **2.5** in $CDCl_3$ (500 Hz)

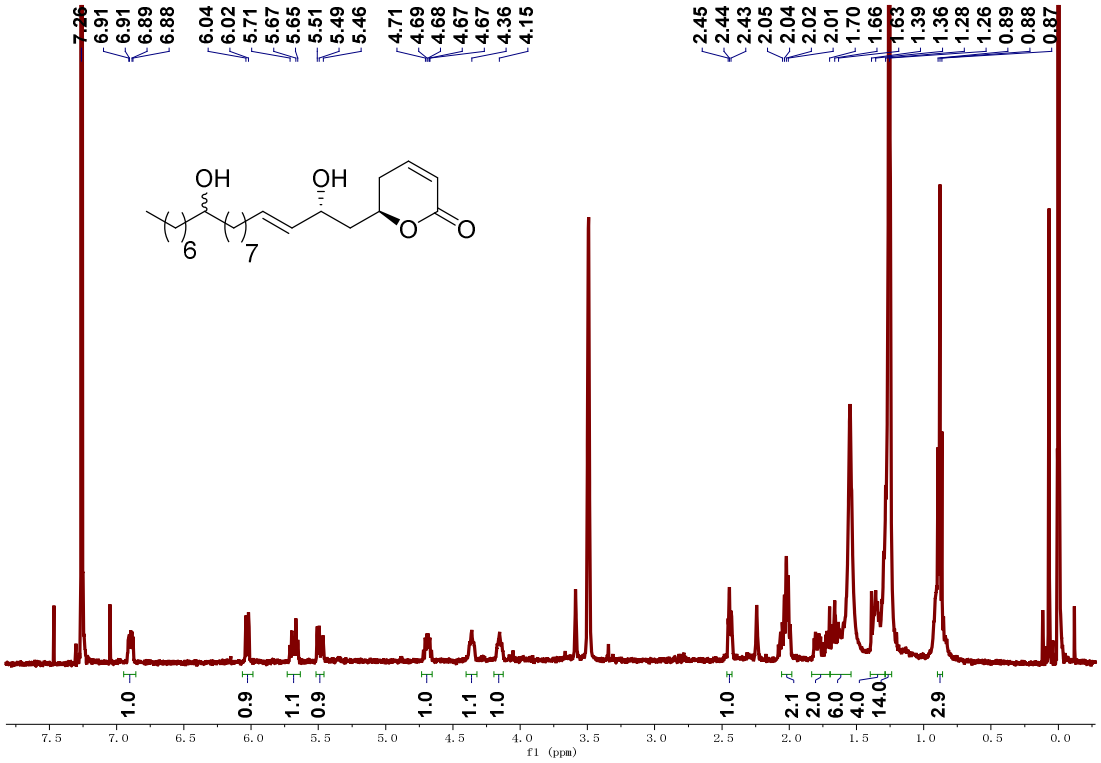

^{1}H NMR spectrum of **2.6** in $CDCl_3$ (500 Hz)

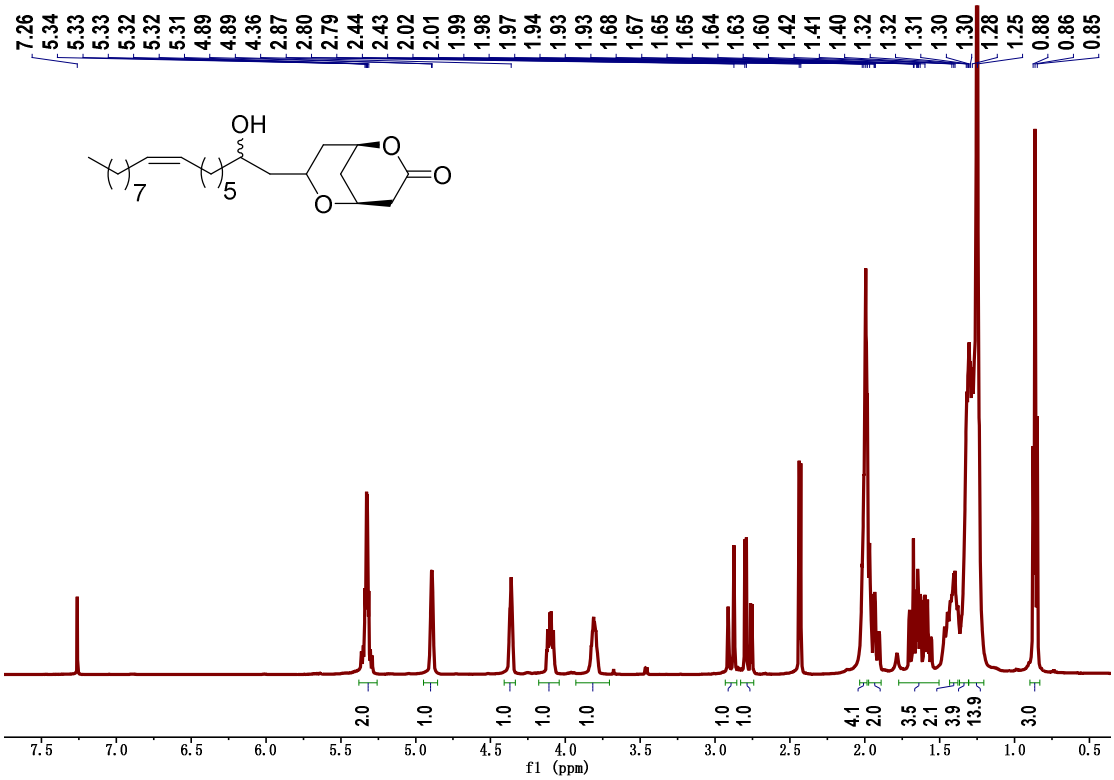

^{1}H NMR spectrum of **2.7** in $CDCl_3$ (500 Hz)

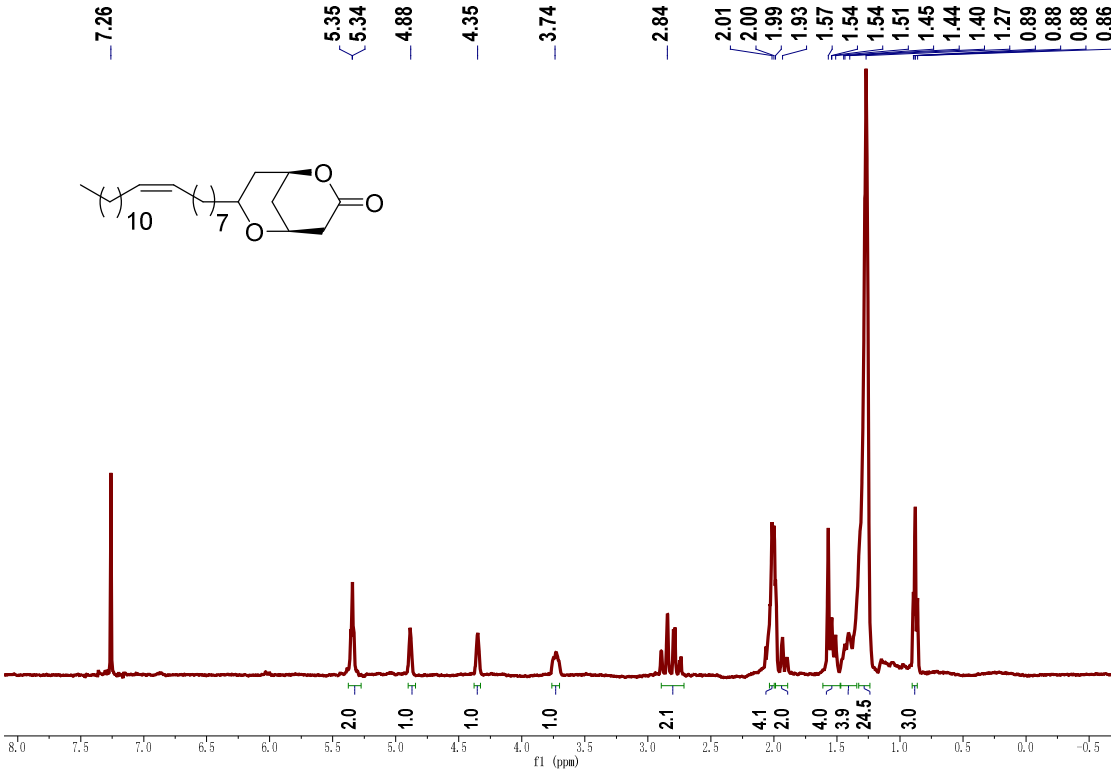

^{1}H NMR spectrum of **2.8** in $CDCl_3$ (500 Hz)

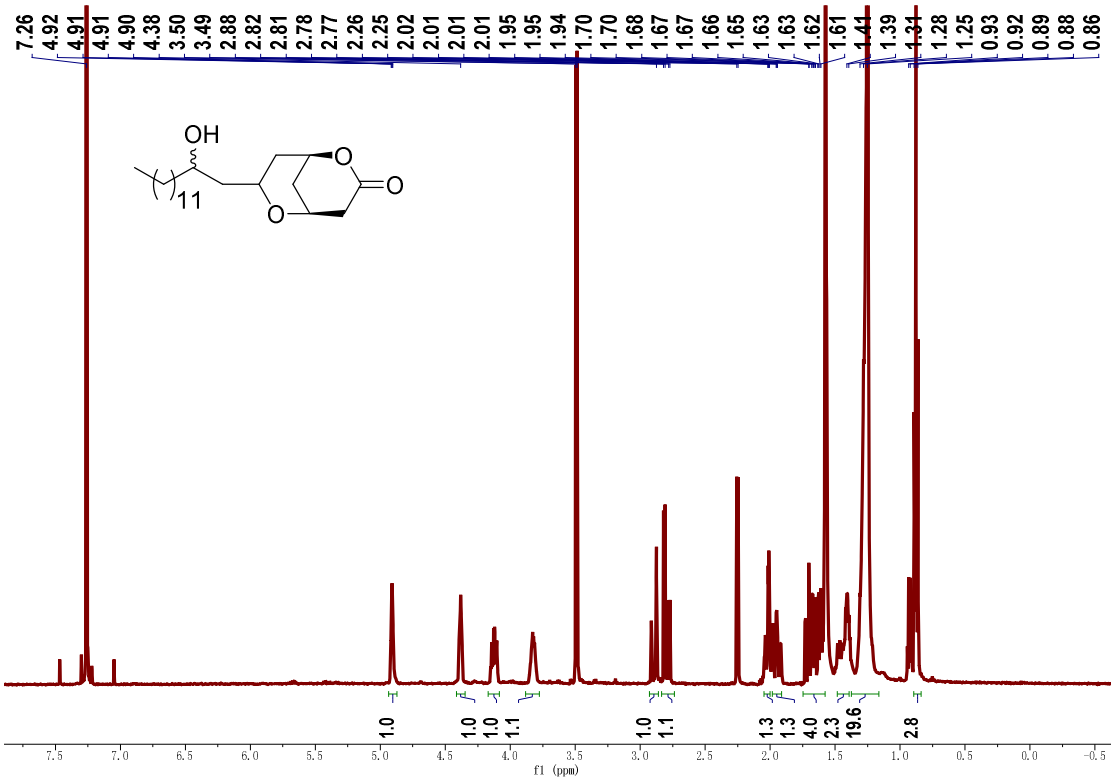

^{1}H NMR spectrum of **2.9** in $CDCl_3$ (500 Hz)

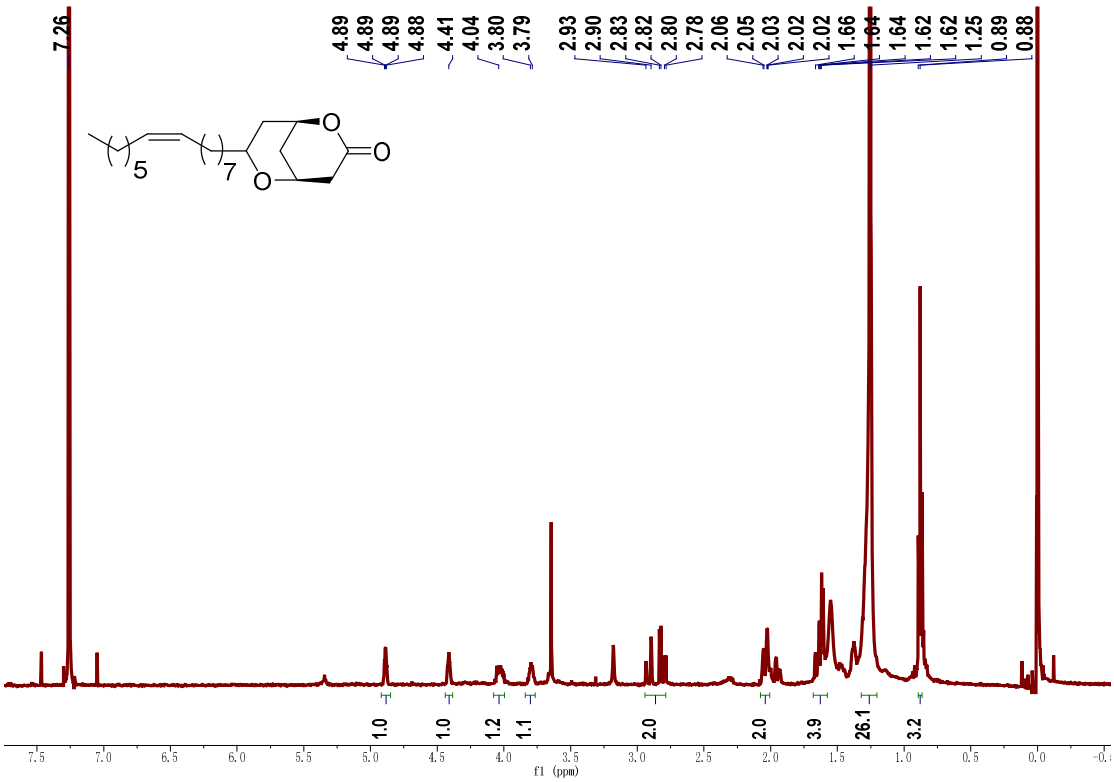

^{1}H NMR spectrum of **2.10** in $CDCl_3$ (500 Hz)

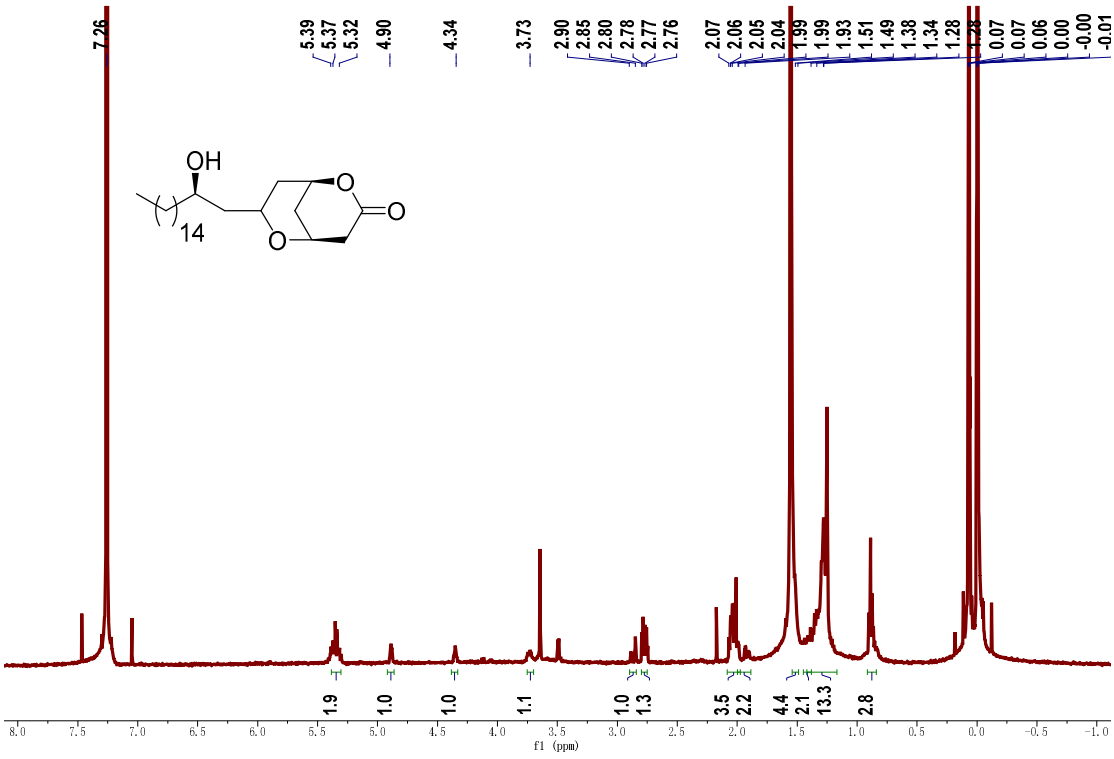

^{1}H NMR spectrum of **2.11** in $CDCl_3$ (500 Hz)

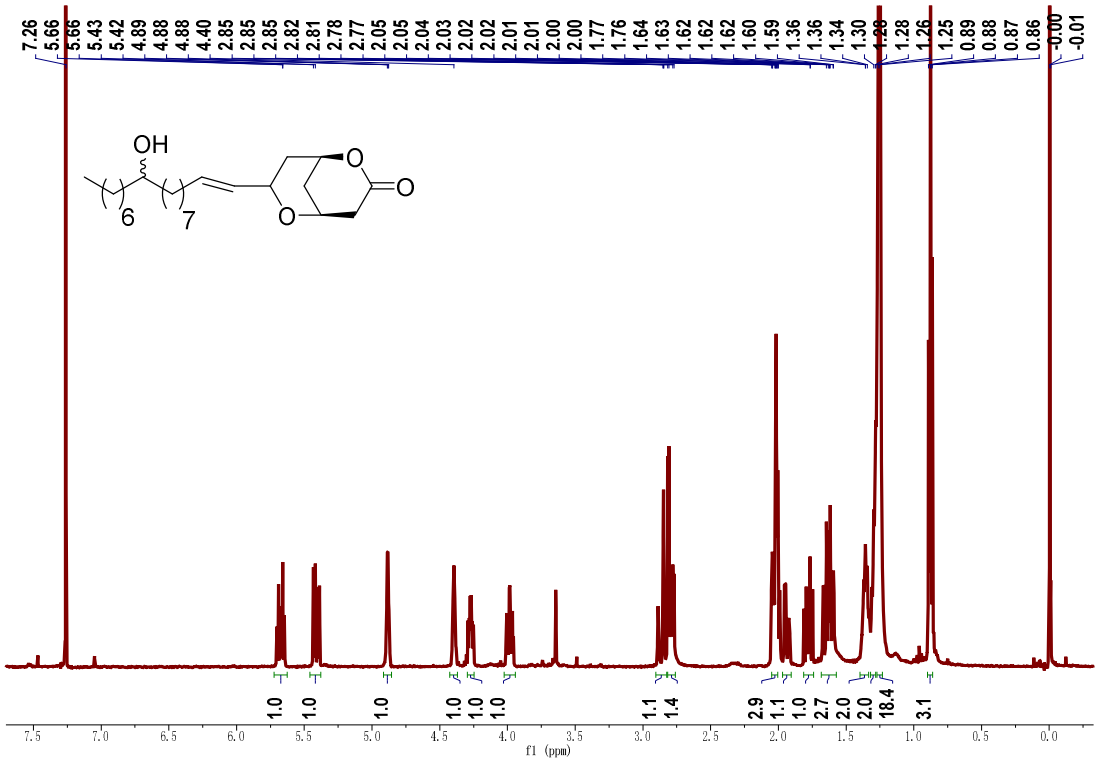

^{1}H NMR spectrum of **3. 1** in CD_3OD (500 Hz)

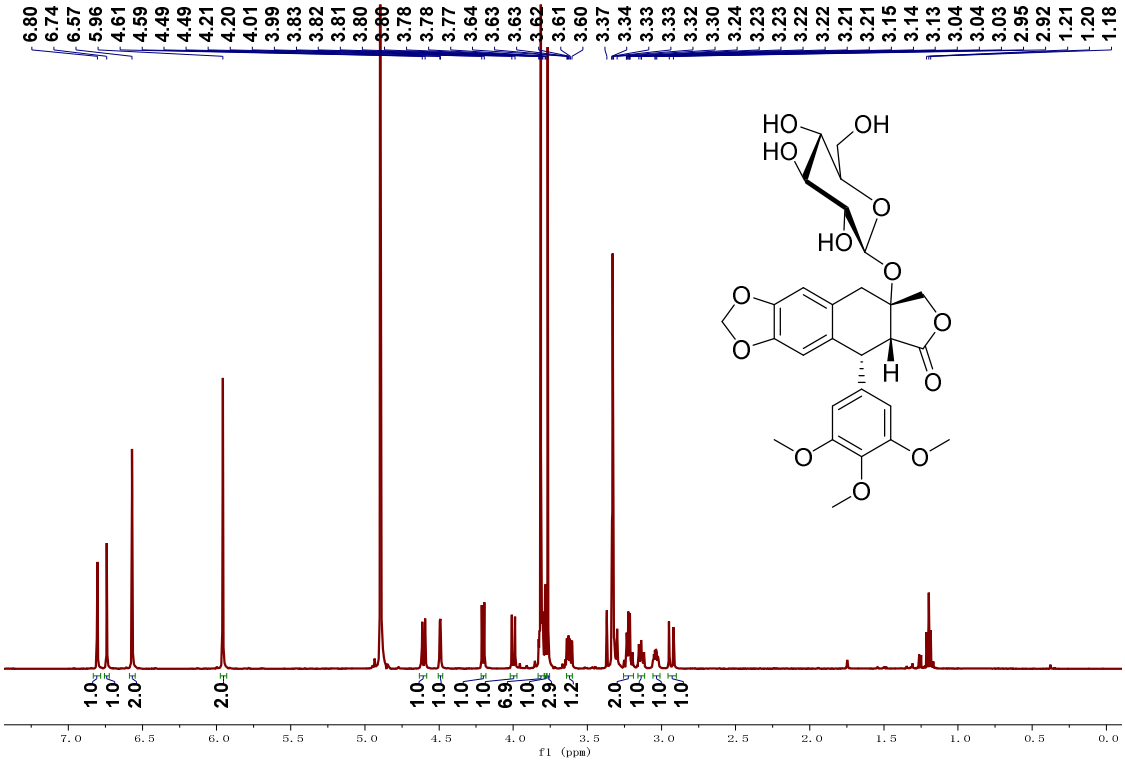

^{1}H NMR spectrum of **3. 2** in CD_3OD (500 Hz)

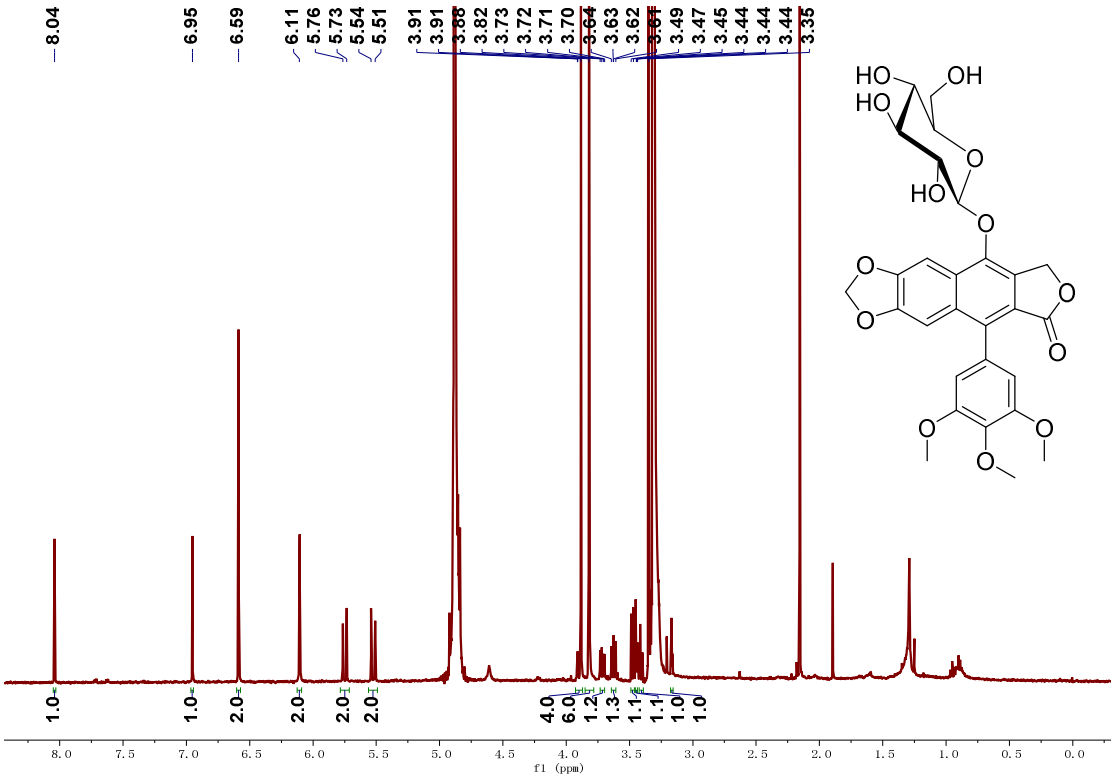

^{1}H NMR spectrum of **3. 3** in $CDCl_3$ (500 Hz)

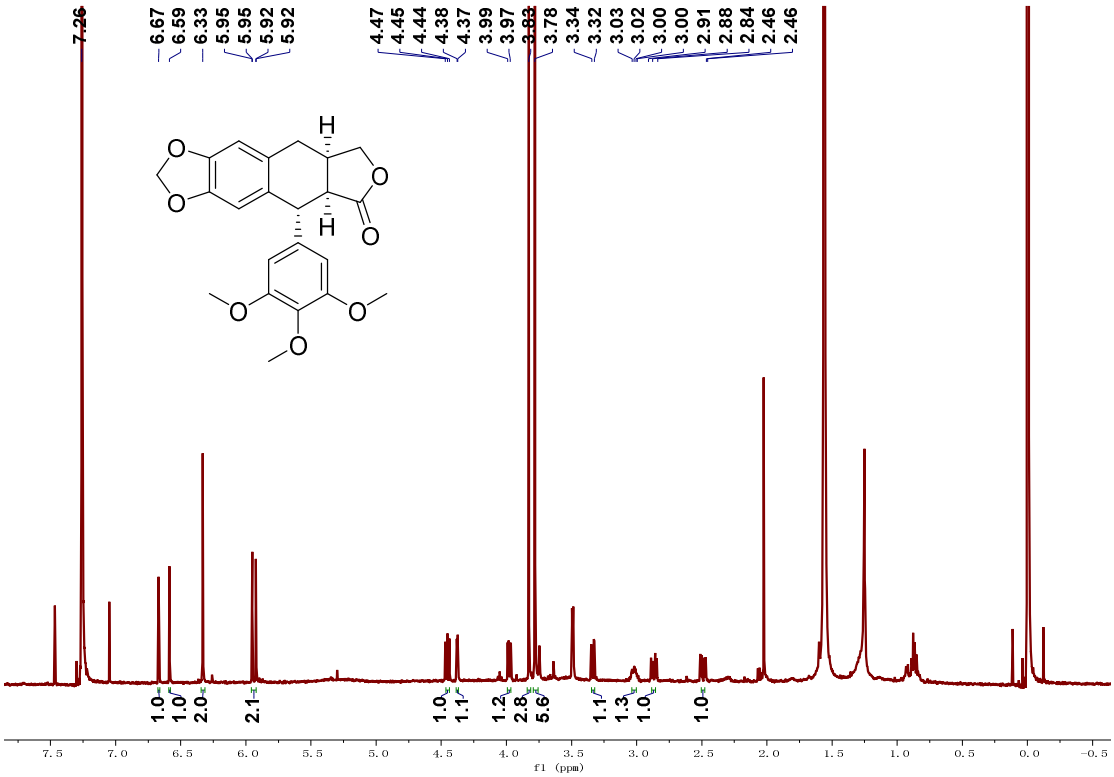

^{1}H NMR spectrum of **3. 4** in $CDCl_3$ (500 Hz)

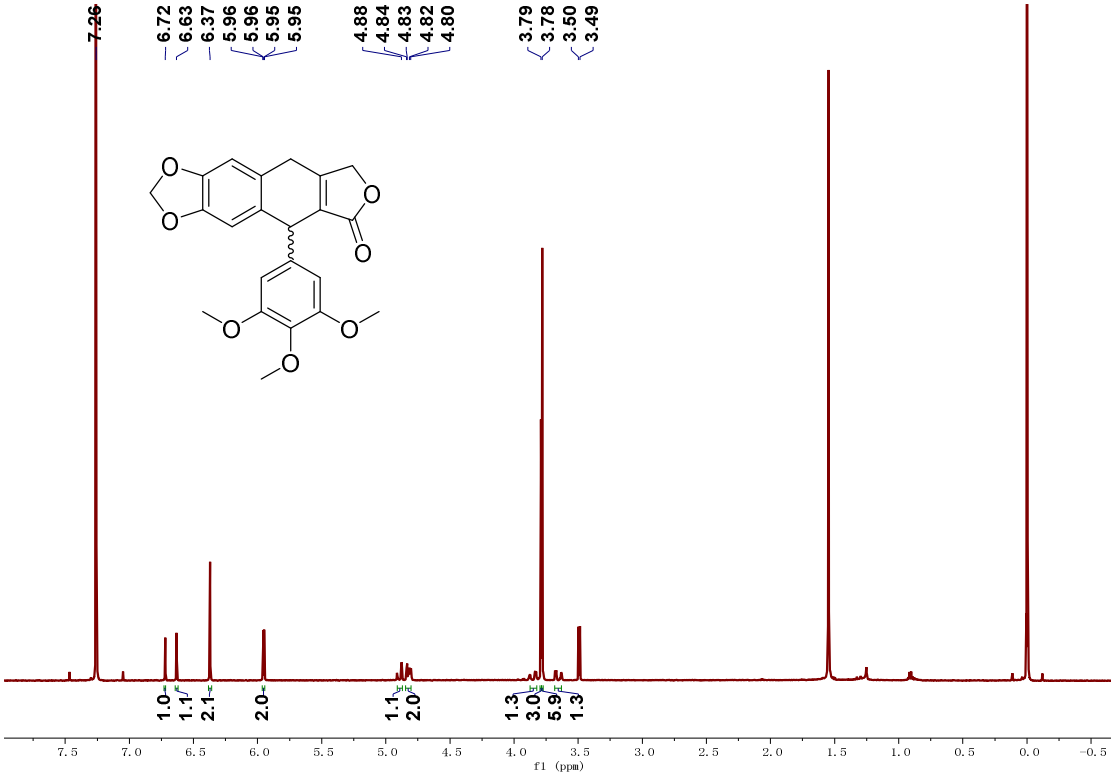

^{1}H NMR spectrum of **3. 5** in $CDCl_3$ (500 Hz)

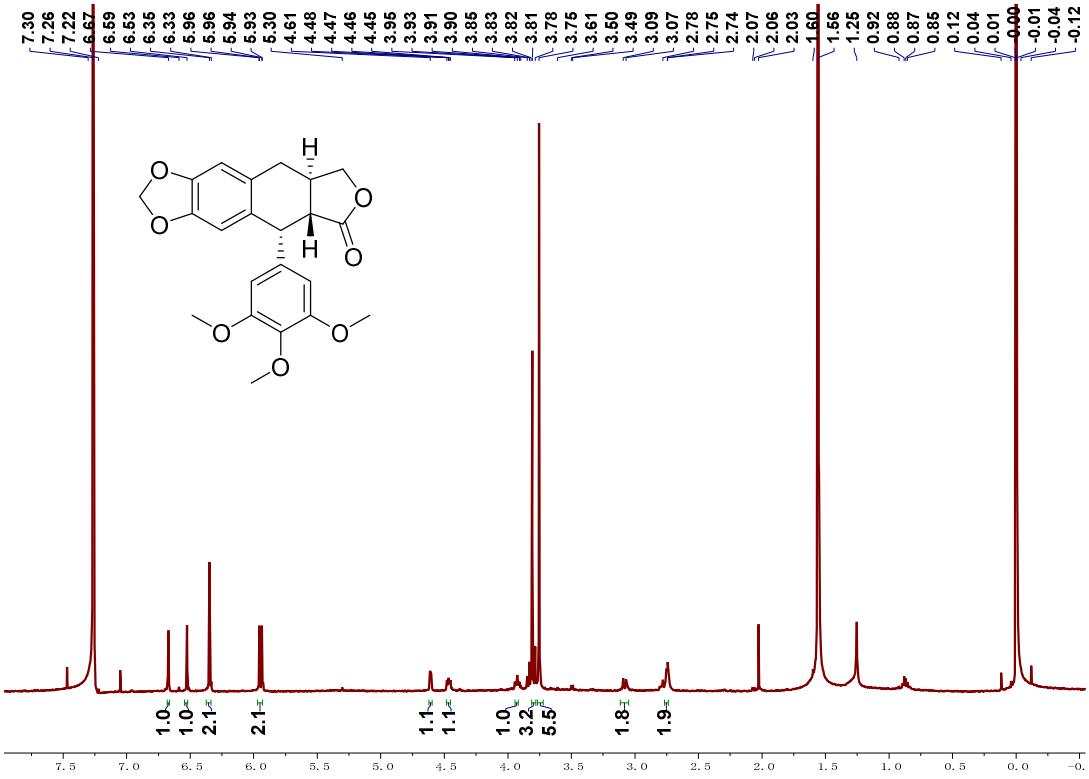

^{1}H NMR spectrum of **3. 6** in $CDCl_3$ (500 Hz)

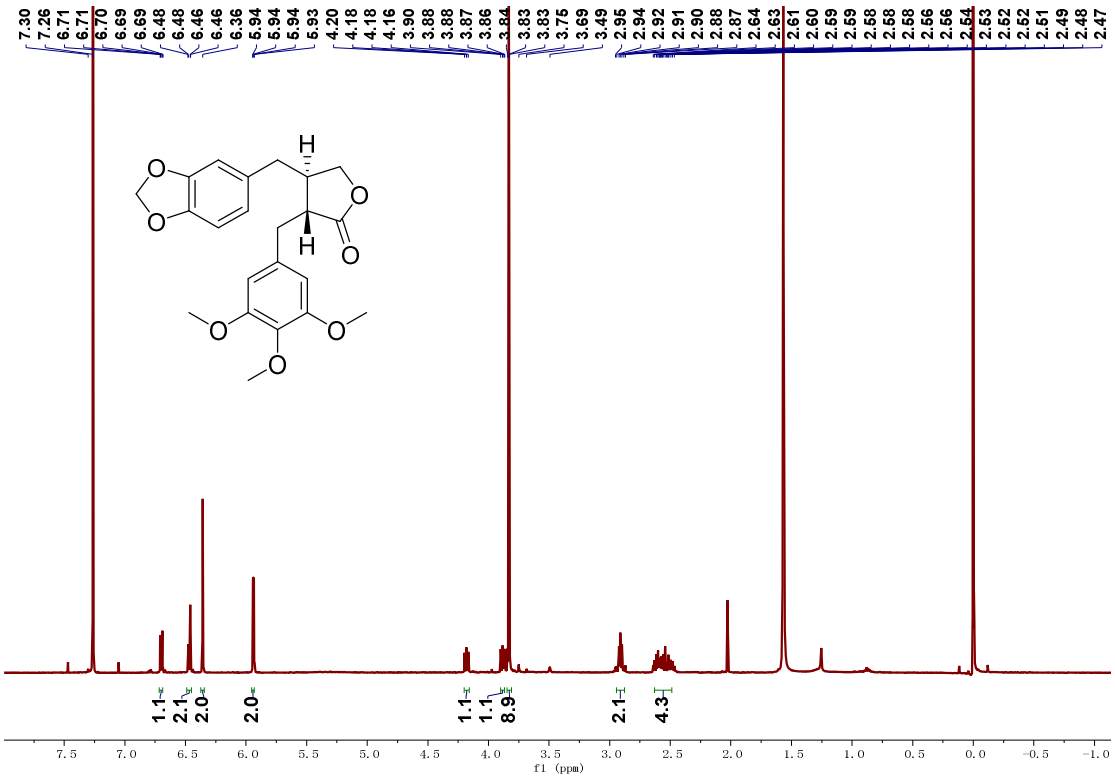

^{1}H NMR spectrum of **3. 7** in CD_3OD (500 Hz)

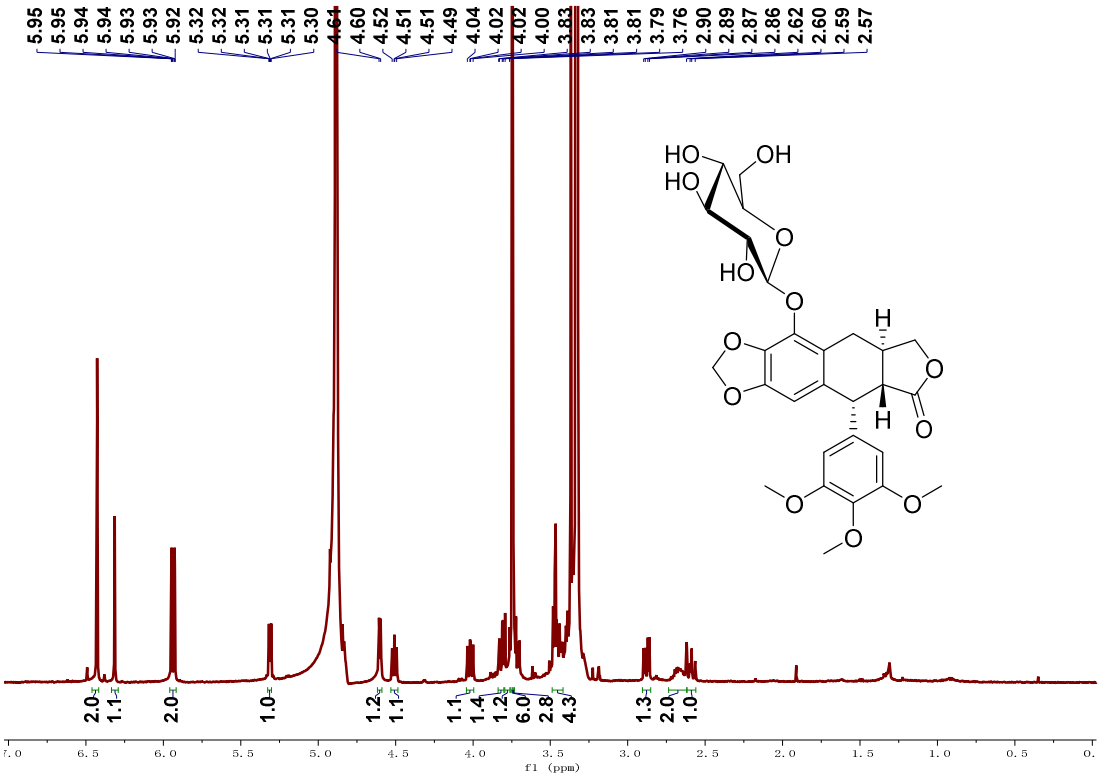

^{1}H NMR spectrum of **4. 1** in $CDCl_3$ (500 Hz)

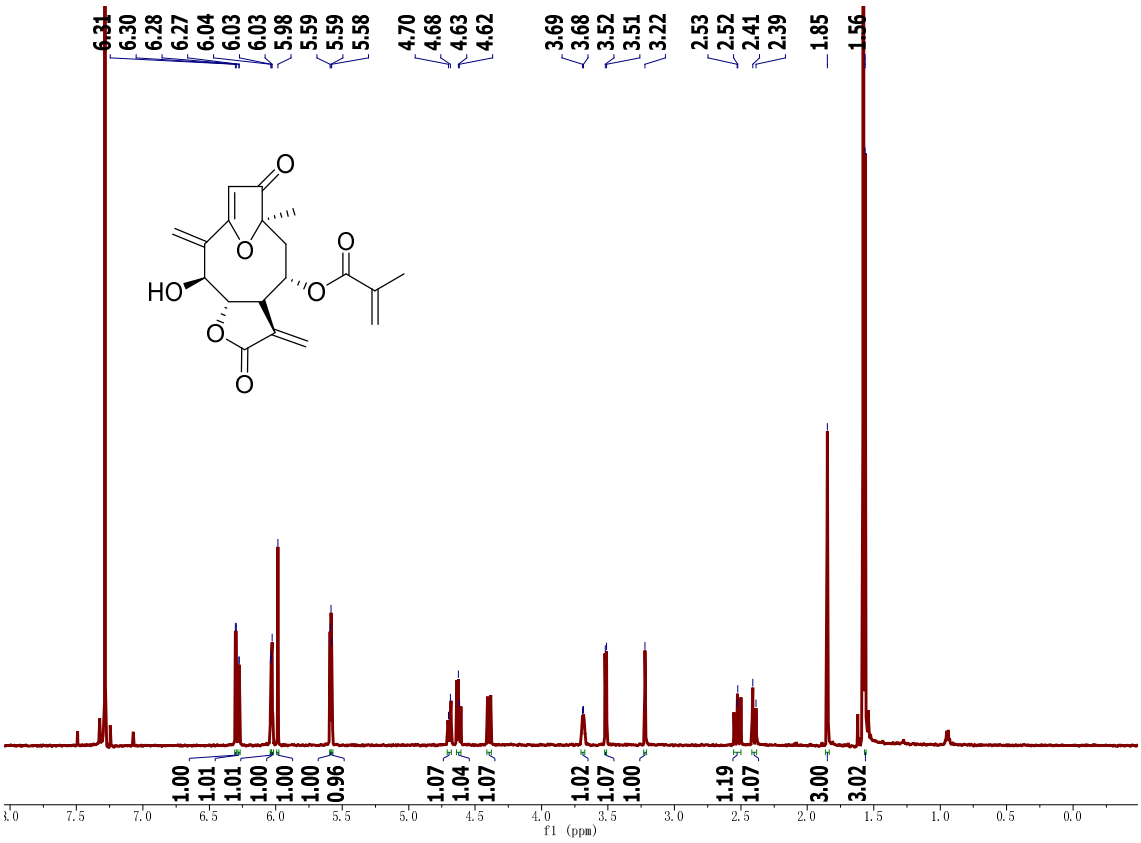

^{1}H NMR spectrum of **4. 2** in $CDCl_3$ (500 Hz)

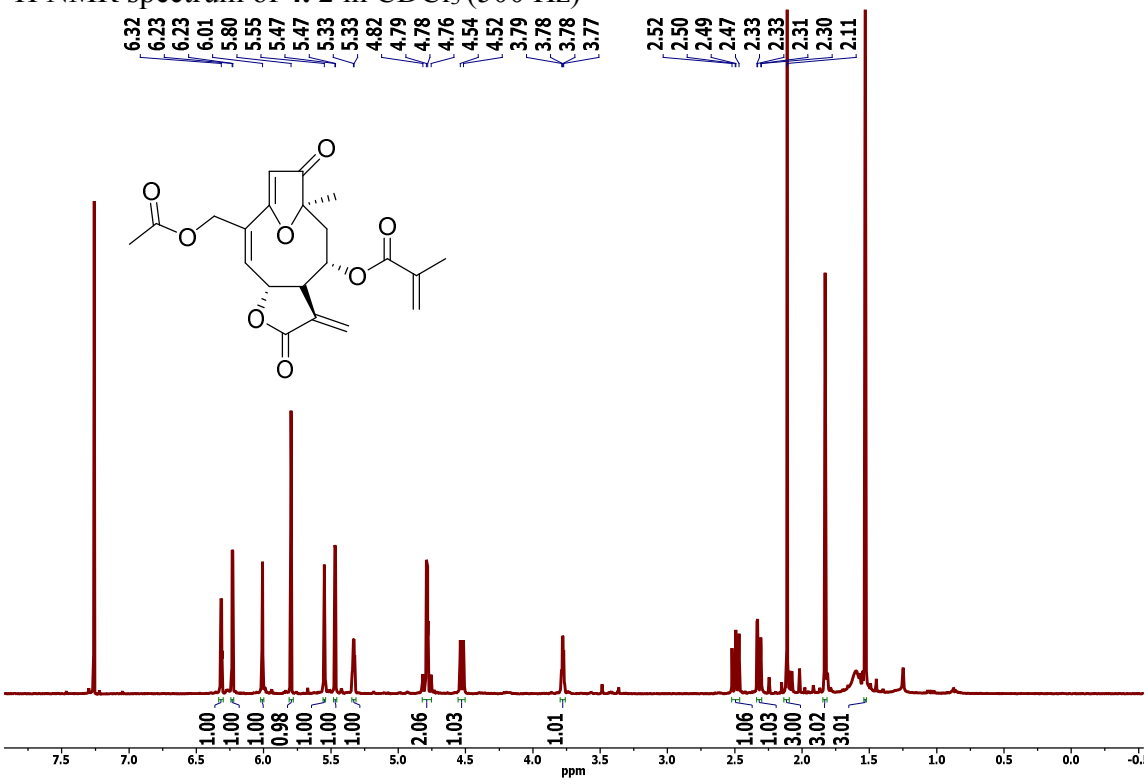

^{1}H NMR spectrum of **4. 3** in $CDCl_3$ (500 Hz)

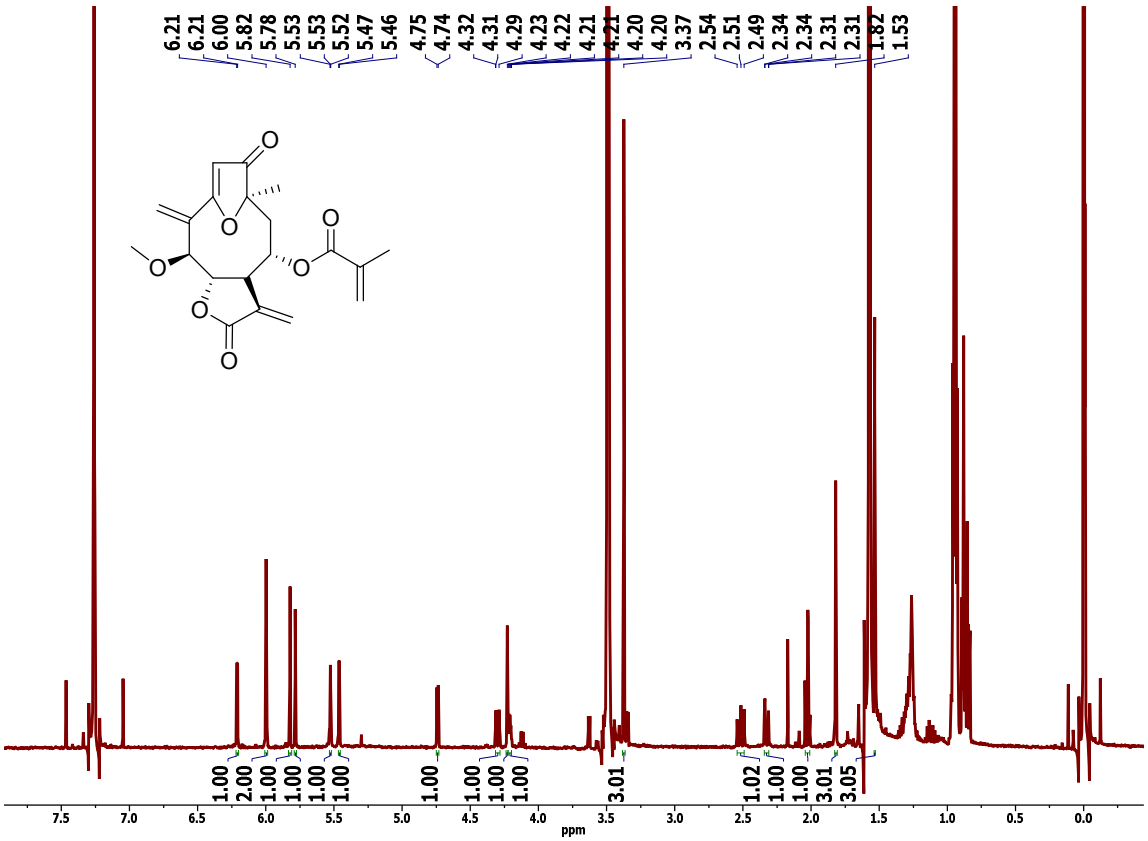

^{13}C NMR spectrum of **4. 3** in $CDCl_3$ (125 Hz)

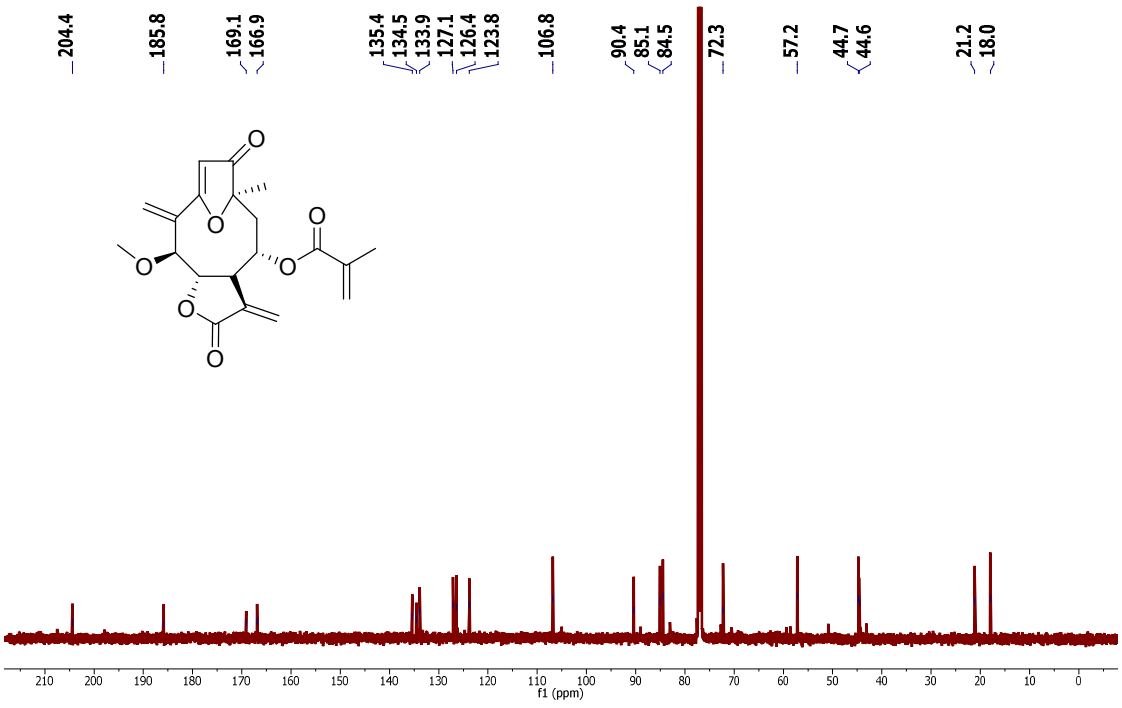

^{1}H NMR spectrum of **4. 4** in $CDCl_3$ (500 Hz)

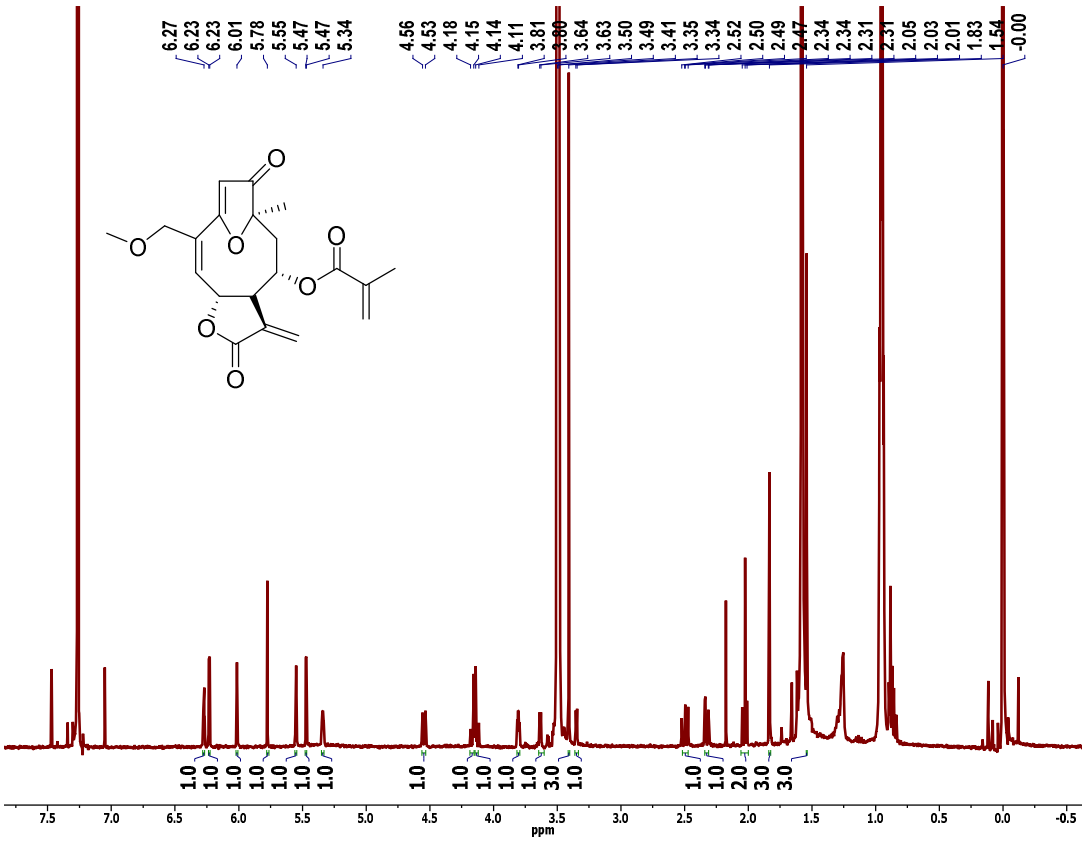

^{13} C NMR spectrum of **4. 4** in $CDCl_3$ (125 Hz)

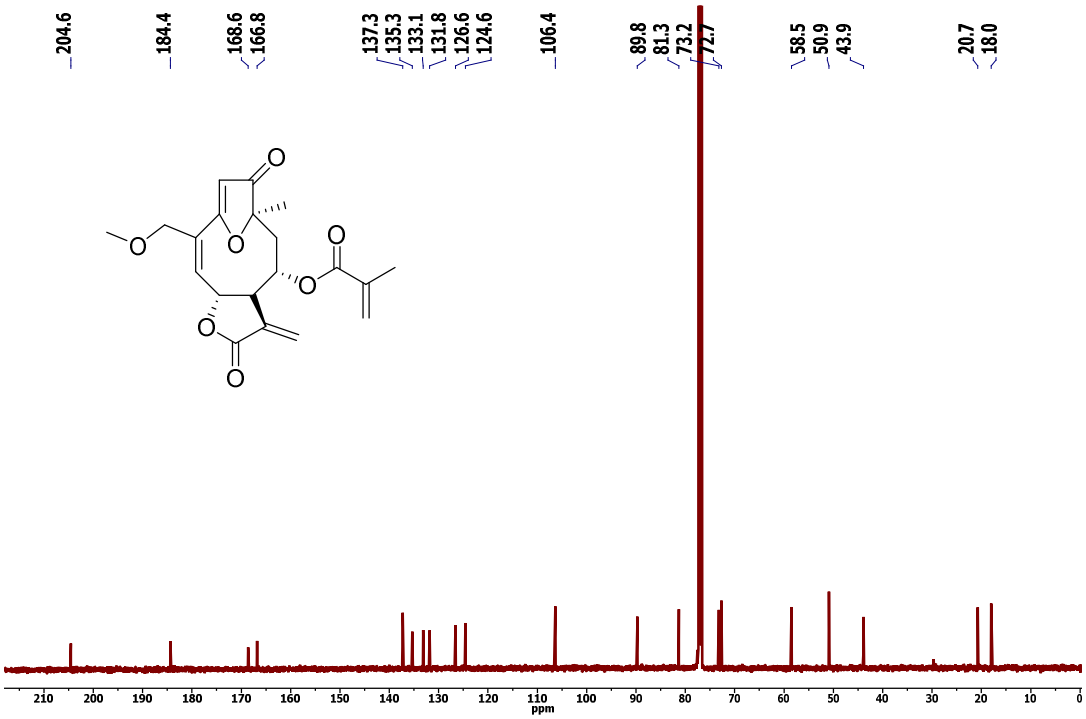

^{1}H NMR spectrum of **5. 1** in $CDCl_3$ (500 Hz)

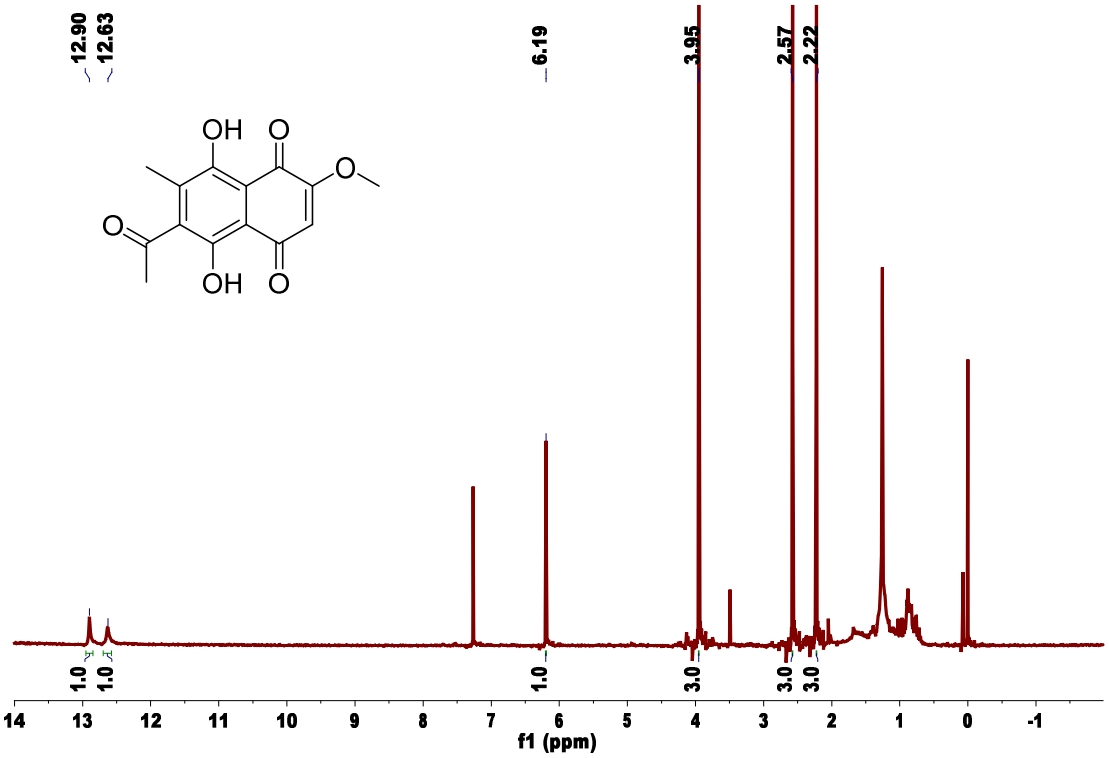

^{13}C NMR spectrum of **5. 1** in $CDCl_3$ (125 Hz)

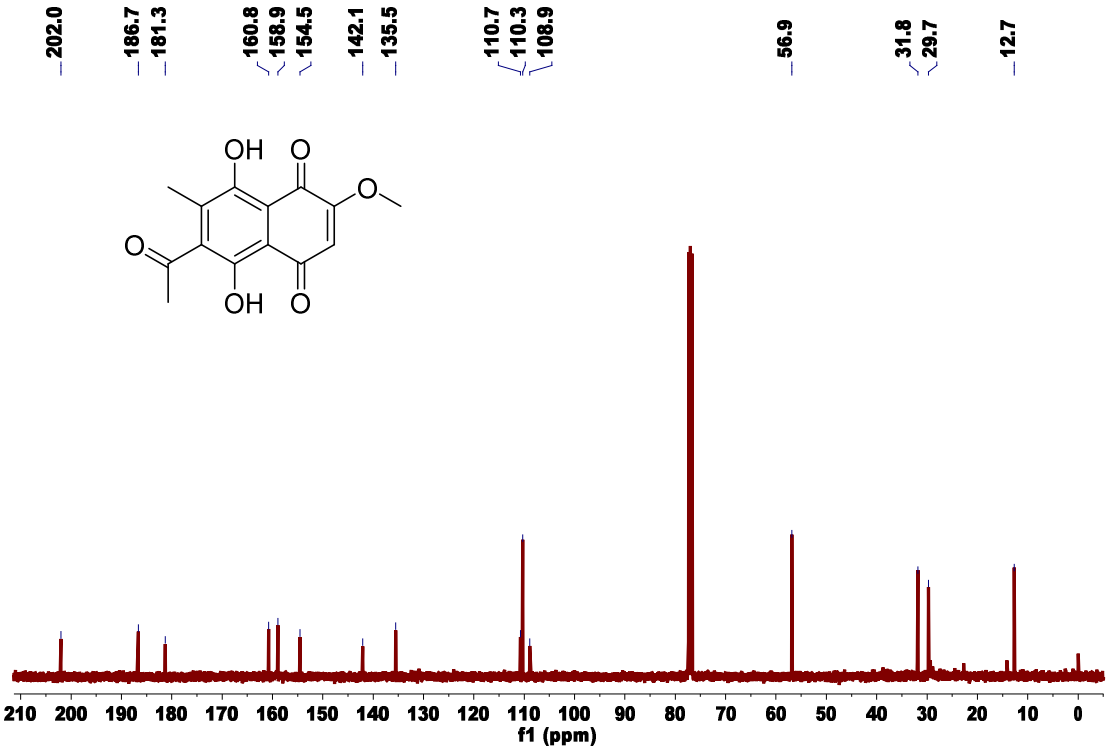

^{1}H NMR spectrum of **5. 2** in CD_3OD (500 Hz)

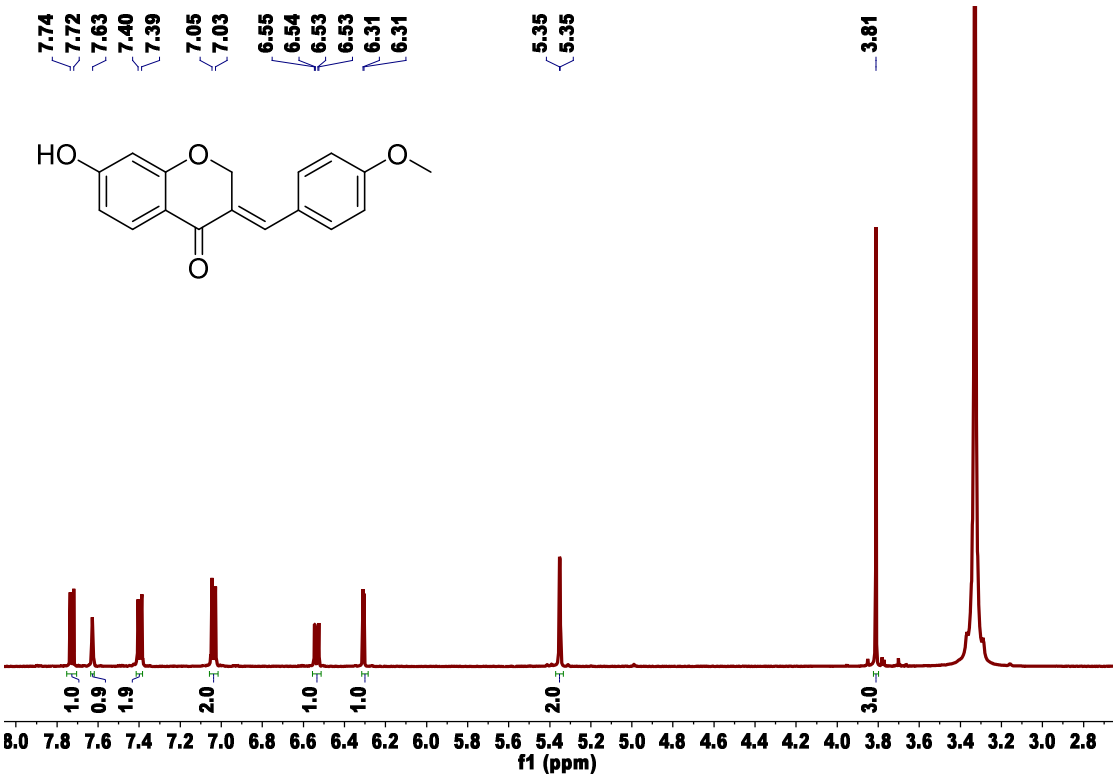

^{1}H NMR spectrum of **5. 3** in CD_3OD (500 Hz)

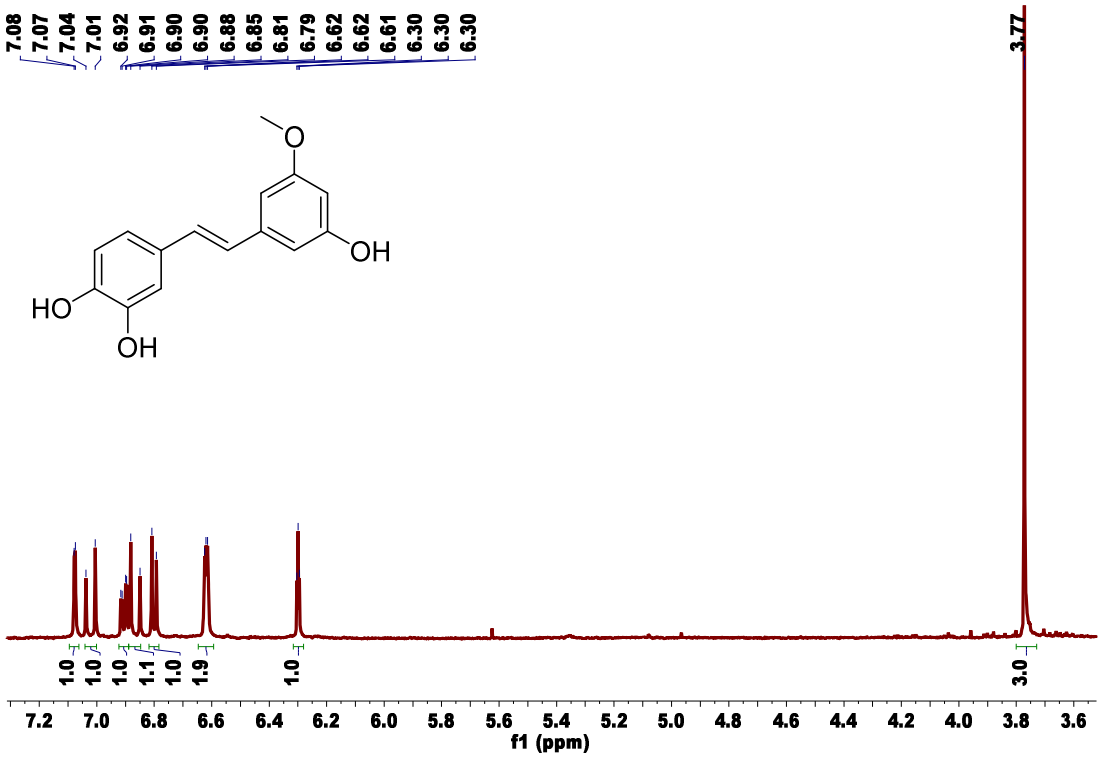

^{1}H NMR spectrum of **5. 4** in CD_3OD (500 Hz)

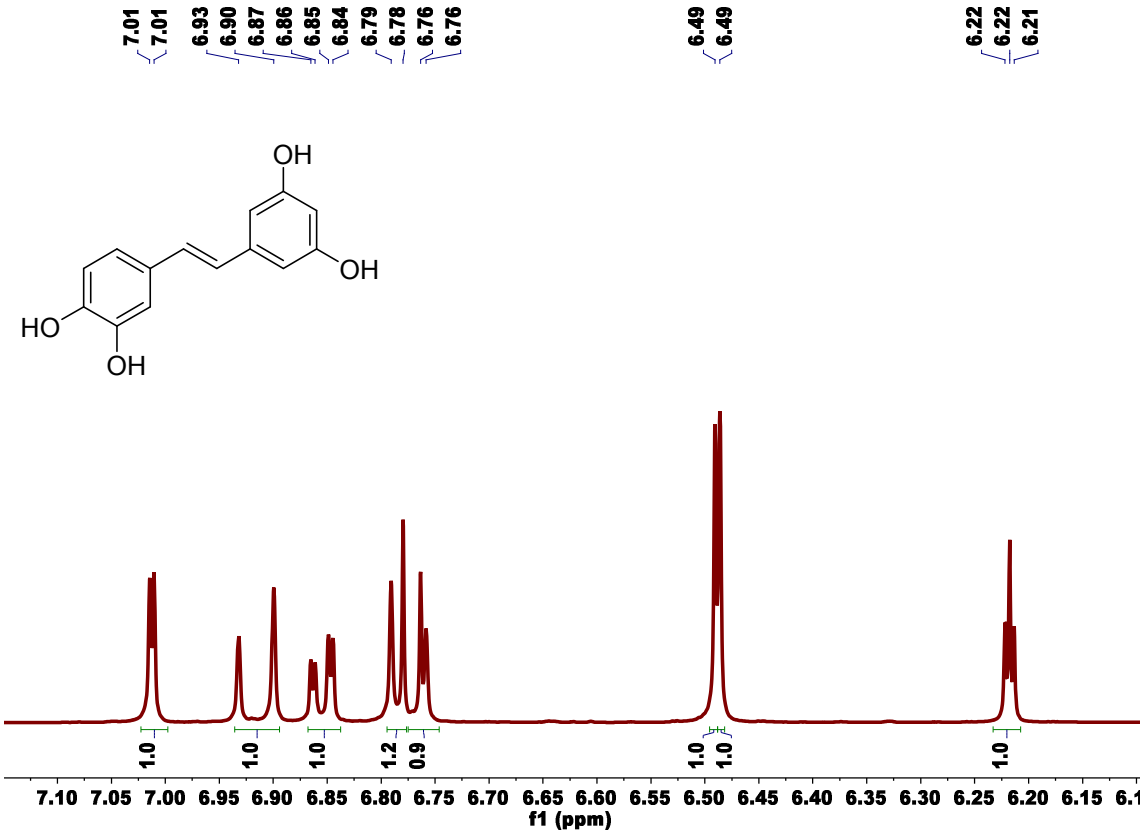

^{1}H NMR spectrum of **5. 5** in CD_3OD (500 Hz)

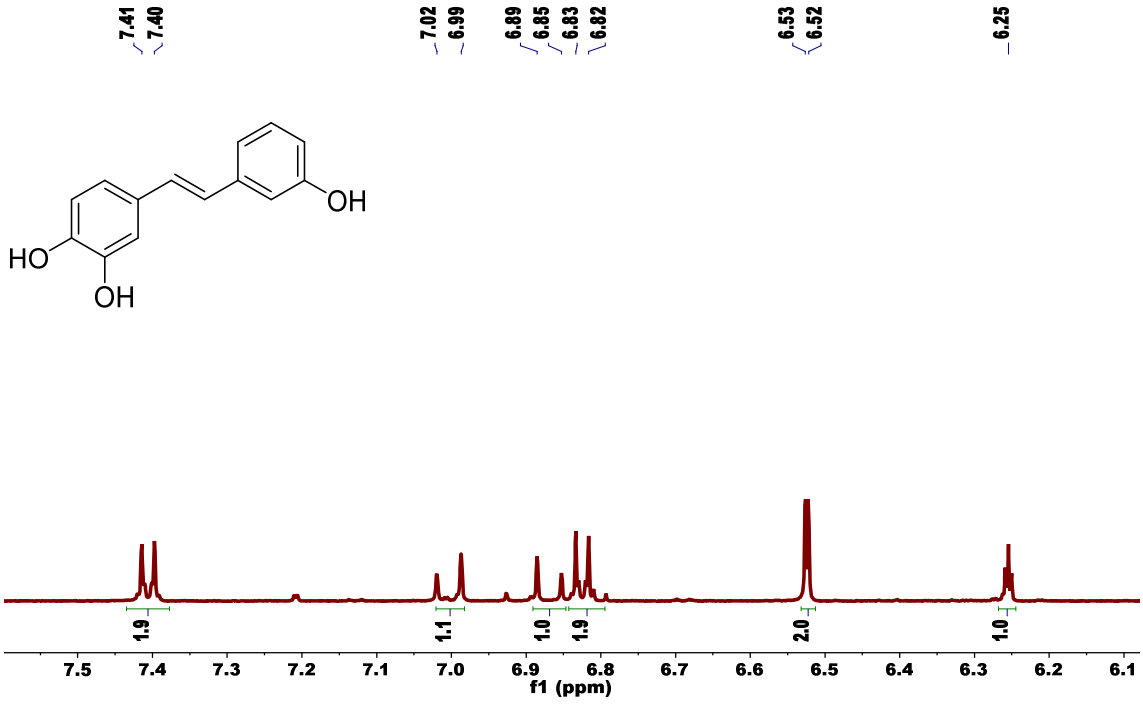

^{1}H NMR spectrum of **5. 6** in CD_3OD (500 Hz)

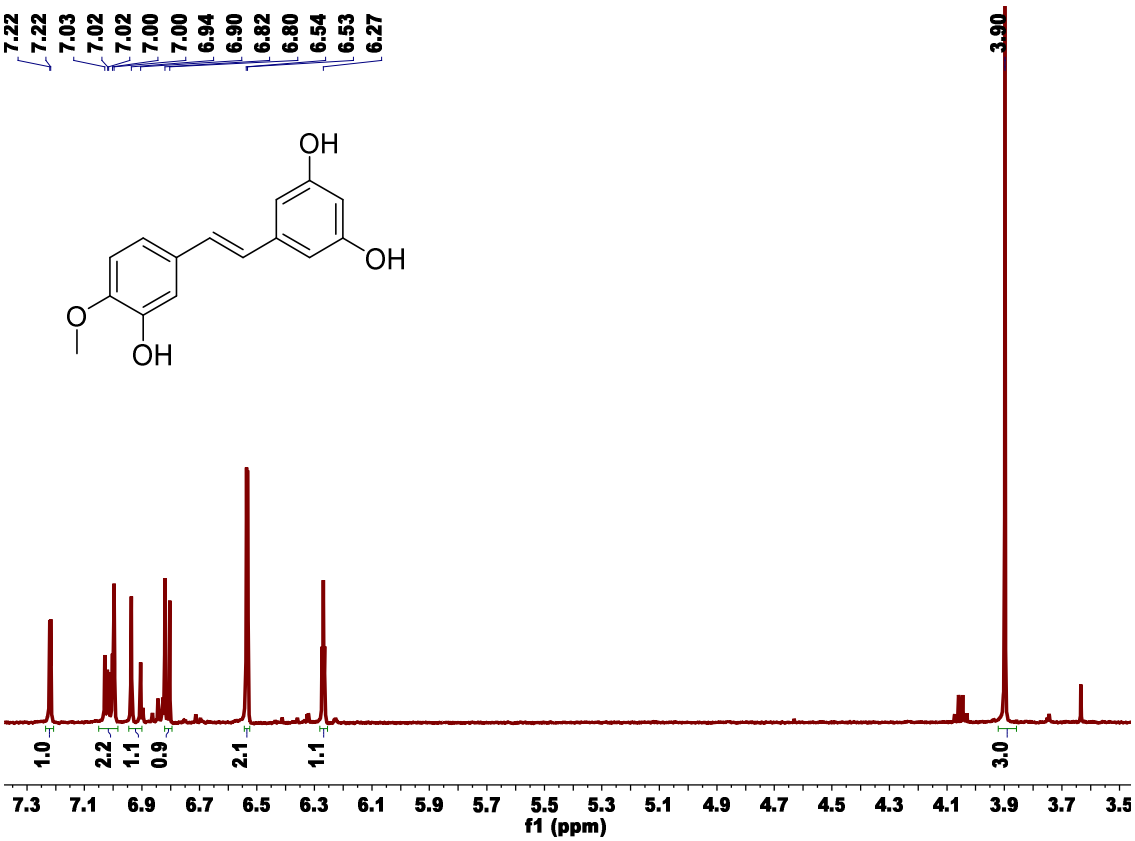

^{1}H NMR spectrum of **5. 7** in CD_3OD (500 Hz)

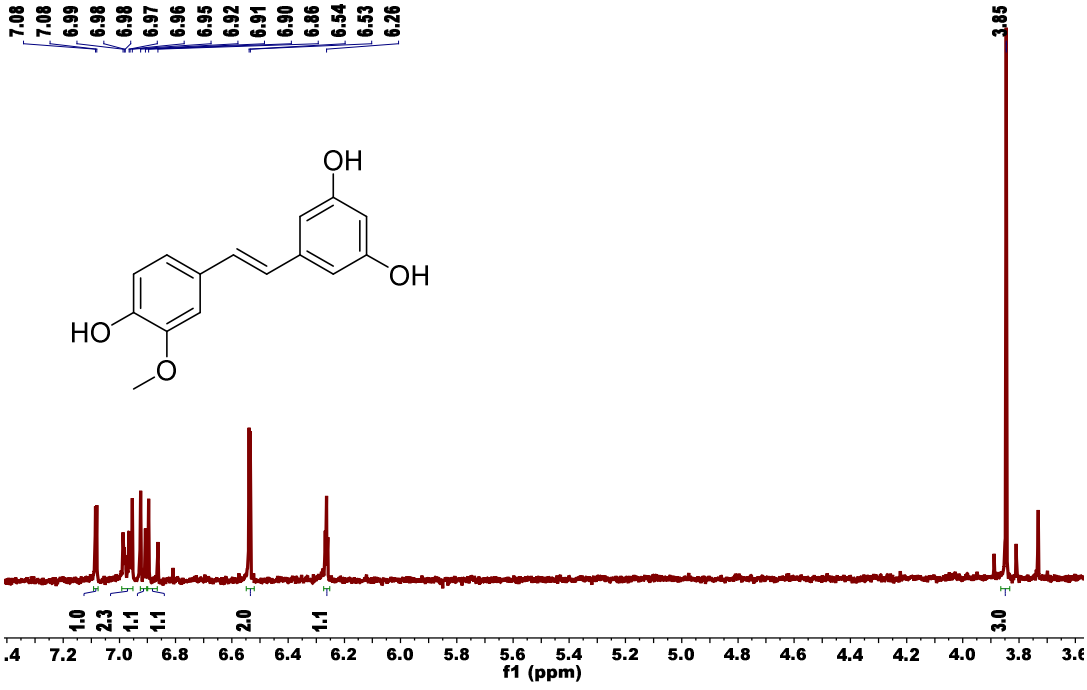

^{1}H NMR spectrum of **6.1** in $CDCl_3$ (500 Hz)

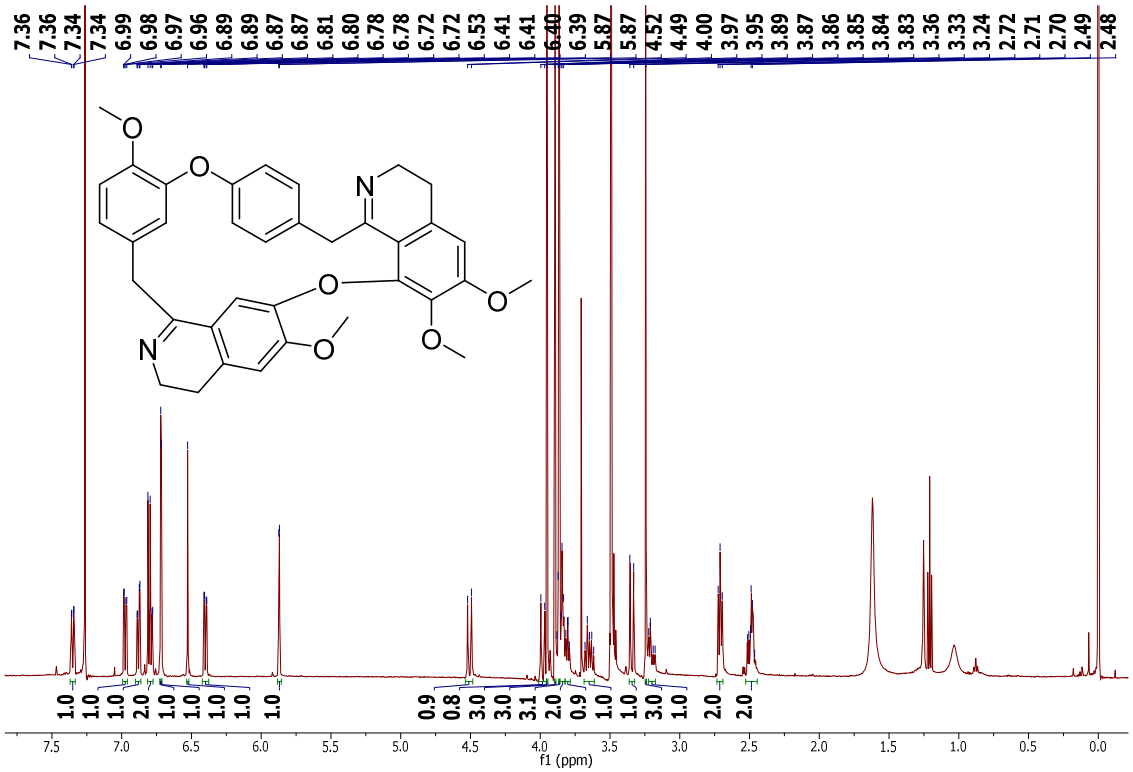

^{13}C NMR spectrum of **6.1** in $CDCl_3$ (125 Hz)

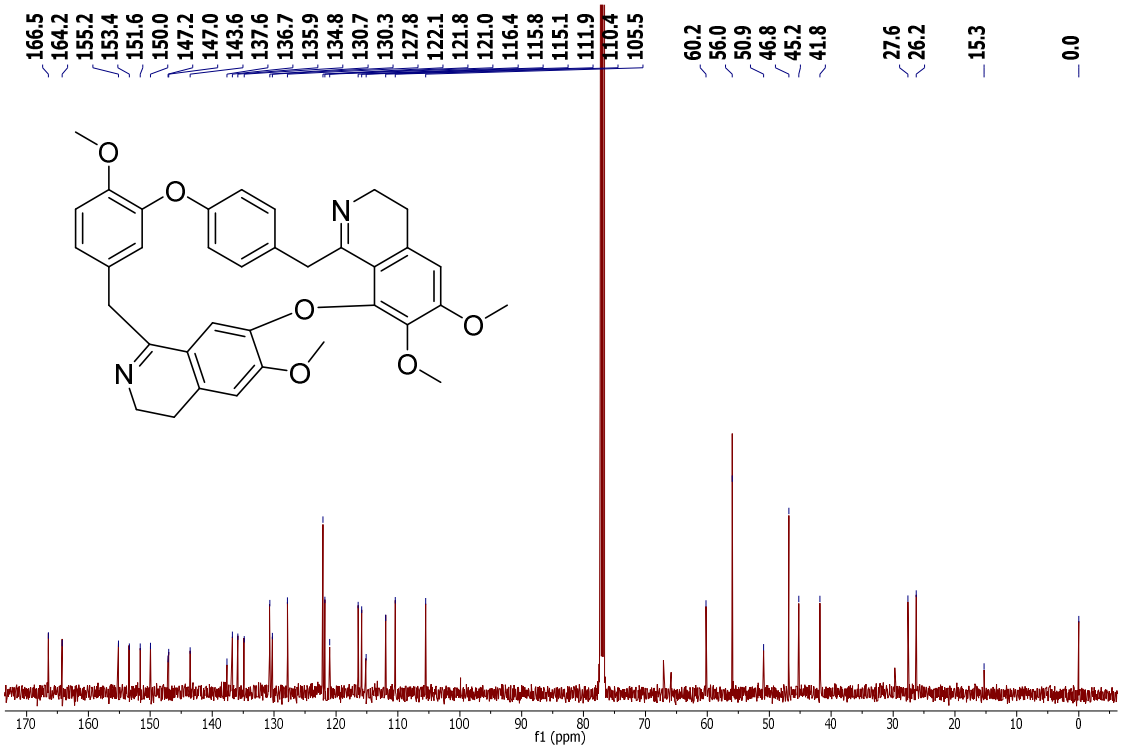

^{1}H NMR spectrum of **6.2** in $CDCl_3$ (500 Hz)

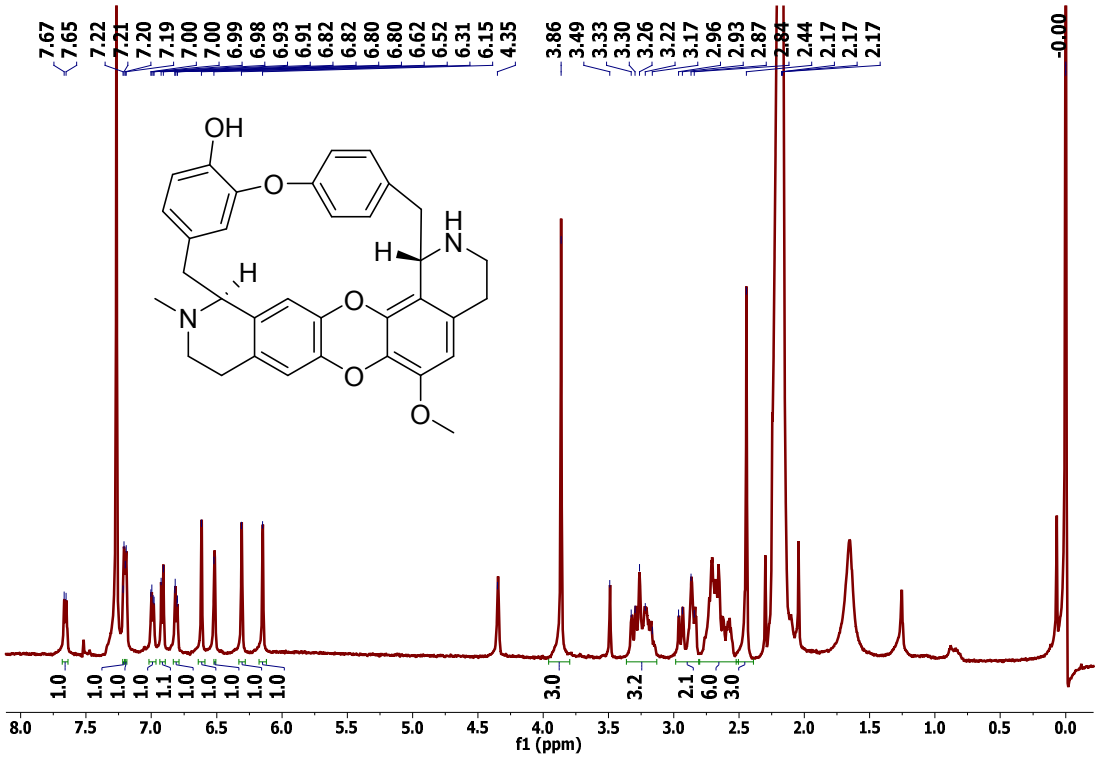

^{13}C NMR spectrum of **6.2** in $CDCl_3$ (125 Hz)

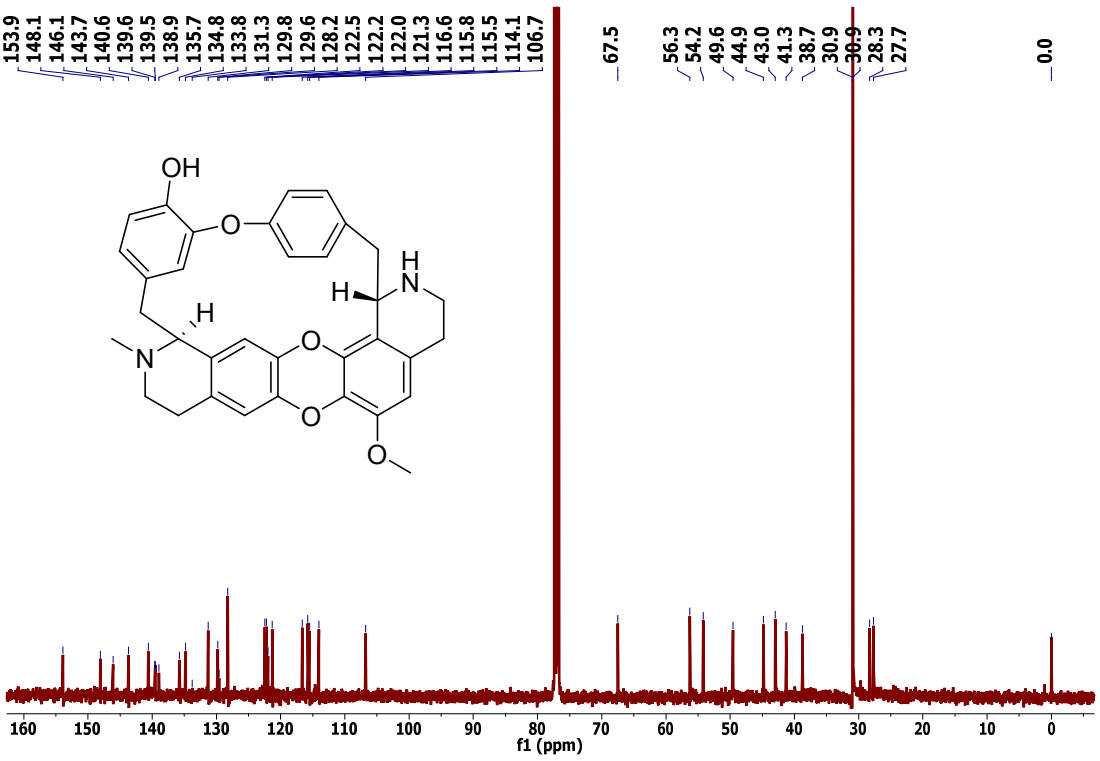

^{1}H NMR spectrum of **6.5** in $CDCl_3$ (500 Hz)

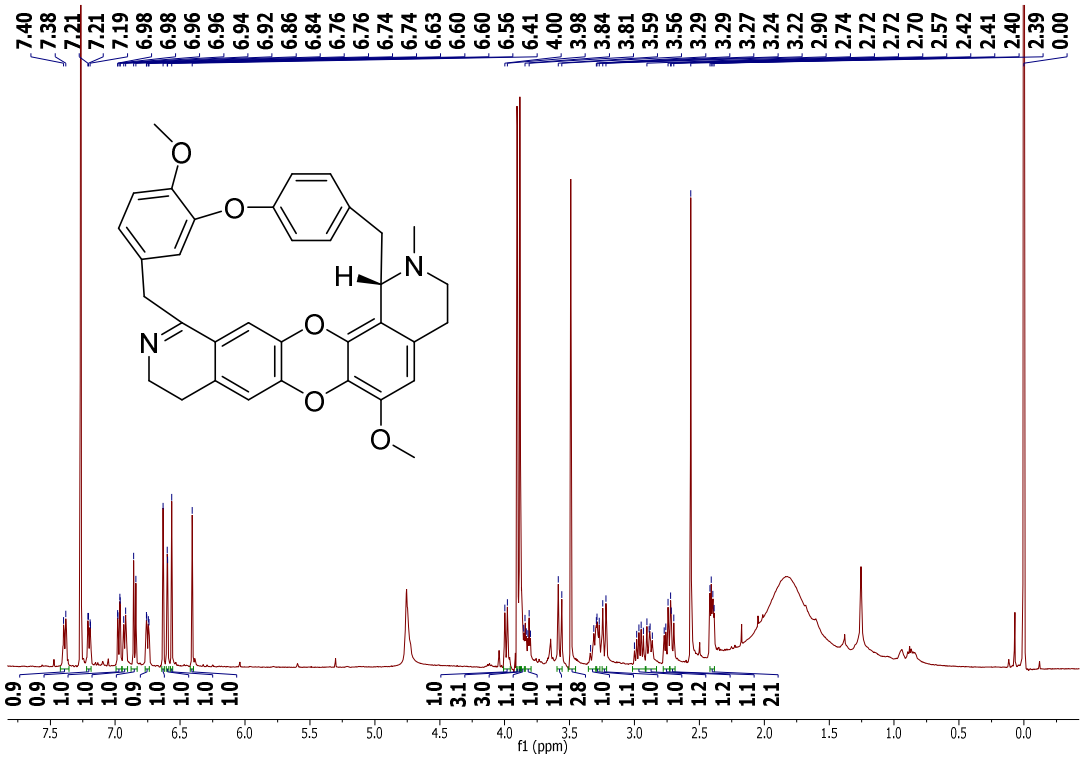

^{13}C NMR spectrum of **6.5** in $CDCl_3$ (125 Hz)

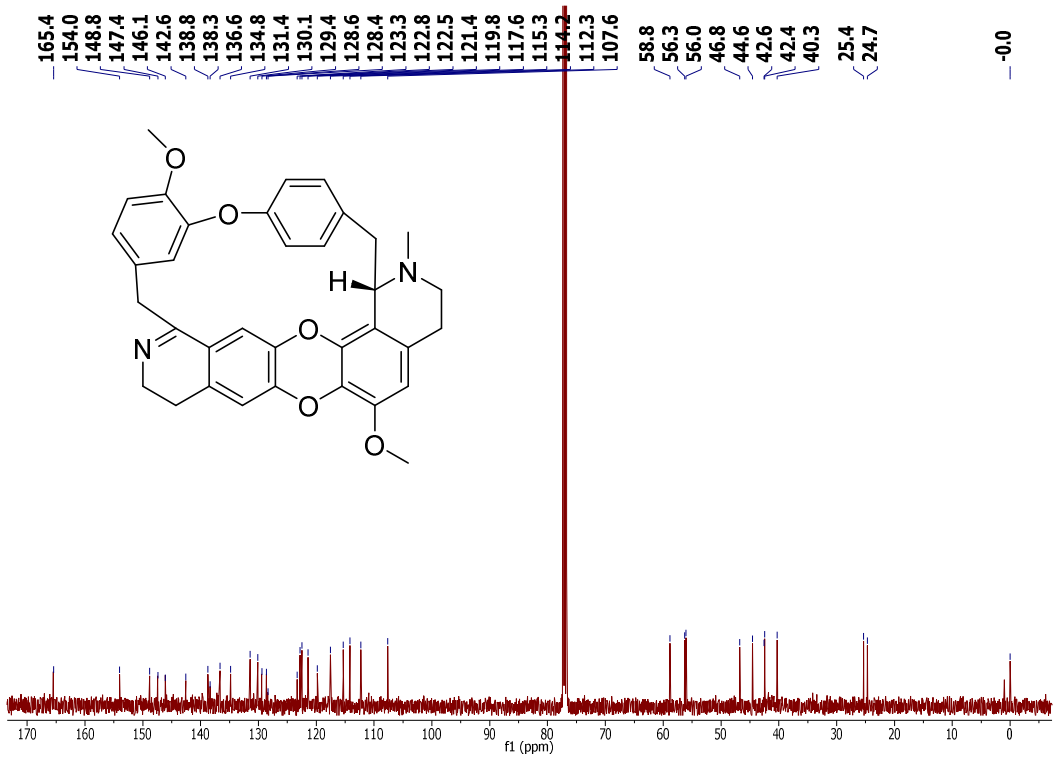

^{1}H NMR spectrum of **6.6** in $CDCl_3$ (500 Hz)

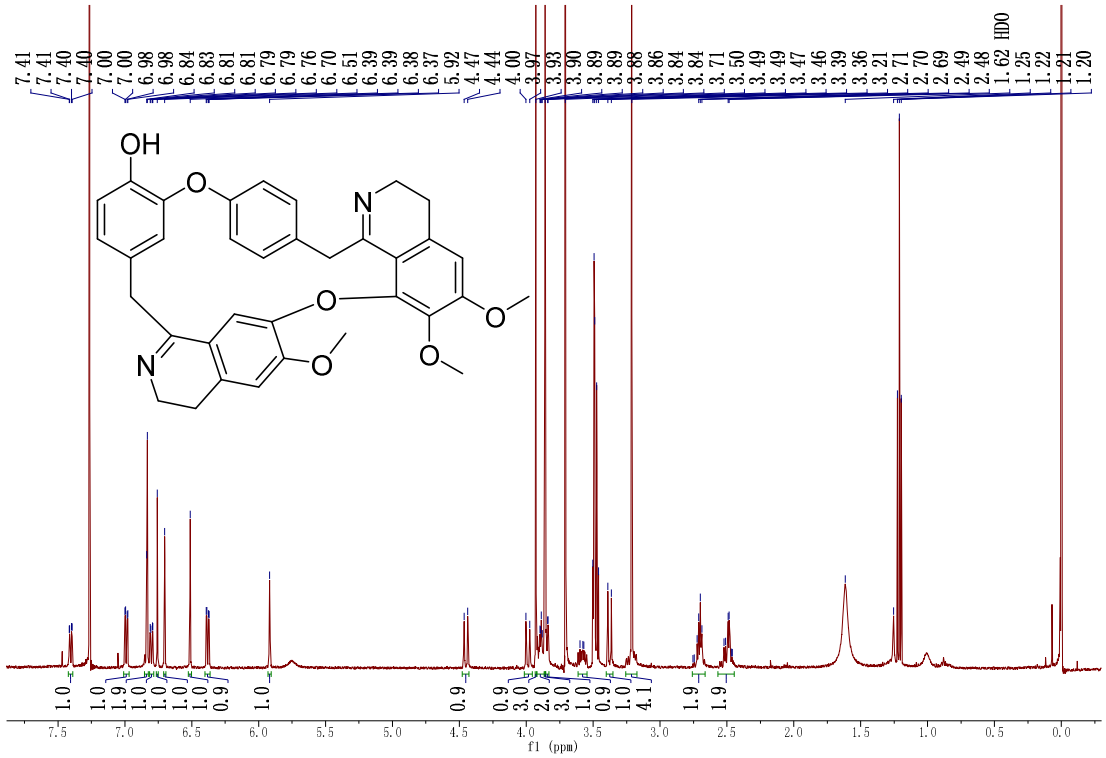

^{13}C NMR spectrum of **6.6** in $CDCl_3$ (125 Hz)

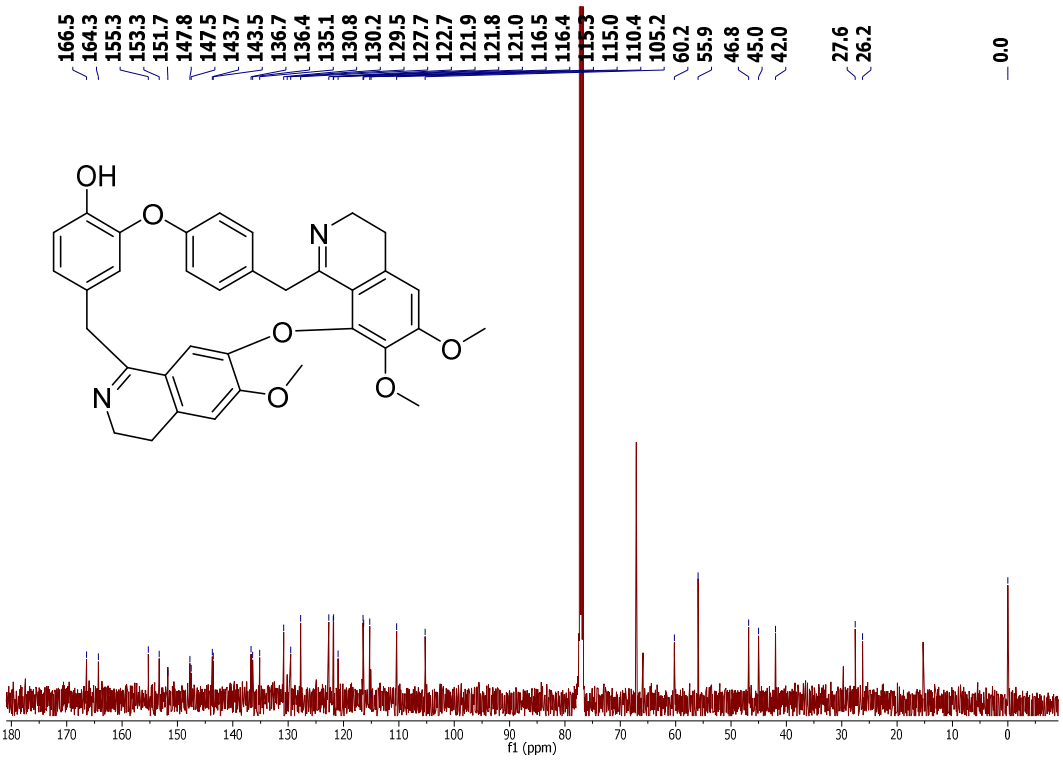

^{1}H NMR spectrum of **7.1** in $CDCl_3$ (500 Hz)

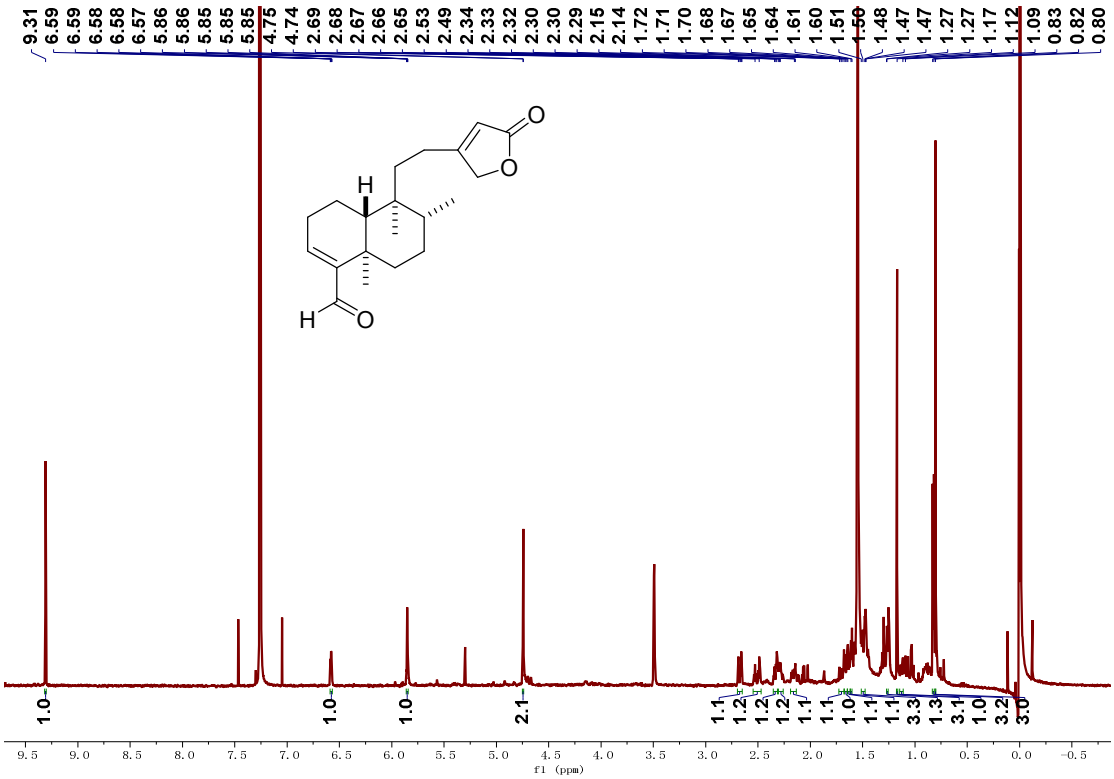

^{1}H NMR spectrum of **7.2** in $CDCl_3$ (500 Hz)

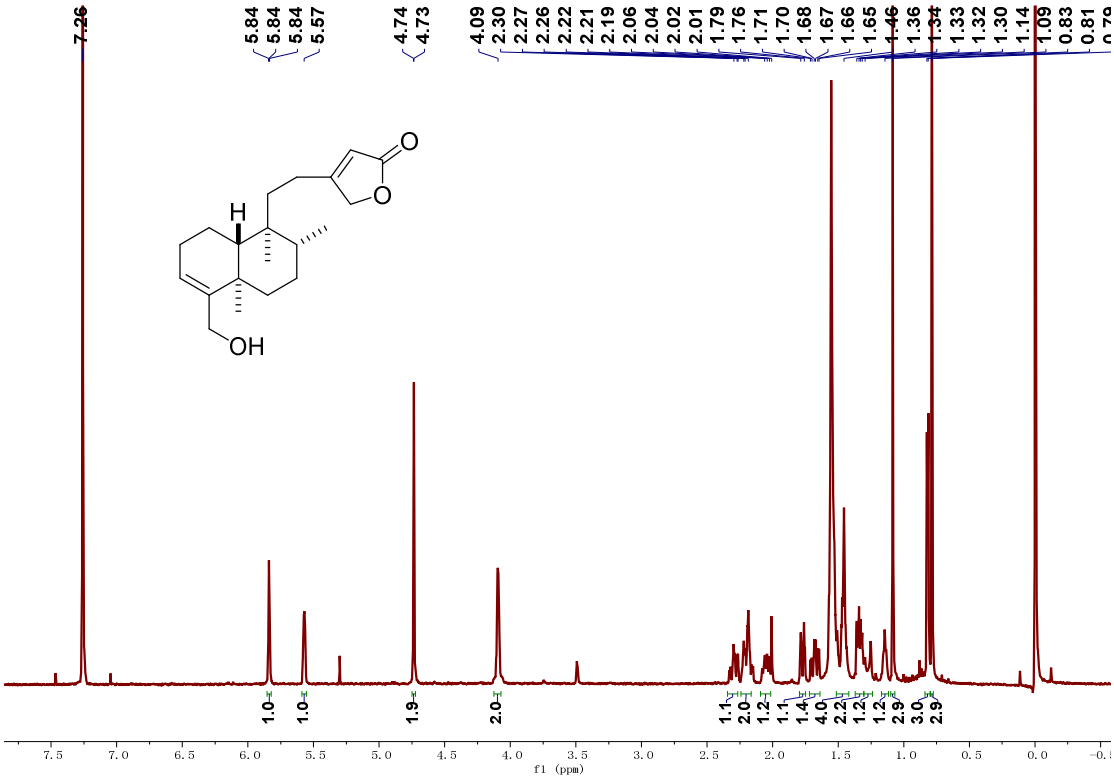

^{1}H NMR spectrum of **7.3** in $CDCl_3$ (500 Hz)

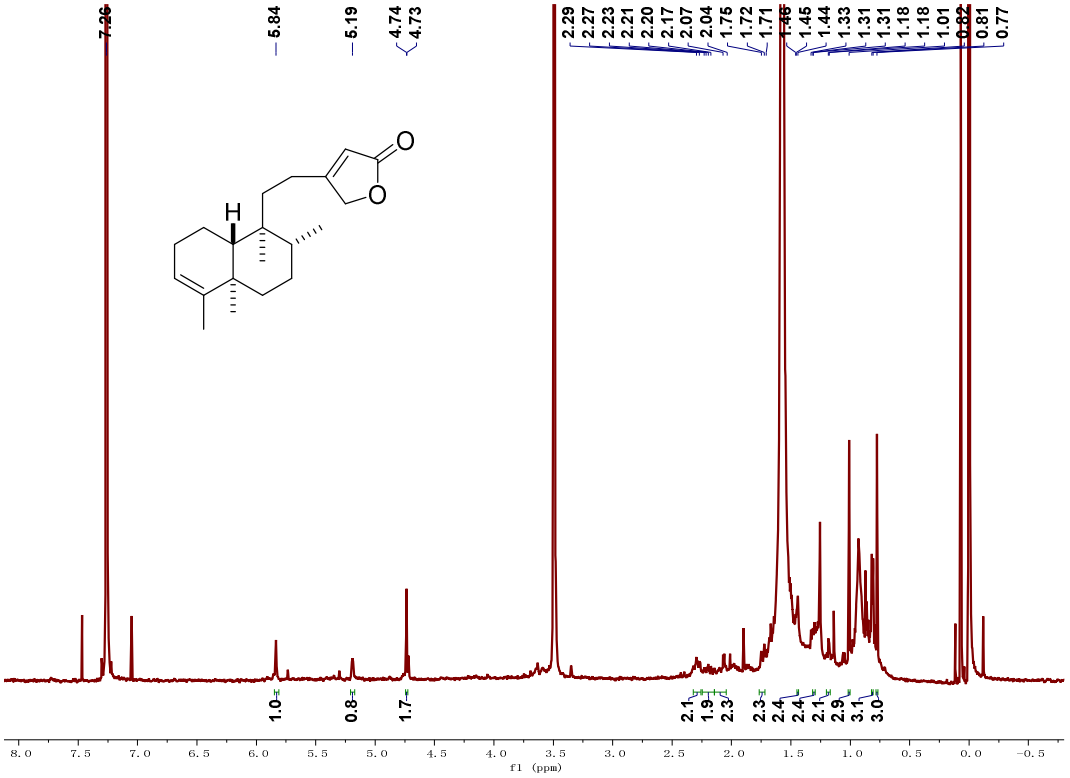

^{1}H NMR spectrum of **7.4** in $CDCl_3$ (500 Hz)

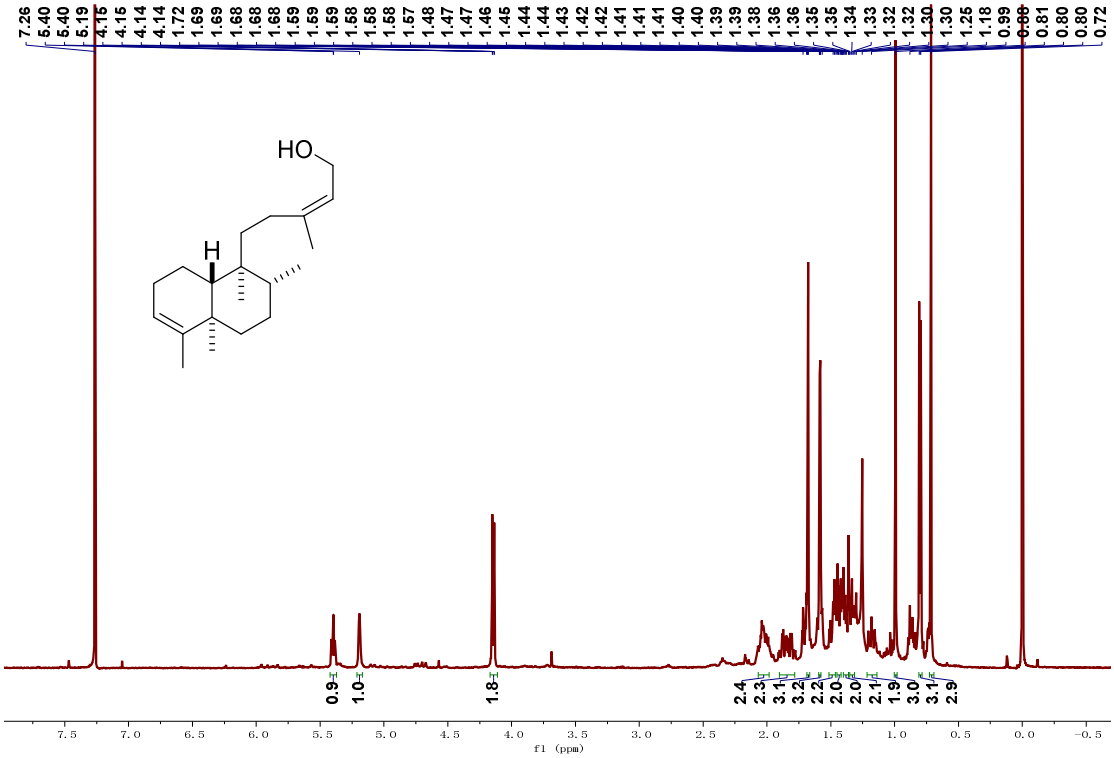

^{1}H NMR spectrum of **7.5** in $CDCl_3$ (500 Hz)